Multifunctional liposomes: Microscale formulation, modification and *in vitro* interaction

Dissertation zur Erlangung des Grades

"Doktor der Naturwissenschaften"

am Fachbereich Chemie, Pharmazie und Geowissenschaften

der Johannes Gutenberg-Universität Mainz

Diplom-Chemiker Thomas Fritz

geboren am 20.02.1987 in Mainz

Mainz, Juni 2016

JOHANNES GUTENBERG UNIVERSITÄT MAINZ

JG|U

Max Planck Graduate Center mit der Johannes Gutenberg-Universität

Dekan: [redacted]

1. Berichterstatter: [redacted]
2. Berichterstatter: [redacted]

Datum der mündlichen Prüfung: 01. September 2016

Prüfungskommission der mündlichen Prüfung:

1. Prüfer [redacted]
2. Prüfer [redacted]
3. Prüfer [redacted]
4. Prüfer [redacted]
5. Prüfer [redacted]

The present dissertation was composed at the Institute of Pharmacy and Biochemistry at the University of Mainz within the Max Planck Graduate Center (MPGC) under supervision of Prof. Dr. [redacted] in the time between the 15th November 2012 and the 31st July 2016.

Supervisors	
Prof. Dr. [redacted] Faculty of Chemistry, Pharmaceutical Science and Geoscience Institute of Pharmacy and Biochemistry Johannes Gutenberg-University Mainz	Prof. Dr. [redacted] Faculty of Chemistry, Pharmaceutical Science and Geoscience Institute of Organic Chemistry Johannes Gutenberg-University Mainz

MPGC Mentors	
Prof. Dr. [redacted] Jena Center for Soft Matter Institute for Organic Chemistry and Macromolecular Chemistry Friedrich-Schiller-University Jena	Dr. [redacted] BioNTech RNA Pharmaceuticals Mainz

I hereby declare that I wrote the dissertation submitted without any unauthorized external assistance and used only sources acknowledged in the work. All textual passages which are appropriated verbatim or paraphrased from published and unpublished texts as well as all information obtained from oral sources are duly indicated and listed in accordance with bibliographical rules. In carrying out this research, I complied with the rules of standard scientific practice as formulated in the statutes of Johannes Gutenberg-University Mainz to insure standard scientific practice.

Place, Date

Thomas Fritz

"There is a way out of every box, a solution to every puzzle; it's just a matter of finding it."

"Things are only impossible until they're not!"

Jean-Luc Picard

Danksagung

[redacted]

Contents

Abstract

Liposomes have been in clinical application for over two decades and are the arguably most important class of nanoparticulate therapeutics. However, the investigation of functionalized liposome systems is yet limited by synthetic access as well as by material and time consumption.

Dual centrifugation (DC) has previously been established as a valuable method for the rapid formulation of liposomes in small batch sizes.[1] However, standard laboratory-scale syntheses of novel polymeric amphiphiles typically only allow for a relatively limited number of preparations. Here, DC formulation was scaled down to the single-digit milligram scale of total lipids, while beneficial properties such as high encapsulation efficiencies (EE) were preserved. This enabled the detailed investigation of the formulation parameter space of liposomes that contained rare prototype compounds.

Efficient surface derivatization routes are key requirements for the use of valuable targeting ligands. After having established CuAAC chemistry for surface modification of liposomes recently,[2] this tool was used to investigate the *in vitro* interaction of a new class of polyglycerol amphiphiles. Live cell imaging revealed a rapid desorption of cholesterol-based amphiphiles from the liposome surface. While the sterical stabilization of these vesicles was intended to prevent unspecific interaction in biological systems, the observed instability rendered the use of such amphiphiles questionable. The permutation of the amphiphile structures, membrane anchors and reactive groups, and the application of orthogonal derivatization *via* CuAAC and IEDDA revealed that solely the cholesterol anchorage caused the mentioned desorption effects. Consistently, less effective active targeting of folic acid-containing cholesterol-amphiphiles was found when compared to dialkyl-substituted anchors. However, these more stable membrane anchors were also found to desorb after binding to cellular folate receptors, which suggested fundamental implications for the rational design of liposome membrane anchors.

While sterical stabilization provides "stealth" properties to liposomes to overcome rapid clearance from the blood stream *in vivo*, it typically also decreases interaction with and delivery to cells in the target tissue. As a potential solution, a novel class of acid-cleavable amphiphiles that contained acetal or ketal groups was investigated for stabilization of liposomes. Half lifes at lysosomal-like pH of 5.4 were found to be 20 h and 15 min, respectively, and therefore illustrated the suitability of these systems for the controlled shedding of liposomes.

Enabled by the substantial decrease of material consumption, polymersomes and polymeric micelles have been prepared *via* micro scale DC formulation in a proof-of-concept study, while characteristics of DC formulations like narrow size distributions and high EE were maintained. In contrast to conventional formulation methods, such as solvent switching, substantial benefits regarding time consumption and preparation yields rendered micro scale DC formulation a highly valuable tool for such systems.

Zusammenfassung

Liposomen sind seit über zwei Jahrzehnten in klinischer Anwendung und die vermutlich wichtigsten nanopartikulären Therapeutika. Die Entwicklung von funktionalisierten Liposomen ist jedoch noch immer limitiert durch synthetische Möglichkeiten sowie Material- und Zeitbedarf.

Duale Zentrifugation (DC) ist eine bereits etablierte Methode zur schnellen Formulierung von Liposomen in kleinen Ansätzen.[1] Gewöhnliche Synthesen von neuartigen Polymeramphiphilen im Labormaßstab erlauben jedoch typischerweise nur eine relativ limitierte Anzahl an Präparationen. DC Formulierung wurde daher in den einstelligen Milligrammbereich der Gesamtlipide herunterskaliert, wobei die vorteilhaften Eigenschaften wie z. B. hohe Einschlusseffizienz (EE) erhalten blieben. Dies ermöglichte die detaillierte Untersuchung des Parameterraums der Formulierung von Liposomen, welche rare Prototypstrukturen enthielten.

Effiziente Strategien zur Oberflächenderivatisierung sind Schlüsselvoraussetzungen für die Anwendung teurer Targetingliganden. Vor kurzem etabliert,[2] wurde CuAAC Chemie zur Modifizierung von Liposomen nun zur Untersuchung der *in vitro* Interaktionen einer neuen Klasse von Polyglycerolamphiphilen genutzt. Mikroskopie an lebenden Zellen zeigte eine schnelle Desorption von cholesterol-basierten Amphiphilen von der Liposomenoberfläche, was wegen der unzureichenden Verhinderung von unspezifischen Interaktionen in biologischen Systemen die Anwendbarkeit solcher Amphiphile infrage stellte. Permutation von Amphiphilstrukturen, Membrananker und reaktiven Gruppen, sowie die Anwendung orthogonaler Derivatisierung *via* CuAAC und IEDDA zeigten, dass ausschließlich Cholesterolanker die genannten Desorptionseffekte verursachten. Zusätzlich zeigte sich das aktive Targeting mit Folsäure-Cholesterol-Amphiphilen als weniger effektiv im Vergleich mit dialkylsubstituierten Ankern. Diese stabileren Lipidanker zeigten jedoch ebenso eine Desorption nach der Bindung an zelluläre Folsäurerezeptoren, was fundamentale Folgerungen für das rationale Design von derartigen Strukturen implizierte.

Während sterische Stabilisierung der schnellen Eliminierung aus dem Blutstrom vorbeugen soll, wird typischerweise auch die Interaktion mit den Zellen des Zielgewebes reduziert. Als ein möglicher Lösungsansatz wurde eine neue Klasse von säurespaltbaren Amphiphilen, welche Acetal- und Ketalgruppen enthielten, zur Stabilisierung von Liposomen untersucht. Halbwertszeiten bei lysosomartigen pH-Werten von 5.4 waren jeweils 20 h und 15 min, was die Verwendbarkeit solcher Systeme für die kontrollierte Destabilisierung von Liposomen bestätigte.

Ermöglicht durch die starke Reduktion des Materialverbrauchs wurden Polymersomen und Polymermicellen *via* Mikro-DC Formulierung in einer Machbarkeitsstudie hergestellt, wobei die Eigenschaften der DC Formulierung, wie z.B. hohe EE, erhalten blieben. Im Vergleich mit konventionellen Methoden wie z.B. Lösungsmittelaustausch, stellten große Vorteile in Zeitbedarf und Ausbeuten die Mikro-DC als ein wertvolles Werkzeug für solche Systeme dar.

Graphical abstract

Section 3.1: Microscale formulation of liposomes *via* dual centrifugation

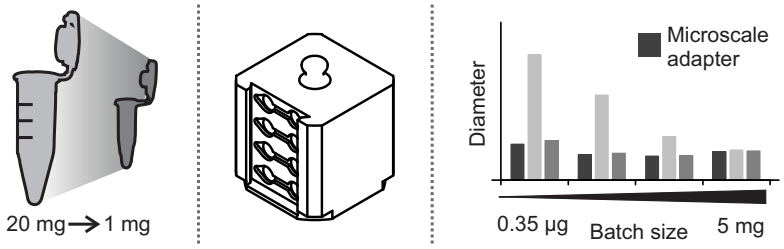

Section 3.2: In vitro interaction of poly(glycerol)-shielded, functionalized liposomes

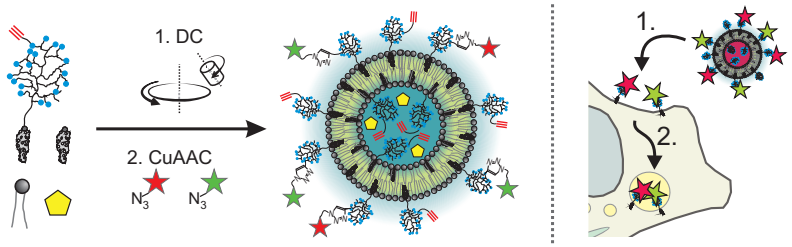

Section 3.3: Orthogonal functionalization of liposomes: multifunctional carriers

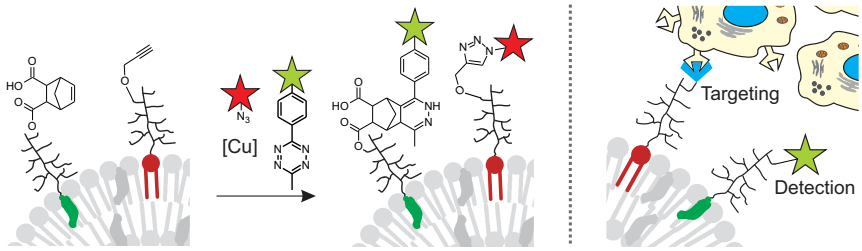

Section 3.4: Acidic shedding of liposomal particles

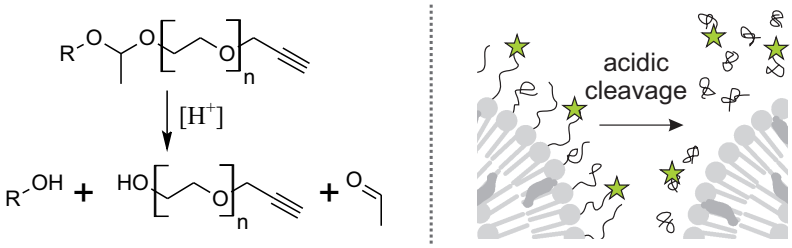

Section 3.5: Application of microscale dual centrifugation to non-lipid particles

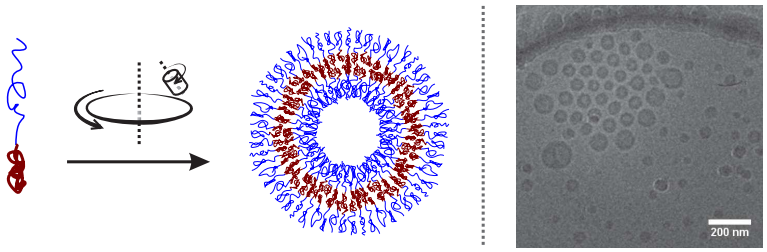

1 Introduction

1.1 Liposomes: Basic concepts

In 1965, Alec Banghamfirst described the lamellar structure of phospholipids that he subjected to rehydration with aqueous buffer, and thus established the term liposome.[3] Liposomes are vesicular, self-assembled particles that can be formed from naturally occurring phospholipids, as well as from other amphiphilic compounds. The hydrophobic effect leads to a thermodynamically driven separation of lipophilic and hydrophilic parts of such amphiphilic compounds, representing one of the main driving forces for structural organization in biological systems.[4, 5] The interactions in this context are mainly defined by VAN DER WAALS forces between aliphatic chains, as well as hydrogen bonds and electrostatic interactions between the polar head groups.[6] Figure 1.1A displays stearoyl-palmitoylphosphatidylcholine (SPPC) and cholesterol, two lipids that can be frequently found in liposome compositions. The mode of self-assembly is illustrated in Fig. 1.1B, with the employed lipids orientated with their polar headgroups (B, top) to both the outside and the aqueous core of the lipid vesicle. Liposomes can be prepared to encapsulate as well hydrophilic payload within the aqueous core and lipophilic payload which integrates within the lipid phase in the membrane, rendering the system highly versatile for encapsulation purposes (Fig. 1.1C). Depending on the intended type of application, liposomes can be prepared in a variety of sizes between 20 nm and several micrometers, as shown in Figure 1.1D, and thus be classified as small, large or giant unilamellar vesicles (SUV, LUV or GUV, respectively). When comprising more than one lipid bilayer per particle, such systems are referred to as multilamellar vesicles (MLV).[7]

A distinct feature of liposomes is the relative ease of how their characteristics can be tailored by the selection of the lipid composition. In 1968, van Deenen reported on the permeability of lipid membranes, that correlated with the degree of unsaturation of the aliphatic chains in phospholipids.[8] The saturated distearoyl phosphatidylcholine (DSPC) exhibited a lower permeability for hydrophilic small molecules than the unsaturated dioleoyl phosphatidylcholine (DOPC). This permeability of lipid membranes is related to the phase transition temperature T_m between the solid ordered (SO) phase and the liquid disordered (LD) phase, with T_m values of 54.5 °C and -18.3 °C for DSPC and DOPC, respectively.[9, 10] Also, cholesterol can be added to the phospholipid composition, which shifts the phospholipid membrane in

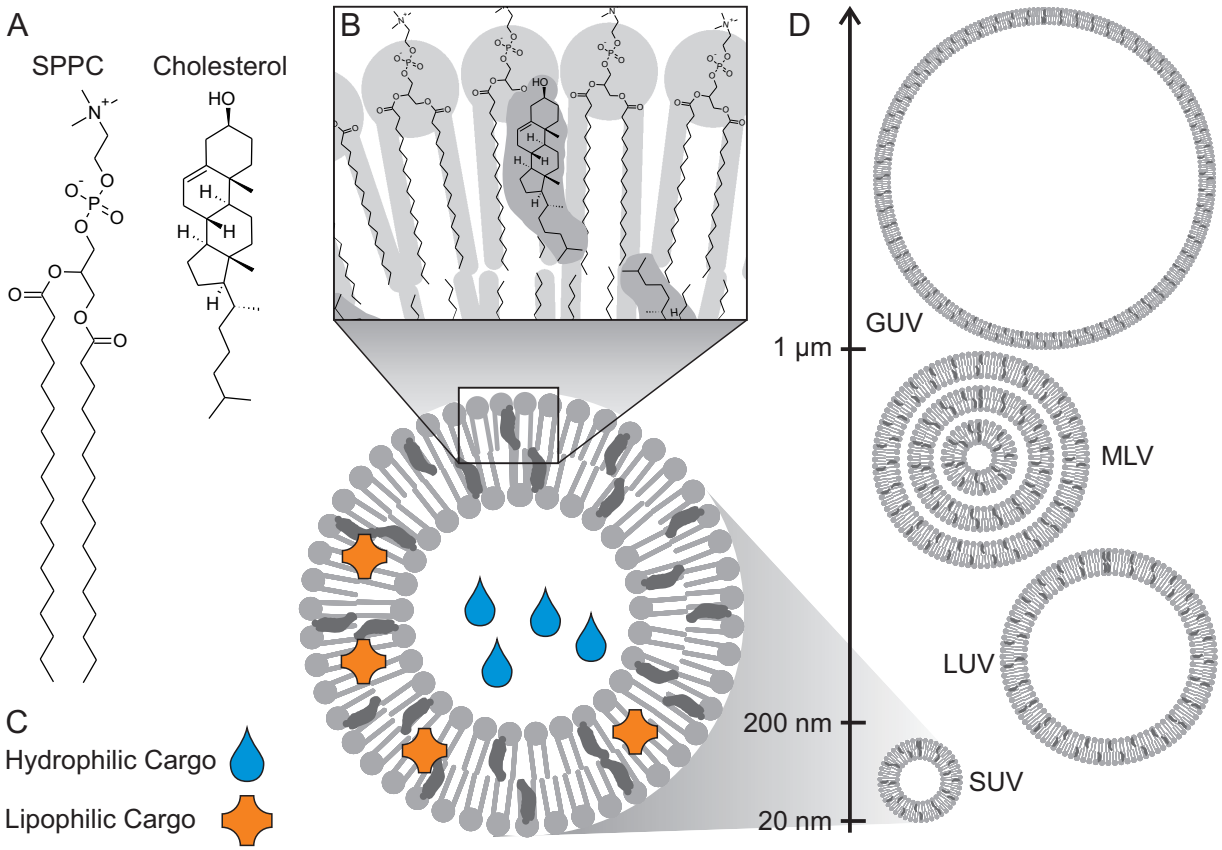

Figure 1.1: Structural concepts of liposomes. Liposomes consist typically of naturally occurring phospholipids (A), i.e. here stearoyl-palmitoylphosphatidylcholine (SPPC), and can comprise also other amphiphiles like cholesterol. These lipids assemble in lipid bilayers (B), which allow for the vesicular encapsulation of hydrophilic cargo in the aqueous core or lipophilic cargo in the lipid phase (C). Liposomes can be prepared in several forms (D), depending on the method of formulation and their composition, including small unilamellar, large unilamellar, multilamellar and giant unilamellar vesicles (SUV, LUV, MLV and GUV, respectively).

a liquid ordered (LO) phase when introduced in a fraction of approx. 33%.[11] In this LO phase, cholesterol was shown to decrease permeability compared to LD phases,[12] while it was also shown to increase fluidity below and to decrease fluidity above the T_m and thus to cause a liquid-crystalline state in a broad temperature range.[13] Cholesterol induces a tighter packing within the phospholipid bilayer by occupying the space between aliphatic chains.[14, 15] Besides influence on the phase transition temperatures, steric demands of the lipophilic chains and hydrophilic headgroups determine the tendencies of amphiphiles to either form micelles, vesicles or other structures, e.g. inverted micelles.[16, 17] As a consequence of this concept, dioleoyl phosphatidylethanolamine (DOPE) forms no lipid bilayers but facilitates membrane fusion between phospholipid bilayers, while DSPC readily forms rather inert membranes.[18]

It is apparent, that the selection of lipids and their composition crucially influences the properties of the resulting vesicles, and the ability to specifically tailor the liposome properties led to the development of applications in a vast variety of fields.

Applications of liposomes

Already in 1932, the two German researchers Klein and Grosse filed a patent on pharmaceutical formulations based on phospholipids.[19] This invention can be described as the first concept of the application of liposomes, although the authors did not know about the specific structure and underlying principles. After Banghams ground-laying findings in the 1960s, the first concepts of the encapsulation of active molecules were proposed by Sessa *et al.*, who incorporated lysozym inside phospholipid vesicles.[20] Other fields of liposome application can be found in food industry[21, 22] and cosmetics[23], for example, the use of liposome-encapsulated enzymes has been applied to accelerate the ripening of cheese,[24] and liposomal formulations have been shown to increase the efficacy of sunscreen protection.[25] However, the application in pharmaceutic research was finally envisaged by Gregoriadis, who proposed liposomes as a potential drug delivery system.[26, 27]

A large and growing body of literature has investigated the distinct advantages of liposomes for the encapsulation of pharmaceutically active compounds. Liposomes in general protect their payload from degradation within the biological environment, which can, e.g., be due to enzymatic digestion, and therefore liposomal formulations show significantly changed pharmacokinetics compared to free small molecular drugs.[28] Furthermore, in the case of parenteral application, renal clearance is typically impossible for nanoparticulate particles with hydrodynamic radii above 5.5 nm, which also leads to higher availability due to changes in renal elimination kinetics.[29] Additionally, liposomes allow to dissolve rather lipophilic drugs within the lipid phase of the vesicle (Figure 1.1C), which enables the intravenous application of such compounds, and with Amphotericin B representing one of the most widely applied

examples.[30, 31, 32] Liposomes consist in most cases of naturally occurring phospholipids like phosphatidylcholines (PC) and other lipids like cholesterol, which render liposomes intrinsically biocompatible and nontoxic. Lastly, liposomes can be versatilely derivatized in order to further manipulate their properties, which subsequently led to the development of sterically stabilized liposomes (SSL), as introduced in the following section.

Sterically stabilized liposomes: The "stealth" effect.

The use of hydrophilic polymer chains on the surface of liposomes evolved to a gold standard for parenteral applications of liposomes. In 1987, Allen and Chonn prepared liposomes that contained sialic acid as part of gangliosides, in order to mimic glycosylation patterns of cellular membranes.[33] The surface grafting with such biopolymers resulted in significantly increased circulation times due to a reduced uptake in the mononuclear phagocytic system (MPS), and was explained by a decrease of the surface adsorption of blood plasma proteins.[34] This adsorption process is part of the innate immune system and facilitates an opsonin-dependent recognition of antigens by macrophages, which typically leads to a fast uptake of conventional liposomes into the liver.[35, 36] However, subsequent investigations focused on polyethylene glycol (PEG) for the sterical stabilization of liposomes, which evolved to the gold standard for liposome derivatization ever since. The first systematic study was conducted by Klibanov *et al.,* who found that a conjugate of PEG and dioleoylphosphatidylethanolamine (PEG-DOPE) facilitated a vast prolongation of blood circulation half-life times from 30 minutes to 5 hours.[37, 38] While the exact mechanisms of PEG-stabilization have been extensively discussed,[39, 40, 41] a stable hydration layer, conformational dynamics and minimized VAN DER WAALS forces lead to a higher colloidal stability and decreased protein adsorption, and are thus resulting in a prolongation of circulation times.[42, 43, 44]

Importantly, Gabizon and Papahadjopoulos investigated the effects of several other polymer-conjugates on the liposome characteristics and deduced the possibility to achieve an enrichment within the tissue of solid tumor with such systems.[45] This passive enrichment, also referred to as passive tumor targeting, is based on effects that have been first described by Maeda in 1986 for polymeric nanoparticles.[46, 47] Maeda demonstrated a passive enrichment of such particles within the tumor tissue, which was due to a decrease in lymphatic drainage from the tumor tissue in combination with an increased permeability of the vascular system within the tumor. This effect is also referred to as the effect of enhanced permeability and retention (EPR effect) and is illustrated in Figure 1.2. The EPR effect is also the major principle behind the first ever approved nanoparticulate drug DOXIL, which was brought to market in 1995 and is a stealth liposome formulation of the chemotherapeutic drug doxorubicin.[48, 49] Subsequent optimization of the lipid and polymer composition has led to long circulation half-

lifes between 20 and 35 hours, resulting in a 60-fold increase of the area under the curve (AUC) compared to the free drug.[50] As a consequence, the effective doses that are necessary to achieve comparable tumoral drug concentrations as with the free drug are considerably lower, which results in substantially decreased unwanted side effects and represents one of the most important advantages of currently applied liposomal chemotherapeutics. In addition, a specific and crucial feature of DOXIL was also the development of the doxorubicin remote loading into vesicles by making use of an ammonium sulfate gradient across the membrane, which allowed for quantitative loading and very high intravesicular concentrations, that resulted in subsequent intravesicular crystallization of doxorubicin sulfate.[51, 52, 53]

Altogether, the use of PEG for steric stabilization has enabled the clinical application of intravenously administered liposome formulations in first place. However, several other biocompatible biopolymers were investigated as well, as introduced in the following.

Beyond PEG: Other hydrophilic polymers for sterical stabilization

Besides the abovementioned biopolymer sialic acid and the biocompatible PEG, a considerable amount of literature has been published on the application of other biocompatible polymers in liposome technology. Water-soluble dextran has been controversially discussed for sterical stabilization, since reports on both an increase[54] in circulation time and no effect[55] on circulation time have been published. Polyacrylamide (PAA) and poly(vinyl pyrrolidone) were investigated by Torchilin *et al.* and were shown to improve the circulation half-lifes of liposomes comparable to PEG.[56] Additionally, previous studies have reported on the use of poly(oxazoline)[57], poly(N-(2-hydroxypropyl)methacryl- amide)) (HPMA)[58], or polyvinyl alcohol (PVA)[59]. Another biocompatible polymer, polyglycerol, was first mentioned for the stabilization of liposomes in 1994 by Maruyama *et al.*[60], and has been gaining increased attention recently.

In 2010, the Frey group reported on a new class of polyether compounds that were accessed by oxyanionic ring opening polymerization, and subsequently evolved the described syntheses to a toolbox for the design of amphiphiles with tailored properties.[61, 62, 63] The strategy involved the intrinsic advantage to employ lipids as initiators during polymerization, which made subsequent conjugation reactions obsolete and lead to very stable amphiphiles with oxyether moieties between lipid anchors and hydrophilic polymers. Furthermore, hyperbranched polyglycerol (*hb*PG) was for the first time introduced for liposome stabilization, and has been investigated in subsequent studies. The Kressler group studied the membrane insertion of cholesterol-based *hb*PG-amphiphiles into GUV.[64, 65] In contrast to PEG-coating, *hb*PG-bearing liposomes were shown to result in lower aggregation when incubated with human blood serum, as investigated by light scattering techniques by Mohr *et al.*[66] Regarding the

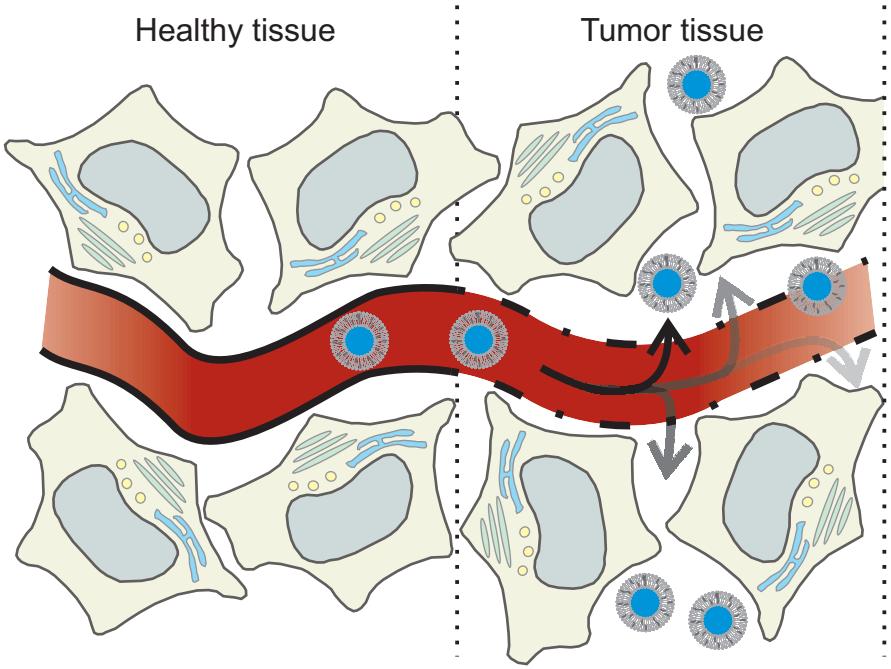

Figure 1.2: Schematic representation of the EPR effect. Liposomes circulating in the blood stream are unable to leave the vascularity within healthy tissue. In tumor tissue, the nanoparticulate drug can translocate through the endothel due to lesions and enhanced permeability, leading to a passive enrichment. Additionally, the particles and their payload shows a decreased elimination from the tumor site, as the lamphatic drainage is decreased.

in vivo pharmacokinetics, *hb*PG-liposomes were found to be comparable to PEG-liposomes by investigation with ^{18}F-labeling and positron emission tomography (PET).[67] This is of particular importance, as one distinct advantage of PG compared to PEG is the availability of a large number of free hydroxyl endgroups, which allow for multifunctinality after derivatization, while PEG offers only one terminal group for such purpose. Also, the effect of accelerated blood clearance (ABC), which has been described for PEG-liposomes and causes accelerated accumulation within the liver tissue due to the production of antibodies against the PEG coating.[68] was recently evaluated for PG-liposomes. In the respective study, Abu Lila *et al.* demonstrated that the use of PG instead of PEG efficiently prevented the occurrence of the ABC phenomenon.[69]

The studies presented thus far provided evidence on the promising characteristics of PG-based liposome-stabilization, which motivated the exploration of such compounds for liposome functionalization in the present thesis. However, also the lipid anchorage has influences on liposome stabilization and was studied in detail.

Role of lipid anchors for sterical stabilization

As outlined above, numerous studies have reported on variations of the type of polymer for sterical stabilization of liposomes. Also, a considerable amount of literature has been published on the use of different lipophilic membrane anchors. Phospholipids can be classified as the most prominent lipid anchors, which are usually modified with polymer residues by conventional conjugation chemistry (see also Section 1.2 on page 12), and with a large number of investigations described in literature.[38, 70] In addition, several artificial phospholipid-mimics have been developed, e.g. based on naturally occurring ceramides[71] or on substituted pyridinium chlorides[72]. A compound class that has recently been gaining increased attention are acyl- or alkyl-substituted glycerols, that in contrast to phospholipids lack the hydrolysis-sensitive phosphoester group.[73] Additionally, the negative net charge of the usually employed phosphatidyl ethanolamine conjugates is omitted.

Liposomes are important systems to solubilize pharmaceutically active compounds that do not comprise the necessary hydrophilicity for parenteral application. However, lipophilic drugs were shown to transfer between liposomes and biological membranes.[74] Followingly, this principle is also applicable to membrane-located lipids, an effect, which has been studied for cholesterol and phospholipids.[75, 76, 77] For liposomal membranes that consist of naturally occurring lipids, the equilibria of desorption and adsorption processes *in vivo* cause no significant changes to the liposomal compositions. However, desorption of sterically stabilizing amphiphiles significantly alters the properties of liposomal formulations, which has been studied in detail for the desorption of DSPE-PEG conjugates and nonionic derivatives of such.[78] Furthermore, Mui

et al. demonstrated that tailoring the desorption rates of stabilizing amphiphiles allowed to control the pharmacokinetics of nanoparticulate systems.[79] The authors demonstrated this controlled shedding with lipid particle systems that were stabilized with myristyl-substituted glycerols.

A significant number of researchers have reported on the use of cholesterol as a lipophilic anchor, which comprises much lower prices for raw material compared to phospholipids, while cholesterol overcomes the sensitivity of phospholipids towards hydrolysis during longer storage. Comparable to the lipid anchors based on aliphatic chains, cholesterol-based PEG-amphiphiles were in many cases shown to provide sterical stabilization and prolonged circulation times *in vivo*.[38, 80, 81, 82, 83, 84] Beugin-Deroo reported on liposomes stabilized with cholesterol-PEG conjugates that showed increased stability and impermeability.[85] However, literature has emerged that offers contradictory findings about whether cholesterol is representing a more[86] or a less[38, 87] stable lipid anchor compared to aliphatic analogues. One systematic study by Carrion *et al.* reported on the role of the linker moiety results from different conjugation routes, and determined the stability of cholesterol within the lipid bilayer.[88] The abovementioned membrane impermeability has also been controversially discussed, as it was also reported to be decreased for hydrophilic small molecules and therefore comprising a disadvantage for drug delivery purposes.[87] Sato *et al.* demonstrated that cholesterol-PEG conjugates desorbed from liposomes and stained cholesterol-rich biological membranes.[89]

Recently, a method for the post-insertion of cholesterol-PEG conjugates has been gaining increased attention,[90, 91] which illustrates the substantial popularity of cholesterol as a membrane anchor.[92] However, the controversy about cholesterol-PEG conjugates for sterical stabilization remains yet unabated, which motivated the investigation of the applicability of such structures within this thesis.

Stimuli responsive liposomes

As outlined above, recent developments regarding the slow desorption of lipid anchors have heightened the interest in a controlled depletion of sterical stabilization.[79] While the PEG chains, that mediate stealth properties *e.g.* in DOXIL, are crucial for the passive tumor targeting *via* the EPR effect, the high stability of long circulating liposomes was also shown to actively hinder the efficient release at the target tissue.[93, 94] Besides this, liposomal anthracyclines like DOXIL are known to often cause severe side effects like hand foot syndrome (or palmar-plantar erythrodysesthesia, PPE), which is an inflammatory process of skin on feet and hands. PPE is pathologically connected with the secretion of liposomal doxorubicin in sweat,[95] and thus a faster enrichment within the tumor tissue with a decrease in total circulation time is expected to reduce such side effects.

In the past three decades, research on the field of liposomes has led to the development of numerous strategies to allow for a controlled degradation of the stabilizing polymer hull or the vesicular structure itself. The first approach reported in literature was the investigation of redox-sensitive amphiphiles based on disulfide linkers, that were shown to be cleaved in the reductive milieu of endolysosomes.[96] In addition, glutathione levels are known to be increased within a tumor by a factor of 100-1000, which also enables a cleavage of disulfides in the tumor milieu.[97] Subsequent studies have reported on cleavable linkers based on cystein, that were found to enable a fast and efficient cleavage *in vitro*.[98, 99]

Another strategy relies on the fact, that the tumor milieu usually goes along with a reduction in pH due to metabolic acidosis.[100, 101] Furthermore, endosomes and lysosomes, *i.e.* intracellular trafficking vesicles in which liposomes can be taken up, comprise pH values of 6 to 4, respectively.[102, 103] Numerous compound classes ere shown to facilitate shedding of liposomes in acidic environment, including acid-labile ortho esters[104, 105, 106], vinyl ethers[107] or esters[108, 109].

Recently investigators have examined the incorporation of multiple acid-cleavable moieties within the same polyether chain,[110] a promising concept, which allowed for tuning the lability to the specific needs, and also allowed for the incorporation of such cleavable groups within polyglycerol amphiphiles.[61] Based on these studies, the investigation of novel acid-cleavable polyether amphiphiles for liposome shedding is also part of this thesis.

Liposomes in clinical application and development

As of 2015, about a dozen liposomal drug formulations are approved for clinical application.[111] These are including Doxil (doxorubicin)[49], its generic Lipodox[112] and the four other chemotherapeutics Myocet (doxorubicin)[113], DaunoXome (daunorubicin)[114], Marqibo (vincristine sulfate)[115] and DepoCyte (cytarabine)[116]. Such chemotherapeutics typically gain the most important benefits from lower systemic toxicities and improved pharmacokinetics. These advantages also apply to liposomal amphotericin B (Ambisome), one of the most important anti fungal therapeutics, which additionally is insoluble in water under physiological conditions.[31] Indeed, liposomal formulation lowers significantly the otherwise severe side effects of conventional intravenous amphotericin B treatment. Other approved formulations include morphine sulfate for analgesia,[117] verteporfin for the use in photodynamic therapy in macular degeneration[118] or the use of liposomes as immunogenicity adjuvants for hepatitis A and influenza vaccination.[119, 120] However, although the basic knowledge about liposomes was established over half a century ago, the number of approved formulations is yet quite low. This is arguably most likely due to the high complexicity of the pharmaceutical processes during liposome formulation, compared to small molecules.

Ongoing development will presumably broaden the field of clinical liposome applications in the near future, as more than a dozen liposomal pharmaceutics are in clinical trials at the moment.[111] Numerous formulations that are currently under clinical investigation employ already established chemotherapeutics that are formulated within liposomal nanocarriers in order to tune their pharmacokinetics and decrease unwanted side effects, e.g. paclitaxel[121, 122], cisplatin[123, 124, 125], annamycin[126, 127] or topotecan[128]. However, a few studies involve entirely new concepts. Needham *et al.* reported on the use of monopalmitoyl phosphatidylcholine (MPPC), which allowed to tune the overall phase transition temperature of the lipid composition. The resulted increase in permeability facilitated the triggered release of doxorubicin from the vesicle upon mild hyperthermia of 40 °C, which was achieved by ultrasound treatment.[129, 130, 131] Therefore, this concept represents yet another type of stimulus-responsiveness, as introduced above.

Another recent clinical trial investigated the use of active targeting ligands, namely antibodies, that were directed against the endothelial growth factor receptor (EGFR).[132] Representing one of the very few clinical trials of an actively targeted liposome formulation (and the only active clinical trial in this context as of 2015), these so-called immunoliposomes allowed for the specific targeting of certain cell surface features, as introduced in the following section.

Active targeting of liposomes

Already in the beginning of the 20th century, the German physician and scientist Paul Ehrlich proposed the concept of a "Magic Bullet". At that time, he envisaged a drug delivery vehicle that should allow for the specific treatment only of the targeted cells, while preserving healthy tissue from related unwanted side effects.[133] For this purpose, one could use *e.g.* antibodies, *i.e.* proteins of the immune system that are able to specifically recognize antigen patterns. Ehrlich was awarded the Nobel Prize for Physiology or Medicine in 1908 for the postulation of the antibody concept in his "side chain theory". The general concept of "Magic Bullet"-like directed drug delivery is illustrated in Figure 1.3. Drug delivery vehicles, here liposomes, that are equipped with targeting ligands, as *e.g.* antibodies, are able to bind specifically to the intended cell population. After internalization and release, their payload can unfold its pharmacological activity only to these cells, while healthy tissue is preserved from unwanted side effects.

The first approach for liposome targeting was reported by Gregoriadis *et al.*, who prepared liposomes in presence of immune globulines and observed an increased uptake.[134] Since then, antibody-mediated targeting has been extensively investigated with liposomal systems.[135] However, only a few targeted liposome systems have progressed to clinical trials, including transferrin receptor targeting[136], the breastcancer-specific HER2 targeting[137, 138],

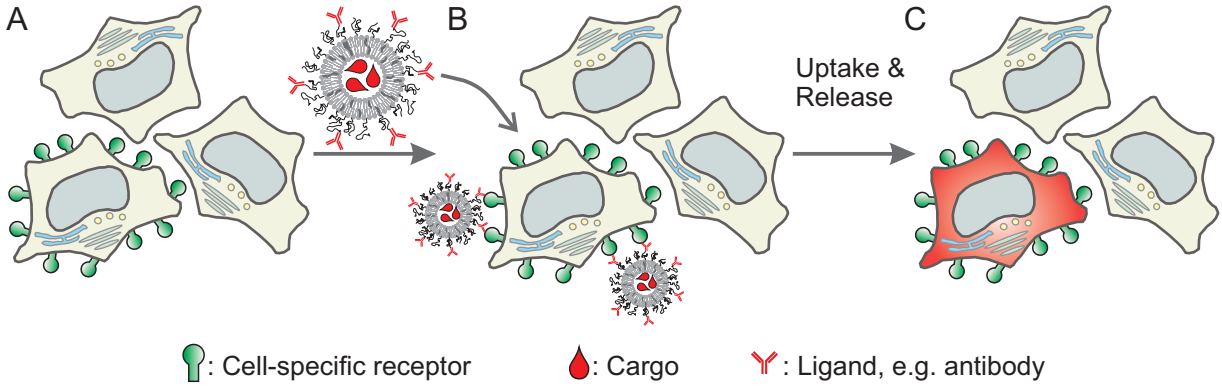

Figure 1.3: Schematic of active directed drug delivery. Cells, that are presenting specific cell surface features as e.g. receptors (A), can be recognized by delivery-vehicle bound ligands, as e.g. antibodies (B). After binding, the therapeutically active payload is delivered solely to the intended cells, while healthy and untargeted cells are preserved from unwanted effects (C).

a transferrin receptor-targeted nanocomplex[139], and the abovementioned EGFR-targeted formulation.[132] It is a subject of current debate that the paramount complexicity of such systems, which subsequently leads to massive costs for development and quality control, is substantially hindering the clinical progress of related research, compared to passively targeted nanomedicines.[140]

Within four decades of liposome research, besides antibodies, various other targeting ligands have been investigated to potentially overcome these drawbacks. Figure 1.4 displays a selection of targeting ligands that have been employed in various reports. One important class of targeting compounds are small molecular receptor ligands, which are typically rather inexpensive and easier to be chemically modified, compared to antibodies, and with the most prominent one being folic acid (FA). Overexpression of the folate receptor (FR) can be commonly found in various types of cancer,[141, 142] since its reduced form, tetrahydrofolate, is essential for the cellular synthesis of nucleic acids and therefore for cell proliferation.[143] The first report of the utilization of FA for liposome targeting was published by Lee *et al.*,[144] who demonstrated an increased uptake of such liposomes in cells overexpressing FR. This concept has earlier been applied to the delivery of a variety of macromolecules.[145] Since its first application, a large and growing body of literature has been published on the use of folic acid as a targeting vector, as recently reviewed.[146, 147] Other alternatives include peptide-based targeting ligands, that consist of short peptide sequences that exhibit an increased stability, are synthetically accessible and often comprise lower immunogenicity than antibodies,[148] which often exhibit an immunogenic potential.[149] Targeting ligands of that class have reportedly been applied to target the tumor vasculature[150], integrins on tumor cells by the RGD motif[151] (Arg-Gly-Asp) or hepatocellular cancer cells[152].

Recently, aptamers as a new class of potential targeting ligands have gained increased attention. Aptamers are short oligonucleotides consisting of ribonucleic acid (RNA) or desoxyribonucleic acid (DNA) that exhibit high binding affinities towards their intended targets, like e.g. cellular receptors or small molecules. They can be generated *in vitro* by the systematic evolution of ligands by exponential enrichment (SELEX) technique.[153, 154] While very low dissociation constants enable similar applications as with antibodies, aptamers can be designed to have superior properties like an increased stability and lower immunogenicity, and can be synthesized by means of solid phase synthesis.[155] Several aptamer systems have been shown to provide targeting properties to liposome systems, directed against the vasculature endothelial growth factor (VEGF), which controls vascularization in tumor tissue[156], against transferrin receptor, which is often overexpressed in cancer cells[157], or even against whole cell populations.[158]

Ligand-based, active targeting of liposomes has been applied to an immense variety of targets and with a versatile selection of ligands. It is yet discussed, that in many cases active targeting has not been able to outperform passive targeting, mainly due to low tissue penetration, low presentation of antigen, or low triggered release after uptake in the targeted cells.[165, 166] Also, the receptor density on the cell surface, which is heterogeneous between patients, strongly effects the targeting efficiency.[167] While these challenges illustrate the paramount importance of the selection of the right application case, the slow progress of clinical development in this context is mainly due to the vast complexicity of such multifunctional delivery vehicles. This underlines the need of effective routes for the immobilization of ligands on the vehicle surface, and a variation of strategies for this purpose is introduced in the following.

1.2 The attachment of ligands to liposomes

One of the most important challenges in the development of actively targeted drug delivery is the efficient and controlled chemical conjugation of ligands to the delivery vehicle. The past thirty years have seen the rapid development of various methods for the attachment of ligands, with the arguably most important approaches represented in Figure 1.5. Classically, ligands were modified with lipophilic or amphiphilic membrane anchors before the particle preparation, in order to facilitate stable surface attachment on the lipid vesicles. This strategy was applied in the majority of the abovementioned cases, while terminally functionalized phospholipid-PEG conjugates were frequently used as the particular membrane anchor.[168] However, the principle to add ligand conjugates *before* formulation causes certain limitations, as on the one hand, the ligands end up statistically distributed also on the inner membrane surface, and therefore inaccessible to the target structure. On the other hand, the attachment of large ligands like antibodies can significantly alter the formulation process and therefore the resulting liposome

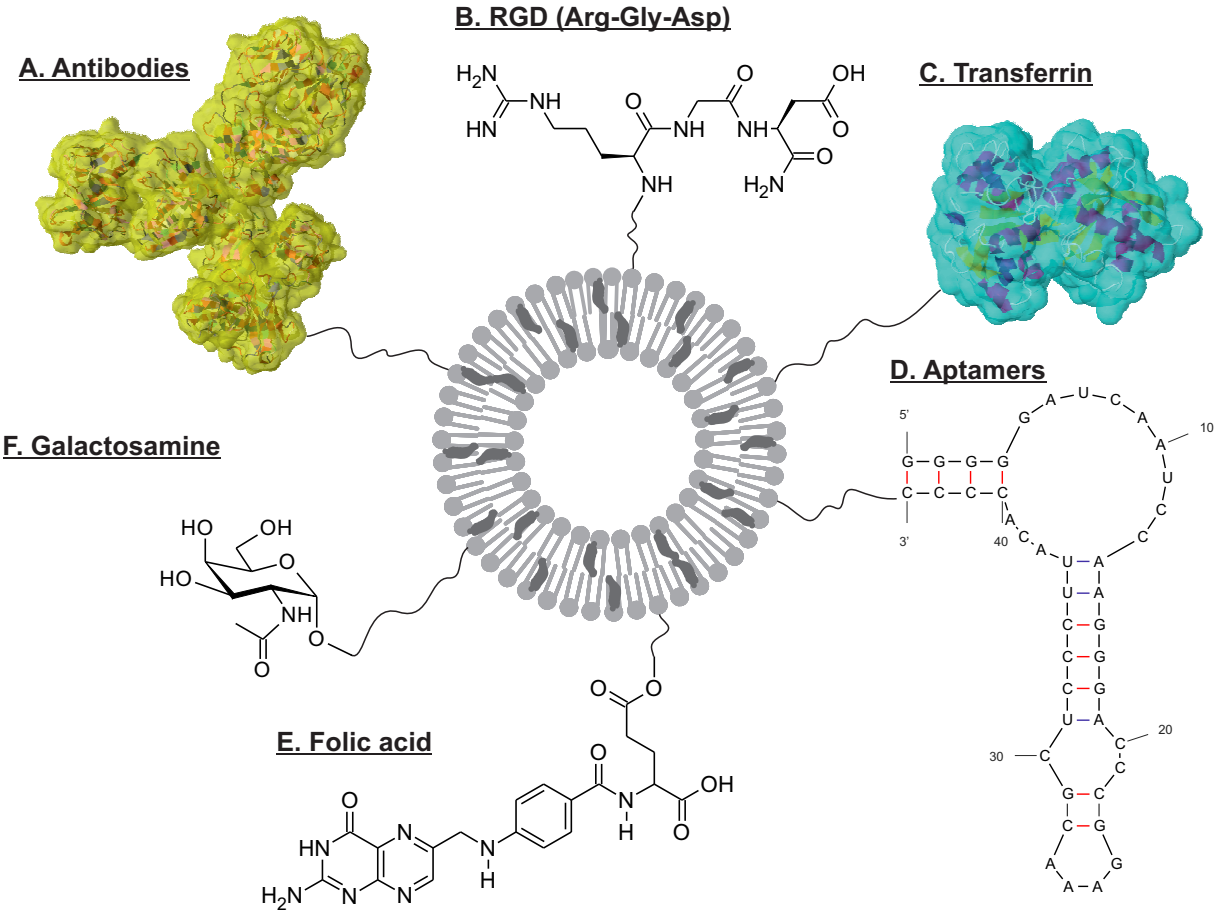

Figure 1.4: Ligands for active targeting of liposomes. A: Antibodies (Structure from PBD ID 1IGY [159]), B: RGD tripeptid as employed in [148], C: Transferrin (structure generated with Jmol[160] from PDB ID 1A8E[161] as obtained from the protein data bank[162]), D: Aptamers, c2.min aptamer against the transferrin receptor (structure predicted by mfold[163] from published sequence[157]), E: Folic acid as employed in [144], F: Galactosamine as a ligand for the liver-specific asialoglycoprotein receptor (ASGPR)[164].

properties. These problems can be overcome by the so called post-insertion technique (Figure 1.5B), were the ligand-functionalized amphiphile is added as a micellar solution to the pre-formed vesicles and readily inserts into the existing phospholipid membranes. Uster *et al.* first reported on the post-insertion of DSPE-PEG amphiphiles in 1996[169], and recent developments have led to a renewed interest in this method utilizing cholesterol-based amphiphiles as established by the Süss group (sterol-based post-insertion technique, SPIT).[91] Post-insertion also has been used to introduce the whole sterically stabilizing polymer shield to the liposome after formulation, which enabled the preparation of highly asymmetric distributions of polymers on the membrane surfaces.[170] However, challenges include the equally distributed, reproducible and efficient insertion of ligands, the leakage of payload during the insertion process and the removal of residual free amphiphile. Furthermore, a polymer-saturated surface has been shown to hinder efficient insertion.[170] Parts of these problems can be overcome by a third variant of ligand attachment, in which the liposome surface can be functionalized *after* formulation, as visualized in Figure 1.5C. This strategy was first applied by Heath *et al.* to immobilize horseradish peroxidase on the liposomal surface.[171] In this particular strategy, the ligand cannot influence the formulation process and is not distributed to the inner surface. However, due to inquantitative reaction, potentially unwanted conjugation sites on the surface can be preserved. Additionally, the ligand can only be conjugated to accessible acceptor sites.

Taken together, the selection of the right attachment strategy is of critical importance and has to be selected for the particular type of application, with each method comprising a different set of characteristics and advantages. In this thesis, mainly post-formulation conjugation has been applied, with a few examples of pre-formulation conjugation. The use of an appropriate conjugation chemistry is essential, and a few of such routes are introduced in the next section.

Conventional conjugation chemistry

Selective chemical conjugation is a commonly applied strategy for the synthesis of multifunctional (bio)molecules.[172] Several synthetical routes have also been applied to liposome surface conjugation, with the most important ones illustrated in Figure 1.6. Disulfide bonds are of paramount importance in proteins, as they allow for the intra- and intermolecular stabilization of protein folding. They can be formed from oxidation of two thiol groups, which enables the conjugation to cysteine residues in proteins. The highly biocompatible disulfide bridge was first used by Gregoriadis and coworkers for the attachment of antibody fragments to liposomes (Fig. 1.6B).[173] Another frequently used route for chemical conjugation of biomolecules is the reaction between hydrazines and aldehydes, that react to hydrazones (Fig. 1.6C). The first use of a hydrazine-modified biotin for the coupling to proteins has been reported by Heitzmann *et al.* in 1974,[174] and consequently, hydrazone coupling has in the following been applied

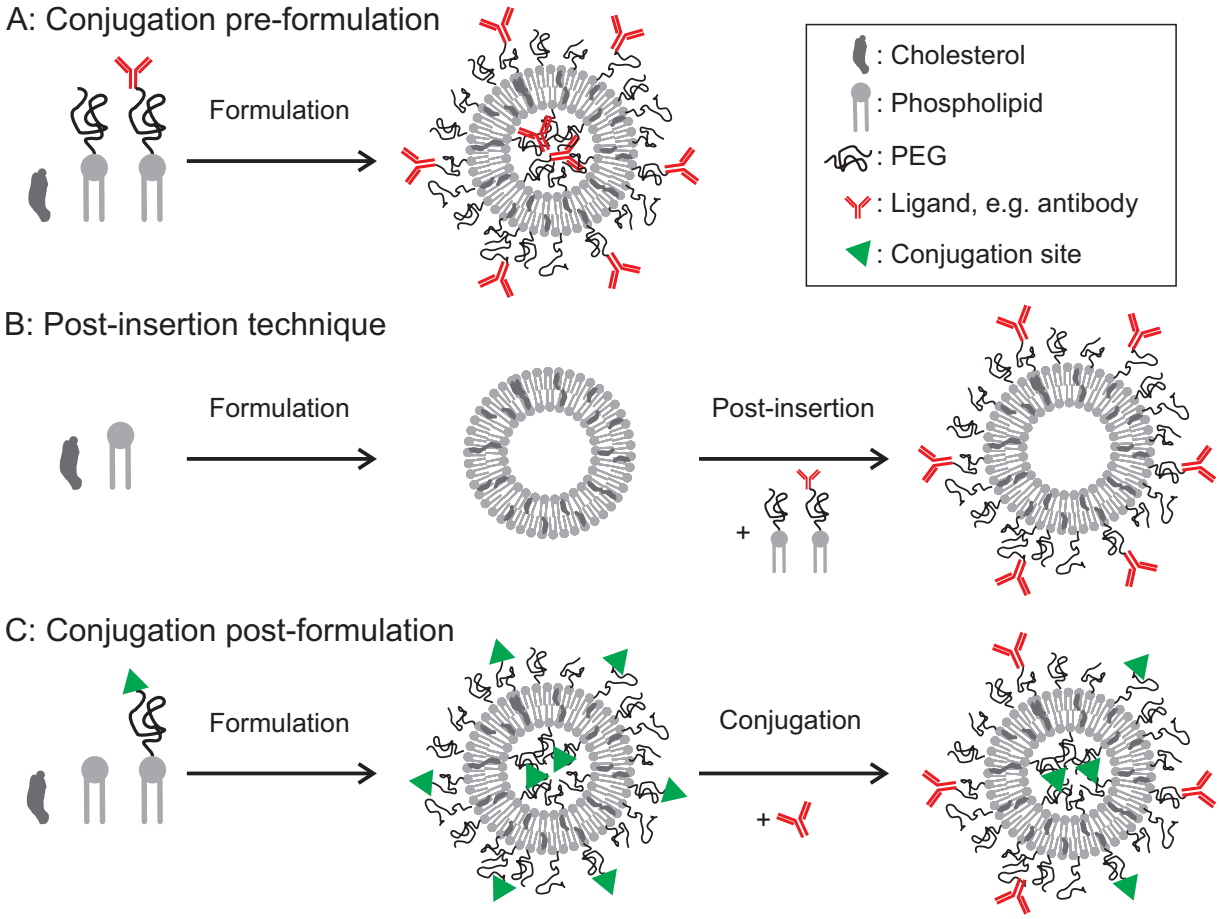

Figure 1.5: Methods for the attachment of ligands on the liposomal surface. The conventional approach comprises a conjugation of the ligand to amphiphiles before formulation, resulting in a distribution of the ligands on both membrane surfaces (A). The post-insertion technique involves the post-insertion of functionalized amphiphiles in pre-formed liposomes (B). Also the PEG-shielding can be introduced in this way, while only the outer surfaces are effected. In contrast, the use of functionalized amphiphiles enables the conjugation of ligands to the surface in a post-preparational approach (C).

for liposome surface conjugation in a broad variety of studies.[175, 176] An also widely utilized derivatization reaction is the MICHAEL addition between a maleimide and a free thiol group (Fig. 1.6D), which also has been used for the modification of peptides and proteins bearing free cysteine residues.[177] The well established maleimide coupling has been applied in many fields of research, as functional compounds that contain maleimide residues are nowadays readily commercially available. Papahadjopoulos and coworkers reported in 1982 for the first time on the utilization in liposome research, when they applied maleimide coupling for the immobilization of antibody fragments.[178] The reaction of primary amines with ester residues can be activated with N-hydroxysuccinimide (NHS, Fig. 1.6A), which yields a rather stable amide bond. Originally first applied for the determination of enzyme structures by crosslinking reactions free lysine residues,[179] the first application to liposomes has been used for the immobilization of antibodies.[168]

The mentioned coupling techniques represent only the arguably most widely applied routes for the chemical derivatization of liposomes, while a vast variety of conjugation methods have been described in literature, as recently reviewed by Nobs *et al.*[180] In the last 15 years, a novel class of conjugation reactions has gained outstanding attention, referred to as "click" reactions.

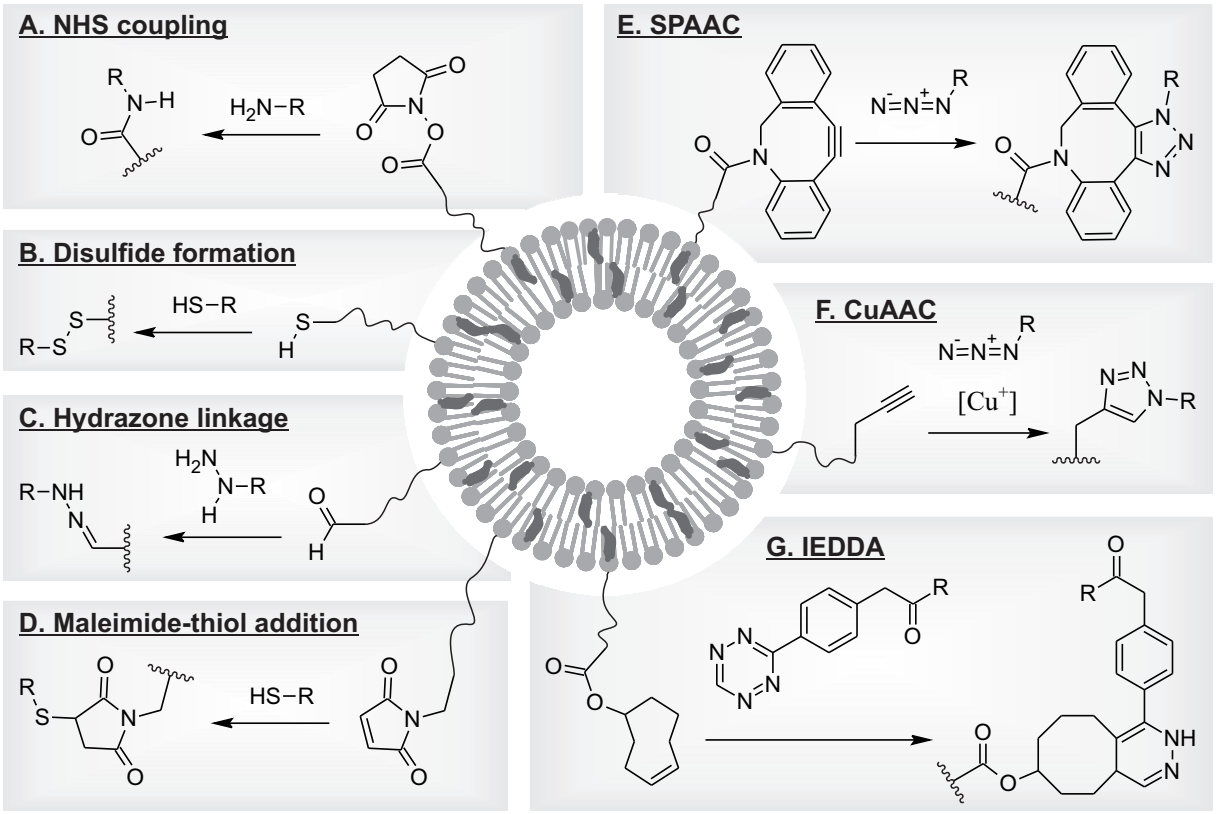

Figure 1.6: Conjugation reactions that have been applied to liposome modification, including conventional conjugation routes (A-D) and "click" reactions (E-G).

"Click" reactions

In 2001, inspired by the tendency of nature to preferentially form bonds between carbon and heteroatoms, Sharpless and coworkers proposed the definition of "click reactions" for a class of reactions that combine specific characteristics.[181] They envisaged a simplification of *how* the development of small molecular pharmaceutics can be performed with the help of this toolbox, to aim rather for functional than for structural novelty.[182] Reactions of the click reaction type have to fulfill a number of criteria, including very high yields, the absence of toxic byproducts, stereospecificity, no need for chromatographic purification and reactivity preferentially in aqueous media in presence of oxygen.[181] Furthermore, specific reactivity of the involved chemical residues enables bioorthogonal reactions, *i.e.* no reactivity towards reactive groups present in biological systems. In the past 15 years, the click chemistry concept has been applied to a broad field of topics, including also conjugation of biomolecules and nanoparticle derivatization.[182, 183, 184]

The reaction between terminal alkynes and azide compounds has evolved to arguably the most important reaction of the click type (Fig. 1.6F). First described by Huisgen in 1963,[185] a copper-catalyzed stereoselective variant was introduced by Sharpless and coworkers in 2002.[186] This copper-catalyzed alkyne azide cycloaddition (CuAAC) has been applied to liposomes in a few cases for post-preparational derivatization, including the coupling of sugar-based targeting ligands to liposomes,[187] or the analysis of coupling kinetics by colorimetric determination.[188] However, the presence of copper renders the bioorthogonality of CuAAC limited due to its cytotoxic potential.[189]

Another type of click-like reaction, a modified type of Staudinger ligation between azides and phosphines, was introduced by Bertozzi and coworkers for the selective labeling of cell-surface bound sugars.[190] This reaction was found to comprise an exceptional bioorthogonality, as it has also been applied inside living animals.[191] The first application to liposomes included the immobilization of sugar ligands on the vesicle surface.[192]

A copper-independent enhancement of CuAAC was first reported by Wittig and Krebs in 1961.[193] In this type of reaction, referred to as strain-promoted alkyne azide cycloaddition (SPAAC, Fig. 1.6E), the high ring strain of cyclic octynes acts as the driving force to facilitate a substantial reaction rate acceleration compared to uncatalyzed Huisgen reactions.[194] Bertozzi and coworkers have applied this principle to the modification of living cells, without the observance of toxic effects.[195] Only a few studies have applied SPAAC to liposomes, either for pretargeting approaches[196], or for surface derivatization[197].

Recently, another type of bioorthogonal conjugation reaction has gained increased attention, namely the inverse electron-demand Diels-Alder reaction (IEDDA, Fig. 1.6G) between electron-rich dieneophils and electron-poor dienes, in this case tetrazine compounds.[198, 199]

Blackman *et al.* envisaged the use of highly strained *trans*-cyclooctenes (TCO)for the use in IEDDA, which were shown to provide elevated reaction rates in biocompatible settings.[200] The to date only application of IEDDA in liposome research involved the intravenous injection of a tetrazine-labeled tumor-targeting peptide as a pretargeting approach, which resulted in an *in vivo* conjugation of subsequently administered TCO-modified liposomes at the target site.[201]

Recent development has revealed promising potential of the attachment of multiple receptor ligands, which has been shown to result in a cooperative increase in targeting efficiency.[202, 203, 204] Several of the mentioned reactions of the click type are also orthogonal with respect to other reactions, as they do not show any cross-reactivity, and which has been demonstrated for the labeling of *e.g.* DNA.[205] The only report of the site-selective double modification of liposomes was published by Salome *et al.* in 2015, who combined SPAAC and the reaction of a dibromomaleimide-lipid derivative as a MICHAEL-acceptor in a one pot reaction.[206] However, due to ubiquitous presence of thiol groups in biological systems, the *in vivo* application of these compounds is questionable. Residual maleimide moieties would have to be quantitatively converted, in order to prevent unspecific reactivity towards thiol groups in biologic environs. As a part of this thesis, CuAAC and IEDDA have been applied in post-preparative, one pot derivatization reactions to yield multifunctional liposomes.

1.3 Formulation Methods

Characterization of liposome properties

Liposomal formulations are characterized by a number of parameters, that allow for an estimation of their performance in the intended application. These properties are either depending on the particular formulation method or on the employed vesicle components, including payload or lipid composition.

The arguably most important property of liposomes for parenteral administration is their size and their size distribution, since tissue penetration, tissue distribution as well as blood circulation times are strongly dependent on the particle sizes. It has been shown that liposomes with diameters below 200 nm exhibit increased circulation times compared to larger vesicles.[207] Numerous analytical techniques are available for the assessment of size distributions, including dynamic light scattering (DLS), (cryo) transmission electron microscopy (TEM or cryoTEM) or size exclusion chromatography (SEC). Due to the availability of benchtop instruments, DLS is a widely applied analytical method, which allows to determine the diffusion coefficients from autocorrelated scattering intensities that are fluctuating due to the Brownian motion of the particles. From this data, hydrodynamic radii of the particles can be derived. The size dis-

tribution of particles is described by the fitting parameter $\mu_2/\bar{\Gamma}^2$, which is derived from the cumulants fit and also referred to as the polydispersity index (PDI).[208] Typically, PDI below 0.3 are rendering a liposomal formulation as suitable for pharmaceutical application.[209, 1] However, DLS is sensitive to particle aggregates and impurities, which requires a cautious interpretation of the obtained values.[210]

In contrast to conventional TEM, in CryoTEM, the evaporation of water is prevented by vitrification of aqueous samples and cryogenic sample handling. Therefore, cryoTEM allows for the analysis of liposomes in their native structure, while also the visual assessment of the lamellarity of liposomal particles is possible. Automated image analysis has been applied for the determination of size distributions.[211] However, elaborate sample preparation and excessive costs are hindering a routine application of this technique. Additionally, as a result of the sample preparation process, smaller particles were shown to occasionally be overrepresented in the obtained micrographs due to a relative enrichment in the thin, vitrified ice film.[212]

Fluorescence correlation spectroscopy (FCS) allows the analysis of fluorescently labeled liposomes. In contrast to DLS, where incident light is scattered and intensity fluctuations quantified, FCS relies on the autocorrelation of emitted fluorescence intensities and allows for the determination diffusion coefficients and therefore sizes.[213] Furthermore, the number of fluorophores per particle and the concentration of particles are accessible.

A rather novel technique is nanoparticle tracking analysis (NTA). For NTA, suspended particles are illuminated with a micrometer-thick laser light sheet and observed in an optical microscope. A video recording that displays the movement of particles within this light sheet is then analyzed by means of automated image analysis, in order to determine diffusion velocities and therefore the diffusion coefficients.[214, 215] Compared to DLS, NTA allows for a particle-wise analysis without the strong overrepresentation of large particles or aggregates.

Phosphatidylcholines are zwitterionic amphiphiles that exhibit no net charge. The use of amphiphiles that are charged, like the positively charged 1,2-dioleoyl-3-trimethylammonium-propane (DOTAP) or the negatively charged phosphatidylserine (PS) result in a non-neutral surface potential of the particles, which is also influenced by environmental properties like pH or dissolved salts.[216] This ζ-potential is typically measured by laser doppler spectroscopy during electrophoretic migration of particles, and has been shown to strongly influence the colloidal stability[217] and the *in vivo* fate of systemically administered liposome formulations.[218] Typically, highly positive or negative charges are known to minimize aggregation of particles due to repulsive forces, however, such particles tend to interact with biological material and therefore yield low systemic circulation times.[219]

A parameter which is defined rather by the particular method for liposome formulation is the encapsulation efficiency (EE). Encapsulations efficiencies also strongly depend on the employed cargo, since lipophilic compounds often readily integrate in the liposomal membrane

and achieve typically much higher EE than hydrophilic compounds.[32] The most widely applied method for EE determination of hydrophilic compounds includes the encapsulation of a water-soluble membrane-impermeant fluorophore inside liposomes, a removal of unencapsulated residue and a subsequent solubilization of the lipid particle, *e.g.* with a detergent like Triton-X. By quantification of the separated unencapsulated cargo and the successfully encapsulated cargo, the EE can be calculated as the encapsulated fraction of total cargo.

Formulation methods

In five decades of liposome research, numerous methods for the preparation of liposomes and the adjustment of their properties were developed. The first controlled method for liposome preparation, the lipid film rehydration technique, was initially described by Bangham in his report on the formation of vesicular structures upon hydration of a thin dried lipid film with aqueous media, as illustrated in Figure 1.7A.[3] Depending of the intensity of mixing of the two phases, the method yielded LUV, GUV and MLV in a rather uncontrolled process. The application of ultrasonication on such vesicular lipid suspensions was shown to homogenize these vesicle populations.[220] In 1979, Papahadjopoulos and coworkers reported on a method for the controlled adjustment of liposome sizes by extrusion through a porous filter membrane, as illustrated in Figure 1.7B.[221] By selecting the pore size, unilamellar lipid vesicles with narrow size distributions have been prepared with specific control over the resulting size.[222] Enabled by the abovementioned remote loading technique as used *e.g.* for DOXIL, membrane extrusion has evolved to the most important method to control liposome size for the manufacturing of pharmaceutic liposome formulations.[223]

Other techniques utilize the removal or dilution of organic solvent. After emulsification of diethyl ether-dissolved lipids in aqueous media, the evaporation of organic solvent was shown to yield well defined liposome formulations.[224] In contrast to film hydration methods, the reverse phase evaporation technique has been shown to efficiently encapsulate aqueous content. In a similar approach, the dilution of ethanolic lipid solutions has been utilized to form vesicular structures upon injection in aqueous buffer.[225] This ethanol injection technique is visualized in Figure 1.7C.

The mentioned formulation methods allow either to prepare vesicles with narrow size distributions (by extrusion), or vesicles with high encapsulation efficiencies of aqueous cargo (by reverse phase evaporation). A method to overcome these limitations is high pressure homogenization (HPH), which was first reported by Mayhew *et al.* for the preparation of phospholipid vesicles.[226] Typical formulation conditions under application of a benchtop homogenizer include homogenization at pressures of 15 MPa, which was reported to yield SUV in the range of 50 nm in diameter.[227] HPH has been shown to yield high encapsulation efficien-

cies for aqueous cargo of up to 45% , that were shown to be dependent on the used lipid concentration.[228] However, modern high pressure membrane extrusion systems also allow for similar encapsulation efficiencies in the range of 20-40%.[229]

Recent advances on the field of microfluidic mixing have led to the application of static microchannel mixers for the preparation of lipid nanoparticles.[230] Cullis and coworkers reported on the preparation of limit size solid nanoparticles by subjecting an aqueous acidic solution of nucleic acids and an ethanolic solution of cationic lipids to millisecond microfluidic mixing .[231] Although originally developed for these solid nucleic acid lipid particles (SNALP), also liposomal vesicles were shown to be accessible with this technique.[232, 233] However, while size distributions were relatively well defined, high encapsulation efficiencies were only achieved with lipophilic payloads.

Dual centrifugation has emerged as a novel method for liposome preparation within the last couple of years, and as it was extensively used in this work, it is introduced in the subsequent section.

Liposome formulation by dual centrifugation

Since its development by Massing *et al.* in 2008[1], dual centrifugation (DC, also referred to as dual asymmetric centrifugation, DAC) emerged to a valuable method for the formulation of liposomes. The basic principle of dual centrifugation is visualized in Figure 1.7D. The main difference to a conventional centrifuge is the presence of a second rotational axis, which is aligned in a certain angle to the main rotational axis and rotates counterwise to the main axis. Inside this secondary rotor, an inset holds the centrifugation vials in place, which leads to the exposure of the lipid samples to intense shear forces. These shear forces originate from the acceleration of the material, as caused by the main rotation, towards the wall of the container, while the wall of the container itself moves relatively to the material content inside the container. These shear forces rely on a certain viscosity of the samples, which is why the method requires appropriate lipid concentrations. The supplementation of a milling aid, *i.e.* glass or ceramic beads, was found to increase the energy input and led to a more intense homogenization.[1] For a DC-based formulation, lipids and aqueous media, typically a solution of the intended cargo, are combined in centrifugation vials and subjected to a DC run, which yields a highly concentrated vesicular phospholipid gel (VPG). VPG are also known to form upon high pressure homogenization of lipids, and can be diluted in a second and shorter DC run to finally yield liposomes.

Dual centrifugation comprises, in comparison to abovementioned liposome formulation methods, several valuable advantages. First, EE for hydrophilic cargo of up to 80% were demonstrated for highly valuable cargo as siRNA.[234, 235] These values for the loading efficiency

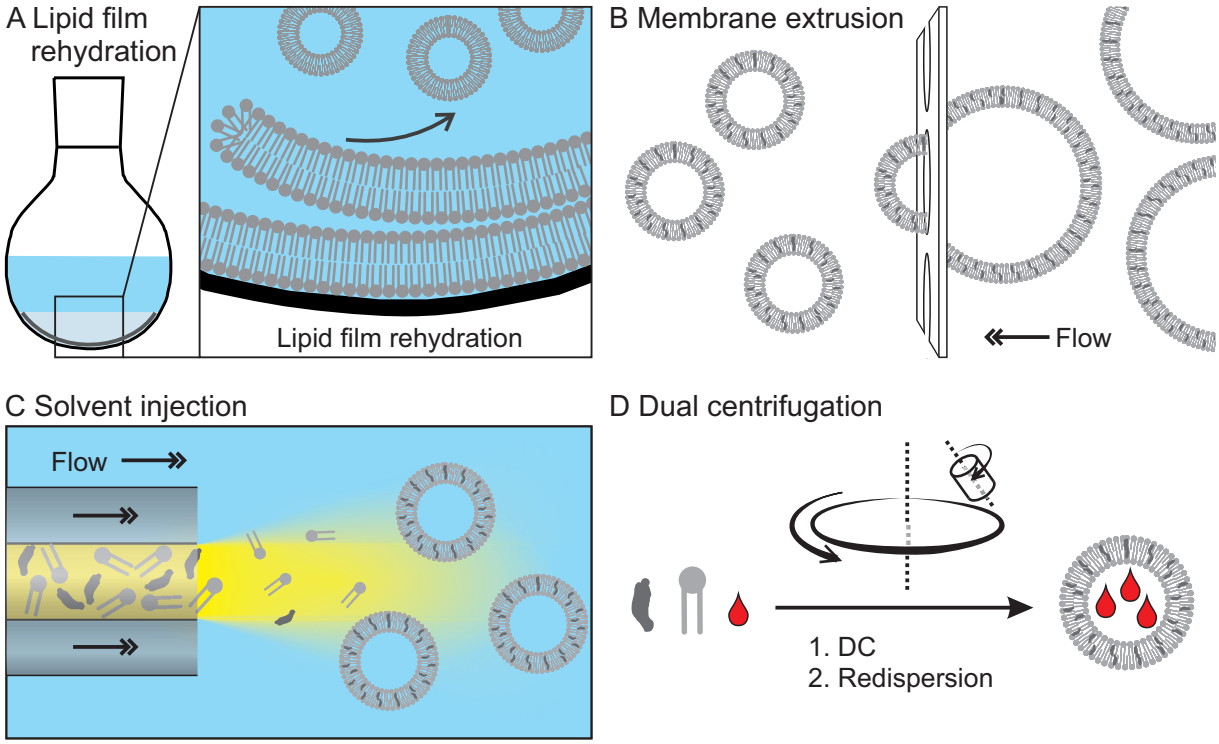

Figure 1.7: Methods for liposome formulation, including lipid film rehydration (A), membrane extrusion to tune the sizes of liposomes (B), solvent injection of organic solutions (yellow) of lipids into in aqueous media (C) and the schematic principle of dual centrifugation (D), bearing two rotational axes, rotating counterwise and oriented in a certain angle.

are very high, compared to the often applied membrane extrusion method, which typically yields EE in the single digit percent range.[30] Second, DC allows for the liposome preparation in a vast range of batch sizes, which was demonstrated in the milligram- to gram-range.[1] This characteristic enables both the laboratory-scale formulation of valuable compounds, as well as formulation of larger batches, *e.g.* for preclinical testing. Furthermore, sealed reaction vials can be used and do not have to be opened during preparation, which allows for convenient preservation of sterility without the need for post-preparational sterilization or elaborate cleaning of equipment, *i.e.* the extrusion apparatus. In addition, the energy intake is lower compared to HPH, which results in a gentler handling of the sample and can be expected to be beneficial for sensitive payloads like peptides. As a proof of milder formulation conditions, DC was also shown to cause a decreased hydrolysis of phospholipids compared to HPH-treated samples.[1] Lastly, since a dual centrifuge typically is a benchtop instrument, neither special training nor expensive instrumentation is needed for the formulation, which is contrary to extrusion or HPH.

Besides the already mentioned reports, a considerable amount of literature has investigated the application of dual centrifugation in a variety of research fields. Adrian *et al.* reported on the delivery to neuroblastoma cells with siRNA-GD2-liposomes, that were ligand-functionalized *via* the post insertion technique.[236] The Fricker group demonstrated the improvement of the oral bioavailability of peptides, that were formulated in liposomes by dual centrifugation.[237] In both cases, the high encapsulation efficiencies virtually enabled the use of siRNA and peptides. Raynor *et al.* used DC for the formulation of liposomes in order to supplement phospholipids during *in vivo* experiments.[238] The use of DC-prepared liposomes as matrices for the intravesicular crosslinking was shown to yield hydrogel particles in the same size range, as was shown by Pohlit *et al.*[239] In this particular contribution, the necessary efficient inclusion of PEG building blocks inside the vesicles was enabled by DC. Recently, the Fricker group reported on the formulation of liposomes that were conjugated to cationized bovine serum albumin, and readily taken up in the central nervous system.[240]

Also, a number of researchers have examined the application of vesicular phospholipid gels which were prepared *via* dual centrifugation.[241, 242, 243, 244] Here, the investigators benefited from the fact that the instrumental demands are substantially lower compared to high pressure homogenization, which renders DC a promising method for the preparation of VPG. Furthermore, the Brandl group reported on the use of dual centrifugation beyond liposome preparation, as they applied DC for the disintegration of cells in order to extract membrane-located lipids from such.[245] Collectively, these studies outline the effectiveness and solidity of dual centrifugation for the preparation of lipid vesicles and other applications, representing a promising platform which is yet to be further evolved.

1.4 Self-assembled polymeric particles

Thirty years after their initial description by Alec Bangham, with the liposomal doxorubicin formulation DOXIL, the first nanoparticulate drug was approved for clinical application. Motivated by this breakthrough of clinical nanotherapy, the past thirty years have also seen increasingly rapid advances in the field of polymeric nanoparticles for the application in drug delivery. Besides the direct polymerization of monomers to yield nano-scaled particles, *e.g.* *via* emulsion polymerization techniques,[246] the use of preformed polymers allows for the preparation of solid particles or core-shell particles that contain a hydrophilic or lipophilic interior.[247] To achieve control over particle sizes and encapsulation, numerous formulation methods have been developed, including solvent evaporation[248], nanoprecipitation[249] or solvent exchange *via* dialysis[250]. A substantial number of these methods utilize a dispersion of an organic polymer solution in aqueous media and therefore rely on the use of surfactants to stabilize the prepared colloids. While the subsequent removal of such stabilizers is often difficult, it is critical for biological applications, as *e.g.* severe side effects are connected to the *parenteral* administration of surfactants to humans.[251]

As a way to overcome these problems, particle systems have been developed that intrinsically comprise colloidal stabilization, *i.e.* particle systems that are based on amphiphilic polymers. Such diblock copolymers can form either micellar or vesicular particle structures, depending on the architecture and characteristics of their polymer blocks.[252] This tendency is to a certain extend determined by the mass fraction of the lipophilic block *f*, which was shown to typically range between 0.25 and 0.4 for polymer vesicles and above 0.5 for micelles.[252] Figures 1.8 A and B illustrate the structure of polymersomes and polymer vesicles, respectively.

Micellar particle systems readily form in aqueous media and are capable of encapsulating lipophilic cargo.[253] Numerous attempts have been made to investigate the encapsulation of pharmaceutically active compounds in polymeric micelles, with several of them being currently

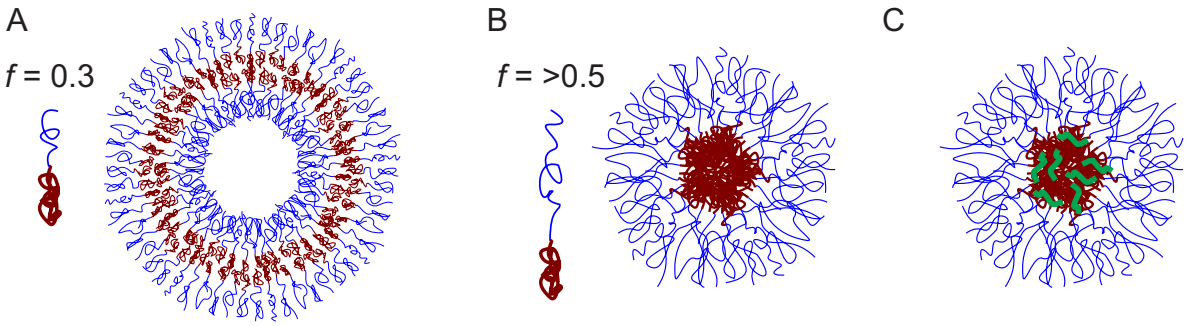

Figure 1.8: Self-assembled polymer nanoparticles. The mass fraction of the lipophilic block determines whether polymersomes (A) or polymeric micelles (B) are formed. One way to stabilize polymer micelles is the crosslinking of the lipophilic core (C).

under clinical investigation.[254] Micellar structures are typically prone to solubilization upon dilution below the critical micelle concentration (CMC) of their building blocks, which has led to the development of stabilization techniques like core crosslinking (Fig. 1.8C).[255] Polymeric micelles can be prepared with diameters between 10 and 100 nm, and these sizes allow for efficient tissue penetration and enrichment *via* the EPR effect.[253]

Vesicular self-assembled polymer particles, also referred to as polymersomes, are under current investigation regarding their suitability for drug delivery applications.[256, 257] The first concept of polymersomes was reported by Discher *et al*. in 1999, who utilized polyethyleneoxide-polyethylethylene block copolymers for vesicle formation.[258] Polymersomes overcome the inability of polymeric micelles to encapsulate hydrophilic cargo within their aqueous core, rendering polymersomes as nanoparticles with similar properties as liposomes. However, by selection of suitable polymer systems, polymersomes can be designed to outperform liposomes regarding their mechanical stability, shelf-life and membrane impermeability.[252]

Amphiphilic diblock copolymers for the preparation of micelles or polymersomes can be prepared from various polymer systems, including PEG, polyacrylic acid (PAA)[259], poly- (N-(2-hydroxypropyl)methacrylamide) (pHPMA)[260], poly(vinyl pyrrolidone) (PVP)[261] or polysarcosine[262] as hydrophilic building blocks. Polyethylethylene (pEE), polystyrene (PS)[259], polylactic acid (PLA)[261] and polylauryl methacrylate (pLMA)[263] have been shown to be suitable lipophilic building blocks for self-assembled polymer particles. Taken together, a vast parameter space has to be navigated for the rational design of such systems. While typical methods for self-aggregation of polymer particles are often time-consuming and provide low yields, a first approach for the formulation *via* dual centrifugation was investigated in the present work.

2 Motivation and Objectives

Microscale formulation of liposomes *via* dual centrifugation The development of novel liposomal systems with classic formulation methods is typically hindered by factors like availability of prototype amphiphile compounds or time-consuming formulation procedures. Especially regarding rare model polymer building blocks with elaborate functionalities, small scale syntheses are often favorable. Additionally, the systematic investigation of structure-function relationships is simplified by small laboratory-scale syntheses, which allow for a higher number of structural variations of polymeric amphiphiles. Since its development in 2008 by Massing *et al.*,[1] dual centrifugation has established itself as a tool which enables highly efficient encapsulation of valuable cargo, while only small amounts of lipids are needed. However, in typical experiments, stabilizing polymeric amphiphiles are still incorporated in amounts in the order of milligrams, limiting the number of experiments per synthesis. Also, regarding the investigation of non-lipid particles, a batch size of single-digit milligram amounts is highly beneficial. The decrease of the batch size of DC-based liposome formulation down to the single-digit milligram range is therefore expected to enable the use of *e.g.* block copolymer compounds for the preparation of polymersomes. Simultaneously, valuable polymer amphiphiles can be conserved in the case of sterically stabilized liposomes. The aim of this initial subproject has therefore been the batch size reduction of DC-based formulation and the investigation of resulting effects on liposome formulation, as reported on in Section 3.1.

***In vitro* interaction of poly(glycerol)-shielded, functionalized liposomes** Sterically stabilized liposomes typically utilize conjugates of hydrophilic polymers such as PEG and lipid anchors, such as DSPE or cholesterol, to provide an inert and hydrophilic layer on the surface of the nanoparticle. While steric stabilization is intended to prevent unspecific interaction with biological systems, previous investigations in this group revealed unexpected effects when a new class of polymeric amphiphiles based on cholesterol and poly(glycerol) were investigated.[2] While a pronounced interaction with cellular membranes has been observed *in vitro*, the origin of these effects remained ambiguous and encouraged further investigations. The objective of this subproject was therefore to establish a structure-function relationship for these novel amphiphile compounds and to assess the mechanistic background of their *in vitro* interaction, which is described in Section 3.2.

Orthogonal functionalization of liposomes: multifunctional carriers Fast and efficient ligand conjugation methods are crucial tools for the design, investigation and application of ligand-targeted drug delivery vehicles. In previous work, one of the most prominent conjugation reactions of the "click" type, namely CuAAC, has been used for the successful surface modification of liposomes.[264] After having established the basic principles of IEDDA as yet another type of biocompatible reaction recently,[265] the major goal of this subproject has been to investigate the resulting effects on the *in vitro* interaction with cells, especially regarding a variety of available polymeric amphiphile structures and anchorages. Furthermore, another aim was to evaluate the use of folic acid as a targeting ligand in the context of the particular amphiphile structure, in order to deduce implications on multifunctional vehicles for directed drug delivery in general. Results from these investigations are detailed in Section 3.3.

Acidic shedding of liposomal particles While sterically stabilized liposomes are known to achieve longer *in vivo* circulation times and higher passive tumor targeting compared to conventional liposomes, the inert PEG shielding comprises the disadvantage to inhibit interaction with cells after their arrival at the target tissue. This problem can be overcome with polymeric amphiphiles that allow for a stimulus-dependent cleavage of their polymer structure, *e.g.* by pH, oxidation or light absorption. The Frey group (Mainz, Germany) reported recently on a concept to incorporate acid cleavable units within PEGs,[110] that allow for potential application in the polymer shell of liposomal structures. The major objective of this subproject was to determine the applicability of this new class of cleavable polymeric amphiphiles for sterical stabilization of liposomes, as well as the development of analytical methods for the assessment of cleavage kinetics. Section 3.4 describes investigations on liposomal formulations that included such structures.

Application of microscale dual centrifugation to non-lipid particles Self-aggregated nanoparticles have evolved to highly promising candidate systems for directed drug delivery. However, formulation methods like mini-emulsion or solvent exchange are often involving the undesired use of surfactants, they result in low yields and sometimes are highly time-consuming due to subsequent purification steps, i.e. dialysis. After the refinement of dual centrifugation for the use with batch sizes in the milligram scale, the aim of this subproject was to perform proof-of-principle studies with different kinds of self-assembling nanoparticle systems. Section 3.5 reports on the application of a variety of systems, with focus on polymersomes from a cooperation with the Zentel group (Mainz, Germany).

3 Results and Discussion

3.1 Microscale formulation of liposomes *via* dual centrifugation

Abstract Dual centrifugation is known to be an efficient formulation method for liposomes in small scales.[1, 234] However, the investigation of composition-dependent effects in formulations involving prototype lipid compounds is still demanding larger amounts of amphiphiles, which are not always available. Here, an approach to scale-down the DC formulation has been investigated for liposome preparation, which allowed to a decrease of batch sizes by an order of magnitude to the single-digit milligram scale. A custom-made DC inset for PCR-vials enabled reproducible sizes and size distributions down to the level of 350 µg total lipid. Microscale formulation therefore crucially enables the systematic investigation of novel polymeric amphiphiles.

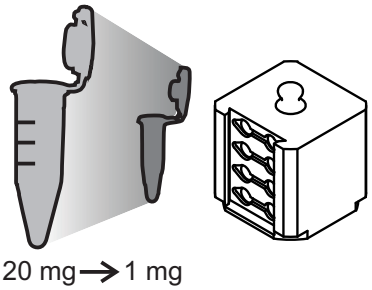

The formulation of liposomal particles *via* dual centrifugation represented the basis of the investigations described in this thesis. Section 1.3 presented an overview on typical formulation techniques and the decent advantages of DC in this context. However, in order to increase the applicability of this formulation method for the investigation of formulations of novel polymeric amphiphiles, the decrease of the necessary batch size has been the aim of the work described in this section. Liposomes were prepared from egg phosphatidylcholine (EPC) and cholesterol, and encapsulated sulforhodamine B (SRB) as a polar tracker of the aqueous content, to evaluate the encapsulation efficiencies throughout the process. Furthermore, as an

Parts of this chapter were a contribution to the Meeting of the Controlled Release Society 2015 on 24th - 29th July 2016, Edinburgh, United Kingdom.[266] Parts of the experiments were performed by Vladislava Schulz during an internship.

commercially available example of a polymeric amphiphile which is also used in clinical application, 1,2-distearoyl-sn-glycero-3-phosphoethanolamine-N-[methoxy(polyethylene glycol)-2000] (DSPE-mPEG2000) was incorporated. The structures of the involved components are shown in Figure3.1.

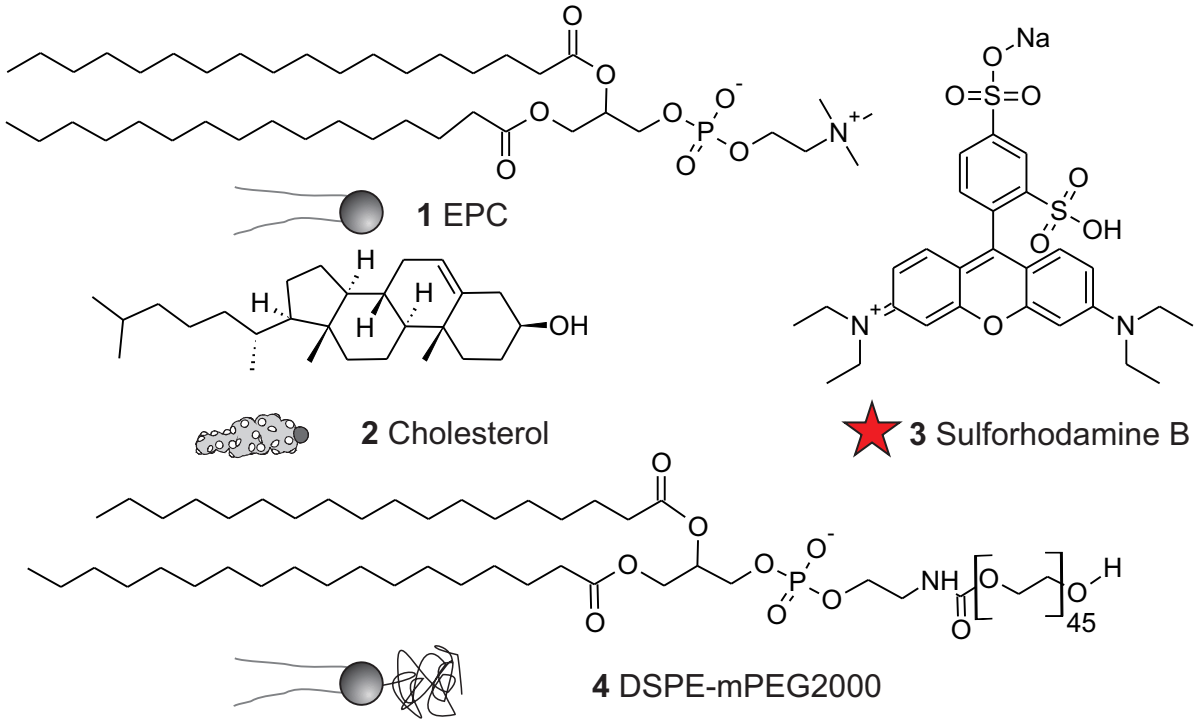

Figure 3.1: Structures of compounds used in this study. Formula **1** shows main species in the used fraction of egg phosphatidylcholine from Lipoid (EPC3).

Liposomes were prepared according to a standard protocol based on previous work,[1, 2] and detailed in Section 5.2. Figure 3.2 illustrates the schematic workflow to yield liposomes *via* dual centrifugation. After all solvent residues from the lipid stocks were removed, the first step was the preparation of a vesicular phospholipid gel (VPG) with only a small volume of aqueous buffer containing the intended cargo and during a rather long DC run of 20 minutes. The VPG was then diluted (redispergated) with additional buffer in another shorter DC run which resulted in the generation of liposomes.

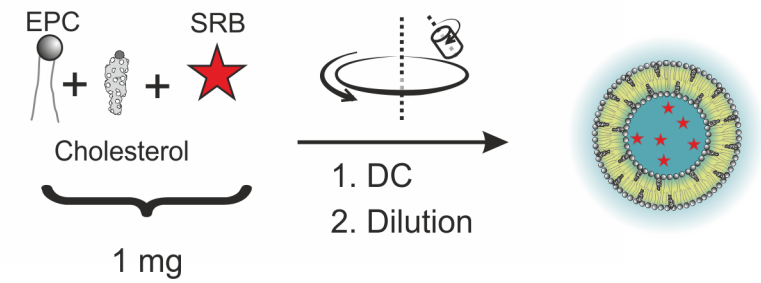

Figure 3.2: Scheme of microscale liposome formulation with dual centrifugation. Small amounts of lipids (down to 350 µg) were combined with SRB as a cargo and subjected to DC runs. Dilution of vesicular phospholipid gels result in liposome suspensions.

As a comparative reference, conventional liposomes (CL) were prepared only from cholesterol and EPC with the abovementioned standard protocol, while for sterically stabilized liposomes (SSL), 5mol% of EPC were substituted with DSPE-mPEG2000. The lipid compositions, resulted sizes, size distributions (from dynamic light scattering) and encapsulation efficiencies are listed in Table 3.1. To this end, the standard protocol involved the use of 17.5 mg of total lipids for CL, and a slightly higher total mass for SSL with the same molar amount.

Table 3.1: Characteristics of CL and SSL (± SD from three measurements)

	$\chi_{EPC} : \chi_{Chol} : \chi_{DSPE-mPEG2k}$	Size (nm)	PDI	EE (%)
CL	55:45:0	174.6 ± 7.3	0.238 ± 0.053	56.6 ± 4.8
SSL	50:45:5	127.3 ± 2.4	0.095 ± 0.016	45.8 ± 5.5

Sizes and size distributions were found to be in good agreement with previously obtained results, and are therefore presenting a good reference for the investigation of variations of formulation parameters. Encapsulation efficiencies were found in the expected range of approximately 50%. While the decrease of the total lipid amount was the main motivation of this work, the influence of the total batch size was next evaluated.

Evaluation of formulation parameters

As a first approach for scaling down the batch size of the liposomal formulation, the amount of lipids was reduced in steps down to 350 µg. In the only systematic investigation available, Massing *et al.* described an independence of liposome characteristics on the batch size, which was investigated in the range between 250 - 3710 mg.[1] In comparison to their results, the approach employed here provides in general larger vesicles, possibly due to the lower batch size or the orientation of the container in the DC inset (here: horizontal, vs. vertical). Figure 3.3 presents the resulting sizes from a variation of the total batch size (batch size = lipid mass +

buffer mass). The lipid concentration was kept constant at 35% m/m, the mass of the ceramic beads that were added as a milling aid was kept constant at 500% of the batch size. One can observe the general trend, that formulation below 2.5 mg total mass resulted in increased sizes and size distributions. Nevertheless, it was expected that the encapsulation efficiency was only dependent on the lipid concentration within the VPG, and was therefore expected to be constant throughout this experiment. This was also in good agreement with the obtained data. The influence on liposome size and size distribution was presumably due to the total amount of solid matter being insufficient to ensure proper homogenization throughout the centrifugation run.

An adequate homogenization of lipids in order to yield a vesicular phospholipid gel has been shown to require a certain minimum viscosity.[1] Since previous studies only investigated significantly larger amounts of lipids (500 mg), the lipid concentration was assessed as an additional parameter of the formulation process. Figure 3.4 A illustrates the effect, that high lipid concentrations above 60% (m/m) resulted in imperfect homogenization and therefore to non-applicable formulations. Interestingly, the sizes and size distributions did not alter towards lower concentrations, which would have been expected from the requirement of a certain minimum viscosity. However, Figure 3.4 B shows the positive correlation between lipid concentration and encapsulation efficiency, and following from this, very low EE for the lower lipid concentrations. Low encapsulation efficiencies in the range of 70-80% of lipid concentration can be explained by residual, inadequately homogenized lipid material which might have been caused by incomplete hydration. It was expected, that during the redispergation step, parts of the insufficiently formulated cargo was not encapsulated in vesicles, but rather was directly diluted in the extravesicular buffer. Sterically stabilized liposomes showed in general the same trends as shown in Figure 3.4 for CL (data not shown).

In total, a first approach to decrease the amount of lipids below 5 mg yielded promising results, while very low amounts led presumably to imperfect homogenization and with that to broad size distributions. To solve this problem, the influence of a smaller sized milling aid was subsequently tested, as well as smaller sized sample vials. These investigations are described in the following sections.

Design of a dual centrifuge PCR-vial inset

Abovementioned formulation experiments were carried out in the routinely used screw-capped reaction vials with volumes of 650 µL. Since a distribution of just a few microliters of liposome suspension throughout this type of vial was suspected to lead to problems during homogenization, an approach to make use of PCR-sized reaction vials with a volume of 200 µL was pursued. A first attempt with an improvisational mount for the standard vial centrifuge inset

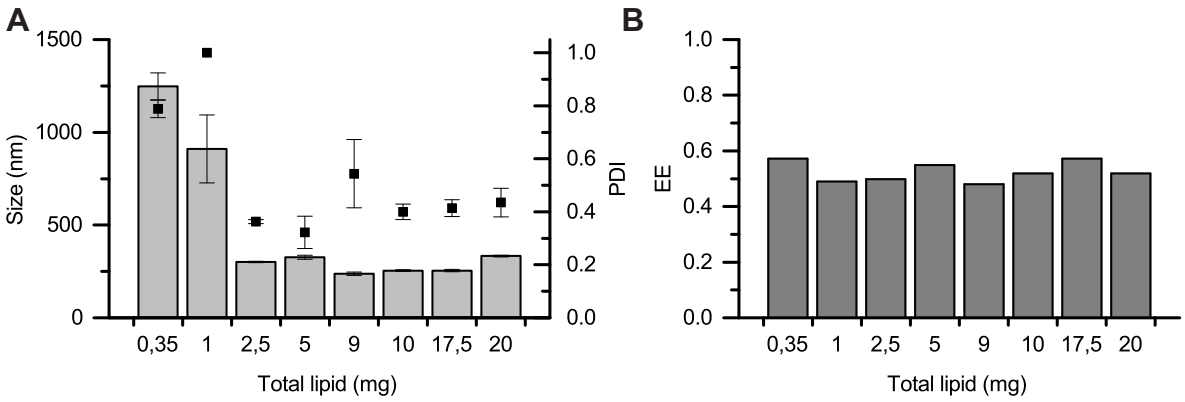

Figure 3.3: Conventional liposomes formulated in different batch sizes. A: Diameters (Columns, left axis) and PDI (squares, right axis) from DLS measurements (± SD from three measurements from same sample). Low lipid amounts yield large and inhomogeneous vesicle populations. B: Encapsulation efficiencies are constant throughout the measurement.

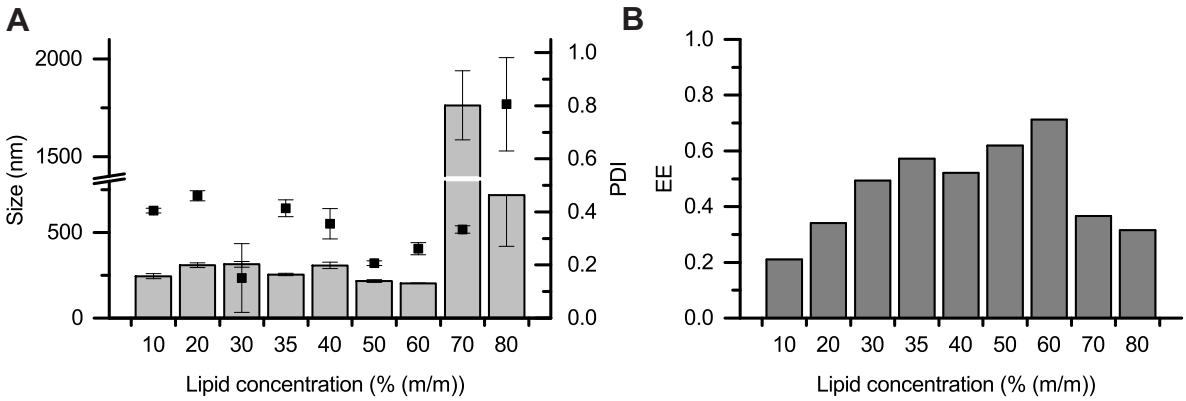

Figure 3.4: Conventional liposomes formulated with different lipid concentrations in the total batch size of 50 mg. A: Diameters (Columns, left axis) and PDI (squares, right axis) from DLS measurements (± SD from three measurements from same sample). Highest lipid concentrations yield large and inhomogeneous vesicle populations. B: Encapsulation efficiencies correlate well with the mass fraction of lipids, above 60% purification was impeded by high sample viscosity.

led to poor reproducibility. Therefore, an optimized sample inset was designed, which allowed for the simultaneous formulation of eight 200 µL sample vials. The design of the sample holder is visualized in Figure 3.5, schematic details and dimensions are listed in the Appendix 1. Furthermore, the occasional loss of sample volume emphasized the importance of structural stability of the used sample vials (as e.g. thicker walls and a tightly closing cap), which led to the use of vials from Kisker Biotech as detailed in Chapter 5. A 3D-printed version of this DC inset was used in the following and in experiments described in the Sections 3.3, 3.4 and 3.5.

Microliter scale formulation

With the custom made PCR-vial inset, which enabled the gentle handling of small volume sample tubes, the influence of tube size and smaller milling aid was systematically investigated. Prior standard protocol involved the use of SiLiBeads ZY® in a size range of 0.6-0.8 mm. These ceramic beads are made of a special zirconium oxide ceramic, stabilized with yttrium, which imparts a high durability to the grinding and milling media with a very low chance to contaminate the sample with ceramic particles. In order to improve the intensity of homogenization, SiLiBeads ZY® in a size range of 0.3-0.4 mm were investigated in a comparative analysis. Figure 3.6 summarizes the results from this study, illustrating the ability to prepare liposomes from sub-milligram lipid amounts by making use of 200 µL vials. The use of 200 µL vials yielded liposome formulations with nearly constant properties throughout all investigated batch sizes. Interestingly, the container size seemed to have an important influence on the ability to efficiently homogenize the sample, as the samples formulated in standard 650 µL vials showed increased sizes and broader size distributions when the lipid mass was decreased below 5 mg of total lipid. This is in general consistence with earlier reports, which concluded that the size of the milling aid is of marginal importance.[1] Additionally, the results indicate again, that the encapsulation efficiency was only dependent on the lipid concentration that

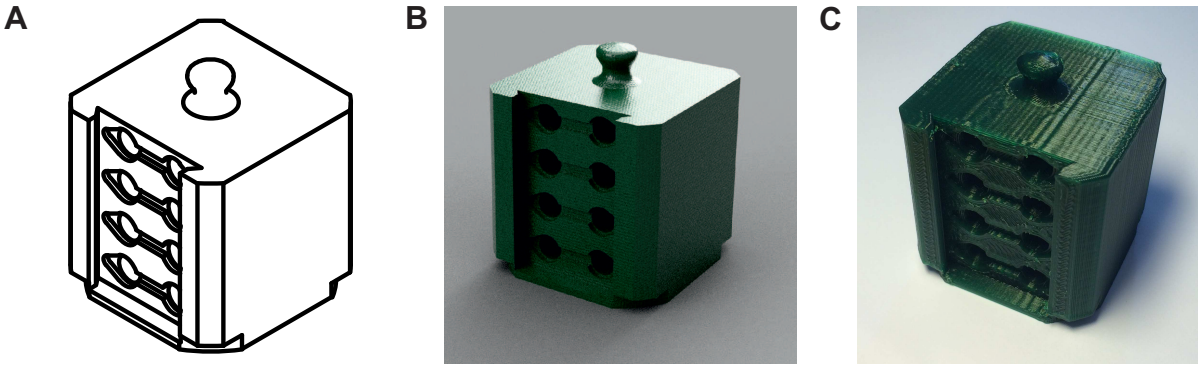

Figure 3.5: The designed sample holder for microscale formulation in PCR vials at three stages of development: A: Drawing of design, B: Rendering of final model, C: Photograph of printed model.

was used to prepare the VPG.

The standard 50 mg batch sizes, which contained approximately 17.5 mg lipids, already enabled the very efficient investigation of liposomal formulations incorporating rare prototype amphiphiles. In this study, the batch size for this method was successfully scaled down more than an order of magnitude while maintaining parameters like size, size distribution and encapsulation efficiency. In a typical preparation in standard batch size for SSL as listed in Table 3.1, one batch incorporated ~4 mg of polymeric amphiphile. A typical laboratory-scale synthesis of polymers as used in the following chapters can be expected to yield 80-100 mg of product, allowing for only ~20 batches to be prepared. It is obvious, that even with the *larger* 5 mg batch sizes, the shrunken formulation setting essentially enables the in-depth characterization of such compounds. Whenever a screening of a parameter space is necessary, the optimized method can save valuable compounds.

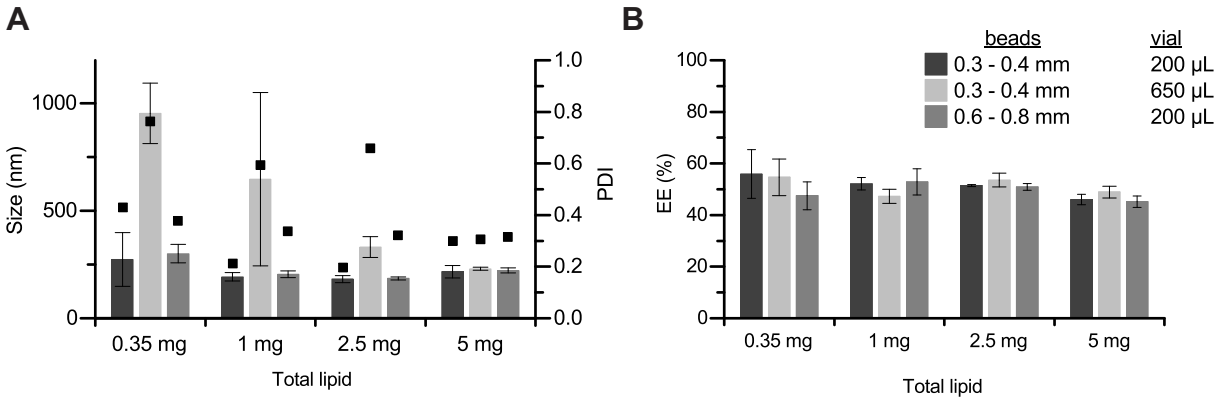

Figure 3.6: Liposomes prepared with the new centrifuge inset in PCR vials with 0.3-0.4 mm ceramic beads compared to preparation in conventional 1.5 mL vials and with original 0.6-0.8 mm beads. A: Sizes and size distributions are in an applicable range for formulations prepared in PCR vials. Larger vials lead to inhomogeneous samples and aggregates. B: Encapsulation efficiencies are constant throughout the measurement (Errorbars represent ±SD from three measurements).

3.2 In vitro interaction of poly(glycerol)-shielded, functionalized liposomes

Abstract Functionalized liposomes are of high interest as drug delivery vehicles, while the *in vitro* fate of amphiphile conjugates often remains unelucidated. Here, small scale liposome preparation with the post-preparational derivatization via CuAAC has been applied as previously established,[2] to study the mode of interaction of a novel class of polymeric amphiphiles based on cholesterol and hydrophilic polyether blocks. Cell incubation revealed a fast and intense membrane staining, which indicated exchange processes to the biological membrane during incubation. These findings suggested strong implications on the use of such compounds as anchors for targeting ligands.

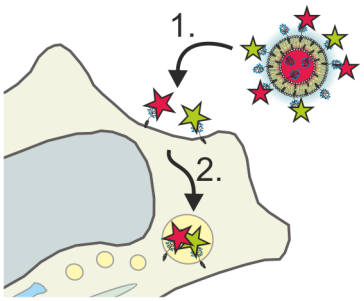

The synthesis of a new class of polymeric amphiphiles has recently been established by the Frey group (Mainz, Germany).[61, 62] The application of oxyanionic ring-opening polymerization to synthesize hydrophilic polyether compounds with lipids like cholesterol as initiator has been applied yield to amphiphiles, which were shown to integrate into artificial membranes of liposomes and giant unilamellar vesicles (GUV). [64] Previous studies by the Helm group gathered elemental knowledge on the application of CuAAC for the post-preparational surface conjugation of such amphiphiles.[2] With these fundamental tools available, CuAAC has been combined with liposome preparation *via* dual centrifugation in a workflow depicted in Figure 3.7, in order to conduct in-depth investigations on the mode of interaction of such liposomes with biological membranes.

Polyglycerol amphiphiles

Polymeric amphiphiles based on cholesterol as a lipophilic anchor and hydrophilic polyether blocks represent promising candidates for the steric stabilization of liposomes. Figure 3.8 shows two compounds 1 and 2, containing hyperbranched polyglycerol (*hb*PG) and linear poly(glycidyl)glycerol (PGG), respectively, that were examined in this study. Compound 3 is a well-established conjugate of DSPE and methoxy poly(ethylene glycol) (DSPE-mPEG), which is also commercially used for sterical stabilization of liposomes, e.g. in DOXIL.[53] Compounds

Parts of this chapter were published in [264]. Parts of the data were acquired by Felix Richter during an internship.

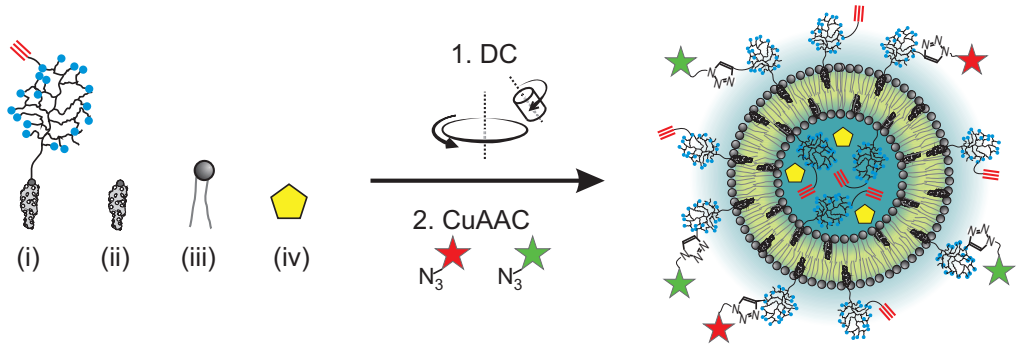

Figure 3.7: Schematic representation of liposome preparation workflow. Hyperbranched polyglycerol-modified amphiphiles (i), based on cholesterol, were combined with helper lipids like cholesterol (ii) and EPC (iii) and hydrophilic cargo (iv), and integrated in liposomes *via* dual centrifugation. After formulation, subsequent CuAAC surface derivatization was applied.

1 and 2 were designed to also contain terminal alkyne groups, which allowed for convenient modification by CuAAC. While in both structures only one propargyl group are represented in Figure 3.8, stochiometry during functionalization was adjusted to yield one and four alkyne moieties for structures 1 and 2, respectively, as determined by ^{1}H NMR measurements (see Appendix 2). One of the distinct advantages of polyglycerol (PG) over the commonly used PEG is the high number of terminal primary and secondary hydroxyl groups, that allow for a higher number of end group derivatizations per molecule. All polymeric compounds employed here were characterized by dispersity indices ($Đ$, M_W/M_N) below 1.12 as listed in Table 3.2, were therefore well-defined and in an applicable range for pharmaceutical applications. PG furthermore has previously been shown to provide similar high biocompatibility as PEG, which rendered PG as a suitable candidate polymer for steric stabilization of nanoparticles.[267]

Liposome preparation and characterization

Liposome formulation was conducted on a 29.5 µmol scale of total lipid, which yielded preparations of ~17.5 mg. CL and DSPE-mPEG2000-incorporating SSL were prepared as reference

Table 3.2: Structures and characteristics of investigated polymers.

	Amphiphile characteristics		
Liposome sample	Structure	$M_W(g/mol)$	M_W/M_N ($Đ$)
CL	*no polymer*		
PGGL	$Chol-PEG_{22}-PGG_8-(CH_2-C{\equiv}CH)_4$	2780	1.08
hbPGL	$Chol-PEG_{25}-hbPG_{21}-(CH_2-C{\equiv}CH)$	3100	1.11
SSL	$DPSE-PEG_{45}-O-CH_3$		n.d.

M_W/M_N ($Đ$): Dispersity index determined by SEC analysis using PEG standards.

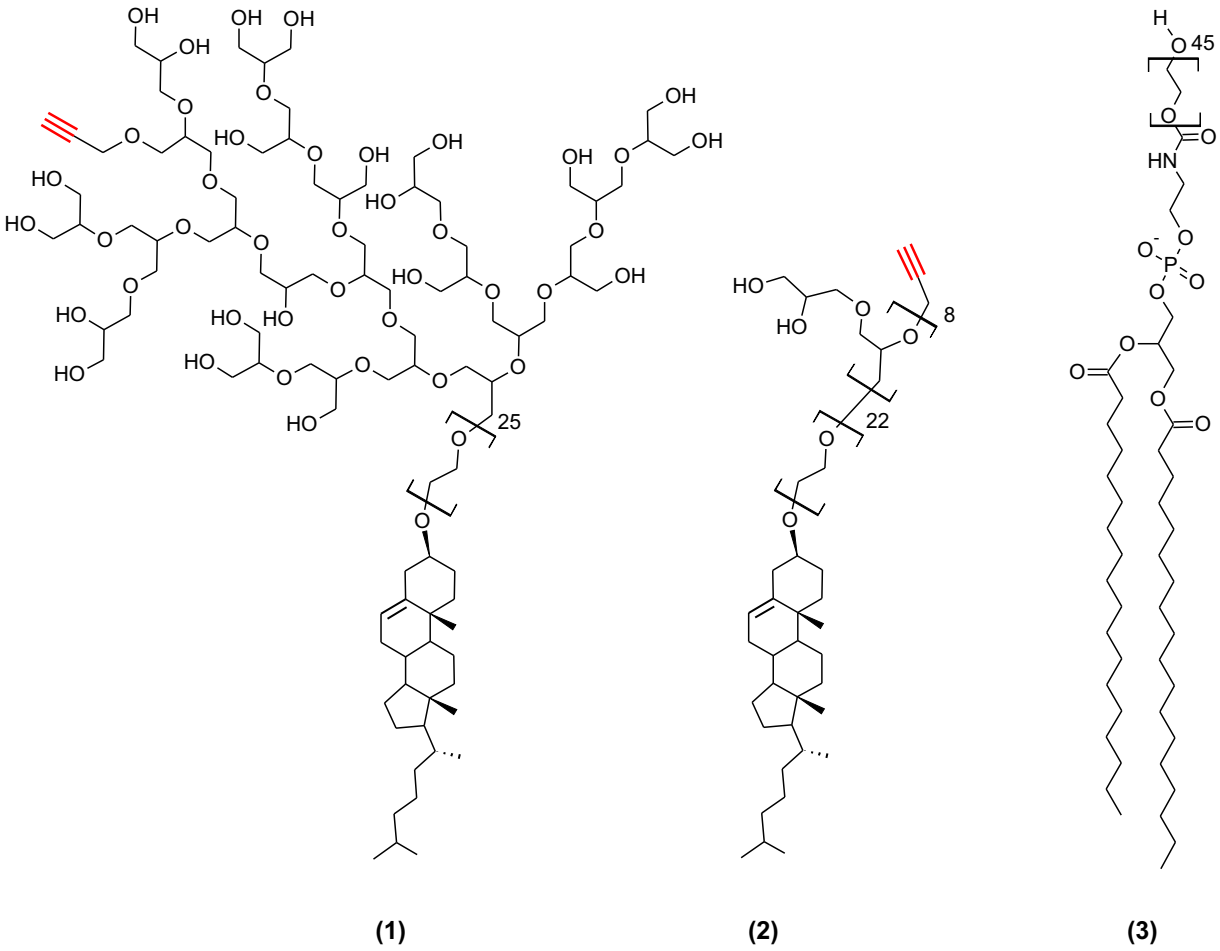

Figure 3.8: Polymeric amphiphiles used in this study, based on hyperbranched polyglycerol (1) $Chol - PEG_{25} - hbPG_{21}$, linear poly(glycidyl)glycerol $Chol - PEG_{22} - PGG_8$ (2) and linear PEG $DSPE - mPEG(2000)$ (3, commercial reference).

standards. Following literature[38], a 5 mol% fraction of either cholesterol (for cholesterol-based amphiphiles 1 and 2, as being referred to as *hb*PGL and PGGL, respectively) or EPC (for SSL) was substituted with the corresponding polymeric amphiphile. Liposomes were subsequently characterized by DLS, and Table 3.3 lists liposome compositions and properties.

The application of liposomes as drug delivery vehicles for parenteral application typically involves the use of unilamellar liposomes, especially when hydrophilic cargo is transported. The lamellar structure of the prepared liposomal formulations was studied by cryo transmission electron microscopy (cryoTEM). Figure 3.9 shows micrographs of CL (A), SSL (B), PGGL (C) and *hb*PGL (D). The observed sizes were in general in good agreement with DLS measurements (compare Table 3.3), with a numerical superiority of unilamellar vesicles in all formulations. However, PGGL and *hb*PGL formulations included a substantial number of multilamellar vesicles, which in total accounted for a non-negligible fraction of the total lipid surface area. This represents an important factor during the estimation of the surface density of functionalities after derivatization. In general, the micrographs confirmed a successful preparation of lipid vesicles without the appearance of non-vesicular aggregates. The finding of high intra-vesicular volume fractions was also in good agreement with the achieved liposomal encapsulation efficiencies of hydrophilic cargo, which were expected to be in the range of 50% (compare Section 3.1) and listed in Table 3.3.

Depending on the method of preparation, the lipid composition within the liposomes after purification does not always represent the initial composition which was used for preparation.[38] Especially for novel lipid amphiphiles with critical micelle concentrations (CMC) that are not always known, a substantial amount of amphiphile can be located in micelles rather than integrated in the lipid bilayers. To resolve this, ^{1}H NMR was applied for the investigation of the lipid composition before and after purification of liposomes, and subsequent comparison of the integrals of unique protons for each of the incorporated lipids. The obtained spectra in Appendix 3 confirmed no sign of variation of this composition after purification, indicating that no significant amount of polymeric amphiphiles were unrecoverable during purification.

Table 3.3: Compositions and characteristics of investigated liposomes.

	Liposome characteristics			
Liposome sample	$\chi_{EPC} : \chi_{Chol} : \chi_{Polymer}$	Diameter ± SD (nm)	PDI	EE
CL	55:45:0	148.8 ± 1.2	0.183	56.6 ± 4.8
PGGL	55:40:5	171.3 ± 0.4	0.123	74.4 ± 1.8
hbPGL	55:40:5	184.9 ± 0.9	0.068	62.9 ± 4.9
SSL	50:45:5	111.6 ± 2.1	0.112	45.8 ± 5.5

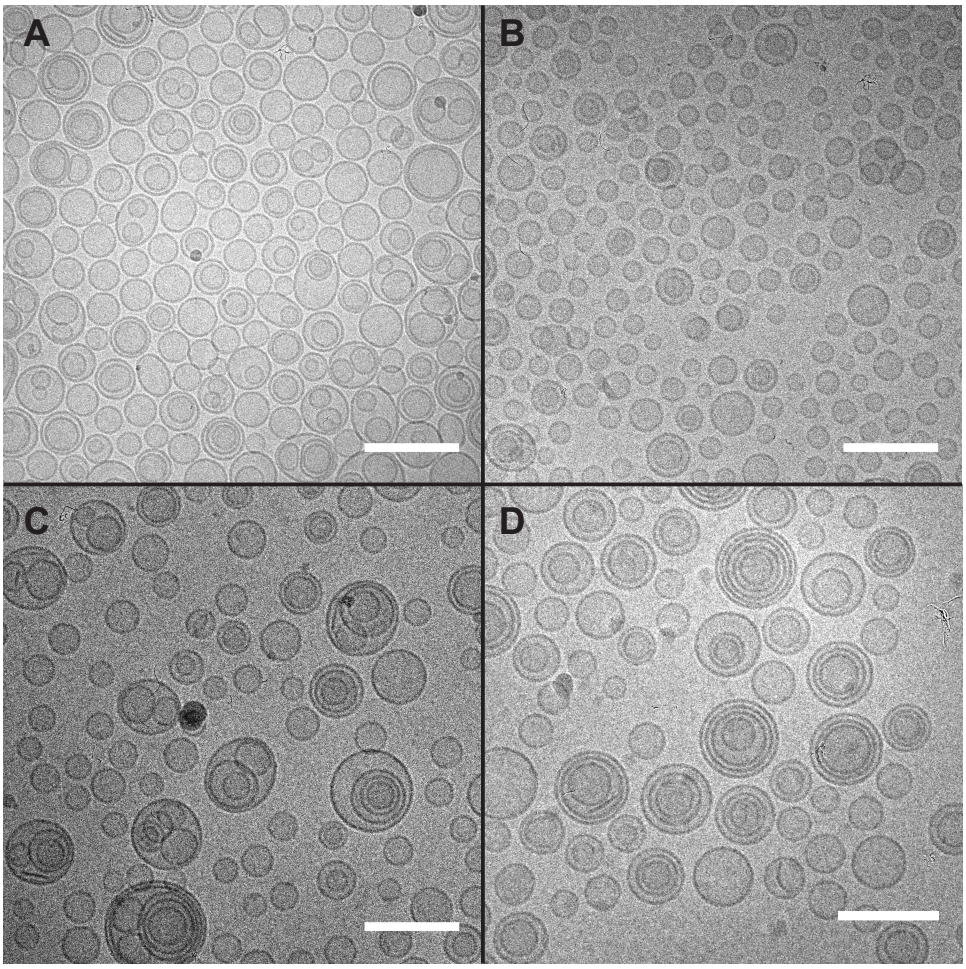

Figure 3.9: Cryo transmission electron micrographs of CL (A), SSL (B), PGGL (C) and hbPGL (D). Scale bar indicates 200 nm.

Functionalization

The investigation of click derivatization on the liposomal surface was previously described in-detail.[2] In the particular contribution, the optimization of reaction conditions, the quantification of surface moieties and the neglectable influence of the mild functionalization reaction on size, size distribution and encapsulation efficiency were described. Also, a conceptual approach to on-surface fluorescence resonance energy transfer (FRET) measurements was introduced, allowing for the measurement of fluorescence emission of an acceptor dye (Alexa 594, red) after excitation of a donor dye (Atto 488, green). Typical methods for quantification of reaction yields are hampered by low material availability, therefore degrees of functionalization have been measured by fluorescence-based techniques as detailed in the methods section. One of the findings of the investigations quoted above was the importance of using fluorophores that were highly hydrophilic, which was the reason why Atto 488 and Alexa 594 were employed in the present study (Figure 3.10). Derivatives of such rhodamine dyes that do not exhibit moieties to increase hydrophilicity as the two sulfonic acid groups in the shown structures, can be expected to cross lipid bilayers and therefore integrate in the liposomal membrane during the click reaction. In general, the number of azide-reactants immobilized on the surface was expected to be in the range of 50-400 per liposome,[2] based on an approximation involving also the size of resulting liposomes and the headgroup size of incorporated lipid compounds. Taking also into account a certain inhomogeneity regarding the lamellarity as was suggested by the electron micrographs in Figure 3.9, the significance of numerical values that describe the average number of fluorophores on the surface of liposomes has to be interpreted with care. More precise evidence can be conducted from fluorescence correlation spectroscopy (FCS) measurements as reported in Section 3.3 below, and the results there indicated that the abovementioned approximation was in moderate to good agreement with FCS analysis.

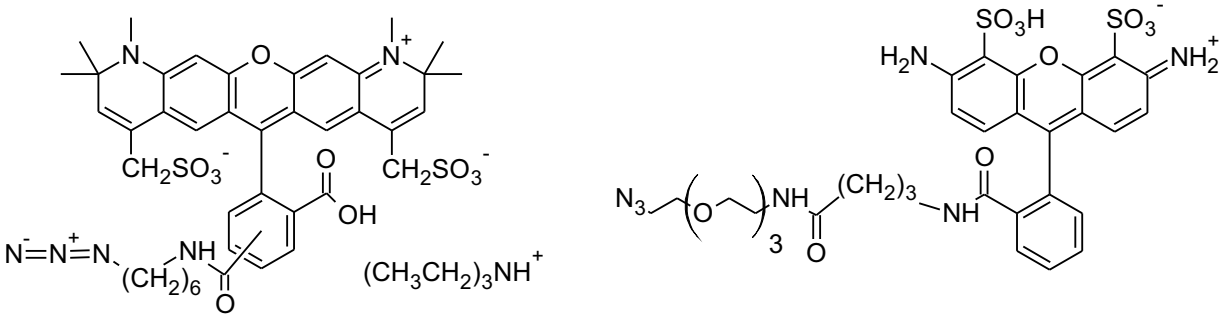

Figure 3.10: Structure of fluorophore azides used in this study.

In vitro interaction

The cellular uptake and interaction of liposomal formulations containing Atto 488- and Alexa 594-labeled polymeric amphiphiles was studied by incubating rat brain endothelial (RBE4) [268] cells. No difference in the interaction with cellular membranes was observed for the two different polyglycerol liposomes PGGL and *hb*PGL, which is why the subsequent investigations were exemplarily conducted with PGGL. Figure 3.11 displays micrographs from confocal laser scanning microscopy (CLSM), showing RBE4 cells, incubated for 4 hours with liposomes that were derivatized either with Atto 488 (A-D), Alexa 594 (E-H) or both fluorophores (I-L). Interestingly, a very intense membrane fluorescence was observable for all samples, a behavior which was not *per se* expected for sterically stabilized liposomes. The membrane fluorescence persisted after the cells were washed with phosphate buffered saline (PBS), which would be expected to diminish if the origin of the membrane staining would have been a weak cell surface adhesion of the labeled vesicles. Besides this, and in consistence with previous work,[2] the FRET channel showed significant fluorescence only in the case of double-labeled particles (Figure 3.11 J). Figure parts B and F indicated an adequate spectral separation of the green and red channels and therefore only neglectable bleed through of the donor fluorophore and also neglectable cross excitation of the acceptor fluorophore.

To date, several studies have reported on the application of cholesterol-anchored polymers for the steric stabilization of liposomes, with PEG representing the most prominent candidate.[80, 269, 85, 270, 271, 84] However, very little is known about the fate of such conjugates in liposomal formulations after incubation on cellular membranes. The strong membrane fluorescence motivated in-depth investigations that addressed the question whether these observations were caused by properties of the particular polyglycerol compounds or by general properties of cholesterol-based amphiphiles. The time-dependence of the staining process was investigated by CLSM observation at different time-points. Figure 3.12 shows merges of the green and red fluorescence channels after different incubation times. Already after 30 minutes, a very strong membrane fluorescence was observable, and was still increasing until the 6 hours time point. Intracellular aggregates were observable after 2 hours, which is in good agreement with the time frame of active endocytosis.[272] The number and intensity of the intracellular structures strongly increased until the last point of observation after 6 hours. Interestingly, the balance between green and red fluorescence seemed to change during internalization. This observation suggested either (i) a preferential uptake of red fluorophore, (ii) an uptake-dependent increase of the FRET efficiency e.g. caused by lower distances between the FRET pairs or (iii) quenching effects during acidification of endosomal compartments.

With the given resolution of CLSM, the exact localization of the labeled amphiphiles within the observed intracellular aggregates were not identifiable. Considering the fast membrane staining within minutes, an integration of the amphiphiles into the membrane upon desorption from

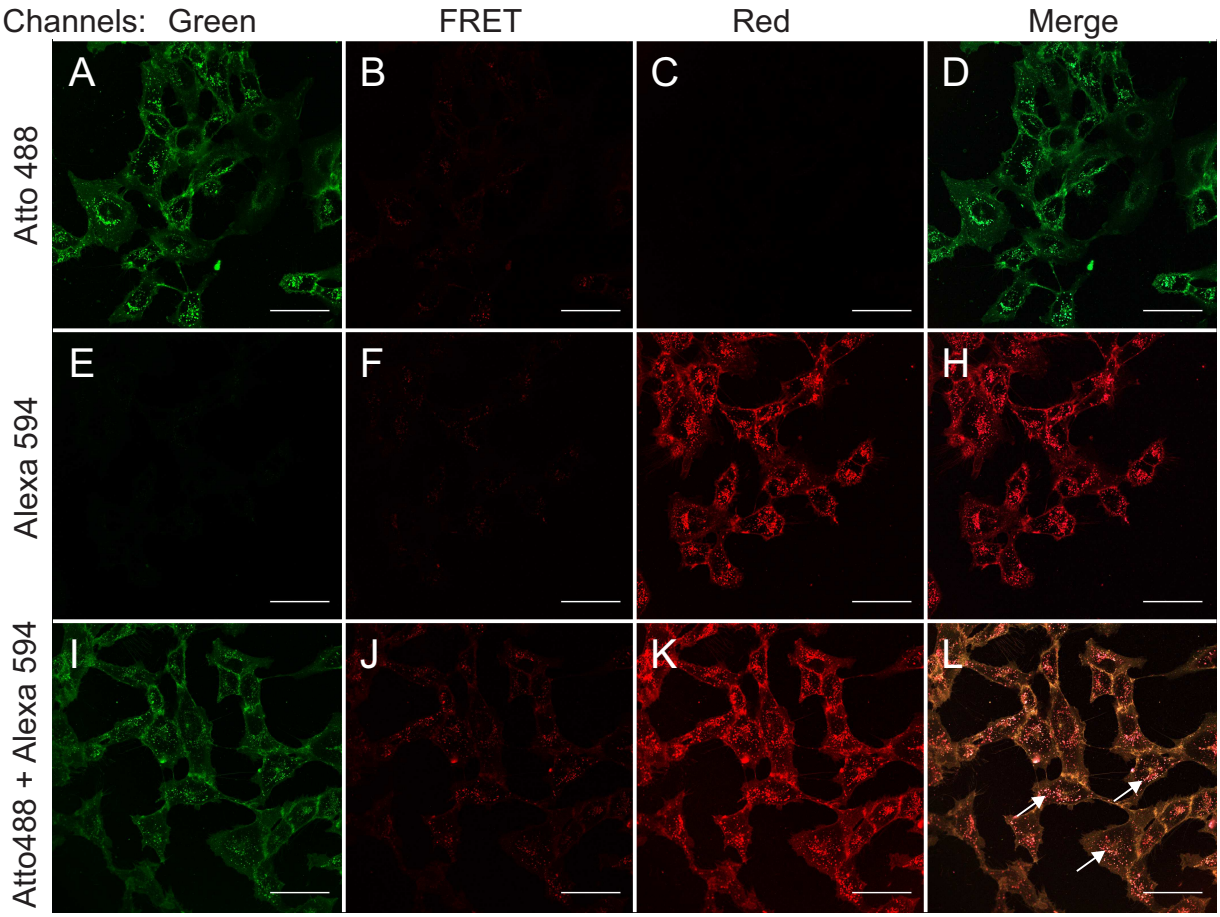

Figure 3.11: CLSM micrographs of RBE4 cells incubated for 4 hours with liposome PGGL, either functionalized with Atto 488 (first row), Alexa 594 (second row) or both fluorophore azides. Columns display the different detection channels for each single fluorophore (green and red), the FRET channel (Atto 488 excitation with Alexa 594 emission) and a merge of green and red channels. Scale bars indicate 50 µm. Arrows indicate areas with intracellular structures that showed a strong fluorescence intensity in both green and red channels.

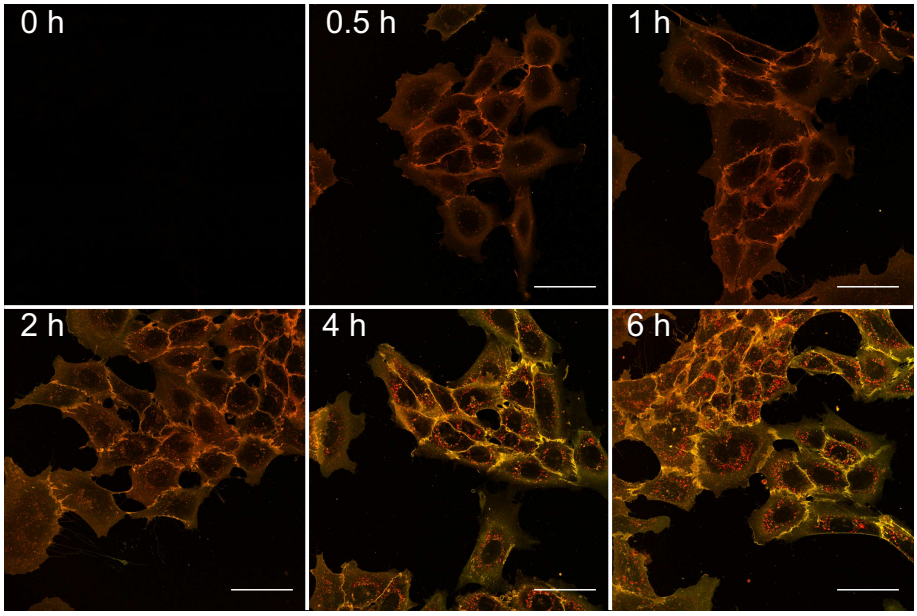

Figure 3.12: CLSM micrographs (merges of green and red channels) of RBE4 cells incubated with Atto 488- and Alexa 594-labeled liposomes at different time points. Already after 30 minutes, a strong membrane fluorescence was observed. Scale bars indicate 50 µm.

the liposome surface was expected to be the most likely mode of action. In order to confirm this suspicion, cells were co-incubated with chloroquine, a membrane-permeant anti-malaria drug which, as a weak base, is known to enrich within endosomes due to protonation during acidification.[273] In the protonated form, chloroquine is membrane-impermeant and therefore accumulates within lysosomal compartments, leading to a significant increase in the volume of these vesicles. Figure 3.13C displays the merge of the green and red channel of a CLSM micrograph of RBE4 cells, that were incubated with Atto 488- and Alexa 594-labeled PGGL and with chloroquine. Confocal cross-sections of intracellular vesicles (white arrows) provided strong evidence, that the labeled amphiphiles were located solely in the membrane of those vesicles and not in the intravesicular lumen. The micrograph displayed in Figure 3.14A furthermore revealed that these vesicles were indeed endosomes that maturated towards lysosomes, since a clear colocalization between Lysotracker Blue® and labeled amphiphiles was observable. The acidification, and therefore the enrichment and fluorescence of Lysotracker Blue®, was efficiently prevented when chloroquine was added to the incubation (Figure 3.14B). By comparison of the micrographs of these chloroquine incubations with the 6 h time point in Figure 3.12, it can also be concluded that the imbalance in emission intensities of both fluorophores as discussed above was most likely due to the decrease of pH that occurred during endosomal maturation. The inhibition of other endocytic pathways did furthermore not yield a decrease of membrane fluorescence, which additionally indicated a completely unspecific mode

of interaction (Appendix 5). Taken together, the findings suggested a fast localization of the used polymeric amphiphiles in the cellular membrane. However, the important question for pharmaceutical applications, regarding the fate of the liposomal cargo, remained unsolved.

Application of liposomes as drug delivery vehicles in most cases includes the encapsulation of pharmaceutically active compounds, and especially targeted delivery often relies on the cell- or tissue-specific delivery of this payload. The abovementioned results provided only imprecise knowledge about the fate of encapsulated cargo. The results of an *in vitro* experiment that addressed this question are set out in Figure 3.15. Here, Atto 488 labeled PGGL were formulated to encapsulate Sulforhodamine B (SRB), which is a highly hydrophilic tracker for the aqueous liposomal lumen. The displayed images detail the effect of membrane integration of the labeled amphiphiles in a shorter time scale, and clearly no colocalization of green and red fluorophores was visible. This indicated that the adhesion of intact liposomes to the cellular membrane did not cause the fluorescent staining, but underlined the previous findings that only the amphiphiles were integrated in the cellular membrane. Also a fusion-like interaction was rather unlikely, since also after longer incubation times no SRB fluorescence has been detected within the cells.

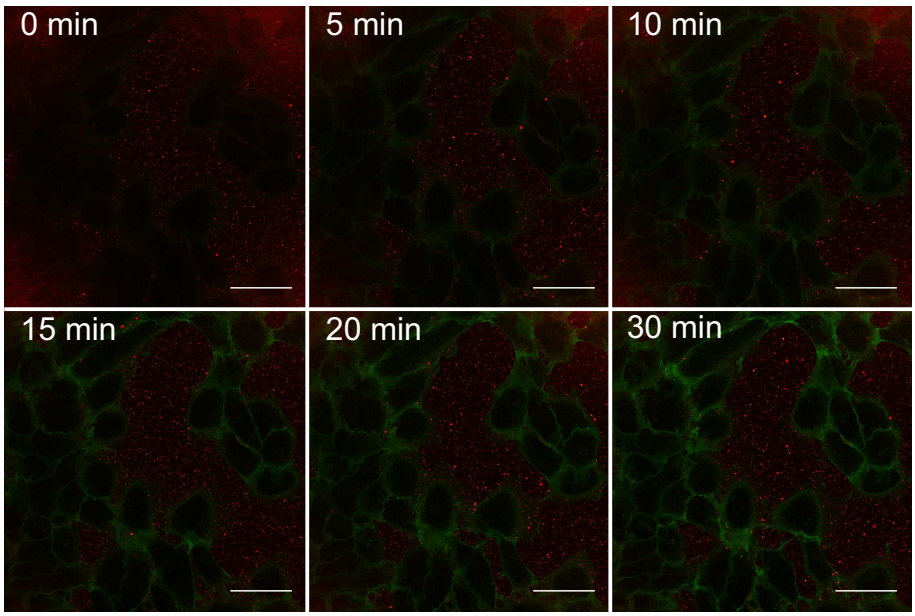

Figure 3.15: Merged channels of Atto488 labeled PGGL (green channel), loaded with sulforhodamine B (red channel) in a short-term live imaging series. The cargo clearly did not colocalize with the green fluorescent amphiphile. Scale bar is 50 µm.

Taken together, these results provided important insights into the mode of interaction of cholesterol-based polyglycerol amphiphiles with cellular environments. The observations were concluded in a mechanism which is depicted in Figure 3.16. After incubation on a cellular

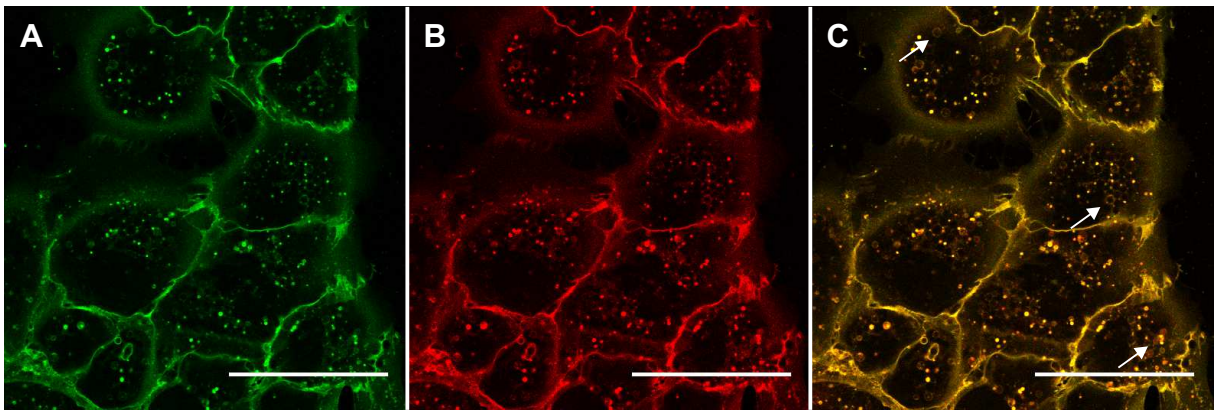

Figure 3.13: Green (A), red (B) and merge of green and red channel (C) of a CLSM micrograph of RBE4 cells incubated with Atto 488- and Alexa 594-labeled PGGL and incubated with chloroquine to prevent endosomal acidification. Arrows in C indicate examples of confocal cross sections of endocytic vesicles. Scale bar represents 50 µm.

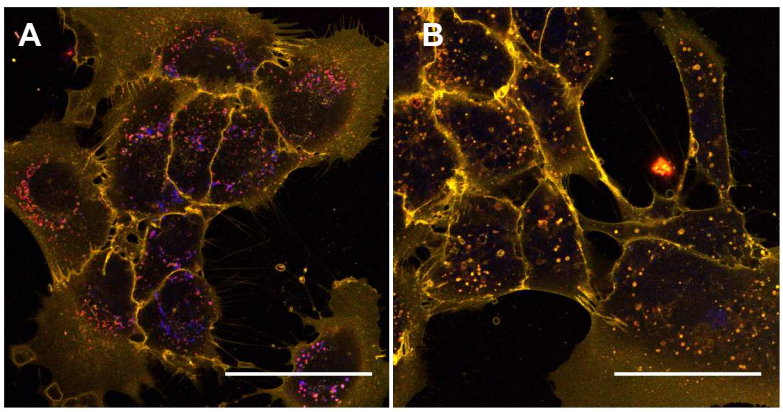

Figure 3.14: RBE4 cells incubated with Lysotracker Blue (blue) and PGGL, labeled with both Atto 488 (green) and Alexa 594 (red), without (A) and with (B) chloroquine. Chloroquine clearly prevented accumulation of Lysotracker in Lysosomes. Scale bar represents 50 µm.

environment, the labeled amphiphiles readily integrated into the cellular membranes which was observable *via* CLSM within minutes. The type of cell line was of no importance, since the effects were observed on several different mammalian cell lines including RBE4, KB, HeLa, HEK and dendritic cells. Liposomal cargo was not observed to be released, neither to the cytosol nor the extracellular environment. During endocytic uptake, the amphiphiles were transported to intracellular vesicles which were at the latest stage located in the perinuclear region, and these vesicles were identified to be lysosomes. In total, this intense interaction was unexpected for such sterically stabilized liposomes, especially regarding the large body of literature on the use of cholesterol as anchor for hydrophilic polymers and sterical stabilization.

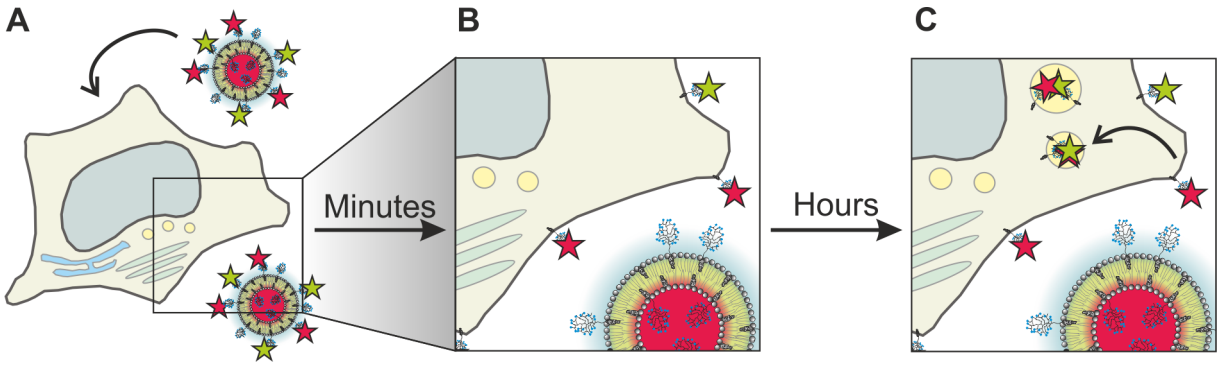

Figure 3.16: Scheme of the proposed mode of interaction of Atto 488- and Alexa 594-labeled PGGL with cellular membranes. In a first step (A→B), amphiphiles integrate rapidly in the order of minutes in the cellular membrane, while the cargo is not released from the liposomes. With ongoing endocytic trafficking, labeled amphiphiles end up in the perinuclear regions of the cytosol in vesicles that can be classified as lysosomes.

3.3 Orthogonal functionalization of liposomes: multifunctional carriers

Abstract Important prerequisites for the application of liposomes in ligand directed targeting are efficient conjugation routes for the ligands of interest. After the basic principles of IEDDA have been recently established,[265] this derivatization method in combination with CuAAC was applied in an orthogonal and site specific manner for liposome functionalization. Folic acid was furthermore employed to facilitate active targeting with multifunctional liposomes, which allowed for active targeting *and* fluorescence-based analysis. The results revealed disadvantages of cholesterol-anchored amphiphiles for active targeting and unexpected desorption processes of alkyl chain-anchored folate amphiphiles, which suggested important implications for the rational design of actively-targeted liposome systems.

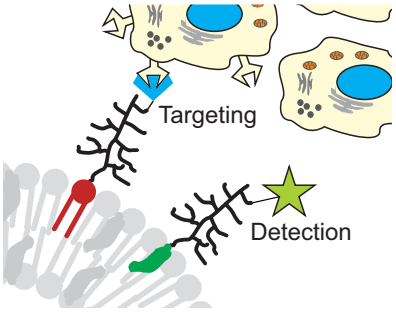

Adequate sterical stabilization of liposomes depends on a stable polymer hull with a particular density to successfully inhibit protein adsorption and therefore prevent fast clearance from the blood stream. After the the strong interaction of cholesterol-based polyglycerol amphiphiles with biological membranes has been established as described in the previous section, the first aim in the following was to investigate the causes of this mode of interaction. Therefore, a systematic variation of the amphiphile structures was explored.

Alkyl chains are more stable membrane anchors

The polymer lipid amphiphiles that were introduced in the previous chapter combined three structural features that defined the properties of these compounds, i.e. the lipid anchor, here cholesterol, the polyglycerol polymer backbone, and the conjugated fluorophore. In a first approach, the influence of the fluorophores on the observed membrane desorption was ruled out. While similar effects irrespective of using Atto 488 or Alexa 594 have been observed as described in the previous sections, Figure 3.17 illustrates that also amphiphiles labeled with cyanine fluorophores like SulfoCy5 showed the same exchange behavior. All in all, the high hydrophilicity that is necessary for successful post-preparational liposome functionalization is

Parts of this chapter were published in [274, submitted]. Matthias Voigt established basic principles of the IEDDA reaction during his diploma thesis[265], Inka Negwer measured FCS data.

expected to prevent an unspecific membrane-labeling of the fluorophores alone. Therefore, the influence of the fluorophores was assumed to be only of minor importance.

As a rather novel polymer for steric stabilization of nanoparticles, the influence of polyglycerol on the properties of nanoparticles was not yet fully characterized at this point. While most reports in literature are devoted to conjugates of cholesterol with PEG and no visualizing studies on the desorption of such compounds from liposomes are available, a comparison between PEG and PG was pursued. Figure 3.18A shows cells, that were incubated with liposomes bearing cholesterol-based, hyperbranched polyglycerol amphiphiles, labeled with Atto 488, and, as expected, cells exhibited intense membrane fluorescence. When comparing this observation to amphiphiles that contained PEG, a similar behavior was observable (B), which indicated no dependence on the type of hydrophilic polymer that was employed. Subsequently, a variation of the lipid anchor to a dialkyl-substituted glycerol derivative (bis(hexadecyl)glycerol, BHG) resulted in liposomes, that virtually did not fluorescently stain cellular membranes within the time of observation. Figures 3.18 C and D show KB cells that were incubated with liposomes containing such compounds, i.e. BHG-*hb*PG and BHG-PEG, respectively. The fluorescence of the membrane and internalized structures was only visible when cholesterol-based structures were used, which indicated a higher stability of BHG-based compounds in the liposomal membrane. While these findings suggested that cholesterol-based polymeric amphiphiles might exhibit unwanted properties in the context of immobilization of targeting ligands on liposomes, the exchange behavior between two artificial phospholipid membranes was further investigated in order to exclude influences from biological environments.

Whenever cells are incubated with liposomes in an *in vitro* setting, the complex extracellular environment might influence the mode of interaction between cells and liposomes. It has been shown adsorbed proteins on nanoparticle surfaces, also referred to as the protein corona, *e.g.* from cell culture media containing fetal bovine serum (FBS), strongly influenced the cellular uptake of such particles.[275] To prevent such influence, exchange experiments between different populations of liposomes were conducted by fluorescence cross-correlation

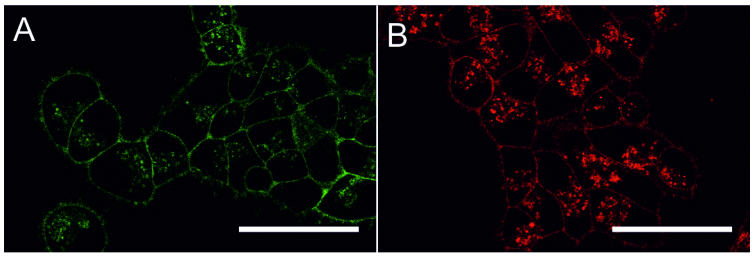

Figure 3.17: KB cells, incubated with Atto 488- (A) or SulfoCy5-labeled (B) *hb*PGL for 4 hours. A clear membrane incorporation was observable, irrespective of the used fluorophore. Scale bar represents 50 µm.

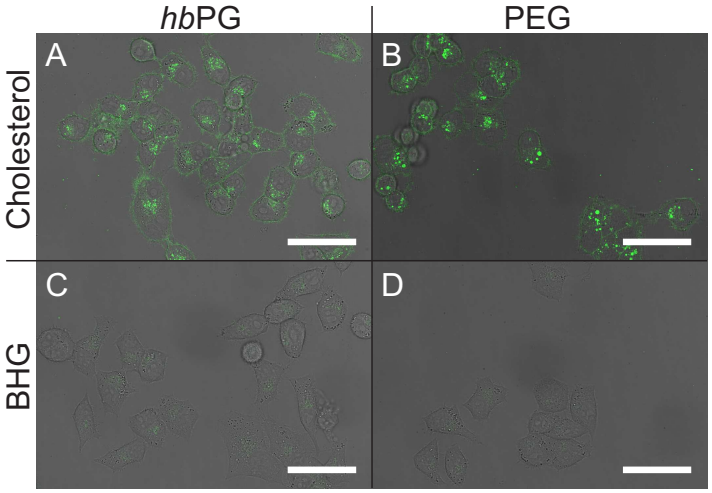

Figure 3.18: KB cells, incubated with liposomes containing Atto 488-labeled amphiphiles of different structures: (A) Cholesterol-hbPG, (B) Cholesterol-PEG, (C) Bis(hexadecyl)glycerol-*hb*PG (BHG-*hb*PG), (D) BHG-PEG. Strong membrane fluorescence in (A) and (B) indicated a cholesterol-dependent desorption of the amphiphiles, which was not detectable for BHG-based amphiphiles. Scale bar represents 50 µm.

spectroscopy (FCCS). Therefore, liposomes incorporating either cholesterol-*hb*PG *or* BHG-*hb*PG amphiphiles were labeled either with Atto 488 *or* with SulfoCy5, which yielded four different particle species. Immediately after mixing either both cholesterol- or both BHG-incorporating liposomes, samples were subjected to FCCS analysis. Figure 3.19 illustrates the difference between both lipid anchors. (A) shows that the cross correlation trace (black) was virtually equal to the autocorrelation function of SulfCy5 (red), which indicated a strong cross-correlation of both fluorophores and therefore a complete exchange of fluorophores between the two particle populations. However, complete in this case refers to a low number of liposomes that remained labeled only with one of the two fluorophores. In contrast, the cross-correlation function $G/(0)$ was much lower in the case of BHG-based amphiphiles (B), which indicated a higher number of single-labeled particles and therefore a slower exchange of the amphiphiles. Exemplary fluorescence correlation spectroscopy (FCS) data of Atto 488-labeled liposomes is shown in Appendix 6, which furthermore confirmed (i) the complete removal of residual free fluorophore azide, (ii) the successful immobilization of the fluorophores on the particle and (iii) a number of fluorophores per particle in the expected range.

In summary, cholesterol-based amphiphiles were shown to rapidly integrate into biological *and* into artificial phospholipid membranes, while these findings questioned the applicability of such compounds *in vivo*. However, since a controlled way of desorption could also be exploited to control the time-dependent stability of liposomes, systems that incorporate both cholesterol- and BHG-based amphiphiles might be promising candidates for specific applications. In order to

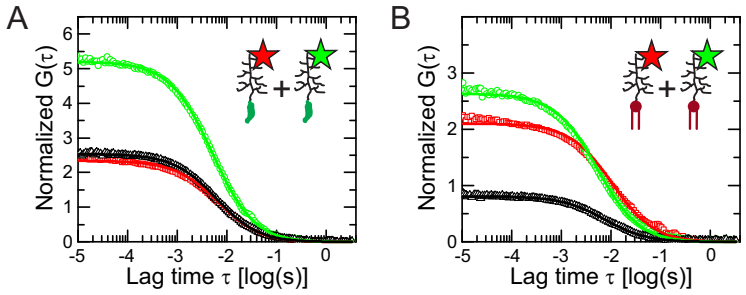

Figure 3.19: FCCS data illustrating strong cross correlation (black trace) for a mixture of liposomes that incorporate either Atto 488- and SulfoCy5-labeled cholesterol-based amphiphiles (A). For BHG-based amphiphiles (B), low cross correlation is indicated by a black cross correlation trace unequal to the trace of either fluorophore (green: Atto 488, red: SulfoCy5).

further expand the scope of the investigated structures and to study multifunctional liposomes that incorporate more than one functionalizable lipid, investigations on the site-specific surface derivatization were conducted as described in the following.

IEDDA on the liposomal surface

The use of the copper-catalyzed cycloaddition between azides and alkynes as a versatile and efficient way for the post-preparational surface modification of liposomes has recently been established.[264] This specific type of reaction is depending on copper as a catalyst, which renders the bioorthogonality limited due to the cytotoxic potential of copper.[189] A reaction that recently gained increasing attention is the DIELS-ALDER cycloaddition between an electron-poor diene and an electron-rich dienophile, and therefore being referred to as an inverse electron demand Diels-Alder (IEDDA) reaction.[198, 200] In order to apply this principle to the post-preparational liposome derivatization, free hydroxyl endgroups in PG-containing amphiphiles were esterified with a norbornene dicarboxylic acid anhydride, since norbornene has been reported to be a suitable dienophile for the use in such reactions. Figure 3.20 displays the major building blocks of the functionalizable amphiphiles that were used in this study. Here, (A) shows the lipid anchors cholesterol 1 and BHG 2, (B) lists the two functional moieties of either alkyne 3 or norbornene 4 functionality, and (C) displays the resulting polymeric amphiphiles 5-8 that were resulting from a permutation of these building blocks. Also, a depiction of these structures is introduced for clearer presentation of results in the following sections, describing membrane-unstable cholesterol compounds in green, membrane-stable BHG compounds in red and also describing the structure of the used polymer in general as either branched or linear. The depictions were designed for easy recognition of either linear PEG structures or of (partially) hyperbranched PG structures, thus all depicted compounds 5-8 were based on hyperbranched PG structures. Further properties of these compounds are

also listed in Table 3.4, where also three additional amphiphiles 9-11 are listed, which were employed in subsequent experiments. Polydispersities below 1.6 indicate well defined polymer structures in the context of hyperbranched polymers, and confirm a potential prerequisite for pharmaceutical application.

Previous work by Matthias Voigt reported on detailed investigations on reaction conditions and reaction kinetics regarding compounds 5-8.[265] The typical workflow that was conducted for liposome preparations and functionalization reactions is visualized in Figure 3.21. From the separation of residual unreacted fluorophore tetrazines via GPC, typical reaction yields of 10-25% with respect to the fluorophore compound were measured, depending on the used amphiphile.[265] Besides the previously introduced fluorophore azides, with Atto 488 and SulfoCy5 tetrazine two tetrazine-fluorophore conjugates were employed in these studies, with the corresponding structures being shown in Figure 3.22. Both fluorophores were selected for a sufficiently high hydrophilicity, as ensured by sulfonic acid groups in both structures.

Liposomes prepared by dual centrifugation and incorporated polymeric amphiphiles 5-8 were characterized by dynamic light scattering and yielded diameters in the expected range between 130 and 200 nm with PDI below 0.3. Liposomal compositions as well as characterization data are listed in Table 3.5. Typically, either cholesterol or EPC were substituted by either cholesterol- or BHG-based amphiphiles, respectively, which yielded liposomes that contained in total 5 mol% of polymeric amphiphile in their lipid composition. Liposomes L1-L8 were defined by their lipid compositions as listed in Table 3.5, and will in the following be referred to either with these abbreviations or the depictions of their corresponding amphiphiles as listed in Table 3.4.

The first set of experiments examined the impact of the conjugation chemistry, namely IEDDA, on the exchange characteristics of the two available lipid anchors as established in Section 3.2 on page 37. Therefore, RBE4 cells were incubated with liposomes L1 to L4, labeled either with Alexa 594 azide or with Atto 488 tetrazine. The resulted CLSM micrographs are displayed in Figure 3.23. Following the incubation of cholesterol-based, tetrazine-labeled

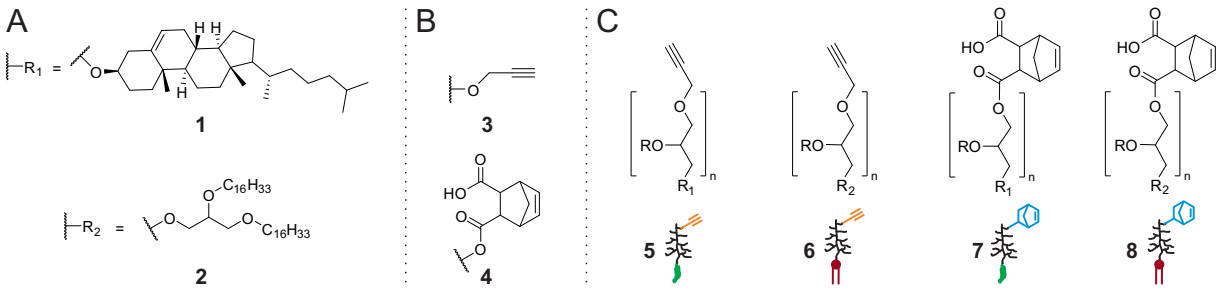

Figure 3.20: Building blocks of polymeric amphiphiles used in this study, including the lipophilic anchors (A) cholesterol 1 and BHG 2, the functional endgroups (B) alkyne 1 and norbornene 2, and the resulting amphiphiles(C) 5 to 8.

Table 3.4: Properties of used amphiphile structures

ID	Lipid anchor	Polymer-Structure	Functionality	M_n / g/mol	M_w/M_n (GPC)	Depiction
5	Chol-	-PEG_{25}-*hb*PG_{21}-	-Propargyl	3078	1.11	
6	BHG-	-PEG_{35}-*hb*PG_{25}-	-$Propargyl_5$	4086	1.5	
7	Chol-	-PEG_{22}-*hb*PG_{35}-	-$Norbornyl_5$	4927	1.4	
8	BHG-	-PEG_{35}-*hb*PG_{25}-	-$Norbornyl_{13}$	6062	1.5	
9	Chol-	-PEG_{41}-	-Propargyl	2228	1.09	
10	BHG-	-PEG_{60}-	-Propargyl	3219	1.05	
11	BHG-	-*hb*PG_{30}-	-$Propargyl_2$	2838	1.2	

Lipid anchors: Chol: Cholesterol, BHG: Bis(hexadecyl) glycerol, M_n: Number average molecular weight as determined by ^1H NMR spectroscopy. M_W/M_N ($Đ$): Dispersity index determined by SEC analysis using PEG standards.

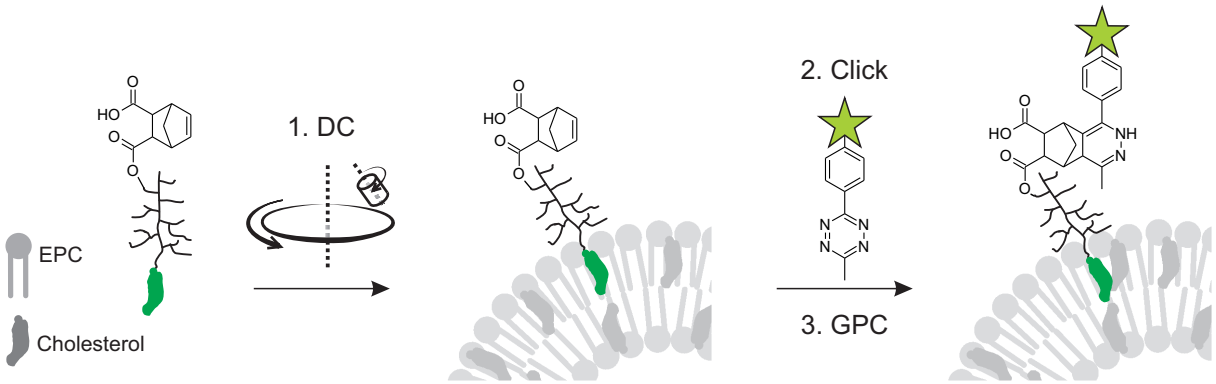

Figure 3.21: Workflow of click modification of liposomes with tetrazine fluorophores. After incorporation of lipid amphiphiles in liposomal structures *via* microscale DC, the surface-anchored norbornene moiety reacts via IEDDA with the tetrazine compound. After removal of free unreacted fluorophores, labeled liposomes are obtained.

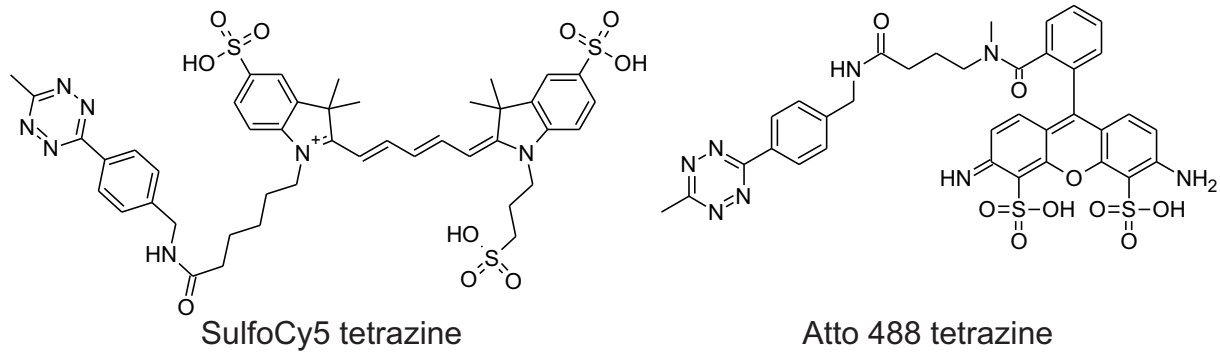

Figure 3.22: Structures of SulfoCy5 tetrazine and Atto 488 tetrazine.

Table 3.5: Compositions and characteristics of liposomes L1 - L8

ID	Composition	Ratio	Functionality	Diameter ± SD (nm)	PDI
L1	EPC : Chol : 5	55 : 40 : 5	P	202.4 ± 7.1	0.134
L2	EPC : Chol : 6	50 : 45 : 5	P	181.6 ± 8.0	0.194
L3	EPC : Chol : 7	55 : 40 : 5	N	135.3 ± 7.9	0.140
L4	EPC : Chol : 8	50 : 45 : 5	N	180.7 ± 3.6	0.186
L5	EPC : Chol : 5 : 7	55 : 40 : 2.5 : 2.5	P/N	152.1 ± 2.4	0.093
L6	EPC : Chol : 6 : 7	52.5 : 42.5 : 2.5 : 2.5	P/N	163.5 ± 2.1	0.082
L7	EPC : Chol : 5 : 8	52.5 : 42.5 : 2.5 : 2.5	P/N	208.5 ± 33.7	0.192
L8	EPC : Chol : 6 : 8	50 : 45 : 2.5 : 2.5	P/N	189.5 ± 24.8	0.153

Functionality: Propargyl (P), Norbornyl (N)

amphiphile 7 (Figure 3.23C), a strong membrane fluorescence was detectable, which did not appear for the corresponding BHG-based polymer. This observation was in good agreement with the interaction expected from alkyne-bearing amphiphiles, and therefore confirmed the previous findings that rendered the lipid anchor as the most important determinant in this context. Interestingly, the incubation with amphiphiles labeled *via* IEDDA had to be carried out *without* FBS in the cell culture media, while otherwise almost no membrane fluorescence was observable. This effect might be explained by aggregation of the IEDDA reaction product with serum proteins, with the liposomal suspension either experiencing colloidal instability with subsequent precipitation or a quenching of the fluorophores. However, the exact causes are yet subject of ongoing investigations, and in order to prevent unwanted interaction with serum, supplementation of FBS was omitted in the subsequent experiments during the incubation and observation periods. Although these findings render the applicability of IEDDA limited in this context, further optimization of the polymer and tetrazine structures can be expected to overcome these issues.

Taken together, these results illustrated IEDDA as yet another type of surface conjugation chemistry for the established liposome system, and allowed in principle for the post-preparational derivatization of liposomes with two different functionalities in a site-selective

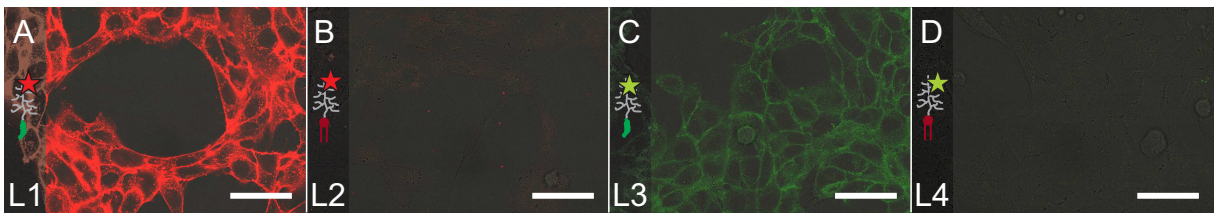

Figure 3.23: RBE4 cells incubated with liposomes L1-L4, incorporating amphiphiles 5-8 for 4 hours. The Atto 488 tetrazine-labeled amphiphiles (C & D) showed similar membrane exchange characteristics as their azide-labeled analogues. Scale bar represents 50 µm.

manner. The next section, therefore, moves on to discuss the combination of the available amphiphiles 5-8 in liposomes L5-L8.

Orthogonal click derivatization of the liposome surface

To this end, the presented studies involved the derivatization of liposome surfaces either with multiple molecules *via* the same chemistry (Section 3.2), or different types of liposomes with particular conjugation routes. CuAAC and IEDDA as established tools for end-group specific conjugation were next applied to liposomes that contained both alkyne *and* norbornene residues on the same particle. Since both conjugation routes are selective towards either alkyne or norbornene moieties, a site-selective derivatization was conducted in a one-pot reaction. The schematic principle is visualized in Figure 3.24, illustrating the possibility to indirectly confirm the selectivity of the reactions by making use of lipid anchors with different membrane stabilities.

Dual-labeled liposomes were prepared by a permutation of the available lipid anchors with either norbornene or alkyne residues, which yielded liposomes L5-L8. When RBE4 cells were incubated with these vesicles, they readily developed intense membrane fluorescence in all cases, where cholesterol-based amphiphiles were the respective acceptor for conjugation. Figure 3.25 presents the results from this *in vitro* investigation. Cells exhibited green and red membrane fluorescence for liposomes L5, which contained only amphiphiles anchored with cholesterol. On the other hand, fluorescence was negligible for fluorophores anchored with BHG-based amphiphiles on the liposome membrane, which was in agreement with previous results. It should be noted that the incubation of cells has been performed with the same concentrations of fluorophore-bound amphiphiles, in order to ensure that the differences in fluorescence originated from the structural properties of the lipid anchorage. However, the findings can

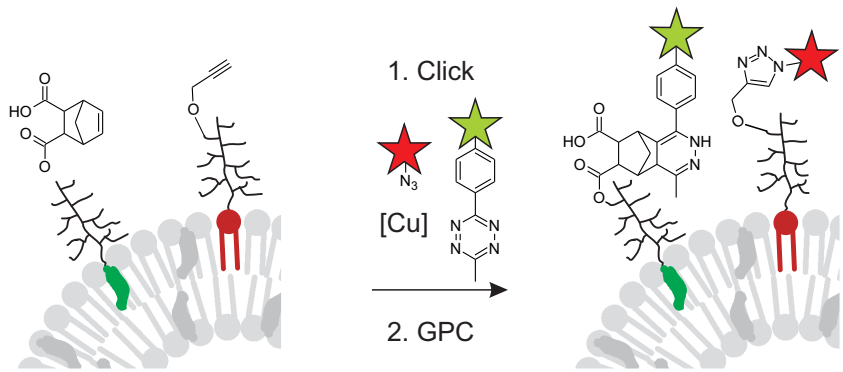

Figure 3.24: Schematic of one-pot orthogonal click reaction on the liposomal surface. Tetrazines and azides site-selectively react with different amphiphile populations on the particle surface.

also be considered as an indirect proof of site-selectivity for the liposome derivatization, which might not be resolvable by conventional analytical techniques. Amounts required for analysis by NMR spectroscopy exceeded the scale of preparation and analysis is in general challenging without the laborious isolation of liposome components. MS-based techniques were impeded by unspecific molecular weights of the ions of interests due to the polymers size distributions. The presented method indirectly provided evidence of the site-selective surface derivatization and therefore represented an elegant solution to this nontrivial question regarding the low amounts of analyte that were available.

Having established the orthogonal post-preparational liposome derivatization in principle, the findings suggested that the stability of the amphiphile anchorage might be exploited in the case of therapeutic drug delivery, *e.g.* to limit the time of circulation in the blood stream by making use of the desorption of sterically stabilizing amphiphiles, as demonstrated earlier.[276] However, since cholesterol can be classified as a very popular anchor for ligand-directed targeting,[92] more detailed investigations on the implications of these desorption processes were conducted, as described in the next section.

Folic acid-mediated targeting

Considered by many as one of the most promising research fields in cancer therapy, ligand-directed nanoparticle targeting is still hampered by the low availability of efficient conjugation methods to immobilize valuable ligand structures on particles. After CuAAC and IEDDA have been established in proof-of-principle studies that involved fluorophores, these conjugation routes were next applied in functional targeting studies to assess their applicability. As a small molecule targeting ligand, folic acid was selected, which can arguably be characterized as the best established small molecule ligand with a large number of reports concerning the targeting of liposomes.[144, 277] Recently, Ross et al. reported on the synthesis of a folic acid azide (FAZ, Figure 3.26A) derivative bearing an azide moiety for convenient application in CuAAC

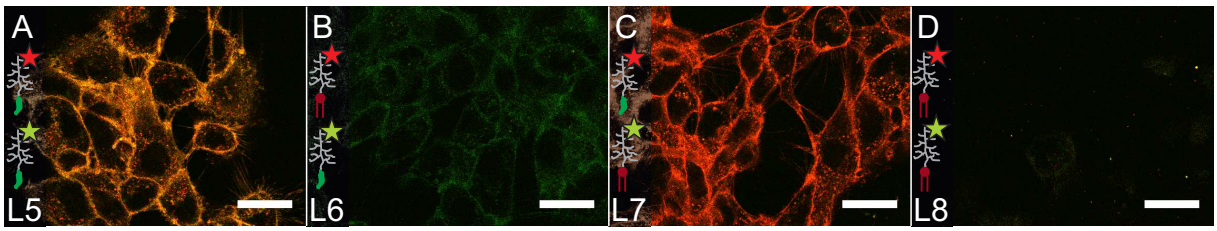

Figure 3.25: RBE4 cells incubated with liposomes L5-L8, labeled with Alexa 594 azide (red) *and* Atto 488 tetrazine. Cells showed intense membrane fluorescence whenever cholesterol-anchored amphiphiles were carrying the fluorescent label. Scale bar represents 25 µm.

chemistry, which is, as of late, also commercially available.[278]

The general requirement for the application of *any* molecules within the presented post-preparational functionalization concept was to have either azide or tetrazine derivatives of such available. However, one additional important prerequisite was a sufficiently high hydrophilicity of these molecules, and with such, a good solubility in water, in order to prevent potential interaction with phospholipid membranes or the used polymers. It turned out that folic acid exhibited unfavorable properties regarding these prerequisites, which resulted only in negligible yields in surface conjugation for the described post-preparational derivatization routes. Therefore, the protocol was re-sorted to apply FAZ in a conjugation reaction with the polymeric amphiphile *prior* to formulation of liposomes, as depicted in Figure 3.26B. In a second step, orthogonal click chemistry was applied after formulation to specifically label the available amphiphiles in order to follow the fate of these compounds *in vitro* (Figure 3.26C).

As detailed in the materials section, the conjugation reaction *before* formulation was carried out in ethanolic solution, in which the polymeric amphiphiles were expected to be present in micellar form and therefore with end groups that were sterically available for conjugation. Since liposome formulation was typically conducted on a 5 mg lipid scale, the previously discussed challenges in analytic evaluation of reaction yields were also true for the FAZ conjugation. The total amount of amphiphile was typically 422 nmol (5 mol% of the batch size and therefore 1-2 mg), which already was a very low amount of analyte for conventional analytical techniques. Additionally, keeping with literature,[279, 280] only 1% of the amphiphile was derivatized by using 4 nmol FAZ in the click reaction. Therefore, the quantitative consumption of FAZ was validated via high performance liquid chromatography (HPLC) as shown in Appendix 7. Potentially, a sophisticated (U)HPLC verification coupled with highly sensitive mass spectrometry might be used for product quantification, but was unavailable at this point.

Liposomes equipped with folic acid and Atto 488 and anchored either with BHG- or cholesterol-based amphiphiles were next investigated *in vitro*. Therefore, the *in vitro* system was switched to KB cells, a nasopharyngeal carcinoma cell line known to overexpress the folate receptor (FR) and well-established in folic acid targeting.[281, 144] The FR expression was maximized by omission of folic acid in the cell culture media, which was done for 3 days prior to seeding the cells in microscopy slides. As a control experiment, folic acid was supplemented to the cell culture media in a 100 µM concentration in order to chase the FA-mediated surface binding, which earlier has been shown to efficiently prevent this specific interaction.[279] Figure 3.27 presents KB cells, which were incubated with liposomes L6 and L5, bearing both Atto 488 and folic acid at the terminal apex of either BHG-based amphiphiles (A, B, L6) or cholesterol-based amphiphiles (C, D, L5). Here, both azides were conjugated to the amphiphiles prior to the formulation in a one-pot CuAAC reaction, while the liposomes were additionally functionalized with SulfoCy5 tetrazine on a cholesterol-based amphiphile after formulation. While a strong

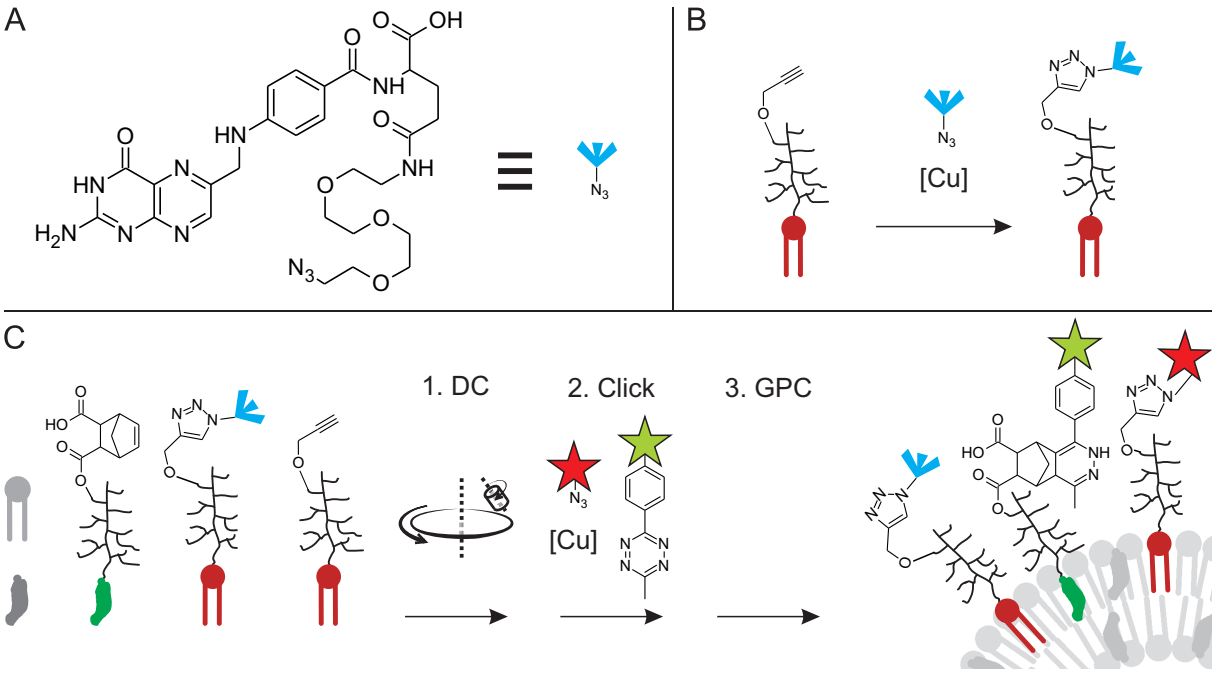

Figure 3.26: A: Structure of folic acid azide and its schematic depiction. B: Schematic of CuAAC with the amphiphile prior to liposome formulation, typically carried out in EtOH. C: Schematic of preparation of trifunctional liposomes. After functionalization of an amphiphile fraction fit FAZ prior to formulation, after DC, post-preparational functionalization and GPC to remove residual free fluorophores, trifunctional liposomes are yielded.

membrane-located green fluorescence was observed also for the BHG-based amphiphiles in L6 (Fig. 3.27A), this interaction was completely inhibited by supplementation of free folic acid (B), which allowed only the SulfoCy5-labeled cholesterol-amphiphiles to stain the lipid structures in the expected way. However, when all functionalities were linked to cholesterol-based amphiphiles, membrane fluorescence was not completely prevented (D), but yet decreased to a certain extend, especially in the green fluorescence channel. These results confirmed therefore also a successful conjugation of the functional folic acid, which facilitated a highly specific cell surface binding that was inhibited by a supplementation of free folic acid. Additionally, this concept represented the first approach for a site-specific orthogonal functionalization of both functional targeting ligands *and* fluorophores to different amphiphiles on the same nanoparticle, a strategy, that demonstrated the structure-function relationship of the lipid anchors in a clear way.

One important advantage of the established orthogonal conjugation toolbox in connection with the small scale liposome preparation was the relative ease, to flexibly test *e.g.* different reaction conditions, ligand densities or simply lipid compositions. Furthermore, findings from well-established targeting ligands like folic acid might easily be transferred to novel, small molecular ligands, in order to assess their targeting qualities. While Figure 3.27 already gave weak evidence on potential drawbacks of cholesterol as a lipid anchor for targeting purposes, the following experiments were conducted to gain deeper insights into the targeting capabilities of cholesterol-bound folic acid.

Targeting efficiency is low with cholesterol-based amphiphiles.

The strong staining behavior of cholesterol-based amphiphiles that anchored fluorophores implied also undesired effects on cholesterol-bound targeting ligands. For more detailed analysis, a liposome system with a strong and specific folate-dependent cell surface binding was employed. These liposomes contained folate conjugated to the terminal alkyne moiety of the BHG-PEG-alkyne amphiphile 10 or the correspondent cholesterol derivative 9, Chol-PEG-alkyne, and abbreviated as liposomes L11 and L12, respectively, as listed in Table 3.6. Both formulations also contained *hb*PG amphiphile 11, that was separately functionalized with Atto 488 azide, in order to track the BHG-based amphiphiles. Furthermore, the fluorescent lipid membrane tracker DiI was used in a concentration of 0.1 mol% with respect to the lipid composition as a model lipophilic cargo, integrated in the liposomal membrane.

Figure 3.28 displays KB cells that were incubated with the multifunctional liposomes L11 and L12 (A, D) and also co-incubated with free folic acid (B, E). The BHG-anchored folate in L11 facilitated a substantial surface binding of particulate structures, while a colocalization of green and red fluorescence indicated the integrity of the particles. This interaction was

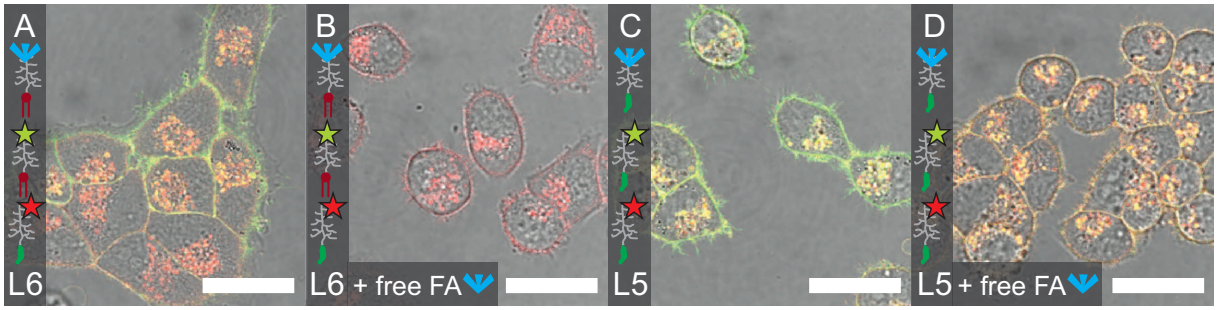

Figure 3.27: KB cells, incubated with FAZ-, Atto 488 azide- and SulfoCy5 tetrazine- functionalized liposomes L6 (A, B) and L5 (C, D) and chased with free folic acid (B, D). The specific interaction in A was efficiently chased with an excess of folic acid (B). If the both fluorophores were cholesterol-anchored, the membrane fluorescence was only reduced slightly. Scale bar represents 25 µm.

Table 3.6: Compositions of liposomes L9 - L12

ID	Composition	Ratio	Functionality
L9	EPC : Chol : 9	55 : 40 : 5	P
L10	EPC : Chol : 10	50 : 45 : 5	P
L11	EPC : Chol : 10 : 11	50 : 45 : 1 : 4	P
L12	EPC : Chol : 9 : 11	51 : 44 : 1 : 4	P
L13	EPC : Chol : 11	50 : 45 : 5	P

Functionality: Propargyl (P)

classified as specific, since supplementation of free folic acid led to complete suppression of the surface binding (B). Of note, the fact that most vesicles remained on the cellular surface is in good agreement with recent reports by the Chau group.[282] In this particular contribution, they reported that folate receptor-mediated uptake showed only slow internalization kinetics for larger particles like those investigated (150 nm), which therefore predominantly remained at the surface. Also for L12, a certain binding to the cellular membrane was observable (D), which in this case was not decreased by the addition of free folic acid (E). This type of unspecific interaction was presumably due to the loss of sterically stabilizing Chol-PEG-amphiphiles, which consequently would have led to a decrease of the surface inertness and therefore to unspecific adhesion to the cellular surface. The amphiphile exchange of both FAZ-functionalized Chol-PEG-amphiphiles and of residual Chol-PEG-alkyne molecules is visualized in Fig. 3.28F. A staining was in this case not observable, since labeling has been omitted for these structures. In total, the findings displayed clearly a benefit of more stable anchorage for ligands in the liposomal bilayer, and the stronger desorption of cholesterol amphiphiles implied potential drawbacks for ligand mediated targeting purposes.

A low stability of targeting ligands on the vesicular surface is in most settings unwanted. KB cells in Figure 3.27C showed yet a certainly stronger green fluorescence compared to the cells in Figure 3.27D. This difference was interpreted as a type of "specificity" of the observed surface interaction, that in this case led to a higher content of labeled amphiphiles on the surface. The folate-dependent interaction was not prevented completely if folate was anchored with cholesterol, which to a certain extend also justified the popularity of cholesterol as a lipophilic anchor for such active targeting systems.[92] However, a clear difference was identified between the folate-dependent interaction of the liposome systems displayed in Figures 3.27A and 3.28A. In Figure 3.27A, the whole membrane of cellular structures was stained in a rather diffuse manner, while in Figure 3.27 only particulate structures were adhering to the cellular surface. Taken together, these observations suggested a difference in the type of membrane interaction, which was investigated in detail and which will be discussed in the following section.

BHG-*hb*PG-folate amphiphiles desorb from the liposome surface.

The ligand-directed targeting with folic acid with fluorescently-labeled nanoparticulate structures can has been expected to cause also the observation of particulate structures by CLSM. While the cells displayed in Figure 3.28A showed particulate structures on their surfaces, the cellular membranes displayed in Figure 3.27A were stained in a diffuse and unstructured manner. The major difference between the liposome systems used in the corresponding experiments was the type of polymer that incorporated the folate residue. Only linear PEG chains led to the observation of particulate structures, that also showed a colocalization of labeled amphiphiles

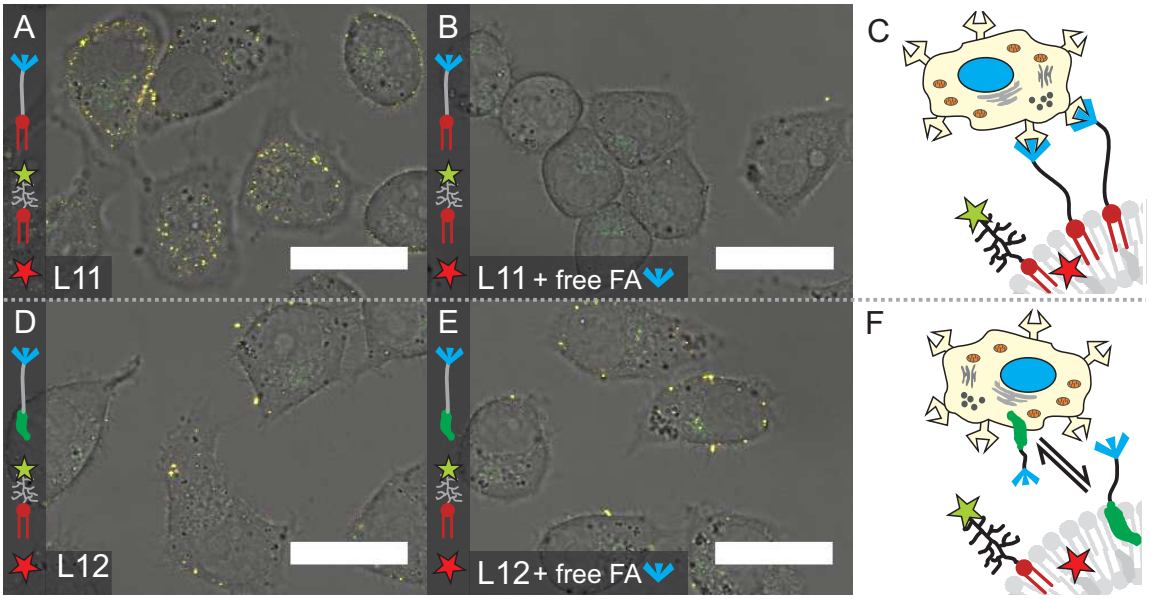

Figure 3.28: KB cells, incubated with liposomes L11 (A+B) and L12 (D+E), bearing BHG- and cholesterol-bound folate, respectively. The strong cell surface adhesion (A) for L11 was specifically chasable with free folate (B), it appeared to be folate-mediated (C). However, lower cell surface binding (D), which was also not chasable and therefore presumably unspecific (E) can be explained with membrane exchange of amphiphiles (F). Scale bar represents 25 µm.

and fluorescent cargo. This observation suggested that the vesicles were intact. Consequently, the *in vitro* interaction of BHG-*hb*PG-folate liposomes that encapsulated sulforhodamine B was investigated next, which is displayed in Figure 3.29. Consistently, the cells developed a strong green membrane fluorescence (A), which was prevented by supplementation of free FA (B). In contrast to Figure 3.28A, no colocalization of green amphiphile fluorescence with the red fluorescence of SRB was observed. These findings suggested that the cell surface staining with fluorophores was not caused by intact liposomes, but rather by labeled amphiphiles that appeared to desorb from the liposome surface. However, this type of interaction clearly seemed to be folate-dependent, since free folic acid was able to efficiently inhibit the membrane staining. In conclusion, the folate-dependent desorption was only observable with BHG-based amphiphiles that incorporated *hb*PG, and not with linear PEG. Taken together, these observations suggested that the observed amphiphiles were prone to multiple functionalization with both FAZ *and* fluorophore, as illustrated in Figure 3.29C.

In order to investigate the potential simultaneous functionalization of *one* amphiphile with FAZ and Atto 488 azide, the derivatization reaction of the amphiphiles *before* formulation was re-sorted. In a one-pot reaction approach, both azides were mixed and simultaneously conjugated to the amphiphile, this mixture was then used for liposome formulation. In a comparative approach that utilized separate reactions, each of the azides was combined with

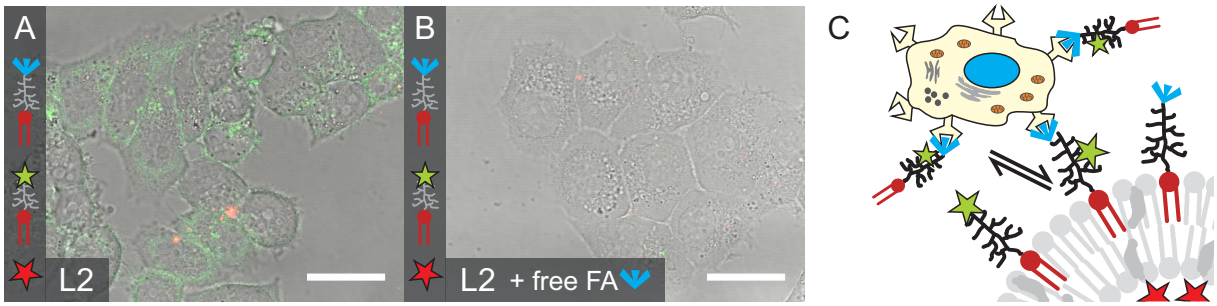

Figure 3.29: KB cells, incubated with Atto 488 labeled liposomes L2 (green) loaded with SRB (red). Cells developed a significant membrane fluorescence (A) which was chasable with free folic acid. Fluorescence from cargo was not colocalized with fluorescence from amphiphiles. The observed effects were presumably due to a multiple functionalization of amphiphiles, which allowed for desorption from the liposome membrane (C). Scale bar represents 25 µm.

the half amount of the needed amphiphile, and the resulting labeled amphiphiles were combined for formulation after the removal of copper as detailed in the materials section. Figures 3.30A and D illustrate these processes schematically for the one-pot reaction and the two separate reactions, respectively. As expected and in agreement with the observations from Figure 3.27A, KB cells incubated with the one-pot reaction products developed a strong membrane fluorescence (Figure 3.30B), which was also inhibited by supplementation of free FA (C). Interestingly, the conjugation of FAZ and Atto 488 in separate reactions led to the observation of particulate structures on the cellular surface, comparable to the BHG-PEG-folate liposomes in Figure 3.28A. Again, the interaction was sensitive towards a supplementation of free folate (F), a finding that emphasized the folate-dependency. While also particulate structures on the cell surface were observable in Figure 3.30B, a final experiment was conducted to confirm these structures as intact liposomes.

In order to assess the folate-dependent binding of intact liposomes after the one-pot conjugation with FAZ *and* fluorophore azides, multifunctional liposomes were prepared using FAZ, Atto 488 azide and SulfoCy5 azide. Figures 3.31A and C illustrate the click functionalization of the used amphiphiles, that employed either SulfoCy5 azide (A) or Atto 488 azide (C) in a separate reaction. The respective other fluorophore azide was combined with FAZ. The resulting liposomes contained in principle the same fluorophore and ligand configuration, however, distinct differences were observable after incubation of KB cells with such systems. Figures 3.31B and D display cells incubated with these liposomes. In both cases, cells developed a strong membrane fluorescence in the channel of the fluorophore which was conjugated simultaneously with folic acid azide (B: SulfoCy5, red channel. D: Atto 488, green channel). The correspondent fluorophore that was conjugated separately, only colocalized in particulate structures on the cellular surface (yellow color in the corresponding figures). These findings indicated that

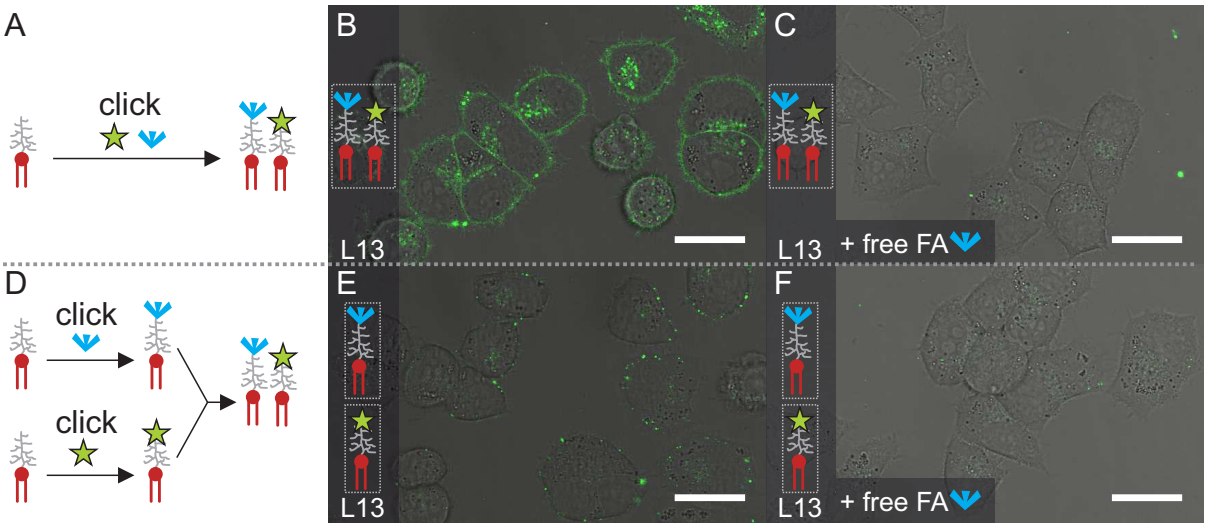

Figure 3.30: Schematic of a one-pot amphiphile conjugation (A) and KB cells, incubated with the resulting FAZ- and Atto 488-labeled liposomes L13 (B). Cells developed a significant membrane fluorescence (B) which was chasable with free folic acid (C). In comparison, the separate functionalization with the azide compounds (D) led to particulate fluorescence on the cellular surface (E), which was also preventable with free folic acid (F). Dashed rectangles indicate combined conjugation reactions. Scale bar represents 25 µm.

the type of fluorophore seemed not to influence the observed interaction, since the crosswise exchange in the conjugation reactions did not alter the mode of interaction. Furthermore, the observed particulate colocalization of fluorophores on the cellular surface suggested the binding of intact vesicles, while a substantial fraction of folate-amphiphile seemed to desorb from the liposomes. A postulated mechanism is depicted in Figure 3.31E, which also proposes a subsequent insertion of the desorbed lipids in the plasma membrane (E, 2.), which represents the arguably most probable target location for such amphiphilic compounds and is in good agreement with the observed internalization of fluorescently labeled structures.

Taken together, these results suggested a folate-dependent desorption of folate-amphiphile conjugates and a subsequent insertion into the plasma membrane of cells. The simultaneous conjugation of FAZ and a fluorophore azide resulted in liposomes, that led to substantial membrane fluorescence when incubated with cells. The observed behavior was presumably due to the formation of dual-functionalized amphiphiles, which was theoretically possible for the employed amphiphile 11, that contained 2 alkyne moieties per polymer chain. However, since FAZ and the fluorophore azides were only applied in 1 mol% with respect to the amphiphile, a double functionalization was expected to be rather unlikely, with a statistical probability of only $1\% \times 1\% = 0.01\%$. Without having examined the absolute amount of fluorophores on the cell surface, it might not be expected that the observed fluorescence was caused only by the 0.01% of amphiphiles that were statistically double-functionalized. One possible explanation for the

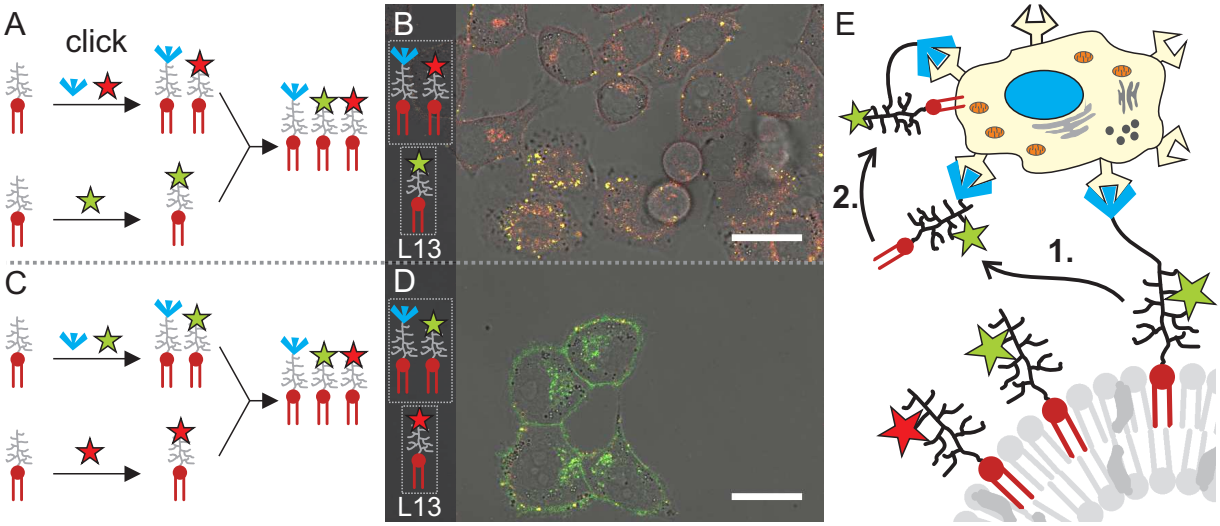

Figure 3.31: Schematic of an amphiphile conjugation with FAZ, Atto 488 and SulfoCy5 azide, employing either Atto 488 azide (A) or SulfoCy5 azide (C) separately. After incubation of KB cells with the resulting liposomes, cells readily developed a strong membrane only in the channel of the fluorophores, which were conjugated in the one-pot reactions (B: SulfoCy5, red. D: Atto 488, green). The seperately conjugated fluorophores colocalized with the respective counterpart in particulate structures on the cell surface, suggesting integrity of these vesicles. Exemplary for the liposome system in A and B, the proposed mechanism (E) relies on the formation of double-functionalized amphiphiles that facilitate folate-dependent binding. The missing colocalization of fluorophores on the cellular membranes suggest a desorption of these multifunctional amphiphiles (1.) and presumably a subsequent insertion in the plasma membrane (2.). Dashed rectangles indicate combined conjugation reactions. Scale bar represents 25 µm.

preferential formation might be the ligation of copper by the resulting triazole-containing conjugates and therefore a type of intramolecular catalysis of the second conjugation reaction. A higher number of terminal alkyne groups might also be an explanation, since the degree of functionalization was obtained by ^{1}H NMR spectroscopy and no inhomogeneity in the sample was considered.

A tendency of the used amphiphiles to desorb from the liposome surface in a folate-dependent manner has been demonstrated. Consequently, this might result in more general implications on lipid-anchored targeting ligands. Typically, terminally modified derivatives of phospholipid-PEG conjugates are used for such purpose, *e.g.* DSPE-PEG-folate conjugates.[144] Classical PEG-based polymers comprise the intrinsic disadvantage to not allow for the attachment of more than one functional moiety, due to just one available polymer chain end. Due to the lack of proper analytical methods it is not surprising, that nobody previously has reported on an increased desorption of such amphiphile-anchored ligands. Although it was not possible to visualize the desorption of BHG-PEG-folate compounds, similar characteristics can also be expected for such. The findings illustrated yet another important advantage of polyglycerol-based amphiphiles, which allowed for simultaneous targeting *and* visualization on a molecular resolution.

Finally, a desorption and therefore a potential destabilization of the liposomes can in certain cases also be beneficial, *e.g.* when long-circulating liposomes are intended to unspecifically interact with the target tissue of interest after enrichment *via* the EPR effect. However, since in the presented cases only a marginal fraction of amphiphiles contained folate residues, the destabilizing effect were presumably insignificant. Another strategy for liposome destabilization in a stimulus-responsive manner is presented in the next section.

3.4 Acidic shedding of liposomal particles

Abstract Liposomal pharmaceutics with steric stabilization by PEGylation have been in clinical application for over two decades. While the polymeric shell was shown to reduce hepatic clearance of these systems, it also was shown to cause a higher stability of the particles after arrival at the target tissue. Here, a new concept for cleavable polymeric amphiphiles that contained acetal or ketal groups has been investigated, including the the assessment of cleavage kinetics within the native environment of liposomal membranes. At lysosome-like pH values of 5.4, acetals and ketals exhibited half life times of 20 hours and 15 minutes, respectively. The conceptual system represents a promising strategy to specifically tailor the polymer stability to the actual needs.

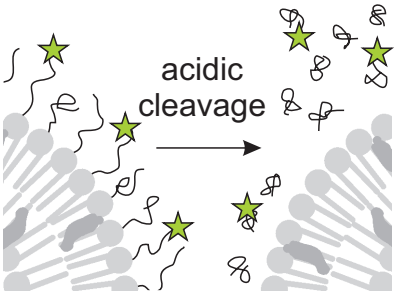

Liposomes represent one of the most important classes of nanoparticulate drug delivery vehicles, and have been in clinical application for over two decades. DOXIL was the first nanodrug that has been approved by the FDA, and consists of PEGylated liposomal doxorubicin for tumor treatment.[284] Since the passive tumor targeting of such STEALTH liposomes is typically dependent on the EPR effect, they are designed to maximize blood circulation times.[38] However, after arrival at the target tissue, the polymeric shell has been shown to also inhibit further interaction and the local release of cargo, which motivated the development of stimuli-responsive particles.[285] As a possible route, the utilization of pH-stimulated shedding of liposomal vesicles has been reported as feasible,[286] typically induced by metabolic acidosis within the tumor milieu and therefore a prevalent decrease of pH.[101]

The group of Prof. Frey has recently reported on the incorporation of acid-cleavable units within specifically tailored polyether structures,[110] a concept, which was applied to liposomes in this study (Figure 3.32). The use of the reported concept in cleavable amphiphiles was expected to impart specific features to the resulting liposomes, *i.e.* (i) a pH-stimulated shedding of the liposomes due to pH drop in the tumor tissue or after endocytic uptake in a lysosome, (ii) the subsequent interaction of the destabilized liposome membranes with cellular or endosomal membranes, in order to deliver payload and (iii) the potential renal elimination of the resulting polymers of lower molecular weights, which is the typical elimination mechanism

Parts of this chapter were published in [283, submitted]. This publication has been prepared in close cooperation with the group of Prof. Holger Frey in Mainz, under contribution of Dr. Sophie S. Müller and Matthias Worm. Fabian Jung contributed substantially to liposome preparation, kinetics measurements and assay design during an internship.

for small polyether structures.[287] The present study describes first basic investigations on toxicity and cleavage kinetics of acetal- and ketal-containing amphiphiles, that were formulated in novel, sterically stabilized liposomes.

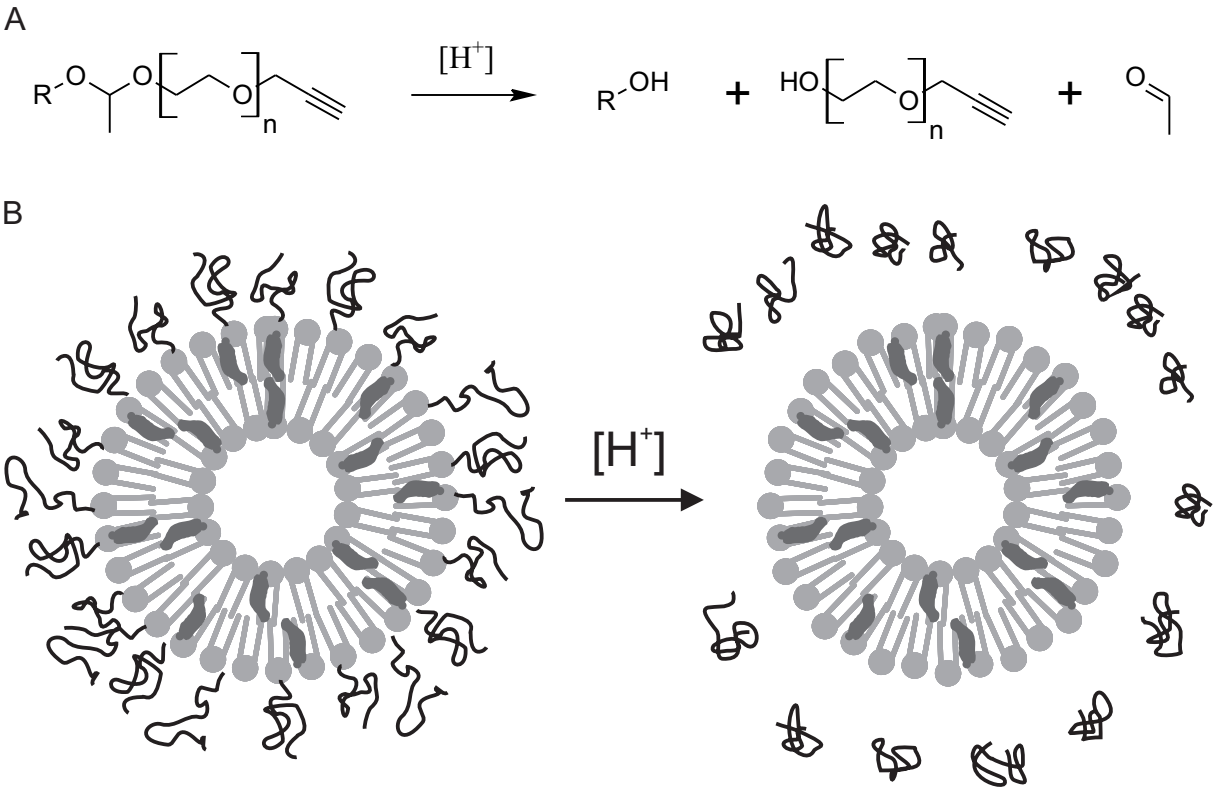

Figure 3.32: Schematic presentation of acid-catalyzed cleavage of acetal-containing polymers (A), that, if incorporated in amphiphiles, allow for a shedding of the liposomal polymer hull after acidification (B), e.g. in lysosomes.

Lipid structures

Lipid structures have been designed and synthesized by Dr. Sophie S. Müller and Matthias Worm as previously described,[110] and were based on cholesterol or bis(hexadecyl)glycerol as lipophilic anchors. In order to apply the previously established surface derivatization routes based on CuAAC to these systems,[264] subsequent functionalization with propargyl bromide were carried out to yield the corresponding alkyne-derivatives, *e.g.* α-(1-(cholesteryloxy)ethoxy)-ω-hydro-PEG_{46}-CH_2-C≡CH (Ch-Ac-PEG_{46}-Alkyne). The different amphiphiles that were employed in the present study are depicted in Figure 3.33. Compounds 1 and 3 were used as negative controls in cleavage experiments as they were missing cleavable building blocks. In contrast, compounds 2 and 4 were incorporating acid-labile acetal groups, while compound 5 was incorporating a ketal group, which was expected to facilitate an increased acid-lability compared to acetal groups.

Table 3.7 lists compositions and characteristics of corresponding liposomes, that were yielded after incorporation of compounds 1-5 and formulation *via* dual centrifugation. Additionally, CL and SSL were prepared as references. Liposomes were characterized by diameters between 150 and 190 nm, as obtained by DLS or NTA, and therefore represented nanoparticulate structures in a size range that in principle allows for pharmaceutical applications. Polymers were applied in a 5 mol% fraction, while either cholesterol or EPC was substituted with cholesterol- or BHG-based amphiphiles, respectively. The molecular weights of all polymers ranged between 2000 and 3300 g/mol, a size-range that was selected due to its proximity to pharmaceutically applied polymeric amphiphiles, such as in DOXIL.

The pharmaceutical application of sterically stabilized liposomes generally depends on a maximal biocompatibility of the components, in order not to cause unwanted toxicity from the particle system itself. While cholesterol and EPC are ubiquitously present in mammalian cell membranes and therefore nontoxic, the employed prototype compounds were of yet unknown influence on cellular systems and therefore subjected to a principal toxicity evaluation, as described in the following section.

Toxicity of cleavable liposomes

In order to evaluate potential toxicity of amphiphiles 1-5, the resulting liposomes L1-L5 were subjected to an *in vitro* toxicity assay, namely an MTT assay. In this well-established assay, the yellow 3-(4,5-dimethylthiazol-2-yl)-2,5-diphenyltetrazolium bromide (MTT) is reduced by cellular reductase enzymes to its corresponding purple and insoluble formazan derivative, (*E*,*Z*)-5-(4,5-dimethylthiazol-2-yl)-1,3-diphenylformazan. Therefore, the MTT assay allows to correlate the formation of formazan to the number of living cells.[288] Figure 3.34 displays the determined viabilities of cells that were incubated with each of the employed liposomes in a variety of lipid concentrations, normalized to an untreated control and in comparison to a cell population that was treated with 10% DMSO. Cells that were treated with CL and SSL did not show any reductions in viability, which is in good agreement to previous reports.[289] Treatment with cholesterol-based amphiphiles showed in general a higher toxicity especially in concentrations of 100 µg/mL, while all BHG-based lipids did not exhibit any substantial toxicity. The observed cytotoxicity of cholesterol-based amphiphiles that were incorporated in liposomes might have been due to the tendency to integrate into cellular membranes as described in the previous chapters, where cellular membrane trafficking potentially might have been perturbed. However, the observed effects illustrated yet another advantage of BHG-based amphiphiles.

Besides a high biocompatibility as the most important requirement, acid-cleavable amphiphiles for pharmaceutic application have to be characterized by a well-defined sensitivity towards

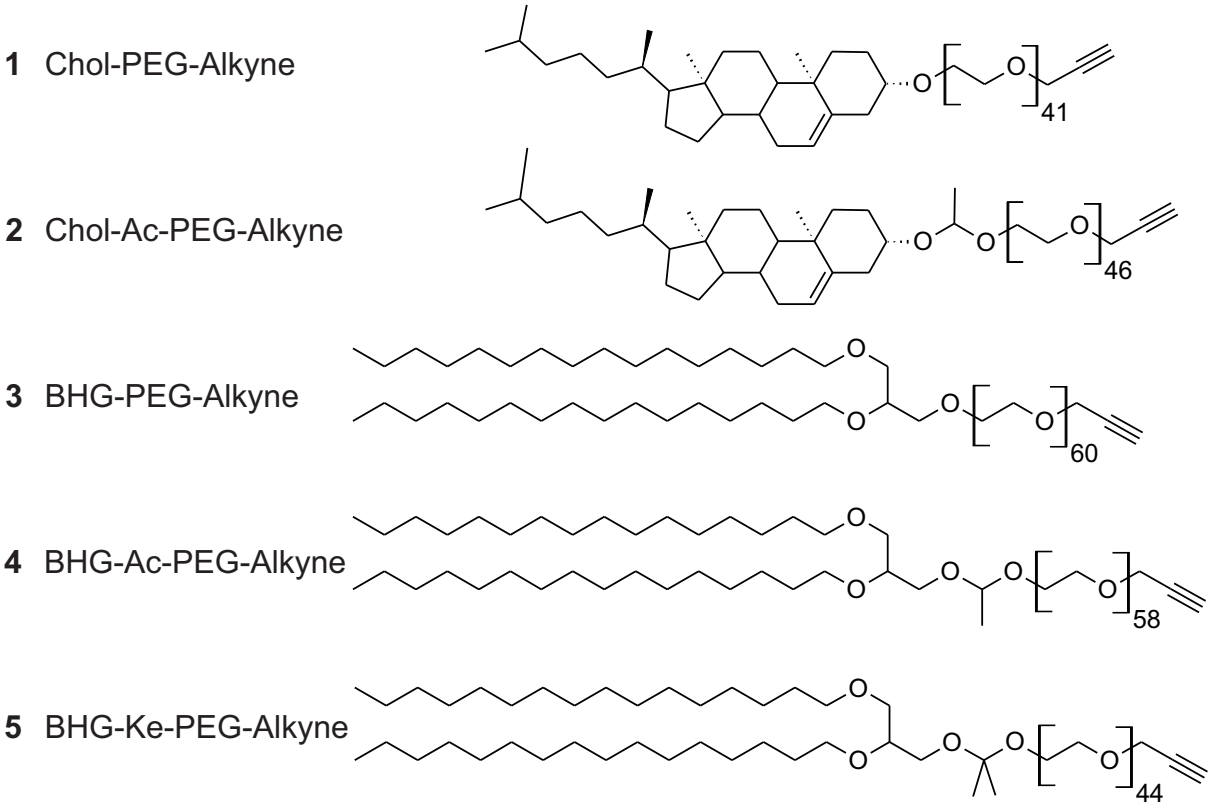

Figure 3.33: Structures of the investigated polymeric amphiphiles based on cholesterol (1, 2) and BHG (3, 4, 5). Compounds 1 and 3 did not contain any cleavable building block and served as references, compounds 2 and 4 contained acetal groups and 5 a more labile ketal.

Table 3.7: Compositions and characteristics of liposomes L1 - L5 and corresponding polymers 1-5.

			Polymers			Liposomes	
ID	Composition	Ratio	Structure	M_n / g/mol	M_w/M_n	Diam. ± SD (nm)	PDI
CL	EPC : Chol	55 : 40				146 ± 2.5[(b)]	-[(b)]
SSL	EPC : Chol	50 : 45 : 5	DSPE-mPEG2k		n.d	184.3 ± 4.2[(b)]	-[(b)]
L1	EPC : Chol : 1	55 : 40 : 5	Chol-PEG_{41}-Alkyne	2240	1.24	154 ± 2.2[(a)]	0.10[(a)]
L2	EPC : Chol : 2	55 : 40 : 5	Chol-Ac-PEG_{46}-Alkyne	2540	1.78	170 ± 2.8[(a)]	0.22[(a)]
L3	EPC : Chol : 3	50 : 45 : 5	BHG-PEG_{60}-Alkyne	3229	1.05	157 ± 7.5[(b)]	-[(b)]
L4	EPC : Chol : 4	50 : 45 : 5	BHG-Ac-PEG_{58}-Alkyne	3219	1.04	152 ± 5.3[(b)]	-[(b)]
L5	EPC : Chol : 5	50 : 45 : 5	BHG-Ke-PEG_{44}-Alkyne	2838	1.07	172 ± 4.0[(b)]	-[(b)]

Lipid anchors: Chol: Cholesterol, BHG: Bis(hexadecyl) glycerol, M_n: Number average molecular weight as determined by ^{1}H NMR spectroscopy. M_W/M_N ($Đ$): Dispersity index determined by SEC analysis using PEG standards. [(a)]: Determined via DLS[(b)]: Determined via nanoparticle tracking analysis (NTA)

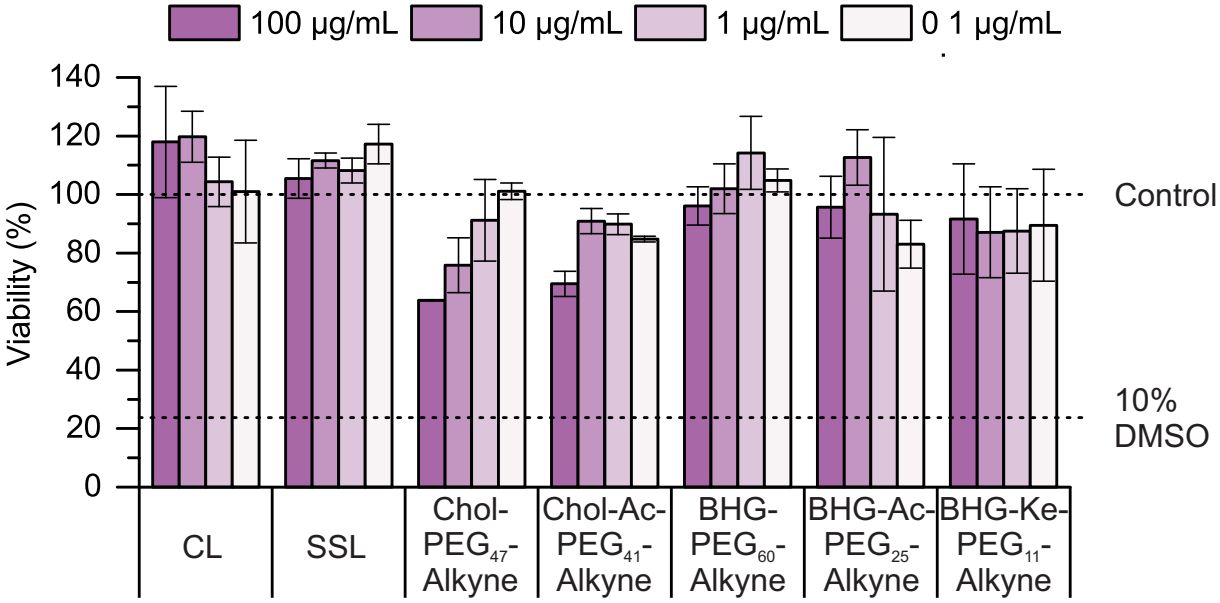

Figure 3.34: Toxicity study by MTT assay of liposomes L1-L5 as indicated by the corresponding polymeric amphiphile, in comparison to CL and SSL. In general, only cholesterol-based liposomes showed a certain toxicity in high concentrations. (n=3)

acidic cleavage. The ideal amphiphile should possess a stability high enough to ensure a reproducible and efficient formulation without any degradation, and low enough, to be readily cleaved in biological environments, which usually do not possess pH values below 5.[102] In order to further detail the applicability of the employed compounds, kinetic measurements of their acid-catalyzed degradation were conducted.

Cleavage analysis assays

In previous studies, the cleavage of acetal-containing polymers was either evaluated by NMR spectroscopy or by acid-catalyzed segregation of micellar amphiphiles in aqueous media.[110] Both of these methods were not applicable to amphiphiles that were formulated in liposomal particles, due to high background from the "main" components cholesterol and EPC, or due to no changes in colloidal stability during cleavage, respectively. In order to determine cleavage kinetics in the designated context of liposome shedding, two different assays were developed to address this question. As depicted in Figure 3.35A, alkyne-containing liposomes L1-L5 were first derivatized with Atto 488 azide to yield fluorescently labeled liposomes. These particles were then transferred to cleavage buffers with pH values between 2 and 8, and the shedding process analyzed by either fluorescence spectroscopy or by an electrophoretic analysis approach (Figure 3.35B and C, respectively).

For the *in situ* approach *via* fluorescence spectroscopy, the cleavage reaction was conducted in

a stirred and tempered cuvette inside the spectrometer. Over time, a pH-dependent increase of fluorescence emission was observed, which was correlated to the cleavage of the membrane-bound fluorophore. Control experiments revealed that this particular increase was not due to an acid-dependent reaction of the fluorophore itself. While the exact cause of this emission increase remained yet unclear, it might be explained with (i) a decrease of the inner filter effect due to the increase in spatial distance between fluorophore and particle; (ii) a decrease of the probability of quenching processes of the fluorophore or (iii) changes in spectral characteristics of the fluorophore due to different micromilieus. Furthermore, the employed amphiphiles were found to adsorb onto the cleaned glass surface of the cuvette, which was therefore saturated with uncleavable derivatives of the corresponding cleavable amphiphiles prior to the incubation.

The *ex situ* assessment involved the time-dependent collection of samples from a cleavage reaction with on-time neutralization and storage at -20 °C until further analysis. Subsequently, the samples were subjected to a polyacrylamide gel electrophoresis (PAGE), which separated liposomes from cleaved polymer-fluorophore conjugates (Figure 3.35C). Atto 488 was selected as a fluorescent probe due to its negative net charge under the electrophoresis conditions, and therefore allowed for electrophoretic migration. A first approach of electrophoretic analysis has been established in previous work, and illustrated that the migration of labeled amphiphiles is dependent on the charge of the fluorophore.[2] In the case of PAGE, intact liposomes did not migrate and therefore remained in the gel pocket, which allowed for a specific separation from low molecular compounds.

Figure 3.36 displays exemplary data from cleavage reactions of Chol-Ac-PEG_{46}-Alkyne that were conducted at different pH values and determined by the fluorescence spectroscopy assay. At pH 2, a very fast increase in fluorescence emission was observed, while at higher pH values only slow increases were measured. On the other hand, the stable derivative Chol-PEG_{41}-Alkyne showed no substantial increase over hours (red trace). However, while these findings rendered the assay qualitatively applicable for the assessment of cleavage kinetics, the reaction at pH 5 predicted the acidic cleavage within a lysosome to be very slow, which questioned the applicability of such systems. Due to the also critical findings regarding cholesterol-based amphiphiles that were presented in the previous sections of this thesis, the investigation of BHG-based amphiphiles was focused on in the following.

Figure 3.37 displays exemplary data that was obtained by the presented PAGE assay. Reactions were conducted in a reaction vial and time-point samples collected, subsequently neutralized to stop the cleavage reaction and loaded onto a polyacrylamide gel. Scanning on a fluorescence imager yielded gel scans as shown in Fig. 3.37A, with clearly separated liposomal residues in the gel pockets and polymers that migrated in the gel matrix. Additionally, the displayed intensities showed a positive correlation to the reaction times. The usage of polyacrylamide gels with a thickness of 2 mm was found to ensure an appropriate resolution of the separation,

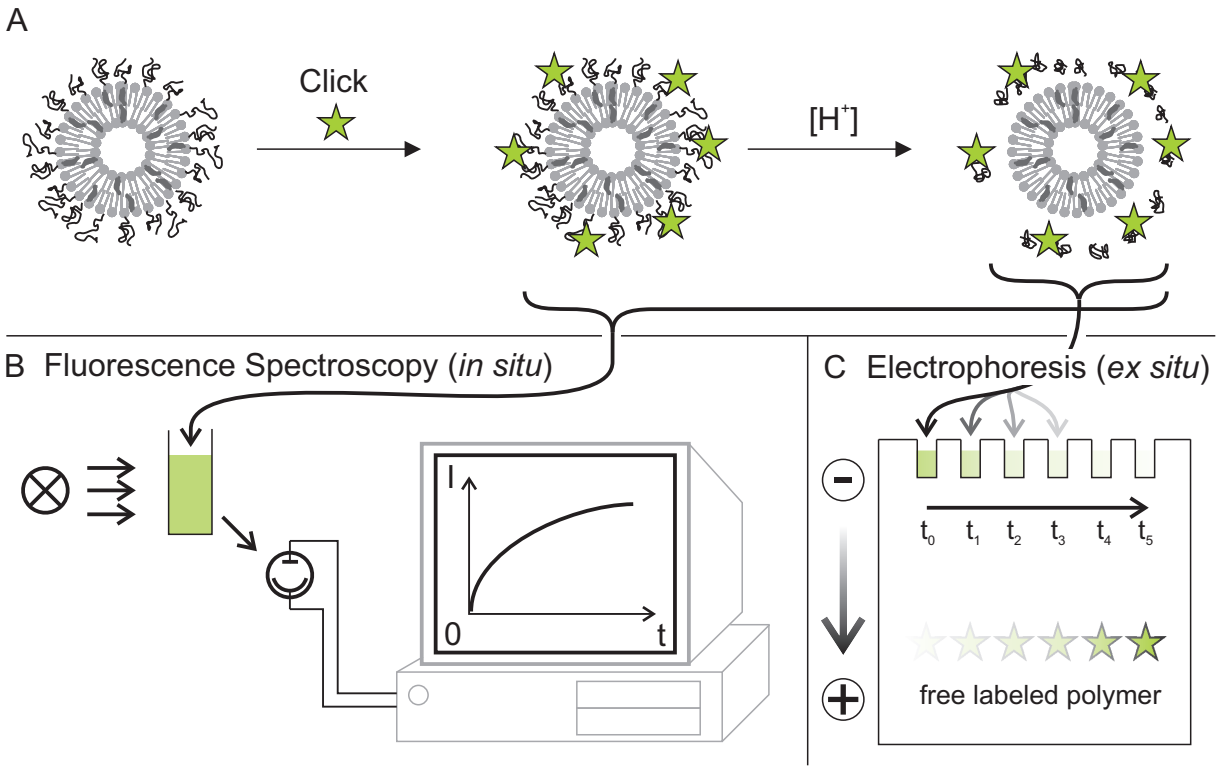

Figure 3.35: Schematic of the developed cleavage assays. A: Alkyne-bearing liposomes were post-preparationally functionalized with Atto 488 azide. Subsequently, the liposome suspension was acidified with buffer and the cleavage of labeled amphiphiles observed by fluorescence spectroscopy. B: In an in situ approach, the cleavage reaction was carried out in a stirred cuvette inside the spectrometer. Over time, a ph-dependent increase in fluorescence intensity was measured. C: Timepoint samples were collected from a cleavage reaction and subjected to PAGE, thus the cleaved polymer-fluorophore conjugates were separated from liposomes, that remained in the gel pocket.

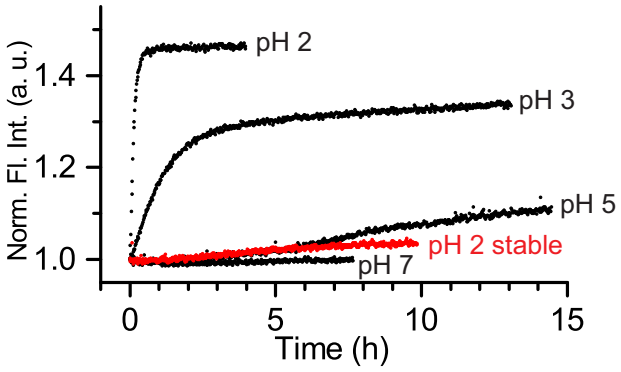

Figure 3.36: Exemplary data from the fluorimetric measurement of acid cleavage of Chol-Ac-PEG_{46}-Alkyne (black traces), compared to a stable derivative Chol-PEG_{41}-Alkyne. While fluorescence emission increased in the case of the cleavable amphiphile in a pH-dependent manner, no substantial increase in fluorescence was observed for the stable analogue.

which allowed for a precise band detection. Subsequent image analysis with ImageJ[290] yielded graphs as shown in Fig. 3.37B, that clearly illustrated the dependence of the reaction rate on the pH. The next section describes therefore the quantitative analysis of the reaction kinetics.

Cleavage kinetics

BHG-based amphiphiles that contained acetal and ketal building blocks were analyzed by abovementioned assays at 25 °C and half-life times from first order exponential fits were calculated. The differences between the *in situ* and *ex situ* assays depicted particular advantages of each, *e.g.* was the fluorimetric *in situ* measurement not readily applicable to long-term measurements, as solvent evaporation and degassing sporadically led to artifacts. Figure 3.38 illustrates the strong differences in reaction kinetics of the ketal containing liposomes, which rendered these particles not measurable with the PAGE assay. Appendix 9 displays this data with exemplary fitting results from a first order exponential fit, as the cleavage reaction in buffered media was expected to follow first order kinetics. Equation 3.1 describes the employed 3 parameter fitting function:

$$y = A_1 \times e^{(-x/t_1)} + y_0 \tag{3.1}$$

Additionally as seen in Appendix 9, correlation coefficients near 1 indicated a good agreement with first order kinetics. From the rate-determining constant t_1, Equation 3.2 leads to the half life time $t_{1/2}$:

$$t_{1/2} = \ln(2) \times t_1 \tag{3.2}$$

Interestingly, the measured half life times are in good linear correlation to the proton concentration, as displayed in Appendix 10. This dependence can be well described ($R^2 = 0.9467$) by equation 3.3:

$$t_{1/2}(pH) = 2 \times 10^{-6} \times e^{(2.2254 \times pH)} \tag{3.3}$$

An overview of half life times for compounds 4 and 5 are listed in Table 3.8. Where applicable, studies of both systems were conducted by utilizing both available assays, allowing for comparison of these results. In general, the half life times determined by the two assays were in very good agreement with only slight differences for the same particular liposome system. Furthermore, the substantially higher reaction rates for the ketal-containing amphiphiles rendered these structures as much more promising for pharmaceutical applications than the

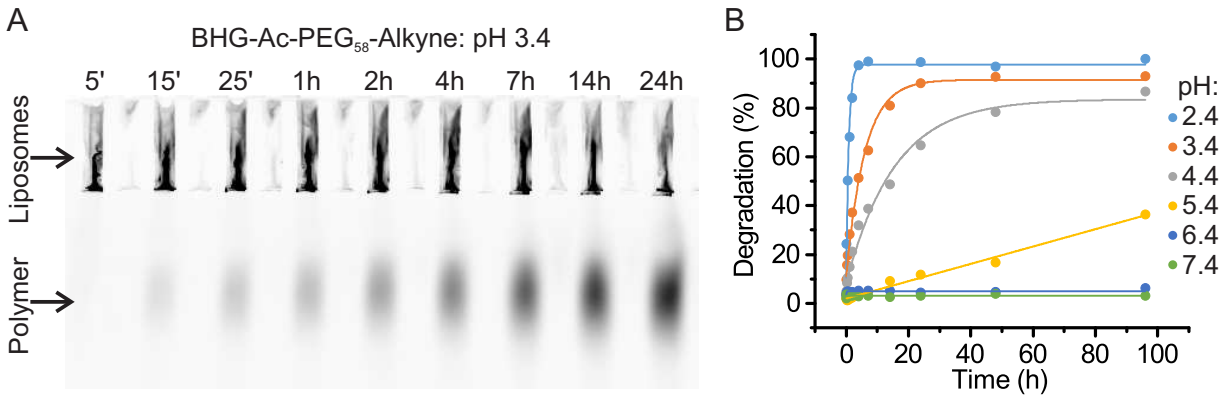

Figure 3.37: A: Exemplary gel fluorescence scan of timepoint samples from a cleavage reaction at pH 3.4 of liposomes that contained BHG-Ac-PEG$_{58}$-Alkyne, subjected to PAGE. While presumably intact liposomes and amphiphiles showed no migration, cleaved polymers migrated through the gel, which resulted in increasing emission intensities with longer incubation times. B: Values resulting from PAGE assay at different pH values with their corresponding exponential decay fits. The findings illustrated well the observed first order kinetics and the qualitative differences between amphiphiles.

corresponding acetal-compounds. However, the measured stability of the ketal compounds might potentially not be high enough, considering half life times of 20 hours at pH 7.4. While an application of such labile structures might be feasible with an on-time, bedside liposome formulation, typical clinically applied liposomes like DOXIL are provided as preformulated suspensions. One important advantage of liposome formulation *via* dual centrifugation is the theoretical possibility of an on-demand formulation in general, however, multiple technical issues like on-site purification have to be yet developed in order to render such applications possible.

Taken together, these findings illustrated the potential applicability of acetal- or ketal-containing

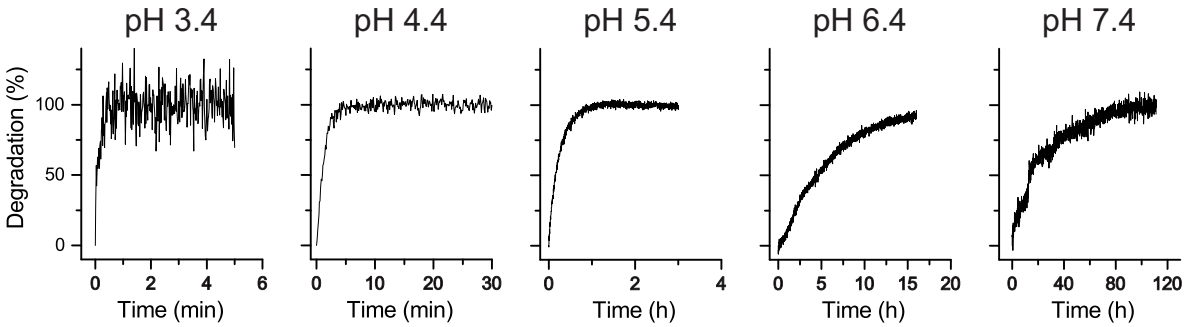

Figure 3.38: Fluorescence traces measured by the fluorimetric cleavage assay for BHG-Ke-PEG$_{44}$-Alkyne liposomes. Strong differences in reaction rate, as illustrated by the x-axis dimensions, impeded the determination of reaction kinetics *via* the PAGE assay.

Table 3.8: Half-life times of BHG-Ac-PEG$_{58}$-Alkyne and BHG-Ke-PEG$_{44}$-Alkyne at 25 °C.

	$t_{1/2}$ [BHG-Acetal-PEG$_{58}$-Alkyne] / h		$t_{1/2}$[BHG-Ketal-PEG$_{44}$-Alkyne] ± SD / h	
pH	PAGE	Fluorimetry	PAGE	Fluorimetry
2.4	0.62	1.04	-	-
3.4	3.78	4.20	-	0.002 ± 0.008 (n=4)
4.4	10.13	-	0.01	0.014 ± 0.004 (n=4)
5.4	20.88	-	0.15	0.18 ± 0.017 (n=3)
6.4	-	-	3.13	4.02 ± 0.96 (n=5)
7.4	-	-	13.13	21.95 (n=2)
8.4	-	-	88.17	104.60 (n=1)

polymeric amphiphiles in pharmaceutical applications. While acetal-based compounds exhibited half life times on the order of days, this type of degradation might display a route to eliminate polyether structures renally even after accumulation in body tissue, since such structures otherwise might not be metabolizable. Ketals on the other hand displayed fast cleavage kinetics, that allowed for cleavage within the order of hours at lysosomal pH. However, the sensitivity towards acidic environment also opens a set of questions regarding the shelf-life and potential bedside formulation of liposomes.

3.5 Application of microscale dual centrifugation to non-lipid particles

Abstract Dual centrifugation has evolved into a highly valuable method for the formulation of vesicular lipid particles, and combines efficient encapsulation with small scale batches. However, in recent years there has been an increasing interest in self-assembled polymeric particles, which were shown to allow for the specific design of their properties and also to outperform liposomes in stability. Here, microscale DC formulation with different polymeric amphiphile systems has been employed in a first proof-of-concept, and yielded either polymersomes or polymeric micelles, while the formulation characteristics of DC as e.g. high encapsulation efficiencies were maintained. The findings rendered DC as a promising alternative to conventional formulation methods for polymeric self-assembled nanoparticles.

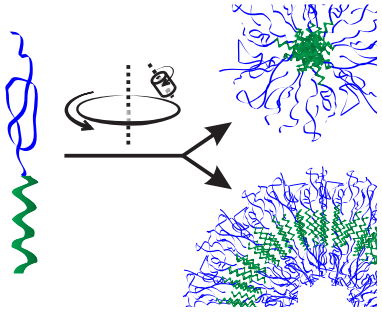

While liposomes have been in clinical application for over two decades, in the last years, artificial polymeric amphiphiles have developed to a level where such systems comprise relevant alternatives to lipid-based drug delivery vehicles.[292] A distinct advantage of self-assembled polymer systems is that they can be designed *ab-initio*, and therefore enable the use of sophisticated and highly functional compounds. Such systems were shown to comprise *e.g.* responsiveness to stimuli[293] or covalent coupling of pharmaceutically active molecules, *e.g.* ligands.[294] However, typical preparation procedures include film hydration[258] or solvent exchange methods,[295] which both are very demanding in time and material consumption as well as characterized by low encapsulation efficiencies for hydrophilic cargo. After having developed dual centrifugation to the level of mg-scale material consumption, the application of DC was therefore tested with novel polymeric systems in a proof-of-principle approach.

Polymersomes as drug delivery vehicles

The Zentel group recently reported on the preparation of diblock copolymers based on N-(2-hydroxypropyl) methacrylamide (HPMA) and lauryl methacrylate (LMA), which were found to efficiently form self-assembled nanoparticulate structures and to be potentially suitable for

Parts of this chapter were published in [291]. This publication has been prepared in close cooperation with the group of Prof. Rudolf Zentel in Mainz. The major part of the work has been carried out by Dr. Martin Scherer.

pharmaceutical application.[263, 296] Due their molecular architecture with high contents of hydrophilic polymer blocks, these particular polymer systems provided solely micellar structures. In this study, derivatives of such polymer systems were employed in order to yield vesicular polymersomes. These polymers were expected to require molecular weight fractions f of the hydrophilic block of $f = 35\% \pm 10\%$, which has previously been shown to be in a suitable range for the formation of polymersomes.[297] However, it turned out that a change to the more hydrophilic (DHPMA) was necessary to push equilibria from micelles towards vesicles, which were then formed with diblock copolymers of varying architecture. Figure 3.39 displays the general structure of such p(DHPMA)-*b*-p(LMA) polymers, as well a schematic of their self-assembly during dual centrifugation.

The polymers that were used in this study are listed in Table 3.9, including their specific molecular compositions and properties. Polydispersities near 1 indicated narrow size distributions and therefore the fulfillment of a potential requirement for medical application. Polymeric vesicles were prepared by the solvent switching technique with polymers P1-P3, which were characterized by hydrophilic weight fractions f between 27-56% and yielded hydrodynamic radii (R_h, as obtained by DLS) between 100-140 nm after membrane extrusion.

In order to apply dual centrifugation, the aforementioned small scale protocol (Section 3.1) was adopted to be used with polymeric systems. After polymer solutions in chloroform were dried in certain centrifugation-compatible PCR vials, they were combined with ceramic beads and aqueous buffer, in which the intended cargo, here SRB, was dissolved. The most important difference compared to liposome formulation was the splitting of the centrifugation run in two consecutive runs. This was necessary as it turned out that the yielded thin polymer films exceeded the dried lipid films in stability, which caused residual film fragments to impede subsequent analysis due to broadening size distributions. Therefore, after half of the intended centrifugation time, the vials were turned by 180° in the sample holder, which efficiently

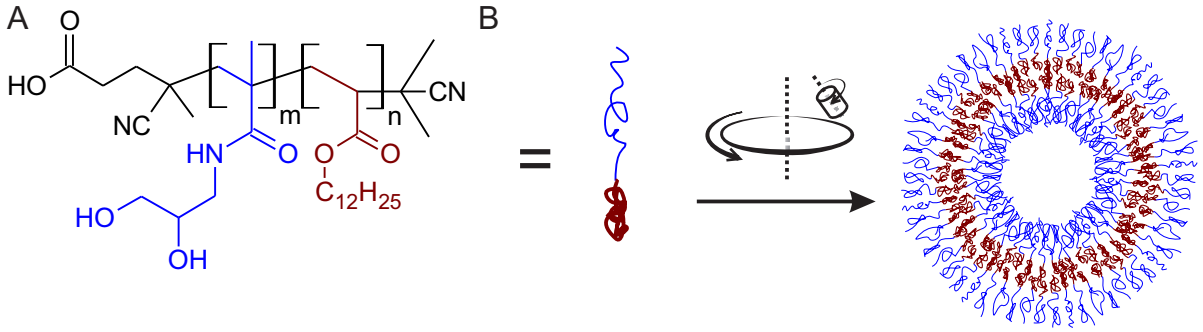

Figure 3.39: Structure of employed p(DHPMA)$_m$-*b*-p(LMA)$_n$ polymers (A) and the formulation of polymersomes *via* DC (B, schematic presentation). Lipophilic LMA blocks (red) assembled to yield spherical vesicles, with layers of hydrophilic polymers on the surfaces.

circumvented the incomplete homogenization of the gel-like mixtures. After redispersion, polymersomes were yielded as highly concentrated suspensions as expected from DC, also indicated by comparable encapsulation efficiencies in the range of 30-40% as listed in Table 3.9.

The prepared polymersomes were furthermore analyzed by cryo transmission electron microscopy. Figure 3.40 displays the obtained micrographs of P3 vesicles after formulation *via* dual centrifugation. The observed sizes were in general in good agreement with the hydrodynamic radii listed in Table 3.9, also, the vesicular structure of the prepared particles was clearly confirmable from the microscopy data. In summary, these results indicated that polymersomes were readily accessible by dual centrifugation, which rendered this method as highly suitable for the formulation of self-assembled nanoparticles. In order to further evaluate the applicability, DC was next employed to yet another polymer system, which was previously shown to self-assemble to micelles.

Polymeric micelles from sarcosine copolymers

Comparable to polymersomes, polymeric micelles represent a promising candidate system primarily for the encapsulation of *lipophilic* pharmaceutical compounds, since these aggregates of polymeric amphiphiles do not exhibit an aqueous core. The system which was applied in this study was previously investigated by Birke *et al.* for the encapsulation of MDL-12,330A, a rather lipophilic adenylate cyclase inhibitor. The particular compound was found to be efficiently encapsulated and the micelles were applied *in vitro* for delivery to melanoma cells, wich resulted in a decrease of cyclic adenosine monophosphate (cAMP) concentrations.[262] Here, a similar polymer compound has been employed in a proof-of-principle approach in vesicle formulation *via* dual centrifugation. Polysarcosine-*block*-polyglutamic acid benzylester p(Sar-*b*-Glu(OBn)) was synthesized by ring-opening polymerization (ROP) of their corresponding *N*-carboxyanhydrides (NCA) as reported earlier.[262] The structure of the employed polymer is visualized in Figure 3.41A, where the amphiphilic structure is represented by the blue and red polymer blocks, indicating hydrophilic and lipophilic sections, respectively. While ^{1}H NMR spectroscopy yielded a composition of p(Sar_{220}-*b*-Glu($OBn)_{26}$) and therefore an M_n of 21,420

Table 3.9: Properties of employed diblock copolymers.

Sample	Composition	M_n / g/mol	$Đ$	Lipophilic weight fraction f	R_h / nm	EE
P1	p($DHPMA)_{33}$-*b*-p($LMA)_{55}$	19600	1.10	26.9%	113	38.4%
P2	p($DHPMA)_{23}$-*b*-p($LMA)_{21}$	9100	1.23	39.8%	101	31.6%
P3	p($DHPMA)_{31}$-*b*-p($LMA)_{16}$	8900	1.16	55.4%	135	39.3%

M_n and $Đ$ (M_W/M_N, dispersity index) determined by SEC analysis using polystyrene standards, R_h determined by DLS after preparation *via* solvent switching.

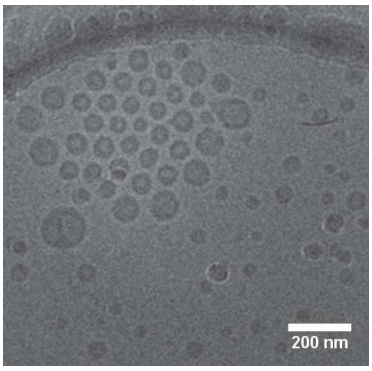

Figure 3.40: Micrograph of P3-based polymersomes as obtained by cryoTEM, clearly displaying a vesicular structure.

g/mol, a polydispersity $Đ$ (M_w/M_n) of 1.18 was determined by hexafluoroisopropanol gel permeation chromatography (HFIP GPC). The molecular weight fraction of the lipophilic block f was determined to be $f = 26.6\%$, a value which was earlier shown for comparable systems of the same polymer to provoke the formation of micelles with R_h in the range of 15 nm, as obtained from FCS measurements.[262]

For the formulation by dual centrifugation, 5 mg of polymer were dried in PCR vials and combined with ceramic beads and aqueous buffer, as detailed in the methods section. In contrast to the abovementioned, rather lipophilic amphiphiles that led to the formation of polymersomes, the sarcosine benzyl glutamate compounds rehydrated readily and therefore allowed for the formulation of micelles in only one DC run without any redispersion. Figure 3.41B illustrates the lipophilic interaction of p(Glu(OBn) sections (green) and therefore the micelle formation, which led to a solid hydrophobic core coated by the hydrophilic polysarcosine shell. The resulting micelles were characterized by DLS, which yielded z-average diameters of 184 nm with PDI of 0.248. In general, these values were in no agreement with the findings of approx.

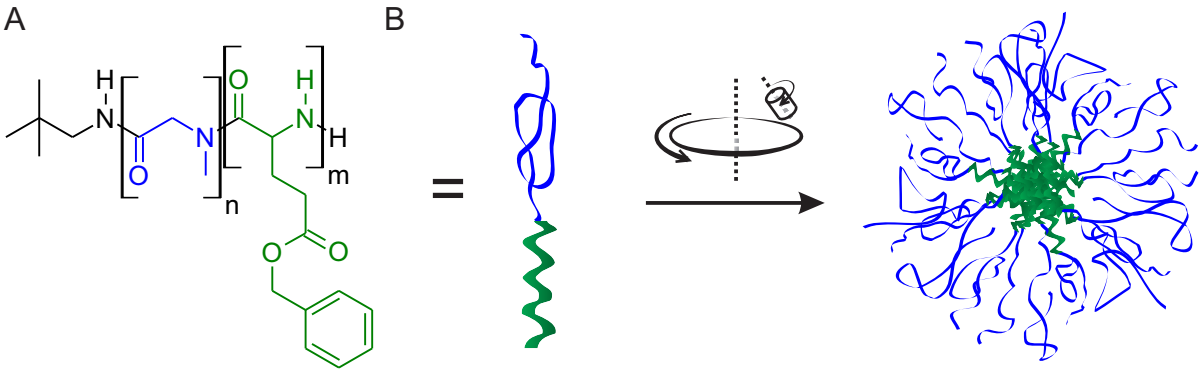

Figure 3.41: A: Structure of the investigated p(Sar)-*b*-p(Glu(OBn)) amphiphile. B: The water-soluble polysarcosine creates an hydrophilic corona around the self-assembled lipophilic core or p(Glu(Bn)).

15 nm for R_h from previous FCS studies, however, they rather indicated the formation of compound micelles. Compound micelles are aggregates of micelles with increased diameters, and their formation has been demonstrated for micelles of polymeric block copolymers.[298] Furthermore, average particle sizes determined with benchtop DLS instruments should be interpreted with care, since necessary compound characteristics like refractive index or homogeneous density are in most cases not known. Also, the measurements are in general very sensitive towards aggregates or contaminations of larger sizes, since scatter intensities scale with r^6 (r: particle radius). However, Figure 3.42 shows an exemplary distribution of scattering intensities, which indicated a monomodal size distribution. The subsequent repetition of micelle preparation resulted in a moderate reproducibility as displayed in Figure 3.42B. The mechanistic background for the variances that were observed between each replicate remained yet unclear and are subject of ongoing investigations. However, the overall findings indicated that dual centrifugation was successfully applied to the preparation of micellar polymeric particles, as the intense DC homogenization led to self-assembled structures with rather narrow size distributions. The formation of compound micelles was indicated by rather large particle diameters, and suggested further determination of these effect.

Taken together, the preparation of self-assembled nanoparticles *via* dual centrifugation, which included the efficient homogenization of amphiphiles with aqueous buffer, was shown to be also applicable for polymeric amphiphiles. Importantly, the microscale approach of DC allowed for the preparation of eight samples in parallel in approximately half an hour. This represented a substantial benefit compared to the very time-consuming solvent exchange by dialysis, which is typically applied on timescales of days. Besides the described benefits in preparation time, also cargo was much more efficiently encapsulated inside the vesicles. Comparable to the lipid systems described in Section 3.1, the encapsulation efficiencies can be expected to correlate with the mass fraction of the used buffer. Furthermore, conventional techniques typically deal with low yields, *e.g.* due to adsorption onto dialysis membranes, which can be ruled out in the case of DC formulation. Lastly, the whole process can conveniently be applied in aseptic conditions, which renders DC as an important alternative for the investigation of self-assembled polymer nanoparticle systems.

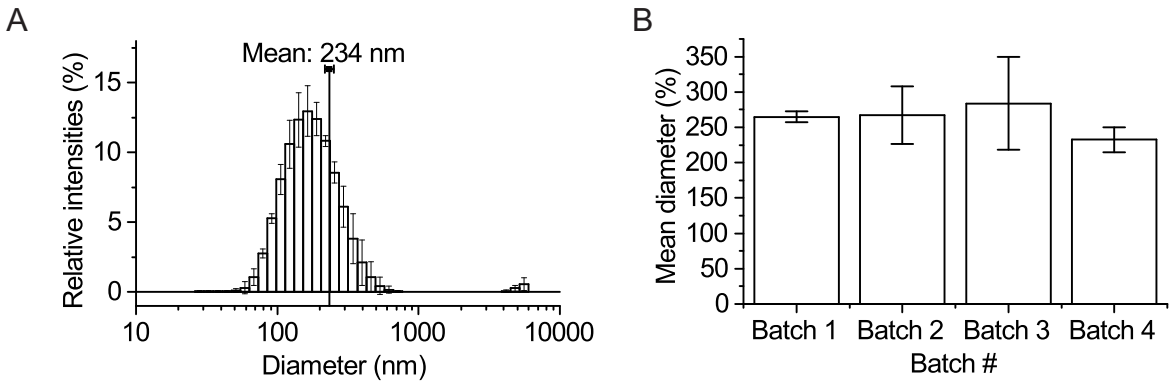

Figure 3.42: A: Exemplary scattering intensity-based distribution of particle sizes indicating a size distribution of moderate dispersity. It should be noted that the mean diameter of 234 ± 17 nm overrepresents larger particles, as scatter intensity scales with r^6. B: Comparison of four reproduced batches, indicating an appropriate reproducibility.

4 Conclusion and Outlook

Microscale formulation of liposomes *via* dual centrifugation Liposome formulation *via* dual centrifugation has been investigated on the single-digit milligram scale. The design of a DC sample inset allowed for the formulation in special PCR vials, which resulted in a preservation of particle characteristics down to a 1 mg batch size. Encapsulation efficiencies were shown to correlate with the lipid concentrations and not with the batch size, thus also inhomogeneous formulations in smallest scales yielded EE of approx. 50%. Microscale liposome formulation essentially enabled subsequent studies, since no excessive batch sizes were necessary for polymer syntheses at laboratory-scales. However, previous reports utilized sample insets with another orientation of the sample vials, and allowed for the preparation of more homogeneous and smaller particles.[1] Therefore, the optimization of the small-scale process is yet topic of ongoing investigations. Furthermore, while the formulation process has been refined to allow for preparation of eight samples in parallel within 30 minutes, the subsequent workup procedure is still laborious and current research is devoted to the automation of such. Altogether, microscale formulation has been shown to provide a valuable tool for the investigation of rare prototype compounds in liposomes.

In vitro interaction of poly(glycerol)-shielded, functionalized liposomes A novel class of poly(glycerol)-stabilized, fluorescently labeled liposomes has been studied in the context of their interaction with cellular environments. The formulation of liposomes by dual centrifugation of 17.5 mg batches yielded particles in the range of 150 nm in diameter and with EE of ~50%. CryoTEM analysis confirmed the numerical predominance of unilamellar vesicles, while also a fraction of multilamellar vesicles was observed. The incubation of living cells with such systems resulted in a fast integration of amphiphiles into cellular membranes on the timescale of minutes, which did not lead to an uptake or delivery of encapsulated cargo, as determined by live cell microscopy. After their uptake by unspecific endocytic trafficking, the cholesterol-based polymeric amphiphiles translocated to the membranes of endolysosomal compartments, and finally to enrich in such compartments near the nucleus. However, the current study has only examined the use of one particular polymeric amphiphile, while the origin of the observed effects remained unelucidated. Therefore, subsequent work included the variation of the particular lipid anchor, polymer architectures and fluorophore characteris-

tics, in order to deduce structure-function relationships. The interrelation of these properties is expected to result in important implications for the future application of such systems in directed drug delivery.

When double-functionalized liposomes were incubated on cells, a difference in the fluorescence emission ratios of the two fluorophores between membrane- and endosome-located amphiphiles was observed. While the fluorescence from both fluorophores was rather equal when located in the membrane, the red fluorophore appeared to increase in brightness during endosome maturation. Future research could possibly include a detailed investigation of the underlying principles, as one could envisage a potential correlation between the pH in the endosome and the fluorescence emission. The system could be developed to a valuable tool for the determination of intracellular pH, which would be membrane-bound in contrast to most other established systems.[299]

Taken together, the findings of this study shed some light on the cellular interactions of a novel class of polyether amphiphiles for steric stabilization of liposomes, and motivated a more detailed analysis of structure-function relationships of such compounds, regarding implications on their use in directed drug delivery.

Orthogonal functionalization of liposomes: multifunctional carriers The application of orthogonal CuAAC and IEDDA functionalization has been evaluated for liposome derivatization. A permutation of the amphiphiles' structural components indicated that the cholesterol anchor caused the previously found desorption effects of cholesterol-based, labeled amphiphiles. In contrast, BHG-based amphiphiles did not cause membrane fluorescence when incubated on cells. The difference in membrane desorption was also confirmed by FCCS analysis for intervesicular exchange. CuAAC and IEDDA allowed for the orthogonal surface derivatization, while site-selectivity was proven by visual assessment of the lipid anchor stability.

Liposomes that contained folic acid-amphiphile conjugates were orthogonally modified with fluorophores, which resulted in folate-dependent cell surface binding that was preventable by an excess of free folic acid. To the author's knowledge, this approach represents the first report of a post-preparational, orthogonal liposome modification, that was capable of active targeting. Importantly, cholesterol-anchored folate targeting was shown to result in substantially decreased surface binding, compared to BHG-based structures. These findings strongly suggested the critical reconsideration of the application of cholesterol as a lipophilic anchor for the attachment of functionalities to liposomes.

Interestingly, BHG-based amphiphiles were also found to desorb from the liposome surface, but in this case in a folate-dependent manner. This effect was only observed for PG-based amphiphiles, which were subjected to a one-pot functionalization with FAZ and fluorophores. A separate conjugation on the other hand resulted in intact liposomes that bound to the

cellular surface without visible desorption. The findings indicated a potential double functionalization of the same amphiphile with both FAZ *and* a fluorophore, although statistically unlikely. However, while the use of polyglycerol has essentially made the detection of such desorption processes possible, these can be expected to reduce the targeting efficiency of such systems. More research is required to determine if the desorbed amphiphiles are indeed double functionalized, and if a more stable anchoring could increase targeting efficiency.

Further work might explore the use of either longer alkyl chains as lipophilic anchors, or completely artificial anchors that comprise an even higher lipophilicity. A conceptual illustration based on an additional glycerol building block is displayed in Figure 4.1A. Similar systems have recently been described by Pasut *et al.*, who utilized PEG-dendron-phospholipid constructs to prepare so-called "super stealth liposomes", with dramatically increased blood circulation times.[300] However, the particular contribution has neither addressed the fate of the amphiphiles nor the attachment of targeting ligands, which might be a promising strategy to increase targeting efficiency.

More research is required to improve the compatibility of the IEDDA products with biological, serum containing environments. A variation of the tetrazine or the dienophile structure towards higher hydrophilicity might result in improved characteristics.

While the general influence of polyglycerol was ruled out to cause the observed desorption processes, the CMC and the stability of such amphiphiles in phospholipid membranes can be expected to correlate with the size of the hydrophilic polymer block. A recent contribution by Schubert and coworkers reported on differences in membrane insertion stabilities of Chol-PEG derivatives with different molecular weights.[301] Consequently, further research might explore the specific role of polymer sizes and architectures of polyglycerol-based amphiphiles, in order to further clarify the structure-function relations.

Altogether, the findings can be considered as prerequisites for the successful application of the presented liposome derivatization platform, which has been designed to allow for a convenient variation and combination of targeting ligands (Figure 4.1B).

Acidic shedding of liposomal particles After a novel concept for the introduction of acid-labile moieties into polyether compounds has recently been reported on, the incorporation of such functionalities into amphiphiles and the resulting liposome characteristics were investigated in this study. Three different lipid-structures were investigated, that based on cholesterol or BHG lipid anchors and linear PEG chains with terminal alkyne moieties, and either contained acetal or ketal groups. An MTT assay-based determination of the *in vitro* toxicity yielded a good biocompatibility for BHG-based amphiphiles, and slightly reduced viabilities for cholesterol-based amphiphiles. For a quantitative analysis of cleavage kinetics, two assays were established. In an *in situ* approach, the cleavage of polymeric amphiphiles

was measured by fluorescence spectroscopy, while PAGE-based separation of cleaved polymers from liposomes allowed for an *ex situ* determination. The findings from both assays were in good mutual agreement and yielded half life times of 20 hours and 15 minutes at pH 5 for acetals and ketals, respectively. These results rendered the investigated compounds as promising structures for the stimulus-responsive shedding of liposomes.

Further research might be devoted to the variation of acetal or ketal structures, in order to tailor the sensitivity towards acid to the specific needs. In addition, a detailed investigation of *in vitro* and *in vivo* performances of the employed systems renders a natural progression of this work. Lastly, the incorporation of cleavable groups within the polar headgroup of the lipid anchor might have promising effects on the triggered destabilization of the whole lipid membrane. This concept is illustrated in Figure 4.1C, and consequently the membrane fluidity can be expected to substantially increase upon the triggered separation of the involved aliphatic chains.

Application of microscale dual centrifugation to non-lipid particles DC formulation has been applied for the preparation of self-assembled particles that contained polymeric amphiphiles. The use of p(DHPMA)-*b*-p(LMA) diblock copolymers yielded polymersomes with encapsulation efficiencies comparable to liposomal formulations. Furthermore, p(Sar-*b*-Glu(OBn)) copolymers, which have previously been used for the preparation of polymeric micelles, yielded particulate structures of narrow polydispersities in the size range of 180 nm, as expected for compound micelles. The preparation of polymersomes was readily transferable from liposome formulation protocols, however, results suggested that subsequent optimization is necessary for the preparation of micellar polymer particles. Altogether, the proof-of-principle investigation pronounced the distinct advantages of DC formulation compared to conventional methods like solvent switching, since these were outperformed in time and material consumption, recovery and, for polymersomes, in reproducibility.

An important area of future research would be to investigate the potential degradation of the polymer systems during the DC runs, since intense shear forces can be expected to lead to a certain amount of degraded polymer. Regarding polymeric micelles, the findings suggested a more detailed analysis of the obtained structures, and further optimization of the formulation protocol. Lastly, it would be interesting to assess the potential application of DC in mini emulsion processes, which could allow the preparation of nanoparticles that do not consist of diblock amphiphiles.

Multifunctional liposomes for targeted drug delivery Altogether, the presented work established a toolbox for the rational design, formulation and derivatization of novel liposome systems. Microscale DC formulation allowed for convenient and fast investigation of liposome

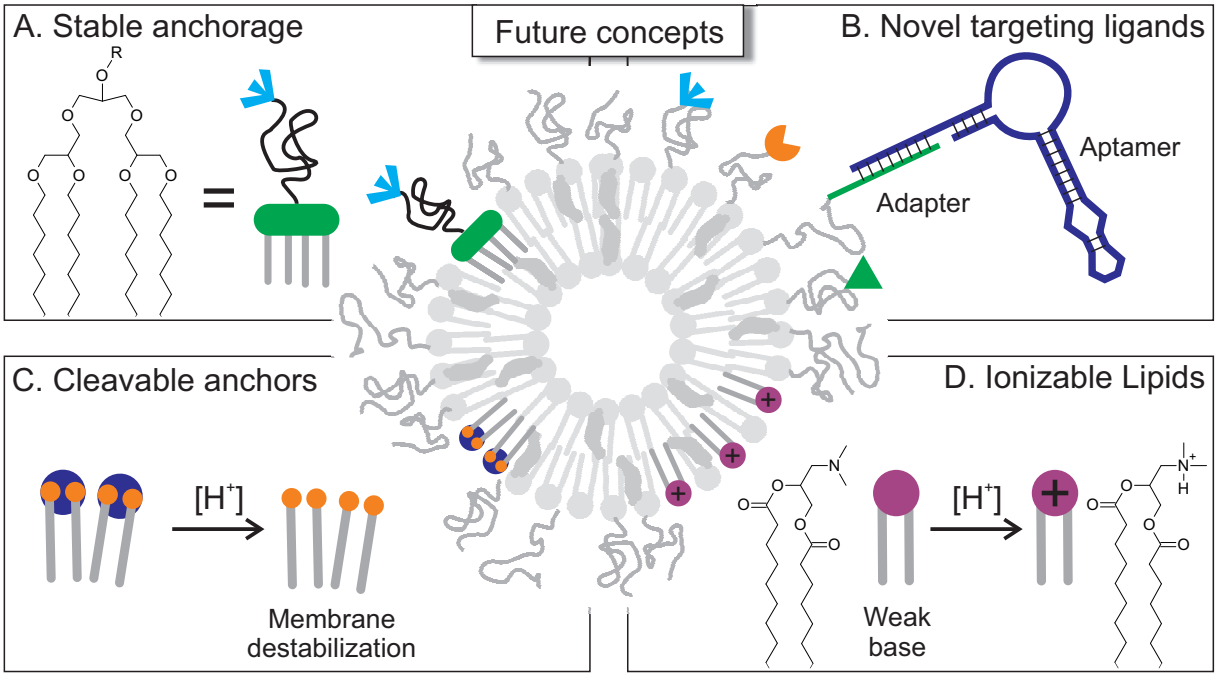

Figure 4.1: Future concepts based on the presented work. A: Multiple anchors might allow the stabilization of targeting ligands. B: The post-preparational functionalization concept allows for flexible variation of targeting ligands. Aptamers could be attached via hybradization to adapter sequences. C: Cleavable units within the polar headgroups might destabilize the vesicles and allow the release of cargo upon acidification. D: With the combination of the presented concepts with ionizable lipids, efficient escape from endolysosomes could be achieved.

compositions and the effects of highly functional prototype compounds. The derivatization system enabled an easy transfer from fluorescent ligand models to functional targeting ligands, and thus can be expanded to a vast variety of ligands. One possibility could include the use of aptamers for targeting, which has earlier been shown to be a promising inasmuch versatile strategy,[156] and aptamers can also contain azide moieties for the direct conjugation *via* click chemistry. The use of hybridization anchors, as illustrated in Figure 4.1B, has previously been shown to allow for a convenient variation of the aptamer structure.[302]

Depending on the mode of interaction between the targeting ligand and the particular cell surface feature, actively targeted nanoparticles either end up just bound to the cell surfaces, or, in most cases, subsequently internalized *via* endocytosis. A major challenge in current research is the escape from endolysosomal compartments, since most therapeutic compounds only unfold their activity after delivery to the cytosol. As a potential strategy, future investigations could include the use of ionizable lipids, which are weak bases that are readily protonated within the acidic milieu in lysosomes. Therefore, they facilitate a disruption of the lysosomal membranes, while they not cause the typical unspecific interaction known from cationic lipids like DOTAP.[303] Figure 4.1D illustrates this concept with an acyl-substituted dimethylaminopropane lipid, *e.g.* 1,2-distearoyl-3-dimethylamino-propane. Importantly, while efficient encapsulation in earlier studies has only been possible by utilization of electrostatic interactions of *e.g.* nucleic acids and the ionizable lipids in acidic solutions,[304] DC formulation could crucially enable the use of such lipids for true *vesicular* encapsulation under neutral pH conditions.

The combination of the established work with the illustrated expansions could evolve the presented liposome system to valuable toolbox for the design of novel liposome targeting concepts.

5 Materials and Methods

5.1 Materials

Chemicals

Acetitc acid, HPLC grade	Sigma-Aldrich (St. Louis, MO, United States)
Acetonitrile, HPLC grade	Sigma-Aldrich
Amiloride	Sigma-Aldrich
Ammonium persulfate (APS)	Carl Roth (Karlsruhe, Germany)
bFGF, human recombinant	Thermo-Fisher Scientific (Waltham, MA, USA)
Bromphenol Blue	Sigma Aldrich
$CDCl_3$	Deutero (Kastellaun, Germany)
Chloroquine Diphosphate	Applichem (Darmstadt, Germany)
Chlorpromazin	Sigma-Aldrich
Cholesterol	Carl Roth
$CuSO_4$	Sigma Aldrich
Dimethyl sulfoxide (DMSO)	Carl Roth
D-MEM indicator free with HEPES #21063	Thermo-Fisher Scientific
D-MEM, #61965	Thermo-Fisher Scientific
D-MEM:F-12 (1:1) indicator free #11039	Thermo-Fisher Scientific
D-PBS, #14190	Thermo-Fisher Scientific
DSPE-mPEG2000	Lipoid GmbH (Ludwigshafen, Germany)
DMSO-d_6	Deutero
Ethylenediaminetetraacetic acid (EDTA)	Carl Roth
Ethanol, 99.5%	Carl Roth
Fetal bovine Serum, #10500	Thermo-Fisher Scientific
Folate azide	Rösch group, JGU Mainz, Germany and BaseClick (Neuried, Germany)
Folic acid	Sigma Aldrich
Genistein	Applichem
Glycerol	Sigma-Aldrich

Ham's F-10, #41550	Thermo-Fisher Scientific
Hellmanex®	Hellma (Müllheim, Germany)
HEPES	Sigma Aldrich
Hydrochloric acid (HCl)	VWR (Darmstadt, Germany)
Hydrogen peroxide (H_2O_2)	Carl Roth
Hydrogenated egg phosphatidylcholin (EPC3)	Lipoid
Lysotracker Blue®	Thermo-Fisher Scientific
OptiMem, #31985	Thermo-Fisher Scientific
PAGE buffer, denaturing	Carl Roth
PAGE concentrate 25 %, denaturing	Carl Roth
PAGE diluent, denaturing	Carl Roth
Penicillin-Streptomycin liquid, #15140	Thermo-Fisher Scientific
Potassium chloride (KCl)	Carl Roth
Potassium dihydrogen phosphate (KH_2PO_4)	Carl Roth
RPMI 1640, Folate free #27016	Thermo-Fisher Scientific
Sepharose 2B CL	Sigma-Aldrich
Sodium Ascorbate	Carl Roth
Sodium chloride (NaCl)	Carl Roth
Sulfuric acid (H_2SO_4)	Merck (Darmstadt, Germany)
TBE 10x buffer	Carl Roth
TEMED	Carl Roth
Triethylamine	Acros Organics (Thermo Fisher Belgium)
Tris(hydroxypropyltriazolylmethyl)amine (THPTA)	Helm group, JGU Mainz, Germany
Trisodium phosphate (Na_3HPO_4)	Carl Roth
Triton-X 100	Sigma-Aldrich
Trypsin EDTA 0.05 %, # 25300	Thermo-Fisher Scientific
Xylene Cyanol	Sigma Aldrich

Chemicals and solvents not listed were acquired from by the chemical supply of the Institute of Pharmacy, University of Mainz, Germany.

Disposables and glassware

8-well chamber, µ-slide	Ibidi (Martinsried, Germany)
96-well optical bottom plates, black	Greiner (Frickenhausen, Germany)
96-well PP plates, black	Greiner
Cell culture flask, 75 cm^2, ventilated cap, tc treated	Sarstedt (Nümbrecht, Germany)

Disposable plastic macro cuvettes	Sarstedt
8-well chamber, glass bottom, Nunc Lab-Tek	Thermo Fisher Scientific
Filter top vacuum bottles, PES, pore: 0.2 µm, 500 mL	Sarstedt
MoBiCol® Classic, disposable PP column 1 mL	MoBiTec (Göttingen, Germany)
NAP-5 column	GE Healthcare (Solingen, Germany)
PCR vials for dual centrifugation 200 µL	Kisker Biotech (Steinfurt, Germany)
Pipet tips, with filter, sterile RNase/DNase free	Greiner
Reaction tube, 1.5 mL and 2.0 mL	Carl Roth
Screw cap vials, 0.65 mL or 2.0 mL	Carl Roth
Screw cap vials for dual centrifugation, 500 µL	Carl Roth
Screw cap vials for dual centrifugation, 650 µL (discont.)	Carl Roth
Serological pipettes, sterile, disposable	Sarstedt
SiLiBeads® ZY Ceramic beads, 0.6 - 0.8 mm #9607-53	Sigmund Lindner (Warmensteinach, Germany)
SiLiBeads® ZY Ceramic beads, 0.3 - 0.4 mm	Sigmund Lindner
Suprasil® quartz glass cuvette, 1 cm	Hellma
Syringe filters units, cellulose, pore: 0.2 µm	Carl Roth

Fluorophores

				CLSM Settings	
Name	Supplier	λ_{exc}/ nm	λ_{em}/ nm	Laser	Bandwidth
Alexa Fluor 594 Azide	Thermo-Fisher Scientific	590	617	561 nm	600 - 630 nm
Atto 488 Azide	Atto-Tec (Siegen, Germany)	500	520	488 nm	510 - 540 nm
Atto 488 Tetrazine	Jena Biosciences (Jena, Germany)	500	520	488 nm	510 - 540 nm
Calcein	Sigma-Aldrich	494	517	488 nm	510 - 540 nm
DiI	Sigma-Aldrich	549	565	561 nm	570 - 600 nm
Lysotracker Blue	Thermo-Fisher Scientific	373	422	405 nm	420 - 450 nm
SulfoCy5 Azide	Sigma-Aldrich	647	663	633 nm	650 - 680 nm
SulfoCy5 Tetrazine	Jena Biosciences	647	663	633 nm	650 - 680 nm
Sulforhodamine	Sigma-Aldrich	565	586	561 nm	570 - 600 nm

Buffers and Media

PBS 10x: 1.4 M NaCl, 27 mM KCl, 15 mM KH_2PO_4, 80.6 mM Na_2HPO_4 in H_2O, resulting in pH of 6.8

PBS: Dilution of PBS 10x with sterile water resulted in a pH of 7.4. With final 140 mM NaCl, 2.7 mM KCl, 1.5 mM KH_2PO_4, 8.06 mM Na_2HPO_4.

Glycin Buffer pH 10: 100 mM glycin in MilliQ H_2O, adjusted to pH 10 with NaOH-

Cleavage buffer pH 2.4 - pH 6.4: Cleavage buffers at the respective pH were yielded from a 1:2 (v/v) dilution with liposomes in PBS 1x pH 7.4 of citric acid solutions of the following concentrations: pH 2.4: 165 mM, pH 3.4: 27.3 mM, pH 4.4: 16.3 mM, pH 5.4: 9.5 mM, pH 6.4: 4.1 mM. Cleavage at pH 7.4 was carried out in PBS. For neutralization, solutions of Na_2HPO_4 in the following concentrations were used: pH 3.4: 723 mM, pH 4.4: 432 mM, pH 5.4: 252 mM, pH 6.4: 108 mM. For neutralization of pH 2.4, a 8.5 mM solution of Na_2HPO_4 was supplemented with 9.8 mM NaOH.

Cleavage buffer pH 8.4 (Sodium tetraborate): 12 mM $Na_2B_4O_7$, 126 mM NaCl, adjusted to pH 8.4 with 2M HCl

RBE growth medium: 45% v/v D-MEM, 45% v/v HAM's F-10, 10% v/v FBS, 100 µg/mL Pen/Strep, 1 ng/mL bFGF

RBE incubation medium: 45% v/v D-MEM, 45% v/v HAM's F-10, 10% v/v FBS, 100 µg/mL Pen/Strep, 1 ng/mL bFGF

RBE incubation medium without FBS: 50% v/v D-MEM, 50% v/v HAM's F-10, 100 µg/mL Pen/Strep, 1 ng/mL bFGF

RBE microscopy medium: 90% v/v D-MEM:F-12 indicator free, 10% v/v FBS, 10 mM HEPES

RBE microscopy medium without FBS: 100% v/v D-MEM:F-12 indicator free, 10 mM HEPES

RBE freezing medium: 35% v/v D-MEM, 35% v/v Ham's F-10, 20% v/v FBS, 10% v/v DMSO

HeLa / KB / HEK growth medium: 90% v/v D-MEM, 10% v/v FBS, 100 µg/mL Pen/Strep

HeLa / KB / HEK growth medium without folate: 90% v/v RPMI 1640 without folic acid, 10% v/v FBS, 100 µg/mL Pen/Strep

HeLa / KB / HEK growth medium with folate: 90% v/v RPMI 1640 without folic acid, 10% v/v FBS, 100 µg/mL Pen/Strep, 100 µM folate

HeLa / KB / HEK incubation medium without folate: 100% v/v RPMI 1640 without folic acid, 100 µg/mL Pen/Strep

HeLa / KB / HEK incubation medium with folate: 100% v/v RPMI 1640 without folic acid, 100 µg/mL Pen/Strep, 100 µM folate

HeLa / KB / HEK microscopy medium: 100% v/v D-MEM indicator free with 10 mM HEPES

HeLa / KB / HEK freezing medium: 70% v/v D-MEM, 20% v/v FBS, 10% v/v DMSO

Polymeric amphiphiles

Polyether amphiphiles All used cholesterol- and BHG-based polyether amphiphiles were provided by the Frey group, JGU Mainz, Germany. All compounds were synthesized by Anna M. Hofmann (Cholesterol-based amphiphiles), Sophie S. Müller (Cholesterol-based [cleavable] amphiphiles), or Matthias Worm (BHG-based [cleavable] amphiphiles) *via* cholesterol-initiated oxyanionic ring-opening polymerization and subsequent derivatization with propargyl bromide as reported previously.[61, 62, 305, 306] Number average molecular weights M_n and degrees of functionalization were obtained *via* from ^{1}H NMR analysis of solutions in deuterated dimethylsulfoxide (DMSO-d_6) or methanol-d_4, using a Bruker AC 300 spectrometer operated at 300 MHz. Diffusion-ordered NMR spectroscopy (DOSY) was applied to verify the conjugation of norbornene moieties to the polymer backbone. DOSY spectra were recorded on a Bruker AC 400 spectrometer with a 5 mm BBO probe operated at 400 MHz and processed using MestReNova Bayesian DOSY Transform Software. Polydispersities ($Đ$, M_w/M_n) were determined by size exclusion chromatography (SEC) in dimethylformamide (DMF, 50 °C, 1 mL/min, containing 0.25 g/L of lithium bromide as an additive), using an Agilent 1100 Series SEC setup with a PSS HEMA column (106/105/104 g/mol) and a UV (254 nm) and RI detector. Polymer sizes were calibrated with poly(ethylene glycol) standards provided by Polymer Standards Service, Mainz, Germany.

P(DHPMA-*b*-LMA) amphiphiles were provided by Martin Scherer (Zentel group, JGU Mainz, Germany) and synthesized by reversible addition-fragmentation chain transfer (RAFT) polymerization as previously described,[263] with the variation that dihydroxypropylamine (DHPA) was used instead of hydroxypropylamine (HPA).[291]

P(Sar-*b*-Glu(OBn)) amphiphiles were provided by Alexander Birke (Zentel group) and synthesized by NCA ring-opening polymerization as previously described.[262]

5.2 Methods

Software and data analysis

CLSM micrographs were inspected with Leica LAS AF Light software and modified with ImageJ.[307] Modifications to CLSM data included cropping, insertion of scale-bars and arithmetic contrast enhancement for visual representation, and, importantly, were performed throughout whole experimental data sets to assure consistence with respective control experiments. All micrographs show representative images from data sets. Charts and plots were prepared with Origin 7.5 (Origin-Lab, Northampton, MA, USA). Figures and schemes were prepared with CorelDraw X8 (Corel Corp., Ottawa, Canada). Computer aided design was performed with AutoDesk Fusion 360 (Mill Valley, CA, USA). LaTeX 2_ε editing was conducted with LyX, and MENDELEY (Mendeley Inc., New York, NY, USA) for reference management.

Amphiphile derivatization

Derivatization before liposome formulation was performed with alkyne-bearing amphiphiles and folic acid azides. Reactants for click reactions were added the following order (final concentration): EtOH 99.9% (to final volume of 80 µL), THPTA (0.5 mM), $CuSO_4$ (0.1 mM), and sodium ascorbate (2.5 mM). 4 nmol of azide compound (folate or fluorophore) were added before an ethanolic solution of the polymer amphiphile was added. The amount of amphiphile was set from composition calculation, *e.g.* 422 nmol for 5 mg of total lipids (5 mol%), or a fraction thereof, if multiple functionalization reactions were conducted separately. However, the amount of amphiphile was representing at least 20 equivalents (or ~1 mol%) with respect to the azide compound, to ensure quantitative reaction of the azide. After 2 h at 25 °C, copper was removed by adding 15 mg Lewatit MonoPlus S 100 H. The ion exchange resin was washed two times with 50 µL EtOH 99.9% and the combined ethanolic solutions dried and combined with the final lipid composition for liposome formulation as detailed below. Reaction control was conducted on an Agilent 1100 system equipped with a quad pump, a diode array detector

recording at 310 nm, an YMC Triart C18 RP column, and running the following acetonitrile (ACN) gradient with a constant concentration of 20 mM triethylammonium acetate (TEAA): 0 min.: 1% ACN, 1 min.: 1% ACN, 25 min.: 97% ACN, 30 min.: 97% ACN, 34 min.: 1% ACN, 40 min.: 1% ACN. Appendix 7 illustrates exemplarily the successful quantitative conjugation without finding residual free folate azide (blue curve) in the reaction mixture (black curve).

Liposome preparation

Liposomes were prepared *via* dual centrifugation according to a modified method as previously described.[1] Stock solutions in absolute ethanol of EPC (50 mg/mL), cholesterol (20 mg/mL) and all polymeric amphiphiles (20 mg/mL) were prepared and combined to yield the intended compositions. Depending on the batch size, either PCR vials (<10 mg) or 500 µL screw cap vials (10-20 mg) were used. The combined lipid solutions were dried in a SpeedVac® vacuum centrifuge (Eppendorf, Hamburg, Germany) at 40 °C for at least 10 h in a first step and then in a lyophilisation unit (Alpha 2-4 LD, Christ, Osterode am Harz, Germany) for at least 72 h. The complete removal of organic solvent turned out to be crucial for subsequent formulation. Dried lipid stocks were stored at -20 °C until usage. Representing an example for a 5 mg total lipid batch, the following values scale linearly with the batch size. For formulation, 9.3 µL of PBS or a solution of designated cargo in PBS and 71 mg ceramic beads were added to the dry lipid films and incubated (preswollen) for 8 minutes at room temperature. The sample tubes were subjected to dual centrifugation in a Rotanta 400 centrifuge, which was customized with a prototype DC-rotor (Hettich, Tuttlingen, Germany) for 20 minutes at 2500. If PCR vials were used, a custom-made, 3D-printed inset was used which was designed as detailed in Appendix 1. The obtained vesicular phospholipid gel was diluted with 28.5 µL PBS and subjected to two more DC runs, in between of which the orientation of the sample tubes was reversed. Stock suspensions were stored at 4 °C until usage.

Post-preparational functionalization

CuAAC in Section 3.2. For post-preparational CuAAC reactions, the reactants were added in the following order (brackets: final concentration): MilliQ water (to final volume of 40 µL), phosphate buffer (5.3 mM NaH_2PO_4, 94.7 mM Na_2HPO_4) pH 8, THPTA (0.5 mM), $CuSO_4$ (0.1 mM), and sodium ascorbate (2.5 mM). Azides were added to these mixtures to achieve final concentrations of 25 - 200 µM, and 10 µL of liposome suspension were added. The fluorophore concentration was selected to yield equal degrees of functionalization throughout each series of experiments. After thorough mixing, the reaction was incubated for 2 h at RT. To fix the reaction endpoint, 1 µL of 20 mM EDTA was added.

CuAAC and IEDDA in Section 3.3. For orthogonal post-preparational derivatization that included CuAAC reactions, the reactants were added in the following order (brackets: final concentration): MilliQ water (to final volume of 40 µL), phosphate buffer (5.3 mM NaH_2PO_4, 94.7 mM Na_2HPO_4) pH 8, THPTA (0.5 mM), $CuSO_4$ (0.1 mM), and sodium ascorbate (2.5 mM). If only IEDDA was applied, the reaction was carried out in PBS. Azides or tetrazines were added to these mixtures to achieve final concentrations of 25 - 200 µM, and 5 µL of liposome suspension were added. The fluorophore concentration was selected to yield equal degrees of functionalization throughout each series of experiments. The reaction was incubated in standard laboratory PCR vials at 45 °C in a PCR-Thermocycler for 4 h. To fix the reaction endpoint, 1 µL of 20 mM EDTA was added.

Gel filtration workup was performed to remove free fluorophore and reactants. In general, either NAP-5-based columns or MoBiCol spin columns were used and packed with Sepharose 2B-CL. Elution volumes of the liposome fraction and free fluorophore fraction were calibrated with calcein-containing liposomes. Therefore, after column packing and equilibration with PBS, drop-sized fractions were collected in 96-well multi-well plates and measured in a plate reader. The obtained elution volumes were used column-specifically to collect purified liposome fractions and free dye fractions of defined volumes for subsequent determination of encapsulation efficiencies. If aseptic conditions were necessary, all purification steps were performed under a laminar flow bench and with sterile D-PBS.

Encapsulation efficiency

For the determination of encapsulation efficiencies, a hydrophilic tracker, *i.e.* calcein or sulforhodamine B, was encapsulated and liposome suspensions were purified via gel permeation chromatography on custom-made Sephadex 2B CL columns (MoBiTec spin columns or NAP-5 column size). Purification yielded two fractions, the liposomal fraction with the volume V_L and the fraction of the free dye with the volume V_F. Samples of the volumes V_{SL} and V_{SF}, typically 10 µL and 50 µL, respectively, were added in black 96-well plates and supplemented with 1% Triton-X 100 and PBS to yield a final concentration of 0.5% Triton-X 100 in 100 µL total volume for all samples. Subsequently, the samples were fluorimetrically quantified on a Tecan M200 pro multiwell plate reader, yielding the intensities I_L and I_F. If necessary, absolute quantification was carried out by external calibration with free fluorophores. From the given parameters, the encapsulation efficiency was calculated as

$$EE = \frac{\frac{V_L}{V_{SL}} \times I_L}{\frac{V_L}{V_{SL}} \times I_L + \frac{V_F}{V_{SF}} \times I_F} \tag{5.1}$$

Degree of functionalization

The degree of functionalization as the number of fluorophores per liposome was obtained from absolute quantification of liposome-associated fluorescence with the same method as described above for the encapsulation efficiencies. Absolute quantification was facilitated with an external calibration with free fluorophore azide or tetrazine, and resulted in an absolute concentration of fluorophore, while spectrometrical changes due to the conjugation reaction were neglected. For tetrazine-modified fluorophores, the external calibration was performed with tetrazine-fluorophore that was reacted for 4 hours with free norbornene dicarboxylic acid anhydride.The number of fluorophores N per liposome was obtained from $N = C_{Fl}/C_L$, with C_{Fl} as the fluorophore concentration in the purified liposome suspension, and C_L the concentration of liposomes. C_L was estimated according to the method of Pidgeon *et al.[308]* which relies on the radius R_L of liposomes as obtained from DLS measurements, the encapsulated volume fraction EE, obtained as shown above, the volume of the cargo buffer used during preparation V_{buf} and the volume of the liposome batch V_{batch}. Assuming a lamellar thickness of $T_{bilayer} = 5\,nm$, C_L follows as

$$C_L = \frac{EE \times V_{buf}}{V_{batch} \times \left(\frac{4}{3}\pi \left(R_L - T_{bilayer}\right)^3\right)} \tag{5.2}$$

From these calculations, the following values were calculated for Atto 488-functionalized PGGL and *hb*PGL, and for an exemplary model liposome with 60% EE and R_h = 80 nm:

Liposome	c_{lipo} / nM	N
Model (EE = 60%, R_h = 80 nm)	122	
PGGL (EE = 74%, R_h = 83 nm)	134	127
*hb*PGL (EE = 63%, R_h = 90 nm)	88	102

However, cryoTEM data illustrated that the assumption of unilamellar liposomes as only a rough approximation, as a substantial fraction of multilamellar liposomes was found. Alternatively, NTA allowed for the determination of particle concentrations and resulted in values that were in moderate agreement with the abovementioned approximations.

Dynamic light scattering

DLS experiments were performed on a Malvern Zetasizer Nano ZS. Samples were measured in disposable polystyrene cuvettes (path length 1 cm), 1 µL of unpurified or 10 µL of GPC-purified liposome suspension was diluted in 1 mL freshly filtered PBS. after equilibration to 25 °C, three measurements were performed, with the instrument optimizing the number of runs for each measurement. Z-averaged hydrodynamic radii and polydispersity indices were

obtained from cumulant analysis. The refractive index (RI) and viscosity of the dispersant (preset: water) was set to 1.330 and 0.8872 cP, respectively, the RI of the particle to 1.59. The absorption of the particle was set to 0.01, both attenuator and measurement position were controlled by the instrument and all measurements were performed at a scattering angle of 173°. The optimization of measurement conditions yielded with the employed dilutions count rates of 300 ± 50 kcounts per second, as recommended by the supplier.

Nanoparticle Tracking Analysis

NTA was conducted on a Malvern NanoSight LM10 equipped with a sCMOS camera, a tempered chamber unit and a 532 nm laser. After purification via GPC, liposomes were diluted 1:2000 in filtered PBS and injected in the sample chamber with a 1 mL syringe. Analysis settings: Camera level: 12, Gain: 350, measurements per sample: 3, duration: 30 seconds, temperature, 25 °C.

Cryo transmission electron microscopy

Micrographs were recorded by Kristiane A. K. Rusitzka (Markl group, JGU Biology dept., Mainz, Germany) on a Tecnai 12 BioTwin cryo transmission electron microscope, FEI, USA at 120 kV. The grid was hydrophilized for 30 seconds in the glow discharger at 25 mA. 3 µL sample volume were applied to the hydrophilized grid in the plunger device (Leica EM GP), while a humidity of at least 93% was assured, and blotted for 3 seconds.

Fluorescence correlation spectroscopy

FCS and FCCS experiments were conducted and interpreted by Inka Negwer (Helm Group, JGU, and Butt group, Max Planck Institute for polymer research, Mainz, Germany) as described in and reproduced from [274]. All experiments were conducted on an inverted Olympus IX70 microscope (with an UPLSAPO 60XW 60x/1.2 water immersion objective) in combination with an Olympus FluoView300 confocal laser scanning unit and a PicoQuant FCS unit. Samples were illuminated with collinear and focused 488 nm ("blue") and 633 nm ("red") laser sources, and fluorescence emission separated with a 635 nm dichroic mirror after passing a confocal pinhole. Channel bandwidths were defined by a 500BP50 filter and a 635LP filter and emission measured with two single photon counting avalanche photodiodes (τ-SPAD, PicoQuant). The dimensions of the two overlapping confocal observation volumes V_b and V_r, that superimpose to a common observation volume V_{br}, were determined with reference standards (Alexa Fluor 488 and Alexa Fluor 647) with known diffusion koefficients. Samples

were mixed in eight-well, polystyrene-chambered cover glass sample cells (Nunc™ Lab-Tek™, Thermo Scientific™) and analyzed after a 1 minute delay.

Fluctuations of the fluorescence intensities $\delta I_b(t)$ and $\delta I_r(t)$ that were caused by diffusion of the labeled particle species through the corresponding observation volumes were independently recorded (30 records of 10 seconds) and analyzed with the corresponding auto- and cross-correlation functions[309]:

$$G_{bb}(\tau) = 1 + \frac{\langle \delta I_b(t) \times \delta I_b(t+\tau) \rangle}{\langle I_b(t) \rangle^2} \tag{5.3}$$

$$G_{rr}(\tau) = 1 + \frac{\langle \delta I_r(t) \times \delta I_r(t+\tau) \rangle}{\langle I_r(t) \rangle^2} \tag{5.4}$$

$$G_{br}(\tau) = 1 + \frac{\langle \delta I_b(t) \times \delta I_r(t+\tau) \rangle}{\langle I_b(t) \rangle \langle I_r(t) \rangle} \tag{5.5}$$

The correlation functions of identical, freely diffusing fluorescent particles, are represented by Equation 5.6:

$$G(\tau) = 1 + \frac{1}{\langle N \rangle \left(1 + \frac{\tau}{\tau_D}\right) \sqrt{1 + \frac{\tau}{S^2 \times \tau_D}}} \tag{5.6}$$

Here, $\langle N \rangle$ represents the mean number of fluorescent species in the confocal volume V, τ_D is the average lateral diffusion time, $S = \frac{z_0}{r_0}$ is the ratio of axial to lateral dimensions of the confocal volume V. After fitting the experimental autocorrelation data (Equations 5.3 and 5.4) in Equation 5.6, N and τ_D were obtained. The particle concentration can be determined from $\langle C \rangle = \langle N \rangle / V$, while the diffusion coefficient D was accessible *via* Equation 5.7.

$$D = \frac{r_0^2 + R_H^2}{4\tau_D} \tag{5.7}$$

Furthermore, the Stokes-Einstein relation 5.8 allowed the evaluation of R_H.

$$R_H = \frac{k_B \times T}{6\pi \times \eta \times D} \tag{5.8}$$

The fluorescence brightness was also determined by dividing the average fluorescent intensity by $\langle N \rangle$, which yielded the brightness per particle and therefore the number of fluorophores per particle, when compared to the brightness per fluorophore.

Fluorescence cross-correlation of vesicles containing single or two different fluorophores was used to investigate the membrane exchange of amphiphiles. Pure Atto 488-labeled and SulfoCy5-labeled liposomes were mixed, and were also found, when no membrane exchange

occurred. In the case of a fast membrane exchange (cholesterol-anchors), particles species showed a correlation between both fluorescence channels, and therefore the temporal fluctuations of fluorescence intensities $\delta I_b(t)$ and $\delta I_r(t)$ were found correlated, with a high amplitude of the cross-correlation function 5.5. The concentration c_{br} of particles that contained both fluorophores was estimated with Equation 5.9.

$$c_{br} = \frac{(G_{br}(0) - 1) \times V_{br} \times N_b \times N_r}{V_b \times V_r} \tag{5.9}$$

Cell culture

All used buffers and media were either sterile filtered or sterile when supplied and prewarmed to 37 °C. All cell lines were cultured at 37 °C in high humidity in HeraCell 150 (Heraeus® , ThermoFisher Scientific) and at 5% CO_2 in 75 cm^2 tissue culture-treated cell culture bottles and handled under a HeraSafe KS12 laminar flow bench (ThermoFisher Scientific). Cells were counted with a Neubauer Improved counting chamber (Marienfeld, Lauda-Königshofen, Germany).Cells were grown to a confluency of 80 - 90% and passaged for 2 - 3 times a week, in order to obtain seeding densities of 40 kcells/cm^2. The following cell lines were used:

- RBE4 cells: Rat brain endothelial cell line, immortalized.[268] The cells were a kind gift from Prof. G. Fricker (IPMB, Dept. Pharmaceutical Technology, Institute of Pharmacy and Molecular Biotechnology, University of Heidelberg, Germany).
- HeLa cells: Human cervix carcinoma cell line (DSMZ #ACC 57).[310] The cells were a kind gift from Prof. B. Epe (Dept. Pharmacology, Institute for Pharmacy and Biochemistry, Johannes Gutenberg-University Mainz, Germany).
- KB cells: Human nasopharyngeal carcinoma cell line (DSMZ #ACC 136).[281] The cells were a kind gift from Prof. B. Epe.
- HEK cells: Human embryonic kidney cell line, immortalized (DSMZ #ACC 305).[311] The cells were a kind gift from Prof. A. Dalpke (Dept. of Infectious Diseases, Medical Microbiology and Hygiene, Heidelberg University Hospital, Heidelberg, Germany).

For in vitro interaction studies, either of the listed cell lines was grown in the respective growth medium as detailed in the materials section. In the case of folate targeting studies, KB cells were grown in standard KB growth medium, and four days prior to the live cell experiment, they were transferred to folate free KB growth medium, in order to induce overexpression of the folate receptor. For live cell imaging, 10 kcells/well were seeded in 8-well µ-slides in 250 µL growth medium 24 h before incubation. Incubation experiments were carried out in the respective HEPES-buffered incubation media that were supplemented with the functionalized liposome suspensions, while the amount of liposomes was typically adjusted to a fixed amount of 10 pmol of each fluorophore-amphiphile conjugate per well (typically resulting in volumes of

5 - 10 µL), unless stated otherwise. Optimization of liposome functionalization yielded similar degrees of functionalizations and therefore similar absolute liposome suspension volumes, which were kept constant throughout each comparative experiment. Importantly, incubation media used in experiments described in Section 3.2 contained FBS (RBE incubation medium), while later experiments described in Section 3.3 were performed with serum free incubation media. For folate chasing experiments, incubation mixtures were supplemented with 100 µM folic acid. Unless stated otherwise, experiments described in Section 3.2 were incubated for 4 h, and experiments described in Section 3.3 were incubated for 24 h. Before imaging, cells were rinsed with DPBS and supplied with fresh, indicator free, HEPES-buffered microscopy medium.

Inhibition of specific endocytosis pathways was conducted by coincubation with either 1 mM Amiloride (inhibition of dynamin-dependent endocytosis[312]), 50 µM Chlorpromazine (inhibition of clathrin-dependent endocytosis, [313]), 25 µM Chloroquine (inhibition of lysosomal acidification, [314]), or 20 µg/mL Genistein (inhibition of caveolae-mediated endocytosis, [315]) and total incubation of 4 h. In keeping with the manufacturers protocol, coincubation with Lysotracker Blue was conducted at a concentration of 0.1 µM.

Confocal laser scanning microscopy

CLSM was performed on either a Leica TCS SP-5 confocal fluorescence microscope, equipped with an Okolab heated stage H301 (Okolab, Pozzuoli, Italy) and 405 nm, 488 nm, 561 nm and 633 nm laser lines on which a 63x/1.4 oil immersion objective was used, or on a Leica TCS STED CW confocal fluorescence microscope, equipped with an incubator box and 488 nm, 561 nm and 633 nm laser lines on which a 100x/1.4 oil immersion objective was used.

Settings for all experiments were: 1024x1024 pixels, 8 bit resolution, laser intensity 25% for 488 nm, 561 nm and 633 nm lasers and 50% for 405 nm laser in acquisition settings, 488 nm laser intensity at 25% in laser settings, a scan speed of 600 Hz and a numerical aperture of one Airy unit. Channel bandwidths were adjusted to 30-50 nm (typical bandwidths are listed with the fluorophores above) around the emission maximum of each respective fluorophore, and, importantly, kept constant throughout each experiment set. Also, photomultiplier (PMT) voltages were kept constant throughout each experiment. While it is in general advisable to fix these settings to specific values during the whole project, effects like detector aging did not always allows to keep PMT voltage and channel bandwidths constant. Therefore, experiments were designed to allow for intrinsically consistent conclusions by including all necessary control measurements without a variation of measurement parameters throughout the experiment. Optical inspection indicated immaculate viability of cells over the whole observation time.

Cytotoxicity: MTT Assay

Cytotoxicity was determined by an 3-(4,5-Dimethylthiazol-2-yl)-2,5-diphenyltetrazoliumbromid (MTT) assay. HeLa cells were seeded in a density of 10 kcells/well in 96-well optical bottom plates 12 h before incubation. For incubation, seeding medium was replaced with fresh medium containing liposomes in total lipid concentrations of 100, 10, 1 and 0.1 mg/mL. After incubation for 24 h, 40 µL of a 5 mg/mL solution of MTT in D-PBS were added to the respective incubation mixture and incubated for 1 hour. After careful removal of the medium, 225 µL of a 1:8 v/v mixture of glycine buffer pH 10 and DMSO were added and the cells shaken for 15 min to dissolve the precipitated crystals. 25 µL from each well were supplemented to 150 µL of glycine buffer pH 10-DMSO mixture (1:8 v/v) in a fresh 96-well plate. Absorbance of MTT was measured at 595 nm with background correction at 670 nm. Measured absorbances were normalized to untreated cells.

Acid cleavage: Polyacrylamide electrophoresis assay

A volume of 88 µL of purified liposomes suspended in PBS were supplemented with 44 µL of citric acid in the following concentrations: pH 2.4: 165 mM, pH 3.4: 27.3 mM, pH 4.4: 16.3 mM, pH 5.4: 9.5 mM, pH 6.4: 4.1 mM. Control of pH was conducted with a FiveEasy™ FE20 pH-meter (Mettler-Toledo, Gießen, Germany). After the intended time points, aliquots of 12 µL were taken and supplemented with 4 µL of the corresponding neutralization solution of Na_2HPO_4: pH 3.4: 723 mM, pH 4.4: 432 mM, pH 5.4: 252 mM, pH 6.4: 108 mM. For neutralization of pH 2.4, a 8.5 mM solution of Na_2HPO_4 and 9.8 mM NaOH was employed. As a gel loading buffer, 4 µL of a 60% (v/v) glycerol solution in PBS was used added and samples were stored at -20 °C until further analysis. Storage did not exceed 24 h. For the determination of cleavage kinetics at pH 7.4, PBS was used instead. For the determination of cleavage kinetics at pH 8.4, a sodiumtetraborate buffer was used, and samples stored at -80 °C after incubation.

PAGE was performed with 10 cm * 20 cm 15% denaturing polyacrylamide gels that were cast with two 1 mm spacers and custom-made combs to yield a thickness of 2 mm. The composition for 15% polyacrylamide contained 10% v/v denaturing PAGE buffer, 60% v/v denaturing PAGE concentrate (25%) and 30% v/v denaturing PAGE diluent. After electrophoresis was conducted for 2 h and 15 min at a constant power of 15 W, using a CBS LSG-400-20 adjustable vertical electrophoresis device (C.B.S. Scientific, San Diego, USA) and a Consort EV232 power supply (Consort, Turnhout, Belgium).

Gels were scanned on a Typhoon 9600 with blue laser unit (GE Healthcare). For the detection of Atto 488-labeled amphiphiles or cleaved polymer fragments, gels were illuminated with the 488 nm laser and analyzed with the 520 nm bandpass (40 nm) filter (520BP40). Image

analysis was performed with ImageJ to measure background-corrected band intensities, which were analyzed as described below.

Acid cleavage: Fluorescence spectroscopy

Hellma Suprasil® quartz glass cuvettes with a 1 cm path length and tight PTFE plugs were used for fluorescence spectroscopy analysis. Measurements were conducted in a Jasco FP-6500 Fluorimeter (JASCO, Tokyo, Japan) equipped with ETC-273T temperature controller , a peltier element stage with magnetic stirrer and a HAAKE® WKL26 cooling unit (Thermo Fisher Scientific). To prevent adsorption of lipids or liposomes to the cuvette surfaces, cuvettes were incubated with a 2.5 µL of unpurified stock suspension of conventional liposomes in 3.8 mL PBS for at least 24 h, before cleavage experiments were performed. After careful removal of this CL suspension, the liposomes of interest were transferred to the cuvette in a total volume of 2.53 mL, while the volume of liposome suspension was chosen to yield a final concentration of 50 nM Atto 488-modified liposomes. Liposome derivatization and purification was conducted as outlined above. After equilibration for 1 h, 1.26 mL of the corresponding acidic solutions were added, yielding 3.8 mL total volume and, importantly, leaving virtually no air space in the cuvette. Fluorescence emission was monitored under constant stirring and at 25 °C. Acetal-cleavage was monitored for 24 h at a data rate of $1\frac{1}{min}$ for all pH values, ketals were monitored at the following data rates (pH: total duration @ data rate): pH 3.4: 3 min @ $5\frac{1}{sec}$, pH 4.4: 15 min @ $0.5\frac{1}{sec}$, pH 5.4: 3 h @ $6\frac{1}{min}$, pH 6.4: 24 h @ $2\frac{1}{min}$, pH 7.4: 4 d @ $12\frac{1}{h}$, pH 8.4: 7 d @ $7.5\frac{1}{h}$. Control measurements were performed to assure no bleaching of the fluorophores during measurement. Other measurement parameters included: Excitation and emission bandwidth 5 nm, excitation wavelength 490 nm, emission wavelength 523 nm, PMT voltage setting high. Cuvettes were cleaned by incubation for 2 h in 2% Hellmanex solution at room temperature, or, for intensive cleaning, by incubation for 1 h with a 3:1 mixture of conc. H_2SO_4 : H_2O_2 30%. Obtained data was exported and analyzed with Origin as detailed below.

Kinetics data analysis

Data from cleavage experiments was first corrected for background values by subtraction of the values at t=0. As the reaction in buffer can be expected to follow first order kinetics, a first order exponential decay fit was applied:

$$y = A_1 \times e^{(-x/t_1)} + y_0 \tag{5.10}$$

For normalization to the degree of degradation, data was normalized to the target value y_0 as

obtained from a first order fit.

Half life times were calculated according to:

$$t_{1/2} = \ln(2) \times t_1 \tag{5.11}$$

Polymersome and polymer micelle formulation

DC formulation of polymersomes and micelles was conducted according to a modified liposome formulation protocol as detailed above. Acrylate-based polymers were dissolved in $CHCl_3$/MeOH 8:2 (v/v), Sar-b-Glu(OBn) polymers were dissolved in CH_2Cl_2.

For polymersomes, a solution of 4.5 mg of polymer compound was transferred to a PCR-vial suitable for dual centrifugation and dried in a vacuum centrifuge. Ceramic beads (41 mg, 0.3-0.4 mm) and 8 µL of PBS or a solution of SRB in PBS were added prior to subjecting the sample to two 16 min DC runs at 2500 RPM, in between of which the sample orientation was reversed. Afterwards, 19.1 µL PBS were added and two additional 2 min centrifugation runs conducted. Purification and EE determination was carried out as described above for liposomes.

Micelles were prepared by drying 5 mg of amphiphile compound in PCR vials and subsequent addition of 50 µL of PBS and 70 mg of ceramic beads. After a 20 min DC run, micelles were yielded and diluted to the needed concentrations.

Bibliography

[1] Massing, U., Cicko, S. & Ziroli, V. Dual asymmetric centrifugation (DAC)–a new technique for liposome preparation. *Journal of controlled release : official journal of the Controlled Release Society* **125**, 16–24 (2008). URL http://www.ncbi.nlm.nih.gov/pubmed/18023907.

[2] Fritz, T. *Functionalizable liposomes made by dual asymmetric centrifugation*. Diploma thesis, Johannes Gutenberg-University Mainz (2012).

[3] Bangham, A. D., Standish, M. M. & Watkins, J. C. Diffusion of univalent ions across the lamellae of swollen phospholipids. *Journal of molecular biology* **13**, 238–52 (1965). URL http://linkinghub.elsevier.com/retrieve/pii/S0022283665800936http://www.ncbi.nlm.nih.gov/pubmed/5859039.

[4] Tanford, C. The hydrophobic effect and the organization of living matter. *Science* **200**, 1012–1018 (1978). URL http://www.sciencemag.org/cgi/doi/10.1126/science.653353.

[5] Chandler, D. Interfaces and the driving force of hydrophobic assembly. *Nature* **437**, 640–647 (2005). URL http://www.ncbi.nlm.nih.gov/pubmed/16193038http://www.nature.com/doifinder/10.1038/nature04162.

[6] Israelachvili, J. N., Marčelja, S. & Horn, R. G. Physical principles of membrane organization. *Quarterly Reviews of Biophysics* **13**, 121 (1980). URL http://journals.cambridge.org/abstract{_}S0033583500001645http://www.journals.cambridge.org/abstract{_}S0033583500001645.

[7] Pidgeon, C., McNeely, S., Schmidt, T. & Johnson, J. E. Multilayered vesicles prepared by reverse-phase evaporation: liposome structure and optimum solute entrapment. *Biochemistry* **26**, 17–29 (1987).

[8] De Gier, J., Mandersloot, J. & Van Deenen, L. Lipid composition and permeability of liposomes. *Biochimica et Biophysica Acta (BBA) - Biomembranes* **150**, 666–675 (1968). URL http://www.sciencedirect.com/science/article/pii/0005273668900564.

[9] Papahadjopoulos, D., Jacobson, K., Nir, S. & Isac, T. Phase transitions in phospholipid vesicles. Fluorescence polarization and permeability measurements concerning the effect of temperature and cholesterol. *Biochimica et biophysica acta* **311**, 330–48 (1973). URL http://scholar.google.com/scholar?hl=en{&}btnG=Search{&}q=intitle:FLUORESCENCE+POLARIZATION+AND+PERMEABILITY+MEASURE-+MENTS+CONCERNING+THE+EFFECT+OF+TEMPERATURE+AND+CHOLE-+STEROL{#}4http://www.ncbi.nlm.nih.gov/pubmed/4729825.

[10] Koynova, R. & Caffrey, M. Phases and phase transitions of the phosphatidylcholines. *Biochimica et Biophysica Acta - Reviews on Biomembranes* **1376**, 91–145 (1998).

[11] Mouritsen, O. G. & Jørgensen, K. Dynamical order and disorder in lipid bilayers. *Chemistry and physics of lipids* **73**, 3–25 (1994). URL http://linkinghub.elsevier.com/retrieve/pii/0009308494901716http://www.ncbi.nlm.nih.gov/pubmed/8001184.

[12] Papahadjopoulos, D. Permeability properties of phospholipid membranes: Effect of cholesterol and

temperature. *Biochimica et Biophysica Acta (BBA) - Biomembranes* **266**, 561–583 (1972). URL http://linkinghub.elsevier.com/retrieve/pii/0005273672903549.

[13] Demel, R. A. & De Kruyff, B. The function of sterols in membranes. *BBA - Reviews on Biomembranes* **457**, 109–132 (1976).

[14] Sankaram, M. B. & Thompson, T. E. Modulation of phospholipid acyl chain order by cholesterol. A solid-state 2H nuclear magnetic resonance study. *Biochemistry* **29**, 10676–10684 (1990). URL http://www.scopus.com/inward/record.url?eid=2-s2.0-0025633287{&}partnerID=40{&}md5=68d7708439be12fd2d0590e479c3e14a.

[15] McMullen, T. P. & McElhaney, R. N. Physical studies of cholesterol-phospholipid interactions. *Current Opinion in Colloid & Interface Science* **1**, 83–90 (1996). URL http://dx.doi.org/10.1016/S1359-0294(96)80048-3http://linkinghub.elsevier.com/retrieve/pii/S1359029496800483.

[16] Israelachvili, J. N., Mitchell, D. J. & Ninham, B. W. Theory of self-assembly of hydrocarbon amphiphiles into micelles and bilayers. *Journal of the Chemical Society, Faraday Transactions 2* **72**, 1525 (1976).

[17] Israelachvili, J. J. N. *Intermolecular and Surface Forces, 3rd Edition* (Cambridge University Press, Cambridge, 2010), 3rd edn. URL http://ebooks.cambridge.org/ref/id/CBO9781107415324A009. arXiv:1011.1669v3.

[18] Allen, T. M., Hong, K. & Papahadjopoulos, D. Membrane contact, fusion, and hexagonal (HII) transitions in phosphatidylethanolamine liposomes. *Biochemistry* **29**, 2976–85 (1990). URL http://www.ncbi.nlm.nih.gov/pubmed/2337577.

[19] Klein, G. & Grosse, A. Pharmaceutical preparation (1932).

[20] Sessa, G. & Weissmann, G. Incorporation of lysozyme into liposomes. A model for structure-linked latency. *The Journal of biological chemistry* **245**, 3295–301 (1970). URL http://www.jbc.org/content/245/13/3295.full.pdfhttp://www.ncbi.nlm.nih.gov/pubmed/5459633.

[21] Gibbs, B., Kermasha, S., Alli, I. & Mulligan, C. Encapsulation in the food industry: a review. *International Journal of Food Sciences and Nutrition* **50**, 213–224 (1999). URL http://informahealthcare.com/doi/abs/10.1080/096374899101256.

[22] Mozafari, M. R., Johnson, C., Hatziantoniou, S. & Demetzos, C. Nanoliposomes and their applications in food nanotechnology. *Journal of liposome research* **18**, 309–327 (2008).

[23] Mu, L. & Sprando, R. L. Application of Nanotechnology in Cosmetics. *Pharmaceutical Research* **27**, 1746–1749 (2010). URL http://link.springer.com/10.1007/s11095-010-0139-1.

[24] Kirby, C., Brooker, B. & Law, B. Accelerated ripening of cheese using liposome-encapsulated enzyme. *International Journal of Food Science & Technology* **22**, 355–375 (1987). URL http://doi.wiley.com/10.1111/j.1365-2621.1987.tb00499.x.

[25] Loukas, Y. L., Jayasekera, P. & Gregoriadis, G. Novel liposome-based multicomponent systems for the protection of photolabile agents. *International Journal of Pharmaceutics* **117**, 85–94 (1995). URL http://linkinghub.elsevier.com/retrieve/pii/0378517394003205.

[26] Gregoriadis, G. The Carrier Potential of Liposomes in Biology and Medicine. *New England Journal of Medicine* **295**, 704–710 (1976). URL http://www.nejm.org/doi/abs/10.1056/NEJM197609232951305.

[27] Gregoriadis, G. Liposomes in Therapeutic and Preventive Medicine: The Development of the Drug-Carrier Concept. *Annals of the New York Academy of Sciences* 343–370 (1978). URL http://onlinelibrary.wiley.com/doi/10.1111/j.1749-6632.1978.tb22034.x/abstract.

[28] Alving, C. R. *et al.* Therapy of leishmaniasis: superior efficacies of liposome-encapsulated drugs. *Proceedings of the National Academy of Sciences of the United States of America* **75**, 2959–2963 (1978).

[29] Choi, H. S. *et al.* Renal clearance of nanoparticles. *Nat. Biotechnol.* **25**, 1165–1170 (2007). URL http://dx.doi.org/10.1038/nbt1340.

[30] Stamp, D. & Juliano, R. L. Factors affecting the encapsulation of drugs within liposomes. *Canadian Journal of Physiology and Pharmacology* **57**, 535–539 (1979). URL http://www.nrcresearchpress.com/doi/abs/10.1139/y79-081.

[31] Meunier, F., Prentice, H. G. & Ringden, O. Liposomal amphotericin B (AmBisome): safety data from a phase II/III clinical trial. *J.Antimicrob.Chemother.* **28 Suppl B**, 83–91 (1991).

[32] Gulati, M., Grover, M., Singh, S. & Singh, M. Lipophilic drug derivatives in liposomes. *International Journal of Pharmaceutics* **165**, 129–168 (1998).

[33] Allen, T. M. & Chonn, A. Large unilamellar liposomes with low uptake into the reticuloendothelial system. *FEBS letters* **223**, 42–6 (1987). URL http://www.ncbi.nlm.nih.gov/pubmed/3666140.

[34] Chonn, A. & Cullis, P. R. Gangliosides and hydrophilic polymers increase liposome circulation times by inhibiting the association of blood proteins. *Journal of liposome research* **2**, 397–410 (1992).

[35] Allen, T. M. & Everest, J. M. Effect of liposome size and drug release properties on pharmacokinetics of encapsulated drug in rats. *The Journal of pharmacology and experimental therapeutics* **226**, 539–44 (1983). URL http://www.ncbi.nlm.nih.gov/pubmed/6875864.

[36] Allen, T. M. The use of glycolipids and hydrophilic polymers in avoiding rapid uptake of liposomes by the mononuclear phagocyte system. *Advanced Drug Delivery Reviews* **13**, 285–309 (1994).

[37] Klibanov, A. L., Maruyama, K., Torchilin, V. P. & Huang, L. Amphipathic polyethyleneglycols effectively prolong the circulation time of liposomes. *FEBS Letters* **268**, 235–237 (1990).

[38] Allen, T., Hansen, C., Martin, F., Redemann, C. & Yau-Young, A. Liposomes containing synthetic lipid derivatives of poly(ethylene glycol) show prolonged circulation half-lives in vivo. *Biochimica et Biophysica Acta (BBA) - Biomembranes* **1066**, 29–36 (1991). URL http://www.ncbi.nlm.nih.gov/pubmed/2065067http://linkinghub.elsevier.com/retrieve/pii/0005273691902465.

[39] Israelachvili, J. The different faces of poly(ethylene glycol). *Proceedings of the National Academy of Sciences of the United States of America* **94**, 8378–8379 (1997).

[40] Papisov, M. I. Theoretical considerations of RES-avoiding liposomes: Molecular mechanics and chemistry of liposome interactions. *Advanced Drug Delivery Reviews* **32**, 119–138 (1998).

[41] Drummond, D. C., Meyer, O., Hong, K., Kirpotin, D. B. & Papahadjopoulos, D. Optimizing liposomes for delivery of chemotherapeutic agents to solid tumors. *Pharmacological reviews* **51**, 691–743 (1999). URL http://www.ncbi.nlm.nih.gov/pubmed/10581328.

[42] Woodle, M. C. Surface-modified liposomes: assessment and characterization for increased stability and prolonged blood circulation. *Chemistry and Physics of Lipids* **64**, 249–262 (1993).

[43] Torchilin, V. P. & Papisov, M. I. Why do Polyethylene Glycol-Coated Liposomes Circulate So Long?: Molecular Mechanism of Liposome Steric Protection with Polyethylene Glycol: Role of Polymer Chain Flexibility. *Journal of Liposome Research* **4**, 725–739 (1994). URL http://www.tandfonline.com/doi/full/10.3109/08982109409037068.

[44] Immordino, M. L., Dosio, F. & Cattel, L. Stealth liposomes: review of the basic science, rationale, and clinical applications, existing and potential. *International journal of nanomedicine* **1**, 297–315 (2006). URL http://www.pubmedcentral.nih.gov/articlerender.fcgi?artid=2426795{&}tool=

pmcentrez{&}rendertype=abstracthttp://www.ncbi.nlm.nih.gov/pubmed/17717971http://www.pubmedcentral.nih.gov/articlerender.fcgi?artid=PMC2426795http://www.ncbi.nlm.nih.gov/pubmed/242679.

[45] Gabizon, A. & Papahadjopoulos, D. Liposome formulations with prolonged circulation time in blood and enhanced uptake by tumors. *Proceedings of the National Academy of Sciences of the United States of America* **85**, 6949–53 (1988). URL http://www.pubmedcentral.nih.gov/articlerender.fcgi?artid=282096{&}tool=pmcentrez{&}rendertype=abstract.

[46] Matsumura, Y. & Maeda, H. A new concept for macromolecular therapeutics in cancer chemotherapy: mechanism of tumoritropic accumulation of proteins and the antitumor agent smancs. *Cancer research* **46**, 6387–92 (1986). URL http://www.ncbi.nlm.nih.gov/pubmed/2946403.

[47] Maeda, H., Wu, J., Sawa, T., Matsumura, Y. & Hori, K. Tumor vascular permeability and the EPR effect in macromolecular therapeutics: a review. *Journal of controlled release : official journal of the Controlled Release Society* **65**, 271–84 (2000). URL http://www.ncbi.nlm.nih.gov/pubmed/10699287.

[48] Lasic, D. D. & Needham, D. The "Stealth" Liposome: A Prototypical Biomaterial. *Chemical Reviews* **95**, 2601–2628 (1995). URL http://pubs.acs.org/doi/abs/10.1021/cr00040a001.

[49] Barenholz, Y. Doxil®–the first FDA-approved nano-drug: lessons learned. *Journal of controlled release : official journal of the Controlled Release Society* **160**, 117–34 (2012). URL http://www.ncbi.nlm.nih.gov/pubmed/22484195.

[50] Gabizon, a., Shmeeda, H. & Barenholz, Y. Pharmacokinetics of pegylated liposomal Doxorubicin: review of animal and human studies. *Clin.Pharmacokinet.* **42**, 419–436 (2003). URL ISI:000183260700002.

[51] Deamer, D. W., Prince, R. C. & Crofts, A. R. The response of fluorescent amines to pH gradients across liposome membranes. *BBA - Biomembranes* **274**, 323–335 (1972).

[52] Madden, T. D. *et al.* The accumulation of drugs within large unilamellar vesicles exhibiting a proton gradient: a survey. *Chemistry and physics of lipids* **53**, 37–46 (1990). URL http://www.ncbi.nlm.nih.gov/pubmed/1972352.

[53] Haran, G., Cohen, R., Bar, L. K. & Barenholz, Y. Transmembrane ammonium sulfate gradients in liposomes produce efficient and stable entrapment of amphipathic weak bases. *BBA - Biomembranes* **1151**, 201–215 (1993). URL http://www.ncbi.nlm.nih.gov/pubmed/8373796.

[54] Pain, D., Das, P. K., Ghosh, P. & Bachhawat, B. K. Increased circulatory half-life of liposomes after conjunction with dextran. *Journal of Biosciences* **6**, 811–816 (1984). URL http://link.springer.com/10.1007/BF02716840.

[55] Torchilin, V. *et al.* Poly (ethylene glycol) on the liposome surface: on the mechanism of polymer-coated liposome longevity. *Biochimica et Biophysica Acta (BBA)-Biomembranes* **1195**, 11–20 (1994). URL http://www.sciencedirect.com/science/article/pii/0005273694900035.

[56] Torchilin, V. P., Shtilman, M. I., Trubetskoy, V. S., Whiteman, K. & Milstein, A. M. Amphiphilic vinyl polymers effectively prolong liposome circulation time in vivo. *Biochimica et biophysica acta* **1195**, 181–4 (1994). URL http://www.sciencedirect.com/science/article/pii/0005273694900256http://www.ncbi.nlm.nih.gov/pubmed/7918561.

[57] Woodle, M. C., Engbers, C. M. & Zalipsky, S. New amphipatic polymer-lipid conjugates forming long-circulating reticuloendothelial system-evading liposomes. *Bioconjugate chemistry* **5**, 493–6 (1994). URL http://www.ncbi.nlm.nih.gov/pubmed/7873652.

[58] Whiteman, K. R., Subr, V., Ulbrich, K. & Torchilin, V. P. Poly(Hpma)-Coated Liposomes Demonstrate

Prolonged Circulation in Mice. *Journal of Liposome Research* **11**, 153–164 (2001). URL http://www.tandfonline.com/doi/full/10.1081/LPR-100108459.

[59] Takeuchi, H., Kojima, H., Yamamoto, H. & Kawashima, Y. Evaluation of circulation profiles of liposomes coated with hydrophilic polymers having different molecular weights in rats. *Journal of controlled release : official journal of the Controlled Release Society* **75**, 83–91 (2001). URL http://www.ncbi.nlm.nih.gov/pubmed/11451499.

[60] Maruyama, K. *et al.* Phosphatidyl polyglycerols prolong liposome circulation in vivo. *International Journal of Pharmaceutics* **111**, 103–107 (1994). URL http://www.sciencedirect.com/science/article/pii/037851739490407 3http://linkinghub.elsevier.com/retrieve/pii/0378517394904073.

[61] Hofmann, A. M. *et al.* Hyperbranched polyglycerol-based lipids via oxyanionic polymerization: Toward multifunctional stealth liposomes. *Biomacromolecules* **11**, 568–574 (2010). URL http://www.ncbi.nlm.nih.gov/pubmed/20121134.

[62] Hofmann, A. M., Wurm, F. & Frey, H. Rapid Access to Polyfunctional Lipids with Complex Architecture via Oxyanionic Ring-Opening Polymerization. *Macromolecules* **44**, 4648–4657 (2011). URL http://pubs.acs.org/doi/abs/10.1021/ma200367c.

[63] Müller, S. S., Dingels, C., Hofmann, A. M. & Frey, H. Polyether-Based Lipids Synthesized with an Epoxide Construction Kit: Multivalent Architectures for Functional Liposomes. In Scholz, C. & Kressler, J. (eds.) *Tailored Polymer Architectures for Pharmaceutical and Biomedical Applications*, chap. 2, 11–25 (American Chemical Society, Washington, DC, 2013). URL http://pubs.acs.org/doi/abs/10.1021/bk-2013-1135.ch002.

[64] Schöps, R., Amado, E., Müller, S. S., Frey, H. & Kressler, J. Block copolymers in giant unilamellar vesicles with proteins or with phospholipids. *Faraday Discussions* **166**, 303–315 (2013). URL http://xlink.rsc.org/?DOI=c3fd00062a.

[65] Scholtysek, P. *et al.* Unusual triskelion patterns and dye-labelled GUVs: consequences of the interaction of cholesterol-containing linear-hyperbranched block copolymers with phospholipids. *Soft Matter* **11**, 6106–6117 (2015). URL http://xlink.rsc.org/?DOI=C5SM01017A.

[66] Mohr, K. *et al.* Evaluation of multifunctional liposomes in human blood serum by light scattering. *Langmuir : the ACS journal of surfaces and colloids* **30**, 14954–62 (2014). URL http://www.ncbi.nlm.nih.gov/pubmed/25469945.

[67] Reibel, A. T. *et al.* Fate of Linear and Branched Polyether-Lipids In Vivo in Comparison to Their Liposomal Formulations by 18 F-Radiolabeling and Positron Emission Tomography. *Biomacromolecules* **16**, 842–851 (2015). URL http://pubs.acs.org/doi/abs/10.1021/bm5017332.

[68] Dams, E. T. *et al.* Accelerated blood clearance and altered biodistribution of repeated injections of sterically stabilized liposomes. *The Journal of pharmacology and experimental therapeutics* **292**, 1071–1079 (2000).

[69] Abu Lila, A. S., Nawata, K., Shimizu, T., Ishida, T. & Kiwada, H. Use of polyglycerol (PG), instead of polyethylene glycol (PEG), prevents induction of the accelerated blood clearance phenomenon against long-circulating liposomes upon repeated administration. *International Journal of Pharmaceutics* **456**, 235–242 (2013). URL http://dx.doi.org/10.1016/j.ijpharm.2013.07.059.

[70] Papahadjopoulos, D. *et al.* Sterically stabilized liposomes: improvements in pharmacokinetics and antitumor therapeutic efficacy. *Proceedings of the National Academy of Sciences of the United States*

of America **88**, 11460–4 (1991). URL http://www.pubmedcentral.nih.gov/articlerender.fcgi?artid=53155{&}tool=pmcentrez{&}rendertype=abstract.

[71] Webb, M. S. *et al.* Comparison of different hydrophobic anchors conjugated to poly(ethylene glycol): Effects on the pharmacokinetics of liposomal vincristine. *Biochimica et Biophysica Acta - Biomembranes* **1372**, 272–282 (1998).

[72] Rejman, J., Wagenaar, A., Engberts, J. B. F. N. & Hoekstra, D. Characterization and transfection properties of lipoplexes stabilized with novel exchangeable polyethylene glycol-lipid conjugates. *Biochimica et Biophysica Acta - Biomembranes* **1660**, 41–52 (2004).

[73] Heyes, J., Hall, K., Tailor, V., Lenz, R. & MacLachlan, I. Synthesis and characterization of novel poly(ethylene glycol)-lipid conjugates suitable for use in drug delivery. *Journal of Controlled Release* **112**, 280–290 (2006). URL http://linkinghub.elsevier.com/retrieve/pii/S0168365906000836.

[74] Fahr, A., Hoogevest, P. V., May, S., Bergstrand, N. & Leigh, M. L. S. Transfer of lipophilic drugs between liposomal membranes and biological interfaces: Consequences for drug delivery. *European Journal of Pharmaceutical Sciences* **26**, 251–265 (2005).

[75] McLean, L. R. & Phillips, M. C. Mechanism of cholesterol and phosphatidylcholine exchange or transfer between unilamellar vesicles. *Biochemistry* **20**, 2893–900 (1981). URL http://www.ncbi.nlm.nih.gov/pubmed/7195733.

[76] McLean, L. R. & Phillips, M. C. Kinetics of phosphatidylcholine and lysophosphatidylcholine exchange between unilamellar vesicles. *Biochemistry* **23**, 4624–4630 (1984).

[77] Bar, L. K., Barenholz, Y. & Thompson, T. E. Fraction of cholesterol undergoing spontaneous exchange between small unilamellar phosphatidylcholine vesicles. *Biochemistry* **25**, 6701–6705 (1986).

[78] Nag, O. K., Yadav, V. R., Hedrick, A. & Awasthi, V. Post-modification of preformed liposomes with novel non-phospholipid poly(ethylene glycol)-conjugated hexadecylcarbamoylmethyl hexadecanoic acid for enhanced circulation persistence in vivo. *International Journal of Pharmaceutics* **446**, 119–129 (2013). URL http://dx.doi.org/10.1016/j.ijpharm.2013.02.026http://linkinghub.elsevier.com/retrieve/pii/S0378517313001610.

[79] Mui, B. L. *et al.* Influence of Polyethylene Glycol Lipid Desorption Rates on Pharmacokinetics and Pharmacodynamics of siRNA Lipid Nanoparticles. *Molecular therapy. Nucleic acids* **2**, e139 (2013). URL http://www.ncbi.nlm.nih.gov/pubmed/24345865http://www.nature.com/doifinder/10.1038/mtna.2013.66http://www.pubmedcentral.nih.gov/articlerender.fcgi?artid=PMC3894582.

[80] Ishiwata, H., Vertut-Doï, A., Hirose, T. & Miyajima, K. Physical-chemistry characteristics and biodistribution of poly(ethylene glycol)-coated liposomes using poly(oxyethylene) cholesteryl ether. *Chemical & pharmaceutical bulletin* **43**, 1005–1011 (1995). URL https://www.jstage.jst.go.jp/article/cpb1958/43/6/43{_}6{_}1005/{_}pdf$\delimiter"026E30F$npapers3://publication/uuid/59D5C8B8-00F8-471E-842A-00E8FA883585http://europepmc.org/abstract/MED/7641302.

[81] Semple, S. C., Chonn, A. & Cullis, P. R. Influence of cholesterol on the association of plasma proteins with liposomes. *Biochemistry* **35**, 2521–2525 (1996).

[82] Bradley, A. J., Devine, D. V., Ansell, S. M., Janzen, J. & Brooks, D. E. Inhibition of liposome-induced complement activation by incorporated poly(ethylene glycol)-lipids. *Archives of biochemistry and biophysics* **357**, 185–94 (1998). URL http://www.sciencedirect.com/science/article/pii/S0003986198907986.

[83] Xiong, S., Yu, B., Wu, J., Li, H. & Lee, R. J. Preparation, therapeutic efficacy and intratumoral localization of targeted daunorubicin liposomes conjugating folate-PEG-CHEMS. *Biomedicine and Pharmacotherapy* **65**, 2–8 (2011).

[84] Kuang, Y., Liu, J., Liu, Z. & Zhuo, R. Cholesterol-based anionic long-circulating cisplatin liposomes with reduced renal toxicity. *Biomaterials* **33**, 1596–1606 (2012). URL `http://dx.doi.org/10.1016/j.biomaterials.2011.10.081`.

[85] Beugin-Deroo, S., Ollivon, M. & Lesieur, S. Bilayer Stability and Impermeability of Nonionic Surfactant Vesicles Sterically Stabilized by PEG-Cholesterol Conjugates. *Journal of Colloid and Interface Science* **202**, 324–333 (1998). URL `http://linkinghub.elsevier.com/retrieve/pii/S0021979798955060`.

[86] Vertut-Doï, A., Ishiwata, H. & Miyajima, K. Binding and uptake of liposomes containing a poly(ethylene glycol) derivative of cholesterol (stealth liposomes) by the macrophage cell line J774: influence of PEG content and its molecular weight. *Biochimica et Biophysica Acta (BBA) - Biomembranes* **1278**, 19–28 (1996). URL `http://linkinghub.elsevier.com/retrieve/pii/0005273695001859`.

[87] Yuda, T., Maruyama, K. & Iwatsuru, M. Prolongation of liposome circulation time by various derivatives of polyethyleneglycols. *Biological & pharmaceutical bulletin* **19**, 1347–51 (1996). URL `http://www.ncbi.nlm.nih.gov/pubmed/8913510`.

[88] Carrion, C., Domingo, J. C. & de Madariaga, M. a. Preparation of long-circulating immunoliposomes using PEG-cholesterol conjugates: effect of the spacer arm between PEG and cholesterol on liposomal characteristics. *Chemistry and physics of lipids* **113**, 97–110 (2001). URL `http://www.ncbi.nlm.nih.gov/pubmed/11687230`.

[89] Sato, S. B. *et al.* Distribution and transport of cholesterol-rich membrane domains monitored by a membrane-impermeant fluorescent polyethylene glycol-derivatized cholesterol. *The Journal of biological chemistry* **279**, 23790–6 (2004). URL `http://www.ncbi.nlm.nih.gov/pubmed/15026415`.

[90] Steenpaß, T., Lung, A. & Schubert, R. Tresylated PEG-sterols for coupling of proteins to preformed plain or PEGylated liposomes. *Biochimica et Biophysica Acta - Biomembranes* **1758**, 20–28 (2006).

[91] Gantert, M. *et al.* Receptor-specific targeting with liposomes in vitro based on sterol-PEG(1300) anchors. *Pharmaceutical research* **26**, 529–38 (2009). URL `http://www.ncbi.nlm.nih.gov/pubmed/19015959`.

[92] He, Z. Y. *et al.* Recent development of poly(ethylene glycol)-cholesterol conjugates as drug delivery systems. *International Journal of Pharmaceutics* **469**, 168–178 (2014).

[93] Holland, J. W., Hui, C., Cullis, P. R. & Madden, T. D. Poly(ethylene glycol)–lipid conjugates regulate the calcium-induced fusion of liposomes composed of phosphatidylethanolamine and phosphatidylserine. *Biochemistry* **35**, 2618–24 (1996). URL `http://www.ncbi.nlm.nih.gov/pubmed/8611565$\delimiter"026E30F$nhttp://pubs.acs.org/doi/abs/10.1021/bi952000vhttp://pubs.acs.org/doi/abs/10.1021/bi952000vhttp://www.ncbi.nlm.nih.gov/pubmed/8611565`.

[94] Hong, R. L. *et al.* Direct comparison of liposomal doxorubicin with or without polyethylene glycol coating in C-26 tumor-bearing mice: is surface coating with polyethylene glycol beneficial? *Clinical cancer research : an official journal of the American Association for Cancer Research* **5**, 3645–52 (1999). URL `http://www.ncbi.nlm.nih.gov/pubmed/10589782`.

[95] Martschick, A. *et al.* The pathogenetic mechanism of anthracycline-induced palmar-plantar erythrodysesthesia. *Anticancer Research* **29**, 2307–2313 (2009).

[96] Kirpotin, D., Hong, K., Mullah, N., Papahadjopoulos, D. & Zalipsky, S. Liposomes with detachable

polymer coating: Destabilization and fusion of dioleoylphosphatidylethanolamine vesicles triggered by cleavage of surface-grafted poly(ethylene glycol). *FEBS Letters* **388**, 115–118 (1996).

[97] Saito, G., Swanson, J. A. & Lee, K. D. Drug delivery strategy utilizing conjugation via reversible disulfide linkages: Role and site of cellular reducing activities. *Advanced Drug Delivery Reviews* **55**, 199–215 (2003).

[98] Zalipsky, S. *et al.* New detachable poly(ethylene glycol) conjugates: Cysteine-cleavable lipopolymers regenerating natural phospholipid, diacyl phosphatidylethanolamine. *Bioconjugate Chemistry* **10**, 703–707 (1999).

[99] Karathanasis, E., Ayyagari, A. L., Bhavane, R., Bellamkonda, R. V. & Annapragada, A. V. Preparation of in vivo cleavable agglomerated liposomes suitable for modulated pulmonary drug delivery. *Journal of Controlled Release* **103**, 159–175 (2005).

[100] Vaupel, P., Kallinowski, F. & Okunieff, P. Blood flow, oxygen and nutrient supply, and metabolic microenvironment of human tumors: a review. *Cancer research* **49**, 6449–65 (1989). URL `http://www.ncbi.nlm.nih.gov/pubmed/2684393`.

[101] De Milito, A. & Fais, S. Tumor acidity, chemoresistance and proton pump inhibitors. *Future Oncology* **1**, 779–786 (2005). URL `http://www.futuremedicine.com/doi/abs/10.2217/14796694.1.6.779`.

[102] Mellman, I., Fuchs, R. & Helenius, A. Acidification of the endocytic and exocytic pathways. *Annual Review of Biochemistry* **55**, 663–700 (1986). URL `http://www.annualreviews.org/doi/pdf/10.1146/annurev.bi.55.070186.003311http://www.annualreviews.org/doi/abs/10.1146/annurev.bi.55.070186.003311`.

[103] Andresen, T. L., Jensen, S. S. & Jørgensen, K. Advanced strategies in liposomal cancer therapy: Problems and prospects of active and tumor specific drug release. *Progress in Lipid Research* **44**, 68–97 (2005).

[104] Guo, X., MacKay, J. A. & Szoka, F. C. Mechanism of pH-triggered collapse of phosphatidylethanolamine liposomes stabilized by an ortho ester polyethyleneglycol lipid. *Biophysical journal* **84**, 1784–1795 (2003). URL `http://dx.doi.org/10.1016/S0006-3495(03)74986-8`.

[105] Choi, J. S., MacKay, J. A. & Szoka, F. C. Low-pH-sensitive PEG-stabilized plasmid-lipid nanoparticles: Preparation and characterization. *Bioconjugate Chemistry* **14**, 420–429 (2003).

[106] Masson, C. *et al.* pH-Sensitive PEG lipids containing orthoester linkers: New potential tools for nonviral gene delivery. *Journal of Controlled Release* **99**, 423–434 (2004).

[107] Shin, J., Shum, P. & Thompson, D. H. Acid-triggered release via dePEGylation of DOPE liposomes containing acid-labile vinyl ether PEG-lipids. *Journal of Controlled Release* **91**, 187–200 (2003).

[108] Xu, H. *et al.* Esterase-catalyzed dePEGylation of pH-sensitive vesicles modified with cleavable PEG-lipid derivatives. *Journal of Controlled Release* **130**, 238–245 (2008).

[109] Clawson, C. *et al.* Synthesis and Characterization of Lipid-Polymer Hybrid Nanoparticles with pH-Triggered Poly(ethylene glycol) Shedding. *Langmuir* **27**, 10556–10561 (2011). URL `http://pubs.acs.org/doi/abs/10.1021/la202123e`.

[110] Dingels, C., Müller, S. S., Steinbach, T., Tonhauser, C. & Frey, H. Universal Concept for the Implementation of a Single Cleavable Unit at Tunable Position in Functional Poly(ethylene glycol)s. *Biomacromolecules* **14**, 448–59 (2013). URL `http://www.ncbi.nlm.nih.gov/pubmed/23256621`.

[111] Pattni, B. S., Chupin, V. V. & Torchilin, V. P. New Developments in Liposomal Drug Delivery. *Chemical Reviews* **115**, 10938–10966 (2015). URL `http://pubs.acs.org/doi/abs/10.1021/acs.chemrev.5b00046http://pubs.acs.org/doi/10.1021/acs.chemrev.5b00046`.

[112] Chou, H.-H. *et al.* Pegylated liposomal doxorubicin (Lipo-Dox®) for platinum-resistant or refractory epithelial ovarian carcinoma: A Taiwanese gynecologic oncology group study with long-term follow-up. *Gynecologic Oncology* **101**, 423–428 (2006). URL http://ovidsp.ovid.com/ovidweb.cgi?T=JS{&}PAGE=reference{&}D=med5{&}NEWS=N{&}AN=16325239http://linkinghub.elsevier.com/retrieve/pii/S0090825805009698.

[113] Gardikis, K., Tsimplouli, C., Dimas, K., Micha-Screttas, M. & Demetzos, C. New chimeric advanced Drug Delivery nano Systems (chi-aDDnSs) as doxorubicin carriers. *International Journal of Pharmaceutics* **402**, 231–237 (2010). URL http://dx.doi.org/10.1016/j.ijpharm.2010.10.007http://linkinghub.elsevier.com/retrieve/pii/S0378517310007696.

[114] Fassas, A. & Anagnostopoulos, A. The use of liposomal daunorubicin (DaunoXome) in acute myeloid leukemia. *Leukemia & Lymphoma* **46**, 795–802 (2005). URL http://www.tandfonline.com/doi/full/10.1080/10428190500052438.

[115] Silverman, J. A. & Deitcher, S. R. Marqibo® (vincristine sulfate liposome injection) improves the pharmacokinetics and pharmacodynamics of vincristine. *Cancer chemotherapy and pharmacology* **71**, 555–64 (2013). URL http://link.springer.com/10.1007/s00280-012-2042-4http://www.ncbi.nlm.nih.gov/pubmed/23212117http://www.pubmedcentral.nih.gov/articlerender.fcgi?artid=PMC3579462.

[116] Glantz, M. J. *et al.* A randomized controlled trial comparing intrathecal sustained-release cytarabine (DepoCyt) to intrathecal methotrexate in patients with neoplastic meningitis from solid tumors. *Clinical cancer research : an official journal of the American Association for Cancer Research* **5**, 3394–402 (1999). URL http://www.ncbi.nlm.nih.gov/pubmed/10589750.

[117] Gambling, D., Hughes, T., Martin, G., Horton, W. & Manvelian, G. A comparison of Depodur, a novel, single-dose extended-release epidural morphine, with standard epidural morphine for pain relief after lower abdominal surgery. *Anesthesia and analgesia* **100**, 1065–74 (2005). URL http://content.wkhealth.com/linkback/openurl?sid=WKPTLP:landingpage{&}an=00000539-200504000-00028http://www.ncbi.nlm.nih.gov/pubmed/15781524.

[118] Bressler, N. M. & Bressler, S. B. Photodynamic therapy with verteporfin (Visudyne): impact on ophthalmology and visual sciences. *Investigative ophthalmology & visual science* **41**, 624–8 (2000). URL http://www.ncbi.nlm.nih.gov/pubmed/10711673.

[119] Usonis, V. *et al.* Antibody titres after primary and booster vaccination of infants and young children with a virosomal hepatitis A vaccine (Epaxal®). *Vaccine* **21**, 4588–4592 (2003). URL http://linkinghub.elsevier.com/retrieve/pii/S0264410X03005097.

[120] Mischler, R. & Metcalfe, I. C. Inflexal®V a trivalent virosome subunit influenza vaccine: production. *Vaccine* **20**, B17–B23 (2002). URL http://linkinghub.elsevier.com/retrieve/pii/S0264410X02005121.

[121] Eichhorn, M. E. *et al.* Vascular targeting by EndoTAGTM-1 enhances therapeutic efficacy of conventional chemotherapy in lung and pancreatic cancer. *International Journal of Cancer* **126**, 1235–1245 (2010).

[122] Slingerland, M. *et al.* Bioequivalence of Liposome-Entrapped Paclitaxel Easy-To-Use (LEP-ETU) Formulation and Paclitaxel in Polyethoxylated Castor Oil: A Randomized, Two-Period Crossover Study in Patients With Advanced Cancer. *Clinical Therapeutics* **35**, 1946–1954 (2013). URL http://dx.doi.org/10.1016/j.clinthera.2013.10.009.

[123] Harrington, K. J. *et al.* Phase I-II study of pegylated liposomal cisplatin (SPI-077) in patients with inop-

erable head and neck cancer. *Annals of oncology : official journal of the European Society for Medical Oncology / ESMO* **12**, 493–6 (2001). URL http://www.ncbi.nlm.nih.gov/pubmed/11398881.

[124] Hoving, S., van Tiel, S. T., Eggermont, A. M. M. & ten Hagen, T. L. M. Effect of low-dose tumor necrosis factor-alpha in combination with STEALTH liposomal cisplatin (SPI-077) on soft-tissue- and osteosarcoma-bearing rats. *Anticancer research* **25**, 743–50 (2005). URL http://www.ncbi.nlm.nih.gov/pubmed/15868905.

[125] Farhat, F. S. *et al.* A phase II study of lipoplatin (liposomal cisplatin)/vinorelbine combination in HER-2/neunegative metastatic breast cancer. *Clinical Breast Cancer* **11**, 384–389 (2011). URL http://dx.doi.org/10.1016/j.clbc.2011.08.005.

[126] Booser, D. J. *et al.* Phase II study of liposomal annamycin in the treatment of doxorubicin-resistant breast cancer. *Cancer Chemotherapy and Pharmacology* **50**, 6–8 (2002).

[127] Wetzler, M. *et al.* Phase I/II trial of nanomolecular liposomal annamycin in adult patients with relapsed/refractory acute lymphoblastic leukemia. *Clinical lymphoma, myeloma & leukemia* **13**, 430–4 (2013). URL http://www.pubmedcentral.nih.gov/articlerender.fcgi?artid=3737573{&}tool=pmcentrez{&}rendertype=abstract.

[128] Tardi, P. *et al.* Liposomal encapsulation of topotecan enhances anticancer efficacy in murine and human xenograft models. *Cancer Research* **60**, 3389–3393 (2000).

[129] Needham, D., Anyarambhatla, G., Kong, G. & Dewhirst, M. W. A new temperature-sensitive liposome for use with mild hyperthermia: characterization and testing in a human tumor xenograft model. *Cancer research* **60**, 1197–201 (2000). URL http://www.ncbi.nlm.nih.gov/pubmed/10728674.

[130] Poon, R. T. P. & Borys, N. Lyso-thermosensitive liposomal doxorubicin: a novel approach to enhance efficacy of thermal ablation of liver cancer. *Expert opinion on pharmacotherapy* **10**, 333–343 (2009).

[131] Yarmolenko, P. S. *et al.* Comparative effects of thermosensitive doxorubicin-containing liposomes and hyperthermia in human and murine tumours. *International journal of hyperthermia : the official journal of European Society for Hyperthermic Oncology, North American Hyperthermia Group* **26**, 485–98 (2010). URL http://www.ncbi.nlm.nih.gov/pubmed/20597627$\delimiter"026E30F$nhttp://www.pubmedcentral.nih.gov/articlerender.fcgi?artid=PMC2956508. NIHMS150003.

[132] Mamot, C. *et al.* Tolerability, safety, pharmacokinetics, and efficacy of doxorubicin-loaded anti-EGFR immunoliposomes in advanced solid tumours: A phase 1 dose-escalation study. *The Lancet Oncology* **13**, 1234–1241 (2012). URL http://dx.doi.org/10.1016/S1470-2045(12)70476-X.

[133] Strebhardt, K. & Ullrich, A. Paul Ehrlich ' s magic bullet concept : 100 years of progress. *Nature reviews, cancer* **8**, 473–480 (2008).

[134] Gregoriadis, G. & Neerunjun, E. D. Homing of liposomes to target cells. *Biochemical and biophysical research communications* **65**, 537–44 (1975). URL http://linkinghub.elsevier.com/retrieve/pii/S0006291X7580180Xhttp://www.ncbi.nlm.nih.gov/pubmed/50067.

[135] Torchilin, V. Antibody-modified liposomes for cancer chemotherapy. *Expert opinion on drug delivery* **5**, 1003–1025 (2008).

[136] Suzuki, R. *et al.* Effective anti-tumor activity of oxaliplatin encapsulated in transferrin-PEG-liposome. *International journal of pharmaceutics* **346**, 143–50 (2008). URL http://www.ncbi.nlm.nih.gov/pubmed/17640835.

[137] Nellis, D. F. *et al.* Preclinical manufacture of an anti-HER2 scFv-PEG-DSPE, liposome-inserting conjugate. 1. Gram-scale production and purification. *Biotechnology Progress* **21**, 205–220 (2005).

[138] Nellis, D. F. *et al.* Preclinical manufacture of anti-HER2 liposome-inserting, scFv-PEG-lipid conjugate. 2. Conjugate micelle identity, purity, stability, and potency analysis. *Biotechnology progress* **21**, 221–32 (2005). URL http://www.ncbi.nlm.nih.gov/pubmed/15903261.

[139] Xu, L. *et al.* Systemic p53 gene therapy of cancer with immunolipoplexes targeted by anti-transferrin receptor scFv. *Molecular medicine (Cambridge, Mass.)* **7**, 723–34 (2001). URL http://www.pubmedcentral.nih.gov/articlerender.fcgi?artid=1949994{&}tool=pmcentrez{&}rendertype=abstract.

[140] Lammers, T., Kiessling, F., Hennink, W. E. & Storm, G. Drug targeting to tumors: principles, pitfalls and (pre-) clinical progress. *Journal of controlled release : official journal of the Controlled Release Society* **161**, 175–87 (2012). URL http://www.ncbi.nlm.nih.gov/pubmed/21945285.

[141] Garin-Chesa, P. *et al.* Trophoblast and ovarian cancer antigen LK26. Sensitivity and specificity in immunopathology and molecular identification as a folate-binding protein. *The American journal of pathology* **142**, 557–67 (1993). URL http://www.pubmedcentral.nih.gov/articlerender.fcgi?artid=1886733{&}tool=pmcentrez{&}rendertype=abstract.

[142] Sudimack, J. & Lee, R. J. Targeted drug delivery via the folate receptor. *Advanced drug delivery reviews* **41**, 147–62 (2000). URL http://www.ncbi.nlm.nih.gov/pubmed/21044432.

[143] Pastore, E. J. & Friedkin, M. The Enzymatic Synthesis of Thymidylate. *The Journal of biological chemistry* **237**, 3794–3801 (1962).

[144] Lee, R. J. & Low, P. S. Delivery of liposomes into cultured KB cells via folate receptor-mediated endocytosis. *The Journal of biological chemistry* **269**, 3198–204 (1994). URL http://www.ncbi.nlm.nih.gov/pubmed/8106354http://www.pubmedcentral.nih.gov/articlerender.fcgi?artid=42157{&}tool=pmcentrez{&}rendertype=abstract.

[145] Leamon, C. P. & Low, P. S. Delivery of macromolecules into living cells: a method that exploits folate receptor endocytosis. *Proceedings of the National Academy of Sciences of the United States of America* **88**, 5572–6 (1991). URL http://www.pubmedcentral.nih.gov/articlerender.fcgi?artid=51919{&}tool=pmcentrez{&}rendertype=abstract.

[146] Low, P. S., Henne, W. A. & Doorneweerd, D. D. Discovery and development of folic-acid-based receptor targeting for imaging and therapy of cancer and inflammatory diseases. *Accounts of chemical research* **41**, 120–9 (2008). URL http://pubs.acs.org/doi/pdf/10.1021/ar7000815http://www.ncbi.nlm.nih.gov/pubmed/17655275.

[147] Low, P. S. & Kularatne, S. A. Folate-targeted therapeutic and imaging agents for cancer. *Current Opinion in Chemical Biology* **13**, 256–262 (2009).

[148] Ruoslahti, E. Rgd and Other Recognition Sequences for Integrins. *Annual Review of Cell and Developmental Biology* **12**, 697–715 (1996). URL http://www.annualreviews.org/doi/abs/10.1146/annurev.cellbio.12.1.697.

[149] Phillips, N. C. & Emili, A. Immunogenicity of immunoliposomes. *Immunology Letters* **30**, 291–296 (1991).

[150] Schiffelers, R. M. *et al.* Anti-tumor efficacy of tumor vasculature-targeted liposomal doxorubicin. *Journal of Controlled Release* **91**, 115–122 (2003).

[151] Dubey, P. K., Mishra, V., Jain, S., Mahor, S. & Vyas, S. P. Liposomes modified with cyclic RGD peptide for tumor targeting. *Journal of drug targeting* **12**, 257–264 (2004).

[152] Terada, T., Iwai, M., Kawakami, S., Yamashita, F. & Hashida, M. Novel PEG-matrix metalloproteinase-2

cleavable peptide-lipid containing galactosylated liposomes for hepatocellular carcinoma-selective targeting. *Journal of Controlled Release* **111**, 333–342 (2006).

[153] Tuerk, C. & Gold, L. Systematic evolution of ligands by exponential enrichment: RNA ligands to bacteriophage T4 DNA polymerase. *Science* **249**, 505–510 (1990). URL http://scholar.google.com/scholar?hl=en{&}btnG=Search{&}q=intitle:Systematic+evolution+of+ligands+by+exponential+enrichment:+RNA+ligands+to+bacteriophage+T4+DNA+polymerase{#}0.

[154] Ellington, A. & Szostak, J. In vitro selection of RNA molecules that bind specific ligands. *Nature* **346**, 818–822 (1990).

[155] Mayer, G. The chemical biology of aptamers. *Angewandte Chemie (International ed. in English)* **48**, 2672–89 (2009). URL http://www.ncbi.nlm.nih.gov/pubmed/19319884.

[156] Willis, M. C. *et al.* Liposome anchored vascular endothelial growth factor aptamers. *Bioconjugate Chemistry* **9**, 573–582 (1998). URL {\T1\textless}GotoISI{\T1\textgreater}://000076242400006.

[157] Wilner, S. E. *et al.* An RNA Alternative to Human Transferrin: A New Tool for Targeting Human Cells. *Molecular Therapy Nucleic Acids* **1**, e21 (2012). URL http://www.nature.com/mtna/journal/v1/n5/pdf/mtna201214a.pdf.

[158] Kang, H., O'Donoghue, M. B., Liu, H. & Tan, W. A liposome-based nanostructure for aptamer directed delivery. *Chemical communications (Cambridge, England)* **46**, 249–51 (2010). URL http://pubs.rsc.org/en/content/articlepdf/2010/cc/b916911chttp://www.ncbi.nlm.nih.gov/pubmed/20024341.

[159] Harris, L. J., Skaletsky, E. & McPherson, a. Crystallographic structure of an intact IgG1 monoclonal antibody. *Journal of molecular biology* **275**, 861–872 (1998).

[160] The Jmol Team. Jmol: an open-source Java viewer for chemical structures in 3D. (2007). URL http://jmol.sourceforge.net/.

[161] MacGillivray, R. T. *et al.* Two high-resolution crystal structures of the recombinant N-lobe of human transferrin reveal a structural change implicated in iron release. *Biochemistry* **37**, 7919–28 (1998). URL http://www.ncbi.nlm.nih.gov/pubmed/9609685.

[162] Berman, H. M. *et al.* The Protein Data Bank. *Nucleic acids research* **28**, 235–242 (2000).

[163] Zuker, M. Mfold web server for nucleic acid folding and hybridization prediction. *Nucleic Acids Research* **31**, 3406–3415 (2003).

[164] Bernardes, G. J. L. *et al.* Design, synthesis and biological evaluation of carbohydrate-functionalized cyclodextrins and liposomes for hepatocyte-specific targeting. *Organic & biomolecular chemistry* **8**, 4987–4996 (2010).

[165] Goren, D. *et al.* Targeting of stealth liposomes to erbB-2 (Her/2) receptor: in vitro and in vivo studies. *British journal of cancer* **74**, 1749–1756 (1996).

[166] Allen, T. M. & Cullis, P. R. Liposomal drug delivery systems: from concept to clinical applications. *Advanced drug delivery reviews* **65**, 36–48 (2013). URL http://www.ncbi.nlm.nih.gov/pubmed/23036225.

[167] Park, J. W. *et al.* Anti-HER2 immunoliposomes: Enhanced efficacy attributable to targeted delivery. *Clinical Cancer Research* **8**, 1172–1181 (2002).

[168] Holmberg, E. *et al.* Highly efficient immunoliposomes prepared with a method which is compatible with various lipid compositions. *Biochemical and Biophysical Research Communications* **165**, 1272–1278 (1989). URL http://linkinghub.elsevier.com/retrieve/pii/0006291X8992740X.

[169] Uster, P. S. *et al.* Insertion of poly(ethylene glycol) derivatized phospholipid into pre-formed liposomes results in prolonged in vivo circulation time. *FEBS Letters* **386**, 243–246 (1996).

[170] Allen, T. M., Sapra, P. & Moase, E. Use of the post-insertion method for the formation of ligand-coupled liposomes. *Cellular & molecular biology letters* **7**, 889–94 (2002). URL http://www.ncbi.nlm.nih.gov/pubmed/12378272.

[171] Heath, T. D., Robertson, D., Birbeck, M. S. & Davies, A. J. Covalent attachment of horseradish peroxidase to the outer surface of liposomes. *Biochimica et Biophysica Acta (BBA) - Biomembranes* **599**, 42–62 (1980). URL http://linkinghub.elsevier.com/retrieve/pii/0005273680900553.

[172] Hermanson, G. T. *Bioconjugate Techniques*, vol. 2nd ed. (Academic Press, 2008). URL http://books.google.com/books?hl=en{&}lr={&}id=Ok6WSgkVq3cC{&}oi=fnd{&}pg=PR21{&}dq=bioconjugate+techniques+hermanson{&}ots=yxxIZis94i{&}sig=h{_}yCat8WuHU2{_}XIQwRKiHNjKqmE.

[173] Martin, F. J., Hubbell, W. L. & Papahadjopoulos, D. Immunospecific targeting of liposomes to cells: a novel and efficient method for covalent attachment of Fab' fragments via disulfide bonds. *Biochemistry* **20**, 4229–4238 (1981).

[174] Heitzmann, H. & Richards, F. M. Use of the avidin-biotin complex for specific staining of biological membranes in electron microscopy. *Proceedings of the National Academy of Sciences of the United States of America* **71**, 3537–41 (1974). URL http://www.pnas.org/content/71/9/3537.full.pdf$\delimiter"026E30F$nhttp://www.ncbi.nlm.nih.gov/pubmed/4139715$\delimiter"026E30F$nhttp://www.pubmedcentral.nih.gov/articlerender.fcgi?artid=PMC433809.

[175] Koning, G. A. *et al.* Selective transfer of a lipophilic prodrug of 5-fluorodeoxyuridine from immunoliposomes to colon cancer cells. *Biochimica et Biophysica Acta - Biomembranes* **1420**, 153–167 (1999).

[176] Bourel-Bonnet, L. *et al.* Anchorage of Synthetic Peptides onto Liposomes via Hydrazone and α-Oxo Hydrazone Bonds. Preliminary Functional Investigations. *Bioconjugate Chemistry* **16**, 450–457 (2005). URL http://pubs.acs.org/doi/abs/10.1021/bc049908v.

[177] Smyth, D., Blumenfeld, O. & Konigsberg, W. Reactions of N -ethylmaleimide with peptides and amino acids. *Biochemical Journal* **91**, 589–595 (1964). URL http://www.pubmedcentral.nih.gov/articlerender.fcgi?artid=1202996{&}tool=pmcentrez{&}rendertype=abstracthttp://biochemj.org/lookup/doi/10.1042/bj0910589.

[178] Martin, F. J. & Papahadjopoulos, D. Irreversible coupling of immunoglobulin fragments to preformed vesicles. An improved method for liposome targeting. *Journal of Biological Chemistry* **257**, 286–288 (1982).

[179] Bragg, P. D. & Hou, C. Subunit composition, function, and spatial arrangement in the Ca2+- and Mg2+-activated adenosine triphosphatases of Escherichia coli and Salmonella typhimurium. *Archives of Biochemistry and Biophysics* **167**, 311–321 (1975).

[180] Nobs, L., Buchegger, F., Gurny, R. & Allémann, E. Current methods for attaching targeting ligands to liposomes and nanoparticles. *Journal of pharmaceutical sciences* **93**, 1980–92 (2004). URL http://www.ncbi.nlm.nih.gov/pubmed/15236448$\delimiter"026E30F$nfile:///C:/DocumentsandSettings/YasinOduk/MyDocuments/MendeleyDesktop/Nobsetal/Nobsetal.-2004-Currentmethodsforattachingtargetingligandstoliposomesandnanoparticles.pdf.

[181] Kolb, H. C., Finn, M. G. & Sharpless, K. B. Click Chemistry: Diverse Chemical Function from a

Few Good Reactions. *Angewandte Chemie (International ed. in English)* **40**, 2004–2021 (2001). URL http://www.ncbi.nlm.nih.gov/pubmed/11433435.

[182] Kolb, H. C. & Sharpless, K. B. The growing impact of click chemistry on drug discovery. *Drug discovery today* **8**, 1128–37 (2003). URL http://www.ncbi.nlm.nih.gov/pubmed/14678739.

[183] Binder, W. H. & Sachsenhofer, R. Click Chemistry in Polymer and Materials Science. *Macromolecular Rapid Communications* **28**, 15–54 (2007). URL http://doi.wiley.com/10.1002/marc.200600625.

[184] Hein, C. D., Liu, X.-M. & Wang, D. Click chemistry, a powerful tool for pharmaceutical sciences. *Pharmaceutical research* **25**, 2216–30 (2008). URL http://www.pubmedcentral.nih.gov/articlerender.fcgi?artid=2562613{&}tool=pmcentrez{&}rendertype=abstract.

[185] Huisgen, R. 1.3-Dipolare Cycloadditionen. *Angewandte Chemie* **75**, 604–637 (1963).

[186] Rostovtsev, V. V., Green, L. G., Fokin, V. V. & Sharpless, K. B. A stepwise huisgen cycloaddition process: copper(I)-catalyzed regioselective "ligation" of azides and terminal alkynes. *Angewandte Chemie (International ed. in English)* **41**, 2596–9 (2002). URL http://www.ncbi.nlm.nih.gov/pubmed/12203546.

[187] Said Hassane, F., Frisch, B. & Schuber, F. Targeted liposomes: convenient coupling of ligands to preformed vesicles using "click chemistry". *Bioconjugate chemistry* **17**, 849–54 (2006). URL http://www.ncbi.nlm.nih.gov/pubmed/16704226.

[188] Cavalli, S., Tipton, A. R., Overhand, M. & Kros, A. The chemical modification of liposome surfaces via a copper-mediated [3 + 2] azide-alkyne cycloaddition monitored by a colorimetric assay. *Chemical communications (Cambridge, England)* 3193–5 (2006). URL http://www.ncbi.nlm.nih.gov/pubmed/17028740.

[189] Gaetke, L. Copper toxicity, oxidative stress, and antioxidant nutrients. *Toxicology* **189**, 147–163 (2003). URL http://linkinghub.elsevier.com/retrieve/pii/S0300483X03001598.

[190] Saxon, E. Cell Surface Engineering by a Modified Staudinger Reaction. *Science* **287**, 2007–2010 (2000). URL http://www.sciencemag.org/cgi/doi/10.1126/science.287.5460.2007.

[191] Prescher, J. A., Dube, D. H. & Bertozzi, C. R. Chemical remodelling of cell surfaces in living animals. *Nature* **430**, 873–877 (2004). URL http://www.nature.com/doifinder/10.1038/nature02791.

[192] Zhang, H., Ma, Y. & Sun, X.-L. Chemically-selective surface glyco-functionalization of liposomes through Staudinger ligation. *Chemical communications (Cambridge, England)* 3032–4 (2009). URL http://www.ncbi.nlm.nih.gov/pubmed/19462077.

[193] Wittig, G. & Krebs, A. On the existence of low-membered cycloalkynes. I. *Chem. Ber* (1961). URL https://scholar.google.de/scholar?hl=en{&}q=On+the+existence+of+low-membered+cycloalkynes{&}btnG={&}as{_}sdt=1{%}2C5{&}as{_}sdtp={#}0.

[194] Shea, K. J. & Kim, J. S. Influence of strain on chemical reactivity. Relative reactivity of torsionally distorted double bonds in MCPBA epoxidations. *Journal of the American Chemical Society* **114**, 3044–3051 (1992). URL http://pubs.acs.org/doi/abs/10.1021/ja00034a042.

[195] Agard, N. J., Prescher, J. A. & Bertozzi, C. R. A strain-promoted [3 + 2] azide-alkyne cycloaddition for covalent modification of biomolecules in living systems. *Journal of the American Chemical Society* **126**, 15046–7 (2004). URL http://www.ncbi.nlm.nih.gov/pubmed/15547999.

[196] Koo, H. *et al.* Bioorthogonal copper-free click chemistry inVivo for tumor-targeted delivery of nanoparticles. *Angewandte Chemie - International Edition* **51**, 11836–11840 (2012).

[197] Oude Blenke, E. *et al.* Liposome functionalization with copper-free "click chemistry". *Journal of controlled release : official journal of the Controlled Release Society* **202**, 14–20 (2015).

URL http://linkinghub.elsevier.com/retrieve/pii/S0168365915000772http://www.ncbi.nlm.nih.gov/pubmed/25626085.

[198] Thalhammer, F., Wallfahrer, U. & Sauer, J. Reaktivität einfacher offenkettiger und cyclischer dienophile bei Diels-Alder-reaktionen mit inversem elektronenbedarf. *Tetrahedron Letters* **31**, 6851–6854 (1990). URL http://linkinghub.elsevier.com/retrieve/pii/S0040403900971880.

[199] Sauer, J. *et al.* 1,2,4,5-Tetrazine: Synthesis and Reactivity in [4+2] Cycloadditions. *European Journal of Organic Chemistry* **1998**, 2885–2896 (1998). URL http://onlinelibrary.wiley.com/doi/10.1002/(SICI)1099-0690(199812)1998:12{\T1\textless}2885::AID-EJOC2885{\T1\textgreater}3.0.CO;2-L/abstracthttp://doi.wiley.com/10.1002/(SICI)1099-0690(199812)1998:12{\T1\textless}2885::AID-EJOC2885{\T1\textgreater}3.0.CO;2-Lhttp://doi.wiley.com/10.1002.

[200] Blackman, M. L., Royzen, M. & Fox, J. M. Tetrazine ligation: fast bioconjugation based on inverse-electron-demand Diels-Alder reactivity. *Journal of the American Chemical Society* **130**, 13518–9 (2008). URL http://www.pubmedcentral.nih.gov/articlerender.fcgi?artid=2653060{&}tool=pmcentrez{&}rendertype=abstracthttp://dx.doi.org/10.1021/ja8053805.

[201] Emmetiere, F. *et al.* (18)F-labeled-bioorthogonal liposomes for in vivo targeting. *Bioconjugate chemistry* **24**, 1784–9 (2013). URL http://www.ncbi.nlm.nih.gov/pubmed/24180480.

[202] Laginha, K., Mumbengegwi, D. & Allen, T. Liposomes targeted via two different antibodies: Assay, B-cell binding and cytotoxicity. *Biochimica et Biophysica Acta - Biomembranes* **1711**, 25–32 (2005).

[203] Chen, C.-H. *et al.* Evaluation of multi-target and single-target liposomal drugs for the treatment of gastric cancer. *Bioscience, biotechnology, and biochemistry* **72**, 1586–1594 (2008).

[204] Ma, Y., Zhang, H., Gruzdys, V. & Sun, X.-L. Azide-reactive liposome for chemoselective and biocompatible liposomal surface functionalization and glyco-liposomal microarray fabrication. *Langmuir : the ACS journal of surfaces and colloids* **27**, 13097–103 (2011). URL http://www.ncbi.nlm.nih.gov/pubmed/21928859.

[205] Schoch, J., Staudt, M., Samanta, A., Wiessler, M. & Jäschke, A. Site-specific one-pot dual labeling of DNA by orthogonal cycloaddition chemistry. *Bioconjugate chemistry* **23**, 1382–6 (2012). URL http://www.ncbi.nlm.nih.gov/pubmed/22709568.

[206] Salomé, C. *et al.* Smart tools and orthogonal click-like reactions onto small unilamellar vesicles. *Chemistry and Physics of Lipids* **188**, 27–36 (2015). URL http://linkinghub.elsevier.com/retrieve/pii/S0009308415000201.

[207] Awasthi, V. D., Garcia, D., Goins, B. A. & Phillips, W. T. Circulation and biodistribution profiles of long-circulating PEG-liposomes of various sizes in rabbits. *International Journal of Pharmaceutics* **253**, 121–132 (2003).

[208] Egelhaaf, S. U., Wehrli, E., Müller, M., Adrian, M. & Schurtenberger, P. Determination of the size distribution of lecithin liposomes : a comparative study using freeze fracture, cryoelectron microscopy and dynamic light scattering. *Journal of Microscopy* **184**, 214–228 (1996).

[209] Moog, R. *et al.* Change in pharmacokinetic and pharmacodynamic behavior of gemcitabine in human tumor xenografts upon entrapment in vesicular phospholipid gels. *Cancer chemotherapy and pharmacology* **49**, 356–66 (2002). URL http://www.ncbi.nlm.nih.gov/pubmed/11976829.

[210] Provder, T. Challenges in particle size distribution measurement past, present and for the 21st century. *Progress in Organic Coatings* **32**, 143–153 (1997).

[211] Crawford, R. *et al.* Analysis of lipid nanoparticles by Cryo-EM for characterizing siRNA delivery vehicles. *International Journal of Pharmaceutics* **403**, 237–244 (2011). URL http://dx.doi.org/10.1016/j.ijpharm.2010.10.025.

[212] Almgren, M., Edwards, K. & Karlsson, G. Cryo transmission electron microscopy of liposomes and related structures. *Colloids and Surfaces A: Physicochemical and Engineering Aspects* **174**, 3–21 (2000). URL http://linkinghub.elsevier.com/retrieve/pii/S0927775700005161.

[213] Krichevsky, O. Fluorescence correlation spectroscopy : the technique. *Reports on Progress in Physics* **65**, 251–297 (2002). URL http://iopscience.iop.org/article/10.1088/0034-4885/65/2/203/meta.

[214] Carr, B. *et al.* Applications of nanoparticle tracking analysis in nanoparticle research - a mini-review. *European Journal of Parenteral & Pharmaceutical Sciences* **14**, 45–50 (2009).

[215] Filipe, V., Hawe, A. & Jiskoot, W. Critical evaluation of Nanoparticle Tracking Analysis (NTA) by NanoSight for the measurement of nanoparticles and protein aggregates. *Pharmaceutical research* **27**, 796–810 (2010). URL http://www.pubmedcentral.nih.gov/articlerender.fcgi?artid=2852530{&}tool=pmcentrez{&}rendertype=abstract.

[216] Delgado, A. V., González-Caballero, F., Hunter, R. J., Koopal, L. K. & Lyklema, J. Measurement and interpretation of electrokinetic phenomena. *Journal of Colloid and Interface Science* **309**, 194–224 (2007).

[217] Woodle, M. C. *et al.* Sterically stabilized liposomes. Reduction in electrophoretic mobility but not electrostatic surface potential. *Biophysical journal* **61**, 902–10 (1992). URL http://www.sciencedirect.com/science/article/pii/S0006349592818970.

[218] Kranz, L. M. *et al.* Systemic RNA delivery to dendritic cells exploits antiviral defence for cancer immunotherapy. *Nature* 1–16 (2016). URL http://www.nature.com/doifinder/10.1038/nature18300.

[219] Gabizon, A. & Papahadjopoulos, D. The role of surface charge and hydrophilic groups on liposome clearance in vivo. *Biochimica et Biophysica Acta (BBA) - Biomembranes* **1103**, 94–100 (1992). URL http://linkinghub.elsevier.com/retrieve/pii/000527369290061P.

[220] Attwood, D. & Saunders, L. A light-scattering study of ultrasonically irradiated lecithin sols. *Biochimica et Biophysica Acta* **98**, 344–350 (1965). URL http://www.sciencedirect.com/science/article/pii/0005276065901268.

[221] Olson, F., Hunt, C. a., Szoka, F. C., Vail, W. J. & Papahadjopoulos, D. Preparation of liposomes of defined size distribution by extrusion through polycarbonate membranes. *Biochimica et biophysica acta* **557**, 9–23 (1979). URL http://www.ncbi.nlm.nih.gov/pubmed/95096.

[222] Szoka, F. *et al.* Preparation of unilamellar liposomes of intermediate size (0.1-0.2 mumol) by a combination of reverse phase evaporation and extrusion through polycarbonate membranes. *Biochimica et biophysica acta* **601**, 559–71 (1980). URL http://linkinghub.elsevier.com/retrieve/pii/0005273680905581http://www.ncbi.nlm.nih.gov/pubmed/6251878.

[223] Wagner, A. & Vorauer-Uhl, K. Liposome Technology: Volume II Entrapment of Drugs and Other Materials into Liposomes, Third Edition. *Journal of drug delivery* **II**, 591325 (2007). URL http://www.pubmedcentral.nih.gov/articlerender.fcgi?artid=3065896{&}tool=pmcentrez{&}rendertype=abstract.

[224] Szoka, F. & Papahadjopoulos, D. Procedure for preparation of liposomes with large internal aqueous space and high capture by reverse-phase evaporation. *Proceedings of the Na-*

tional Academy of Sciences of the United States of America **75**, 4194–8 (1978). URL http://www.ncbi.nlm.nih.gov/pubmed/279908$\delimiter"026E30F$nhttp://www.pubmedcentral.nih.gov/articlerender.fcgi?artid=PMC336078.

[225] Pons, M., Foradada, M. & Estelrich, J. Liposomes obtained by the ethanol injection method. *International Journal of Pharmaceutics* **95**, 51–56 (1993). URL http://www.sciencedirect.com/science/article/pii/037851739390389Whttp://linkinghub.elsevier.com/retrieve/pii/037851739390389Whttp://www.sciencedirect.com/science/article/pii/037851739390422C.

[226] Mayhew, E., Lazo, R., Vail, W. J., King, J. & Green, A. M. Characterization of liposomes prepared using a microemulsifier. *BBA - Biomembranes* **775**, 169–174 (1984).

[227] Brandl, M., Bachmann, D., Drechsler, M. & Bauer, K. H. Liposome Preparation by a New High Pressure Homogenizer Gaulin Micron Lab 40. *Drug Development and Industrial Pharmacy* **16**, 2167–2191 (1990). URL http://informahealthcare.com/doi/abs/10.3109/03639049009023648http://www.informapharmascience.com/doi/abs/10.3109/03639049009023648.

[228] Brandl, M. *et al.* Preparation and characterization of semi-solid phospholipid dispersions and dilutions thereof. *International Journal of Pharmaceutics* **170**, 187–199 (1998). URL http://linkinghub.elsevier.com/retrieve/pii/S037851739800146X.

[229] Berger, N., Sachse, A., Bender, J., Schubert, R. & Brandl, M. Filter extrusion of liposomes using different devices: comparison of liposome size, encapsulation efficiency, and process characteristics. *International journal of pharmaceutics* **223**, 55–68 (2001). URL http://www.ncbi.nlm.nih.gov/pubmed/11451632.

[230] Stroock, A. D. *et al.* Chaotic mixer for microchannels. *Science (New York, N.Y.)* **295**, 647–51 (2002). URL http://www.ncbi.nlm.nih.gov/pubmed/11809963.

[231] Zhigaltsev, I. V. *et al.* Bottom-up design and synthesis of limit size lipid nanoparticle systems with aqueous and triglyceride cores using millisecond microfluidic mixing. *Langmuir : the ACS journal of surfaces and colloids* **28**, 3633–40 (2012). URL http://www.ncbi.nlm.nih.gov/pubmed/22268499.

[232] Kastner, E. *et al.* High-throughput manufacturing of size-tuned liposomes by a new microfluidics method using enhanced statistical tools for characterization. *International Journal of Pharmaceutics* **477**, 361–368 (2014). URL http://dx.doi.org/10.1016/j.ijpharm.2014.10.030.

[233] Kastner, E., Verma, V., Lowry, D. & Perrie, Y. Microfluidic-controlled manufacture of liposomes for the solubilisation of a poorly water soluble drug. *International Journal of Pharmaceutics* **485**, 122–130 (2015). URL http://dx.doi.org/10.1016/j.ijpharm.2015.02.063.

[234] Hirsch, M., Ziroli, V., Helm, M. & Massing, U. Preparation of small amounts of sterile siRNA-liposomes with high entrapping efficiency by dual asymmetric centrifugation (DAC). *Journal of Controlled Release* **135**, 80–8 (2009). URL http://www.ncbi.nlm.nih.gov/pubmed/19124051.

[235] Kim, I., Hirsch, M. & Fischer, R. FRET imaging of cells transfected with siRNA/liposome complexes. *Methods Mol. Biol* (2010). URL http://www.springerlink.com/index/X734158415P51558.pdf.

[236] Adrian, J. E., Wolf, A., Steinbach, A., Rössler, J. & Süss, R. Targeted delivery to neuroblastoma of novel siRNA-anti-GD2-liposomes prepared by dual asymmetric centrifugation and sterol-based post-insertion method. *Pharmaceutical research* **28**, 2261–72 (2011). URL http://www.ncbi.nlm.nih.gov/pubmed/21594716.

[237] Parmentier, J. *et al.* Improved oral bioavailability of human growth hormone by a combination of liposomes containing bio-enhancers and tetraether lipids and omeprazole. *Journal of Pharmaceutical Sciences* **103**, 3985–3993 (2014).

[238] Raynor, A. *et al.* Saturated and mono-unsaturated lysophosphatidylcholine metabolism in tumour cells: a potential therapeutic target for preventing metastases. *Lipids in health and disease* **14**, 69 (2015). URL http://www.pubmedcentral.nih.gov/articlerender.fcgi?artid=4499168{&}tool=pmcentrez{&}rendertype=abstract.

[239] Pohlit, H. *et al.* Biodegradable pH-Sensitive Poly(ethylene glycol) Nanocarriers for Allergen Encapsulation and Controlled Release. *Biomacromolecules* **16**, 3103–3111 (2015).

[240] Helm, F. & Fricker, G. Liposomal conjugates for drug delivery to the central nervous system. *Pharmaceutics* **7**, 27–42 (2015).

[241] Tian, W., Schulze, S., Brandl, M. & Winter, G. Vesicular phospholipid gel-based depot formulations for pharmaceutical proteins: Development and in vitro evaluation. *Journal of Controlled Release* **142**, 319–325 (2010). URL http://dx.doi.org/10.1016/j.jconrel.2009.11.006.

[242] Zhong, Y. *et al.* Vesicular phospholipid gels using low concentrations of phospholipids for the sustained release of thymopentin: pharmacokinetics and pharmacodynamics. *Die Pharmazie* **68**, 811–5 (2013). URL http://www.ncbi.nlm.nih.gov/pubmed/24273885.

[243] Pantze, S. F., Parmentier, J., Hofhaus, G. & Fricker, G. Matrix liposomes: A solid liposomal formulation for oral administration. *European Journal of Lipid Science and Technology* **116**, 1145–1154 (2014).

[244] Buchmann, S. *et al.* Growth factor release by vesicular phospholipid gels: in-vitro results and application for rotator cuff repair in a rat model. *BMC musculoskeletal disorders* **16**, 82 (2015). URL http://www.pubmedcentral.nih.gov/articlerender.fcgi?artid=4417541{&}tool=pmcentrez{&}rendertype=abstract.

[245] Jensen, S. M., Christensen, C. J., Petersen, J. M., Treusch, A. H. & Brandl, M. Liposomes containing lipids from Sulfolobus islandicus withstand intestinal bile salts: An approach for oral drug delivery? *International Journal of Pharmaceutics* **493**, 63–69 (2015). URL http://dx.doi.org/10.1016/j.ijpharm.2015.07.026.

[246] Asua, J. M. Emulsion polymerization: From fundamental mechanisms to process developments. *Journal of Polymer Science Part A: Polymer Chemistry* **42**, 1025–1041 (2004). URL http://dx.doi.org/10.1002/pola.11096.

[247] Rao, J. P. & Geckeler, K. E. Polymer nanoparticles: Preparation techniques and size-control parameters. *Progress in Polymer Science (Oxford)* **36**, 887–913 (2011). URL http://dx.doi.org/10.1016/j.progpolymsci.2011.01.001.

[248] Anton, N., Benoit, J. P. & Saulnier, P. Design and production of nanoparticles formulated from nano-emulsion templates-A review. *Journal of Controlled Release* **128**, 185–199 (2008).

[249] Fessi, H., Puisieux, F., Devissaguet, J. P., Ammoury, N. & Benita, S. Nanocapsule formation by interfacial polymer deposition following solvent displacement. *International Journal of Pharmaceutics* **55**, 1–4 (1989).

[250] Jeong, Y. I. *et al.* Preparation of poly(DL-lactide-co-glycolide) nanoparticles without surfactant. *Journal of Applied Polymer Science* **80**, 2228–2236 (2001).

[251] Hentschel, R. & Jorch, G. Acute side effects of surfactant treatment. *Journal of Perinatal Medicine* **30**, 143–148 (2002).

[252] Discher, D. E. & Ahmed, F. Polymersomes. *Annual Review of Biomedical Engineering* **8**, 323–341 (2006). URL http://www.annualreviews.org/doi/abs/10.1146/annurev.bioeng.8.061505.095838.

[253] Kataoka, K., Harada, A. & Nagasaki, Y. Block copolymer micelles for drug delivery: Design, characterization and biological significance. *Advanced Drug Delivery Reviews* **47**, 113–131 (2001). 0402594v3.

[254] Cabral, H. & Kataoka, K. Progress of drug-loaded polymeric micelles into clinical studies. *Journal of Controlled Release* **190**, 465–476 (2014). URL http://dx.doi.org/10.1016/j.jconrel.2014.06.042.

[255] Talelli, M. *et al.* Core-crosslinked polymeric micelles: Principles, preparation, biomedical applications and clinical translation. *Nano Today* **10**, 93–117 (2015). URL http://dx.doi.org/10.1016/j.nantod.2015.01.005.

[256] Brinkhuis, R. P., Rutjes, F. P. J. T. & van Hest, J. C. M. Polymeric vesicles in biomedical applications. *Polymer Chemistry* **2**, 1449 (2011).

[257] Gaitzsch, J., Appelhans, D., Wang, L., Battaglia, G. & Voit, B. Synthetic bio-nanoreactor: Mechanical and chemical control of polymersome membrane permeability. *Angewandte Chemie - International Edition* **51**, 4448–4451 (2012).

[258] Discher, B. M. *et al.* Polymersomes: tough vesicles made from diblock copolymers. *Science (New York, N.Y.)* **284**, 1143–6 (1999). URL http://www.sciencemag.org/cgi/doi/10.1126/science.284.5417.1143http://www.ncbi.nlm.nih.gov/pubmed/10325219.

[259] Choucair, A., Lavigueur, C. & Eisenberg, A. Polystyrene- b -poly(acrylic acid) Vesicle Size Control Using Solution Properties and Hydrophilic Block Length. *Langmuir* **20**, 3894–3900 (2004). URL http://0-pubs.acs.org.pugwash.lib.warwick.ac.uk/doi/full/10.1021/la035924p.

[260] Nuhn, L., Barz, M. & Zentel, R. New perspectives of HPMA-based copolymers derived by post-polymerization modification. *Macromolecular Bioscience* **14**, 607–618 (2014).

[261] Benahmed, A., Ranger, M. & Leroux, J.-c. Novel Polymeric Micelles Based on the Amphiphilic Diblock Copolymer Poly (N -vinyl-2-pyrrolidone) - block - poly (D , L-lactide). *Pharmaceutical Research* **18**, 2–7 (2001).

[262] Birke, A. *et al.* Polypeptoid- block -polypeptide Copolymers: Synthesis, Characterization, and Application of Amphiphilic Block Copolypept(o)ides in Drug Formulations and Miniemulsion Techniques. *Biomacromolecules* **15**, 548–557 (2014). URL http://pubs.acs.org/doi/abs/10.1021/bm401542z.

[263] Barz, M. *et al.* From defined reactive diblock copolymers to functional HPMA-based self-assembled nanoaggregates. *Biomacromolecules* **9**, 3114–3118 (2008).

[264] Fritz, T. *et al.* Click modification of multifunctional liposomes bearing hyperbranched polyether chains. *Biomacromolecules* **15**, 2440–2448 (2014).

[265] Voigt, M. *Orthogonal click reactions on bifunctional stealth liposomes*. Ph.D. thesis, Johannes Gutenberg-University Mainz (2015).

[266] Fritz, T., Voigt, M., Schulz, V., Massing, U. & Helm, M. Micro-scale liposome formulation via dual centrifugation. In *Proceedings of the 2015 Annual Meeting Controlled Release Society* (Edinburgh, 2015).

[267] Kainthan, R. K. *et al.* Blood compatibility of novel water soluble hyperbranched polyglycerol-based multivalent cationic polymers and their interaction with DNA. *Biomaterials* **27**, 5377–90 (2006). URL http://www.ncbi.nlm.nih.gov/pubmed/16854460.

[268] Roux, F. *et al.* Regulation of gamma-glutamyl transpeptidase and alkaline phosphatase activities in immortalized rat brain microvessel endothelial cells. *Journal of cellular physiology* **159**, 101–13 (1994). URL http://www.ncbi.nlm.nih.gov/pubmed/7908023.

[269] Beugin, S., Edwards, K., Karlsson, G., Ollivon, M. & Lesieur, S. New sterically stabilized vesicles based on nonionic surfactant, cholesterol, and poly(ethylene glycol)-cholesterol conjugates. *Biophysical journal* **74**, 3198–210 (1998). URL http://www.pubmedcentral.nih.gov/articlerender.fcgi?artid=1299660{&}tool=pmcentrez{&}rendertype=abstract.

[270] Sugiyama, I. & Sadzuka, Y. Characterization of Novel Mixed Polyethyleneglycol Modified Liposomes. *Biological & Pharmaceutical Bulletin* **30**, 208–211 (2007). URL http://joi.jlc.jst.go.jp/JST.JSTAGE/bpb/30.208?from=CrossRef.

[271] Xu, L. & Anchordoquy, T. J. Effect of cholesterol nanodomains on the targeting of lipid-based gene delivery in cultured cells. *Molecular Pharmaceutics* **7**, 1311–1317 (2010).

[272] Huotari, J. & Helenius, A. Endosome maturation. *The EMBO journal* **30**, 3481–500 (2011). URL http://www.pubmedcentral.nih.gov/articlerender.fcgi?artid=3181477{&}tool=pmcentrez{&}rendertype=abstract.

[273] De Duve, C. *et al.* Lysosomotropic agents. *Biochemical Pharmacology* **23**, 2495–2531 (1974). URL http://scholar.google.com/scholar?hl=en{&}btnG=Search{&}q=intitle:lysosomotropic+agents{#}0http://scholar.google.com/scholar?hl=en{&}btnG=Search{&}q=intitle:Lysosomotropic+agents{#}0http://linkinghub.elsevier.com/retrieve/pii/0006295274901749.

[274] Fritz, T. *et al.* Orthogonal click conjugation to the liposomal surface reveals stability of lipid anchorage as crucial for targeting. *Chemistry - A European Journal* (2016).

[275] Müller, R. H., Rühl, D., Lück, M. & Paulke, B. R. Influence of fluorescent labelling of polystyrene particles on phagocytic uptake, surface hydrophobicity, and plasma protein adsorption. *Pharmaceutical Research* **14**, 18–24 (1997).

[276] Akinc, A. *et al.* Targeted delivery of RNAi therapeutics with endogenous and exogenous ligand-based mechanisms. *Molecular therapy : the journal of the American Society of Gene Therapy* **18**, 1357–64 (2010). URL http://www.pubmedcentral.nih.gov/articlerender.fcgi?artid=2911264{&}tool=pmcentrez{&}rendertype=abstract.

[277] Gabizon, A., Shmeeda, H., Horowitz, A. T. & Zalipsky, S. Tumor cell targeting of liposome-entrapped drugs with phospholipid-anchored folic acid-PEG conjugates. *Advanced drug delivery reviews* **56**, 1177–92 (2004). URL http://www.ncbi.nlm.nih.gov/pubmed/15094214.

[278] Ross, T. L. *et al.* Fluorine-18 click radiosynthesis and preclinical evaluation of a new 18F-labeled folic acid derivative. *Bioconjugate chemistry* **19**, 2462–70 (2008). URL http://www.ncbi.nlm.nih.gov/pubmed/19053298.

[279] Gabizon, A. *et al.* Targeting folate receptor with folate linked to extremities of poly(ethylene glycol)-grafted liposomes: In vitro studies. *Bioconjugate Chemistry* **10**, 289–298 (1999).

[280] Goren, D. *et al.* Nuclear delivery of doxorubicin via folate-targeted liposomes with bypass of multidrug-resistance efflux pump. *Clinical Cancer Research* **6**, 1949–1957 (2000).

[281] Eagle, H. Propagation in a Fluid Medium of a Human Epidermoid Carcinoma, Strain KB. *Experimental Biology and Medicine* **89**, 362–364 (1955). URL http://ebm.sagepub.com/lookup/doi/10.3181/00379727-89-21811.

[282] Suen, W. L. L. & Chau, Y. Size-dependent internalisation of folate-decorated nanoparticles via the pathways of clathrin and caveolae-mediated endocytosis in ARPE-19 cells. *Journal of Pharmacy and Pharmacology* **66**, 564–573 (2014).

[283] Müller, S. S. *et al.* Biodegradable Hyperbranched Polyether-Lipids with In-Chain pH-Sensitive Linkages. *Polymer Chemistry* (2016).

[284] Working, P. K. *et al.* Pharmacokinetics, Biodistribution and Therapeutic Efficacy of Doxorubicin Encapsulated in Stealth® Liposomes (Doxil®). *Journal of Liposome Research* **4**, 667–687 (1994). URL http://informahealthcare.com/doi/abs/10.3109/08982109409037065http://www.tandfonline.com/doi/full/10.3109/08982109409037065.

[285] Mura, S., Nicolas, J. & Couvreur, P. Stimuli-responsive nanocarriers for drug delivery. *Nature Materials* **12**, 991–1003 (2013). URL http://dx.doi.org/10.1038/nmat3776.

[286] Ganta, S., Devalapally, H., Shahiwala, A. & Amiji, M. A review of stimuli-responsive nanocarriers for drug and gene delivery. *Journal of Controlled Release* **126**, 187–204 (2008).

[287] Yamaoka, T., Tabata, Y. & Ikada, Y. Distribution and Tissue Uptake of Poly(ethylene glycol) with Different Molecular Weights after Intravenous Administration to Mice. *Journal of Pharmaceutical Sciences* **83**, 601–606 (1994). URL http://linkinghub.elsevier.com/retrieve/pii/S0022354915494444.

[288] Gerlier, D. & Thomasset, N. Use of MTT colorimetric assay to measure cell activation. *Journal of Immunological Methods* **94**, 57–63 (1986). URL http://linkinghub.elsevier.com/retrieve/pii/0022175986902152.

[289] Al Sabbagh, C. *et al.* Formulation and Pharmacokinetics of Thermosensitive Stealth® Liposomes Encapsulating 5-Fluorouracil. *Pharmaceutical Research* **32**, 1585–1603 (2015). URL http://link.springer.com/10.1007/s11095-014-1559-0.

[290] Schneider, C. a., Rasband, W. S. & Eliceiri, K. W. NIH Image to ImageJ: 25 years of image analysis. *Nature Methods* **9**, 671–675 (2012). URL http://dx.doi.org/10.1038/nmeth.2089http://www.nature.com/doifinder/10.1038/nmeth.2089.

[291] Scherer, M. *et al.* Pentafluorophenyl Ester-based Polymersomes as Nanosized Drug-Delivery Vehicles. *Macromolecular Rapid Communications* **37**, 60–66 (2016). URL http://doi.wiley.com/10.1002/marc.201500444.

[292] Pawar, P. V., Gohil, S. V., Jain, J. P. & Kumar, N. Functionalized polymersomes for biomedical applications. *Polymer Chemistry* **4**, 3160 (2013). URL http://xlink.rsc.org/?DOI=c3py00023k.

[293] Borchert, U. *et al.* pH-induced release from P2VP-PEO block copolymer vesicles. *Langmuir* **22**, 5843–5847 (2006).

[294] Lee, J. S., Groothuis, T., Cusan, C., Mink, D. & Feijen, J. Lysosomally cleavable peptide-containing polymersomes modified with anti-EGFR antibody for systemic cancer chemotherapy. *Biomaterials* **32**, 9144–9153 (2011). URL http://dx.doi.org/10.1016/j.biomaterials.2011.08.036http://linkinghub.elsevier.com/retrieve/pii/S014296121100963X.

[295] Lee, J. C.-M. *et al.* Preparation, stability, and in vitro performance of vesicles made with diblock copolymers. *Biotechnology and Bioengineering* **73**, 135–145 (2001). URL http://doi.wiley.com/10.1002/bit.1045.

[296] Allmeroth, M. *et al.* PEGylation of HPMA-based block copolymers enhances tumor accumulation in vivo: A quantitative study using radiolabeling and positron emission tomography. *Journal of Controlled Release* **172**, 77–85 (2013). URL http://dx.doi.org/10.1016/j.jconrel.2013.07.027http://linkinghub.elsevier.com/retrieve/pii/S0168365913004379.

[297] Aranda-Espinoza, H., Bermudez, H., Bates, F. S. & Discher, D. E. Electromechanical limits of polymersomes. *Physical review letters* **87**, 208301 (2001). 0107039.

[298] Paira, T. K. *et al.* Peptide-polymer bioconjugates via atom transfer radical polymerization and their solution aggregation into hybrid micro/nanospheres for dye uptake. *Macromolecules* **43**, 4050–4061 (2010).

[299] Chauhan, V. M., Burnett, G. R. & Aylott, J. W. Dual-fluorophore ratiometric pH nanosensor with tuneable pKa and extended dynamic range. *The Analyst* **136**, 1799–801 (2011). URL http://www.ncbi.nlm.nih.gov/pubmed/21416087.

[300] Pasut, G. *et al.* Polyethylene glycol (PEG)-dendron phospholipids as innovative constructs for the preparation of super stealth liposomes for anticancer therapy. *Journal of Controlled Release* **199**, 106–113 (2015). URL http://dx.doi.org/10.1016/j.jconrel.2014.12.008.

[301] Molnar, D., Linders, J., Mayer, C. & Schubert, R. Insertion stability of poly(ethylene glycol)-cholesteryl-based lipid anchors in liposome membranes. *European Journal of Pharmaceutics and Biopharmaceutics* **103**, 51–61 (2016). URL http://dx.doi.org/10.1016/j.ejpb.2016.03.023.

[302] Baek, S. E. *et al.* RNA aptamer-conjugated liposome as an efficient anticancer drug delivery vehicle targeting cancer cells in vivo. *Journal of Controlled Release* **196**, 234–242 (2014). URL http://linkinghub.elsevier.com/retrieve/pii/S0168365914007160.

[303] Semple, S. C. *et al.* Rational design of cationic lipids for siRNA delivery. *Nature biotechnology* **28**, 172–6 (2010). URL http://www.ncbi.nlm.nih.gov/pubmed/20081866.

[304] Semple, S. C. *et al.* Efficient encapsulation of antisense oligonucleotides in lipid vesicles using ionizable aminolipids: formation of novel small multilamellar vesicle structures. *Biochimica et Biophysica Acta (BBA) - Biomembranes* **1510**, 152–166 (2001). URL http://linkinghub.elsevier.com/retrieve/pii/S0005273600003436.

[305] Hofmann, A. M. *Amphiphilic polyethers via oxyanionic polymerization: From liposomes to liquid crystals*. Ph.D. thesis, Johannes Gutenberg-University Mainz (2011).

[306] Müller, S. S. *Polyether-based Lipids and Copolymers: From Biomedical Applications to Thermoresponsive Materials*. Ph.D. thesis, Johannes Gutenberg-University Mainz (2014).

[307] Abràmoff, M. D., Magalhães, P. J. & Ram, S. J. Image processing with imageJ. *Biophotonics International* **11**, 36–41 (2004). URL http://dspace.library.uu.nl/handle/1874/204900http://unisciel.irenala.edu.mg/Observatoire{_}de{_}paris/lumiere/4-Application/Pour-faire-le-TP-reduction-m57/doc-ImageJ/ImageJ.pdf. 1081-8693.

[308] Pidgeon, C. & Hunt, C. a. Calculating number and surface area of liposomes in any suspension. *Journal of pharmaceutical sciences* **70**, 173–6 (1981). URL http://www.ncbi.nlm.nih.gov/pubmed/7205223.

[309] Rigler, R. & Elson, E. S. *Fluorescence Correlation Spectroscopy*, vol. 65 of *Springer Series in Chemical Physics* (Springer Berlin Heidelberg, Berlin, Heidelberg, 2001). URL http://link.springer.com/10.1007/978-3-642-59542-4.

[310] Scherer, W. F., Syverton, J. T. & Gey, G. O. Studies on the propagation in vitro of poliomyelitis viruses. IV. Viral multiplication in a stable strain of human malignant epithelial cells (strain HeLa) derived from an epidermoid carcinoma of the cervix. *The Journal of experimental medicine* **97**, 695–710 (1953). URL http://www.pubmedcentral.nih.gov/articlerender.fcgi?artid=2136303{&}tool=pmcentrez{&}rendertype=abstracthttp://www.ncbi.nlm.nih.gov/pubmed/13052828http://www.pubmedcentral.nih.gov/articlerender.fcgi?artid=PMC2136303http://www.jem.org/cgi/doi/10.1084/jem.97.

[311] Graham, F. L., Smiley, J., Russell, W. C. & Nairn, R. Characteristics of a human cell line transformed

by DNA from human adenovirus type 5. *The Journal of general virology* **36**, 59–74 (1977). URL http://www.ncbi.nlm.nih.gov/pubmed/886304.

[312] Kleyman, T. R. & Cragoe, E. J. Amiloride and its analogs as tools in the study of ion transport. *The Journal of membrane biology* **105**, 1–21 (1988). URL http://www.ncbi.nlm.nih.gov/pubmed/2852254.

[313] Wang, L. H., Rothberg, K. G. & Anderson, R. G. W. Mis-assembly of clathrin lattices on endosomes reveals a regulatory switch for coated pit formation. *Journal of Cell Biology* **123**, 1107–1117 (1993).

[314] Cain, C. C., Sipe, D. M. & Murphy, R. F. Regulation of endocytic pH by the Na+,K+-ATPase in living cells. *Proceedings of the National Academy of Sciences of the United States of America* **86**, 544–8 (1989). URL http://www.pubmedcentral.nih.gov/articlerender.fcgi?artid=286508{&}tool=pmcentrez{&}rendertype=abstract.

[315] Akiyama, T. *et al.* Genistein, a specific inhibitor of tyrosine-specific protein kinases. *The Journal of biological chemistry* **262**, 5592–5 (1987). URL http://www.ncbi.nlm.nih.gov/pubmed/3106339.

Nomenclature

ASGPR Asialoglycoprotein receptor

AUC Area under the curve

BHG Bis(hexadecyl) glycerol

cAMP Cyclic adenosine monophosphate

CL Conventional liposomes

CLSM Confocal laser scanning microscopy

CMC Critical micelle concentration

cryoTEM Cryo transmission electron microscopy

CuAAC Copper-catalyzed alkyne azide cycloaddition

DAC Dual asymmetric centrifugation

DC Dual centrifugation

DHPA Dihydroxypropylamine

DHPMA N-(2,3-dihydroxypropyl) methacrylamide

DLS Dynamic light scattering

DOPC Dioleoyl phosphatidylcholine

DOPE Dioleoyl phosphatidylethanolamine

DOSY Diffusion-ordered NMR spectroscopy

DOTAP 1,2-dioleoyl-3-trimethylammonium-propane

DSPC Distearoyl phosphatidylcholine

DSPE Distearoylphosphatidylethanolamine

EGFR Endothelial growth factor receptor

FA Folic acid

FAZ Folic acid azide

FBS Fetal bovine serum

FCCS Fluorescence cross-correlation spectroscopy

FCS Fluorescence correlation spectroscopy

FR Folate Receptor

FRET Fluorescence resonance energy transfer

GUV Garge unilamellar vesicle

GUV Giant unilamellar vesicles

hbPG hyperbranched polyglycerol

HFIP GPC Hexafluoroisopropanol gel permeation chromatography

HPA Hydroxypropylamine

HPH High pressure homogenization

HPLC High performance liquid chromatography

HPMA N-(2-hydroxypropyl) methacrylamide

LMA Lauryl mathacrylate

LUV Large unilamellar vesicle

MLV Multilamellar vesicle

MPPC Monopalmitoyl phosphatidylcholine

MTT 3-(4,5-dimethylthiazol-2-yl)-2,5-diphenyltetrazolium bromide

NCA N-carboxyanhydrides

NHS N-hydroxysuccinimide

NTA Nanoparticle tracking analysis

PAA Polyacrylic acid

PAGE Poly(acrylamide) gel electrophoresis

PBS Phosphate buffered saline

PC Phosphatidylcholine

PDI Poly dispersity Index

PEG Polyethyleneglycol

PET Positron emission tomography

PG polyglycerol

PGG poly(glycidyl)glycerol

PPE Palmar-plantar erythrodysesthesia

PS Phosphatidylserine

PVA Polyvinyl alcohol

RAFT Reversible addition–fragmentation chain transfer

Rh Hydrodynamic radius

ROP Ring opening polymerization

SEC Size exclusion chromatography

SELEX Systematic evolution of ligands by exponential enrichment

SNALP Solid nucleic acid lipid particles

SPAAC Strain-promoted alkyne azide cycloaddition

SPPC Stearoyl-palmitoylphosphatidylcholine

SRB Sulforhodamine B

SSL Sterically stabilized liposomes

SUV Small unilamellar vesicle

TCO Trans-cyclooctene

TEM Transmission electron microscopy

VEGF Vasculature endothelial growth factor

VPG Vesicular phospholipid gel

List of Publications

Peer-Reviewed Publications

T. Fritz, M. Hirsch, F. C. Richter, S. S. Müller, A. M. Hofmann, K. a K. Rusitzka, J. Markl, U. Massing, H. Frey, M. Helm, *Biomacromolecules* **2014**, 15, 2440–2448.

"Click modification of multifunctional liposomes bearing hyperbranched polyether chains

T. Fritz, M. Voigt, V. Schulz, U. Massing, M. Helm, in *Proc. 2015 Annu. Meet. Control. Release Soc.*, Edinburgh, **2015**.

"Micro-scale liposome formulation via dual centrifugation"

M. Scherer, K. Fischer, F. Depoix, T. Fritz, R. Thiermann, K. Mohr, R. Zentel, *Macromol. Rapid Commun.* **2016**, 37, 60–66.

"Pentafluorophenyl Ester-based Polymersomes as Nanosized Drug-Delivery Vehicles"

S. S. Müller, T. Fritz, F. Prochnow, M. Gimnich, M. Worm, M. Helm, H. Frey, *Polym. Chem.* **2016**. *(submitted)*

"Biodegradable Hyperbranched Polyether-Lipids with In-Chain pH-Sensitive Linkages"

T. Fritz, M. Voigt, M. Worm, I. Negwer, S. S. Müller, K. Kettenbach, T. L. Ross, F. Roesch, K. Koynov, H. Frey, M. Helm, *Chem. - A Eur. J.* **2016**. *(accepted)*

"Orthogonal click conjugation to the liposomal surface reveals stability of lipid anchorage as crucial for targeting"

Oral Presentations

T. Fritz, SFB 1066 Summer School 2014, Stromberg, Germany, 23 Sep **2014**

"Preparation, stability, uptake, and surface conjugation of liposomes"

Poster Presentations

T. Fritz, M. Hirsch, S. S. Müller, H. Frey, U. Massing, M. Helm
International Liposome Society Meeting 2013, London, United Kingdom, 14 - 17 Dec **2013**
TAU Summer School on Nanomedicine and Innovation 2014, Tel Aviv, Israel, 15 -19 Jun **2014**
"Tracking the intracellular fate of new hyperbranched polymer-conjugated lipids in liposomal siRNA formulations prepared via dual asymmetric centrifugation "

T. Fritz, M. Voigt, S. S. Müller, M. Worm, A. Ziller, P. Langguth, H. Frey, M. Helm
SFB 1066 Summer School 2014, Stromberg, Germany, 22 - 26 Sep **2014**
"Aufnahme und intrazelluläre Verteilung von RNA Formulierungen in neuartigen Stealth Liposomen"

T. Fritz, M. Voigt, S. S. Müller, H. Frey, U. Massing, M. Helm
RNA Biochemistry 2014, Bonn, Germany, 09 - 12 Oct **2014**
"In vitro fate of novel sterically stabilized liposomes for aptamer-directed targeting"

T. Fritz, M. Voigt, M. Worm, H. Frey, U. Massing, M. Helm
Controlled Release Society Meeting 2015, Edinburgh, United Kingdom, 08 - 12 Oct **2015**
International Liposome Society Meeting 2015, London, United Kingdom, 19 - 22 Dec **2015**
Max Planck Graduate Center Retreat 2016, Mainz, Germany, 14 Apr **2016**
"Micro-scale liposome formulation via dual centrifugation"

Appendix

1 Detail drawing of DC inset for PCR vials

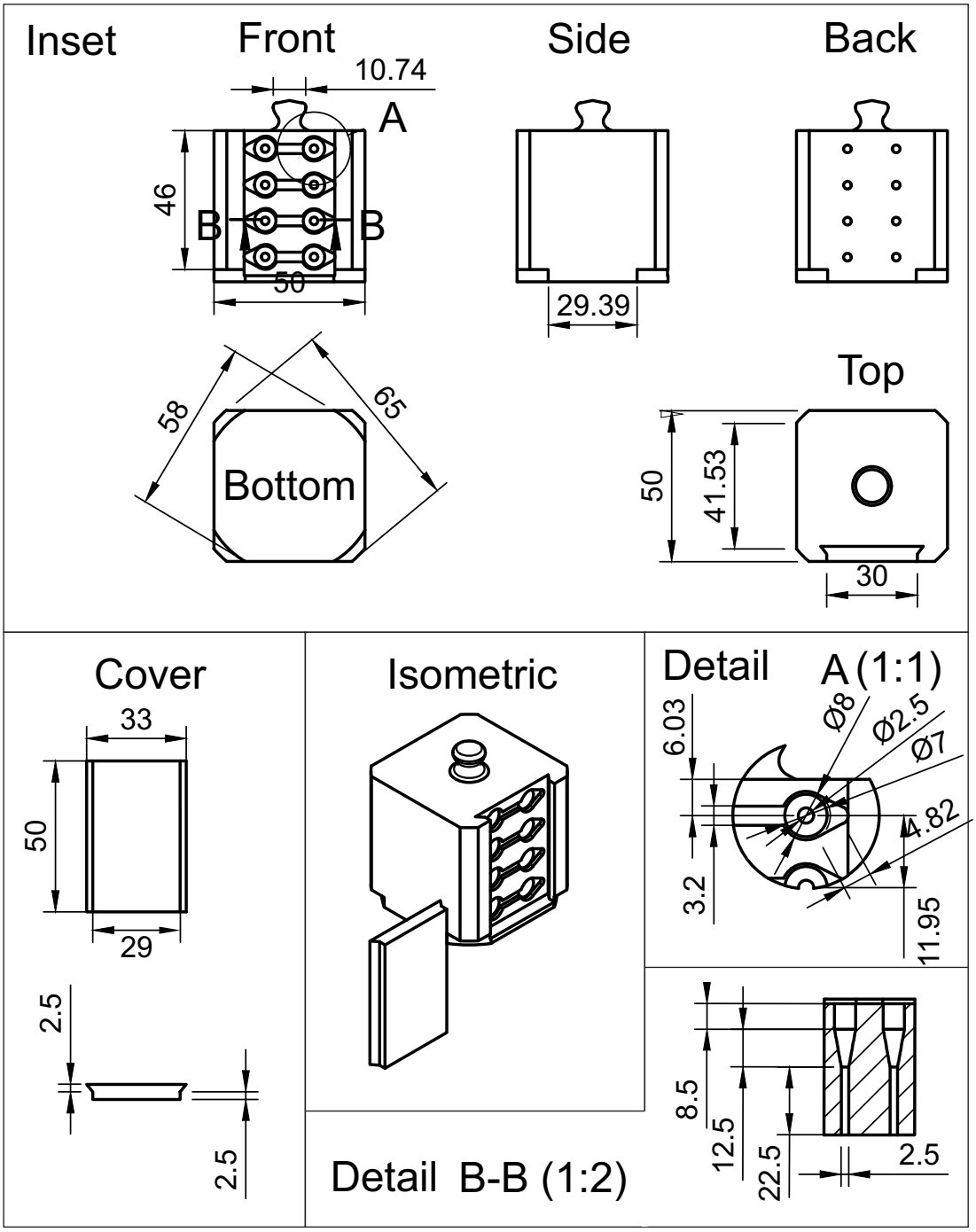

Appendix 1 Detail drawing of PCR-vial sample holder.

2 Quantification of alkyne residues

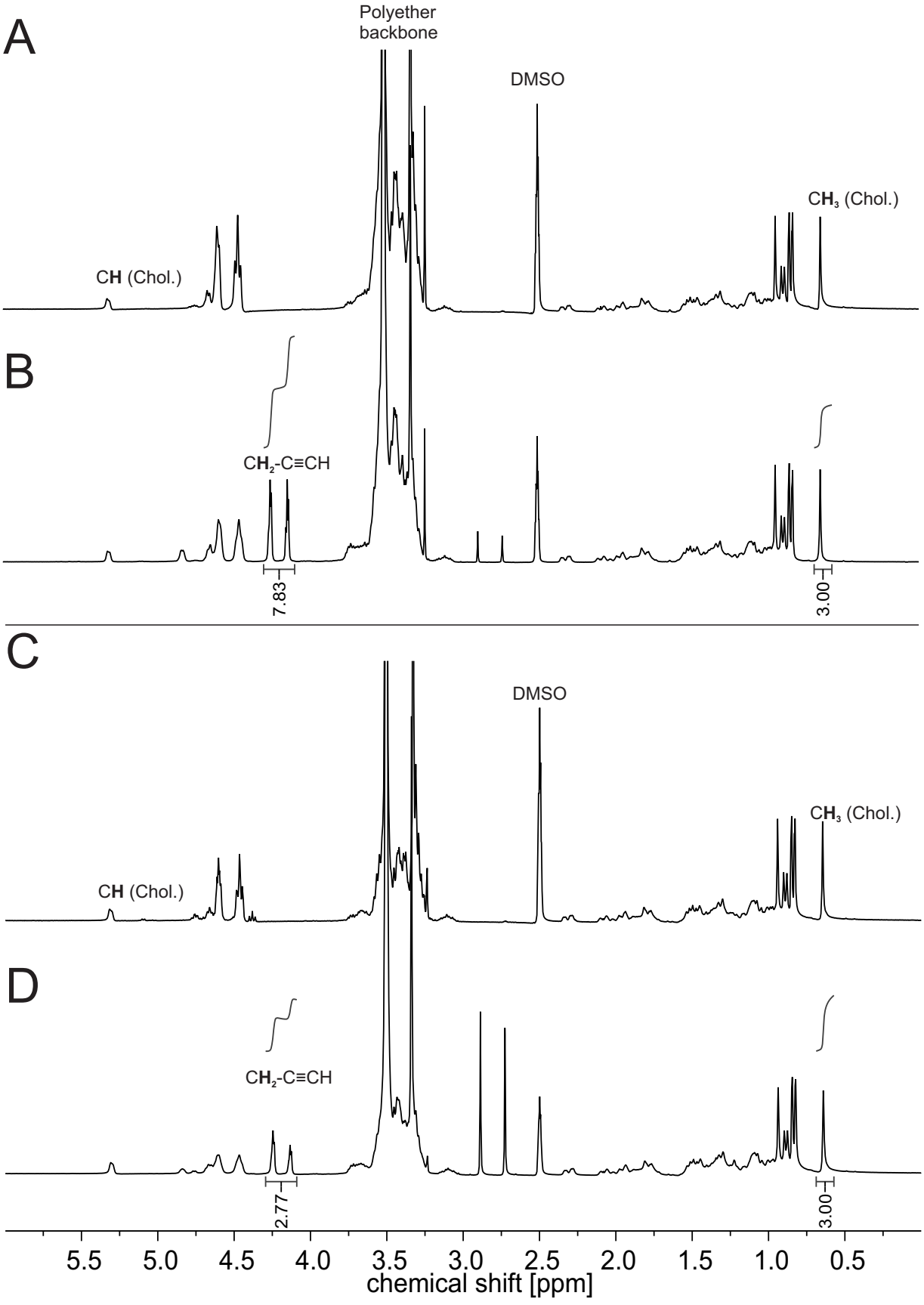

Appendix 2 ^{1}H NMR spectra (300 MHz, DMSO-d_6) of Cholesterol-PEG$_{22}$-PGG$_{8}$ (A), Cholesterol-PEG$_{22}$-PGG$_{8}$-(-CH$_2$-C≡CH)$_4$ (B), Cholesterol-PEG$_{25}$-*hb*PG$_{21}$ (C), Cholesterol-PEG$_{25}$-*hb*PG$_{21}$-(-CH$_2$-C≡CH) (D). Integrals reveal four alkyne residues per cholesterol for (B) and one alkyne residue for (D).

3 Lipid composition after preparation

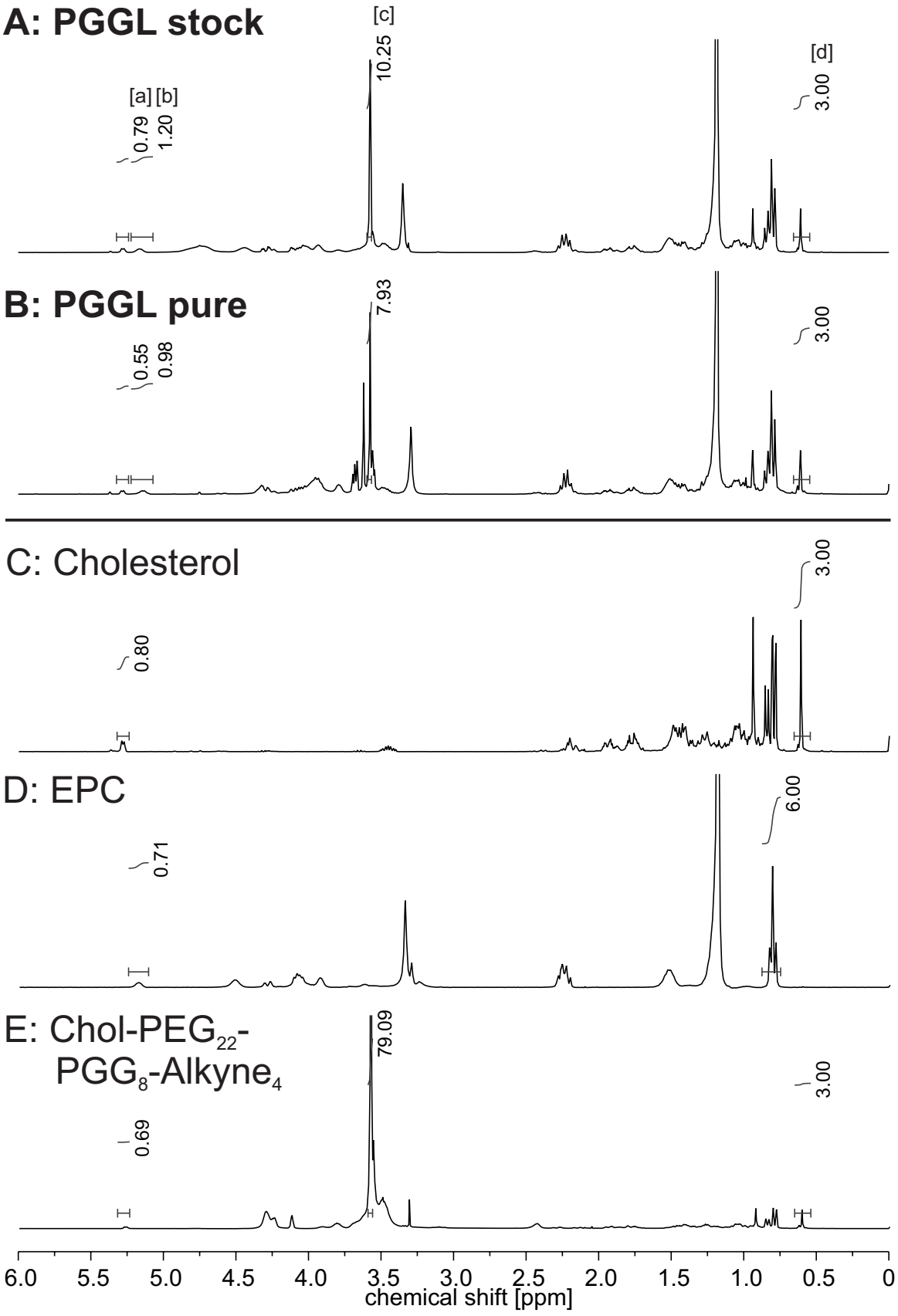

Appendix 3 ^{1}H NMR spectra (300 MHz, $CDCl_3$) of PGGL stock (A), after formulation, purification *via* GPC and lyophilization (B), cholesterol (C), EPC (D) and the used amphiphile (E). Compositions A and B show analog ratios between the integrals of unique protons of each substance, indicating no changes in composition during liposome preparation and purification. Additionally, the integrals of the polyether backbone (3.6 ppm, [c]) and the ratio between unique protons of cholesterol (5.3 ppm, [a]) and of EPC (5.2 ppm, [b]) are consistent with a molar ratio of 40:55:5 for cholesterol:EPC:Cholesterol-PEG$_{22}$-PGG$_8$-(-CH$_2$-C≡CH)$_4$. Signals: [a]: Cholesterol =CH; [b]: EPC (RO-CH$_2$)$_2$-CH-OR; [c]: polyether backbone; [d]: Cholesterol CH_3.

4 Exemplary gel permeation chromatogram from liposome purification

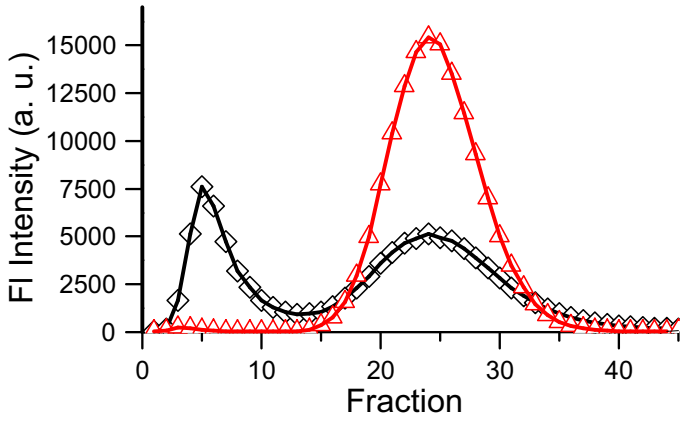

Appendix 4 Gel permeation chromatogram from liposomes purified with a custom-made Sepharose 2B CL column. Liposomes are eluting in fractions 3-10 (black rectangles) and free dye between fractions 14 and 36. The measurement of free dye (red triangles) indicates adequate resolution for this separation problem.

5 Inhibition of other endocytosis Pathways

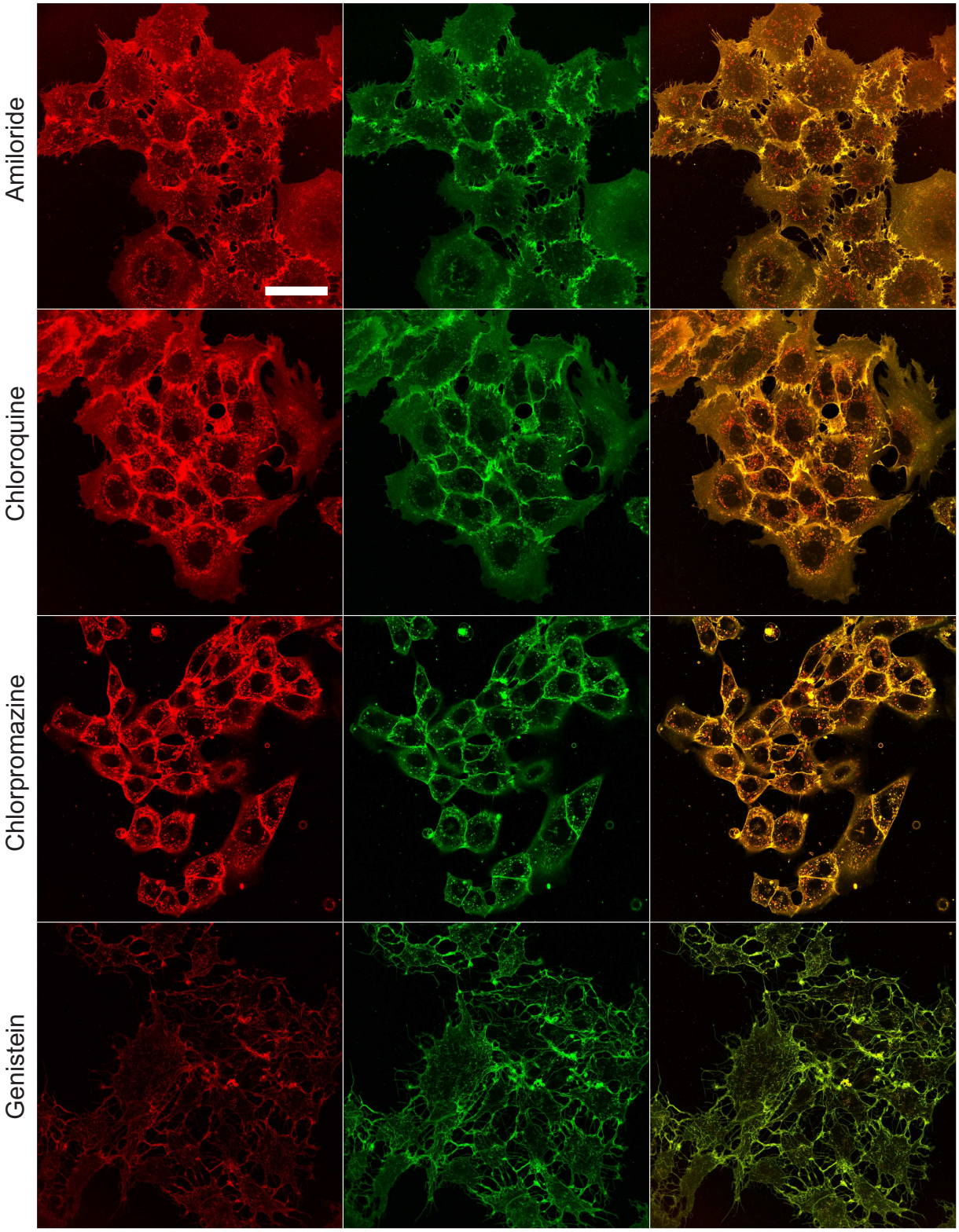

Appendix 5 Inhibition of endocytic uptake pathways. RBE4 cells were incubated with Atto 488- and Alexa 594-labeled PGGL and either Amiloride (inhibition of dynamin-dependent

endocytosis[312]), Chloroquine (inhibition of lysosomal acidification, [314]), Chlorpromazine (inhibition of clathrin-dependent endocytosis, [313]), or Genistein (inhibition of caveolae-mediated endocytosis, [315]). All cells showed unspecific membrane staining and intracellular aggregates, which suggested the endocytic uptake of labeled amphiphiles to be highly unspecific. Scale bar represents 25 µm.

6 FCS data of labeled liposomes

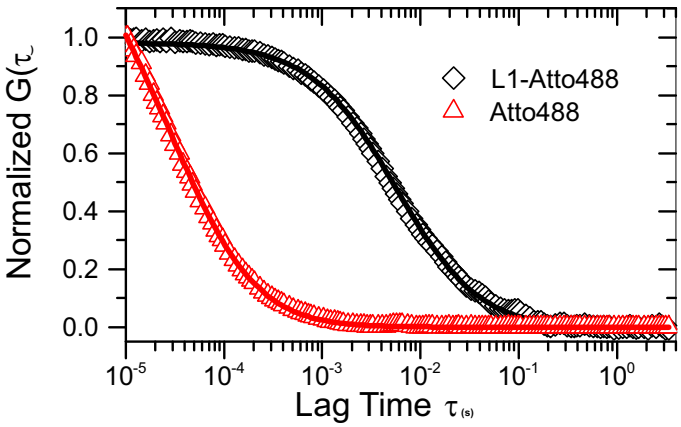

Appendix 6 Fluorescence correlation spectroscopy data of Atto 488-labeled formulation L1 (black diamonds) and free Atto 488 azide (red triangles). An accurate fit with eq. 5.6 (black line) indicates no significant amount of free dye.

7 HPLC verification of FAZ click

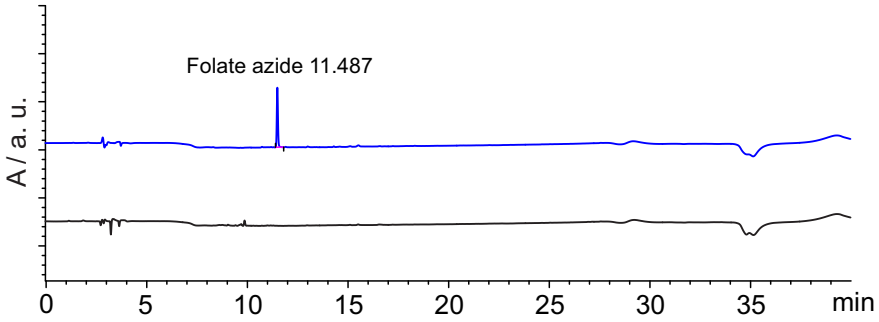

Appendix 7 HPLC chromatograms of free folic acid azide (Blue) and an exemplary click reaction mixture after successful conjugation to alkyne bearing amphiphile (black). While in both injections 20 pmol FAZ were injected, no residual free azide was detected in the click reaction, indicating a quantitative consumption.

8 One-pot labeling of folate liposomes

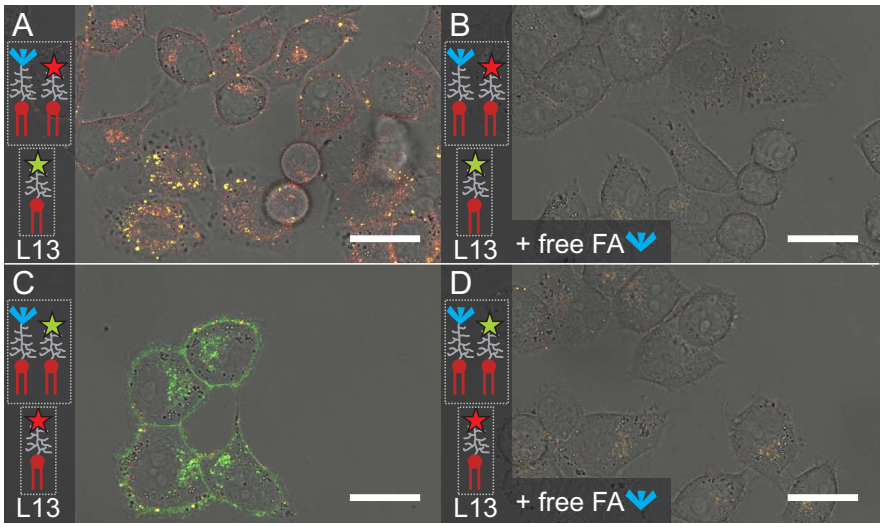

Appendix 8 One-pot labeling of folate liposomes. Only when fluorophores were present during folate conjugation, cells exhibited fluorescent membrane staining in the correspond channels (A: red, C: green). Particulate aggregates, presumably intact liposomes, showed colocalization of both fluorophores. All binding was chasable with free folic acid (B, D). Scale bars represent 25 µm.

9 Cleavage kinetics of BHG-Ke-PEG$_{44}$-Alkyne

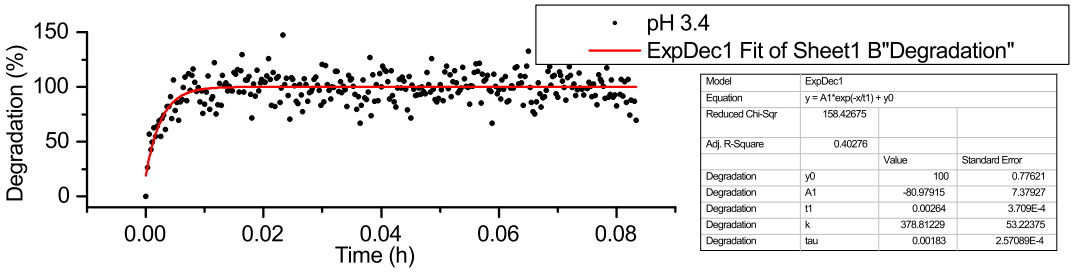

Model	ExpDec1		
Equation	y = A1*exp(-x/t1) + y0		
Reduced Chi-Sqr	158.42675		
Adj. R-Square	0.40276		
		Value	Standard Error
Degradation	y0	100	0.77621
Degradation	A1	-80.97915	7.37927
Degradation	t1	0.00264	3.709E-4
Degradation	k	378.81229	53.22375
Degradation	tau	0.00183	2.57089E-4

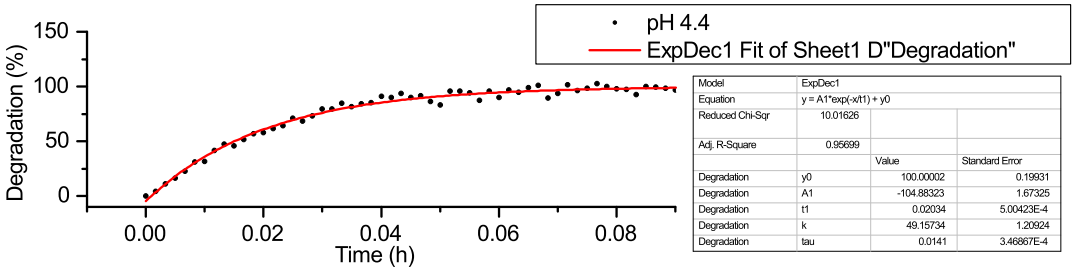

Model	ExpDec1		
Equation	y = A1*exp(-x/t1) + y0		
Reduced Chi-Sqr	10.01626		
Adj. R-Square	0.95699		
		Value	Standard Error
Degradation	y0	100.00002	0.19931
Degradation	A1	-104.88323	1.67325
Degradation	t1	0.02034	5.00423E-4
Degradation	k	49.15734	1.20924
Degradation	tau	0.0141	3.46867E-4

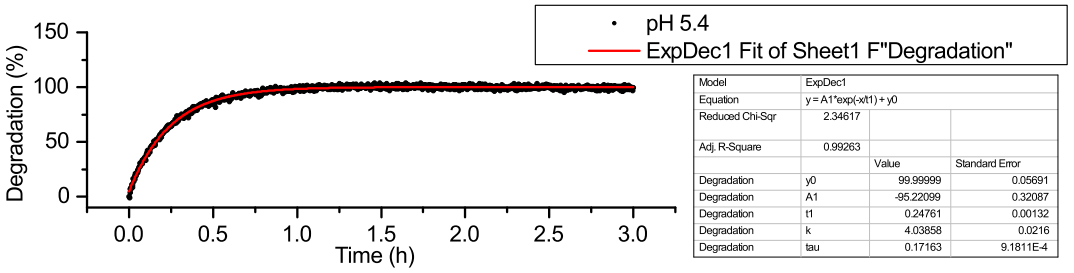

Model	ExpDec1		
Equation	y = A1*exp(-x/t1) + y0		
Reduced Chi-Sqr	2.34617		
Adj. R-Square	0.99263		
		Value	Standard Error
Degradation	y0	99.99999	0.05691
Degradation	A1	-95.22099	0.32087
Degradation	t1	0.24761	0.00132
Degradation	k	4.03858	0.0216
Degradation	tau	0.17163	9.1811E-4

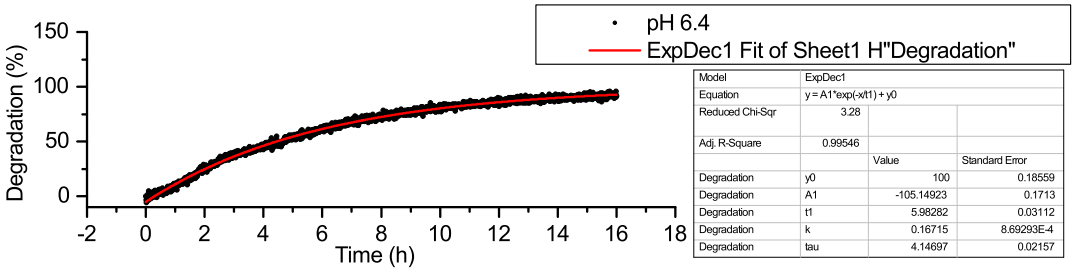

Model	ExpDec1		
Equation	y = A1*exp(-x/t1) + y0		
Reduced Chi-Sqr	3.28		
Adj. R-Square	0.99546		
		Value	Standard Error
Degradation	y0	100	0.18559
Degradation	A1	-105.14923	0.1713
Degradation	t1	5.98282	0.03112
Degradation	k	0.16715	8.69293E-4
Degradation	tau	4.14697	0.02157

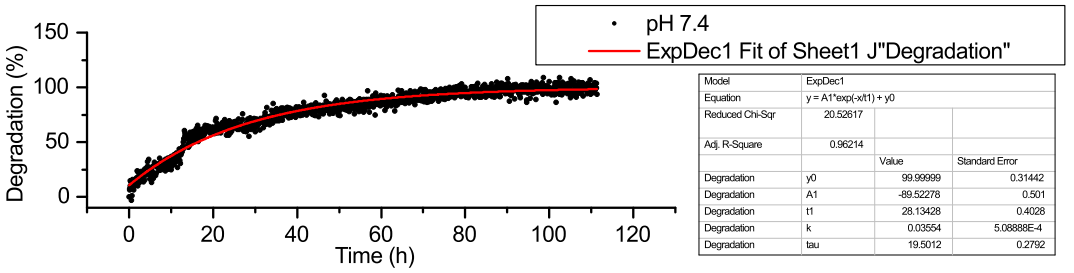

Model	ExpDec1		
Equation	y = A1*exp(-x/t1) + y0		
Reduced Chi-Sqr	20.52617		
Adj. R-Square	0.96214		
		Value	Standard Error
Degradation	y0	99.99999	0.31442
Degradation	A1	-89.52278	0.501
Degradation	t1	28.13428	0.4028
Degradation	k	0.03554	5.08888E-4
Degradation	tau	19.5012	0.2792

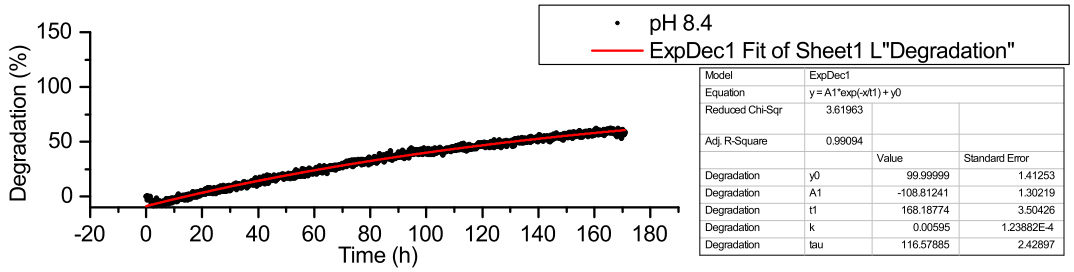

Model	ExpDec1		
Equation	y = A1*exp(-x/t1) + y0		
Reduced Chi-Sqr	3.61963		
Adj. R-Square	0.99094		
		Value	Standard Error
Degradation	y0	99.99999	1.41253
Degradation	A1	-108.81241	1.30219
Degradation	t1	168.18774	3.50426
Degradation	k	0.00595	1.23882E-4
Degradation	tau	116.57885	2.42897

Appendix 9 Cleavage kinetics of BHG-Ke-PEG$_{44}$-Alkyne at different pH values, including fitting data.

10 Dependence of $t_{1/2}$ on pH

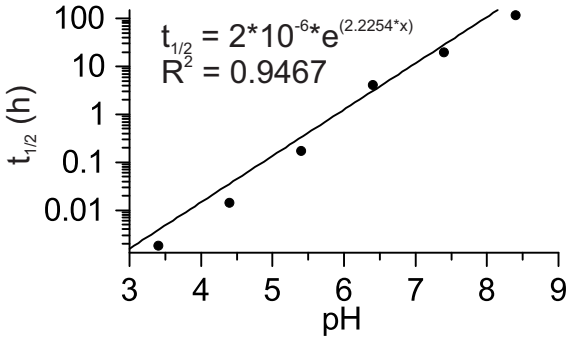

Appendix 10 Dependence of halflife $t_{1/2}$ on the pH value.

Curriculum Vitae

Thomas Fritz

Anschrift:	[redacted]
Nationalität:	[redacted]
Geburtsdatum:	[redacted]
Geburtsort:	[redacted]

Ausbildung

[redacted]

Ort, Datum

Thomas Fritz